Identification of protein interactions between *Salmonella* and the mammalian host during intracellular survival

By

Andrea Déborah V. Briones Gómez

A thesis submitted for the degree of Doctor of Philosophy

Supervisor: Dr. Alessandra Devoto

Royal Holloway University of London

September 2016

Declaration of Authorship

I Andrea D.V. Briones Gómez hereby declare that this thesis and the work presented in it is entirely my own. Where I have consulted the work of others, this is always clearly stated.

September 1st, 2016

Abstract

Salmonella typhimurim is the major cause of gastroenteritis in the developed and developing world. This research focuses on the hypothesis that the Salmonella atypical fimbriae (Saf) plays an important role in attachment and re-infection of cells. Salmonella atypical fimbriae (Saf) is mainly composed of several SafA subunits and one SafD unit at the tip of the SafA polymer. SafA's sequence is variable within *Salmonella* strains but SafD's is not, indicating that SafD is most likely a conserved adhesin, whereas SafA is involved in host specificity.

The Saf fimbriae was studied by designing recombinant dual tagged protein SafA' (GST-SafA-6xHis). This was immobilised in a repertoire of systems until finding a suitable one that would allow us to study protein-protein interactions between *Salmonella* and the mammalian host. Finally, any SafA-6xHis binding partners identified in the large intestine affinity-enrichments were identified by mass spectrometry.

The experiments were performed with a variety of negative controls, including GST, BSA, cleaved SafA' (SafA-6xHIs), SafA’ (GST-SafA-6xHis), among others to identify specific interactions. The analysis was carried out with Scaffold, a bioinformatics tool that increases confidence in protein identification reports through the use of several statistical methods. A stringent analysis was performed, leading to the identification of five SafA-6xHis interacting proteins.

Whilst hypothetical, a role for the Saf fimbriae other than in surface attachment is suggested on the basis of the results. Different functions for the Saf fimbriae that will allow *Salmonella* to modulate crucial events during the infection process are discussed: mitochondrial apoptosis, effect on the transcription of host genes, neutrophil induced cell death and the binding to host transmembrane proteins.

Acknowledgements

I am grateful to Dr. Devoto for her support in the initial four years as an Advisor and in the last year and a half as a Supervisor. To re-direct and complete this work has taken much effort, yet regardless of this and the adjustments of working in a different environment, it did not seem impossible and at no point I felt overwhelmed by the challenges. I believe this is due to your understanding and support– Thank you.

To my first supervisor, Dr. Soloviev, thank you for the basic training received. It would have been impossible to move forward without a solid basis.

My appreciation also extends to Prof. Klein- Seetharaman, Dr. Jones (both from University of Warwick) and Dr. Bindschedler for her role as my Advisor during the last year of my work. I would also like to thank all the members of staff who helped me with corrections, feedback and technical advice so that I could progress.

To my Father, who passed away in late 2013, I am sorry it took so long but I can assure you I worked every day until I had nothing left to give. Thank you for raising me to never give up and to refuse to be second best. To my mother, for rubbing her unstoppable optimism on me and making me feel that impossible is nothing, the advantages of having a good attitude are invaluable. The truth is, I have been fortunate to have you both and I would like to think your ways have blended in me. I would also like to thank my siblings and friends for the support and who have been neglected for (too) long, but I had to work!

Finally, to Royal Holloway University of London for their financial support.

Table of Contents

List of Figures

List of Tables

List of Abbreviations

(*m/z*)	Mass-to-charge ratio
2DIR	Two-dimensional infrared
a.u	Arbitrary units
ABHD14B	Alpha/beta hydrolase domain-containing protein 14B
ABU	Asymptomatic bacteriuria
Ag	Antigen
AP-MS	Affinity purification mass spectrometry
BCR	B cell receptor
BMDM	Bone Marrow-derived Macrophages
BSA	Bovine Serum Albumin
CBP	Calmodulin Binding Protein
CD	Circular dichroism
CG	Cathepsin G
Co-IP	Co-immunoprecipitation
cRAP	Common Repository of Adventitious Proteins
DAEC	Diffusely Adherent *E. coli*
DMD	Duchenne muscular dystrophy
DSC	Donor strand complementation
DSE	Donor strand exchange mechanism
DSF	Differential Scanning Fluorimetry
E. coli	*Escherichia coli*
ELISA	Enzyme-linked immunosorbent assay
ER	Endoplasmic reticulum
ESI	Electrospray ionisation

FAE	Follicle-associated epithelium
FDR	False Discovery Rate
FPs	fluorescent proteins
FTIR	Fourier transform
GALT	Gut-associated lymphoid tissue
GFP	Green fluorescent protein
GI	Gastrointestinal
GO	Gene ontology
GRAVY	Grand average of hydropathy
GSH	Reduced glutathione
GST	Glutathione S-transferase
HA	Influenza Hemagglutinin
HCD	Higher-energy collisional gas dissociation
His-tag	Poly-Histidine tag
HPLC	High-pressure liquid chromatography
HRP	Horseradish Peroxidase
HRV	Human Rhinovirus
Ig	Immunoglobin
IL-1β	Interleukin-1β
IMAC	Immobilized Metal Affinity Chromatography
JNK	Jun N-terminal kinase
LAMP	Lamp membrane protein
M cells	Microfold cells
MALDI	Matrix Assisted Laser Desorption Ionization

MAPEG	Membrane associated proteins in eicosanoid and glutathione metabolism
IMPC	International Mouse Phenotyping Consortium
MAPEG	Membrane associated proteins in eicosanoid and glutathione metabolism
MAPK	Mitogen-activated protein kinases
MBP	Maltose-binding protein
MGST	Microsomal glutathione transferases
MGST3	Microsomal glutathione S-transferase 3
MOTC	MT-organizing center
MRW	Mean Residue Weight
MS	Mass spectrometry
NC	Nitrocellulose
NEs	Elastases
NRMSD	Normalized root mean square displacement
NSPs	Serine proteases
Nte	N-terminal
OG	Octyl β-D-glucopyranoside
PBS	Phosphate-buffered Saline
PCD	Apoptosis is a type of programmed cell death
PE3	Proteinase-3
PEM	Photo Elastic Modulator
PEM	Photo Elastic Modulator
PI	Protease inhibitor
PMF	Peptide Mass Fingerprinting
PMN	Polymorphonuclear neutrophil
PP	Peyer’s patch
PPI	Protein-protein interaction

QAA	Quantitative Amino Acid Analysis
Quad, Q	Quadrupole
RFU	Relative Fluoresence Intensity
RMS	Root mean square
RMSE	Root-mean-square error
RNS	Reactive Nitrogen Species
ROS	Reactive oxygen species
RP	Reverse phase
Saf	Salmonella atypical fimbriae
SafA’	GST-SafAx6His
SCV	Salmonella-containing-vacuole
SDS	Sodium dodecyl sulphate
SPI	*Salmonella* pathogenicity island
SPR	Surface plasmon resonance
T3SS	Type III secretion system
TCA	Trichloroacetic acid
Tm	Melting temperature
TMB	3,3′,5,5′-Tetramethylbenzidine
TNFα	TNFα
TOF	Time-of-Flight
UDE	Uracil-DNA degrading protein
UPEC	Uropathogenic *E. coli*
UPR	Unfolded Protein Response
WT	Wild type
ZNF23	Zinc finger nuclear protein 23

CHAPTER I – GENERAL INTRODUCTION

1. *Salmonella*: General Concepts

1.1 *Salmonella enterica*

Salmonella enterica serovar Typhimurium is the major cause of gastroenteritis in the developed and developing world (Gal-Mor et al 2014). The different serovars of *Salmonella* depict the ability of this bacterium to infect different hosts and of its ability to prevail over harsh environments within the host (Ochoa and Rodríguez et al 2005). *Salmonella* infection in humans is zoonotic and the main route of infection is through the consumption of contaminated foods, like eggs, meat, poultry and milk (Gómez-Aldapa et al 2012, Meyer et al 2012, Phalen et al 2010, Ravishankar et al 2010). It is possible to get infected by consuming vegetables and fruits contaminated by sewage in the water or manure (Gómez-Aldapa et al 2012, Heaton and Jones et al 2008). After 12 to 72 hours of infection the subject experiences fever, diarrhoea, vomiting and stomach pain. The disease must be controlled as dehydration occurs quickly and without treatment the infection can be extended from the intestines to the blood system by getting through the intestinal epithelial barrier (Foley et al 2008).

1.2 *Salmonella* taxonomy and serological classification

Salmonella is a bacterium that may have possibly originated as a result of plasmid or phage mediated horizontal transfer from *Escherichia coli* (Bäumler et al 1997, Ochman et al 2000, Vernikos et al 2007). *Salmonella* is taxonomically divided into *Salmonella enterica* and *Salmonella bongori*. *Salmonella enterica* is subdivided into six subspecies: *Salmonella enterica* or *I*, *salamae* or *II*, *arizonae or IIIa*, *diarizonae* or *IIIb*, *houtenae* or *IV* and *indica* or *VI* (Rabsch et al 2002, Tindall et al 2005, Figure 1). These are further divided into over 2,500 serovars. The main classification of these serovars is based on the Kauffman and White scheme (Grimont et al 2007) which defines the serogroup according to the O antigen and the serovar by the expression of the H antigen, located at the flagellum of the bacterium (Brenner et al 2000).

Salmonella is a well-adapted bacterium capable of infecting a range of hosts (Schwartz et al 1992, Uzzau et al 2000). Its different serovars are manifestations of its ability to infect and survive within a diverse range of hosts, such as, reptiles, fishes, poultry, avians and humans, and even plants (Schikora et al 2012, Singh et al 2013, Switt et al 2013). All

Salmonella species can cause high morbidity and mortality in animals and humans. *Salmonella enterica* subspecies I in particular contains the largest number of species that cause disease in warm blooded animals (Holt et al 2009) . Within subspecies I, *S. enterica serovar* Typhimurium and *S. enterica serovar* Typhi, infect humans the most. *S. enterica serovar* Typhimurium causes acute gastroenteritis and can be deadly in the malnourished and the elderly. It can also infect mice (Rabsch et al 2002). On the other hand, *S. enterica serovar* Typhi infects solely humans and is a major problem in the African continent where the disease is endemic in sub-Saharan Africa (Morpeth et al 2009). In this work, *Salmonella enterica* subspecies I, serovar Typhimurium strain LT2 has been used.

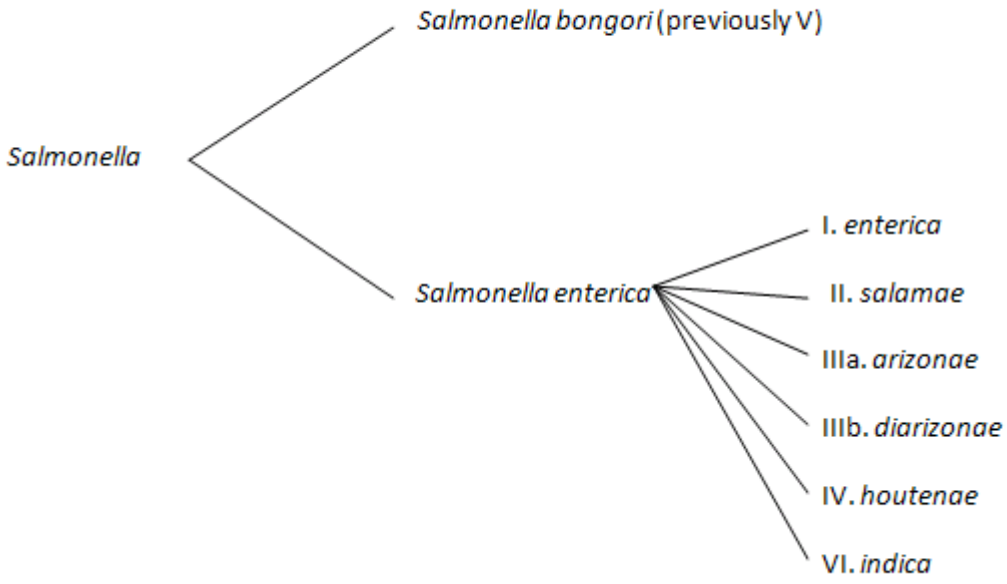

Figure 1. Phylogenetic tree of *Salmonella*. Representation of *Salmonella*'s main species and the six subspecies under *Salmonella enterica*. Adapted from Swearingen et al (2012).

1.3 Pathogenicity Islands and the Type III secretion system (T3SS or injectisome)

Pathogenicity islands are genetic clusters that are pivotal for the encoding of virulence factors (Schmidt and Hensel et al 2004). *Salmonella enterica* Typhimurium has six pathogenicity islands encoded in its genome. *Salmonella* pathogenicity island 1 (SP-1) produces the secreted factors involved in the formation of the pore making proteins and the effectors that will direct actin rearrangement; therefore SPI-1 is referred to as the invasion island (Sukhan et al 2003). *Salmonella* pathogenicity island 2 (SPI-2) has the role of secreting the proteins that will allow *Salmonella* to burst out from the host's

vacuole making it important for systemic infection and intracellular accumulation (Hapfelmeier et al 2005). *Salmonella* pathogenicity island 3 (SPI-3) is needed for intramacrophage survival, virulence in certain hosts and to adapt itself to its environment, especially the ones low in Mg^{2+} (Blanc-Potard et al 1999). It was thought the role of *Salmonella* pathogenicity island 4 (SPI-4) was solely of importance for intracellular survival (Gerlach et al 2007) but Main-Hester's work demonstrated SPI-1 and SPI-4 are co-regulated in the interaction of *Salmonella* Typhimirium and the host by encouraging cell adherence (Main-Hester et al 2008). *Salmonella* pathogenicity island 5 (SPI-5) plays a role in the inflammatory reaction (Rychlik et al 2009) and bacteria enteropathogenicity (Amavisit et al 2003).

In *Salmonella enterica* subspecies *enterica* I, *Salmonella* pathogenicity island 6 (SPI-6) encodes type six secretion system (T6SS) and also the Salmonella atypical fimbriae (Saf) (Blondel et al 2009, Cao et al 2014). T6SS has been associated with roles in adherence, biofilm formation, cytotoxity and cell invasion (Cascales et al 2008).

Additionally, pathogenicity islands also encode for Type III secretion systems (T3SS), or injectisomes, which are biological machines that consist of a needle like apparatus, an inner rod and a basal body (Figure 2). (Gophna et al 2003). In different bacteria the injectisome secretes their own repertoire of toxins but despite the difference between secreted proteins among these, the injectisome structure seems highly conserved (Roy et al 2010). These similarities make it possible to study the function and infection ability of *Salmonella* by cross studying the already known information for this system on other bacterium. It is known *Salmonella* has two type 3 secretion systems located within SPI-1 (T3SS) and SPI-2 (T3SS) islands. The difference between SPI-1 (T3SS) and SPI-2 (T3SS) is that SPI-1 (T3SS) promotes bacterial pathogenicity for invasion and it is the means by which *Salmonella* injects its effectors during infection. On the other hand, SPI-2 (T3SS) is activated only after *Salmonella* has entered the host's cytosol (Büttner et al 2012).

Gram negative bacteria, such as, *Shigella*, *E. coli*, *Yersinia*, *Chlamydia* and *Pseudomonas* use this complex to infect eukaryotic cells by secreting proteins from the bacteria directly into the target cell (Coburn et al 2007, Hueck et al 1998). The functions of the injectisome are to translocate virulent proteins into the host in order to change host cell functions, translocate proteins across host membrane, export proteins across bacterial envelope and to bring bacterial and host cells closer (Winstanley and Hart et al 2001). Inside the injectisome reside translocators to create a pore in the host's membrane, effectors and

chaperones that act as transcription factors for the translocators and effectors (Worrall et al 2011).

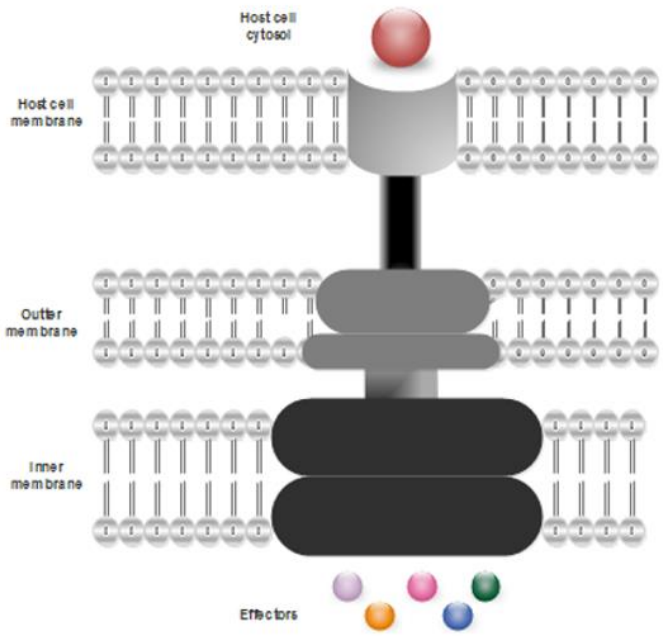

Figure 2. Diagram of the Type 3 secretion system (T3SS or Injectisome). The base and needle components are in black and grey. Effector proteins are translocated from the bacterium cytoplasm to the host cytosol. Adapted from Dewoody et al (2014).

1.4 Survival and infection mechanism

Salmonellae are intracellular bacteria that need the host for its replication. In order to survive, *Salmonella* has adapted itself to live outside the host and can live up to six weeks in fallow soil with the ability to contaminate plants (Barak and Liang et al 2008).

Human pathogenesis of *Salmonella* starts when the subject ingests contaminated food. It makes its way to the alimentary system; some survive the acidic conditions of the stomach and reach the intestine by using their flagella to swim through the surface of the intestinal epithelial cells (Reis et al 2011). Components on the *Salmonella* surface are known to facilitate the attachment to the intestinal epithelial cells (Knodler et al 2010; Figure 3). Previous studies have demonstrated that is possible that after oral ingestion the preferred site of penetration is the jejunum followed by the ileum and lastly, the caecum (Brown et al 2005); this is because *Salmonella* finds itself at the right pH and with the necessary nutrients for invasion. Work carried by Deng shows that only after 8 hours of inoculation the jejunum and ileum are positive for *Salmonella* and after 12 hours post inoculation the presence of *Salmonella* in the caecum is significant. Very low concentrations were found in the duodenum, colon, rectum, oesophagus and stomach (Eswarappa et al 2010).

After anchoring itself into the host's surface it proceeds to invade the interior of the cells by using its first needle-like system SPI-1 (T3SS) to deliver toxins directly into the cytoplasm of the host (Kim et al 2011). Through the injectisome, secreted factors SopE, SopE2 and SopB are transported into the host; SipA triggers membrane ruffling by targeting actin and T-plastin leading to membrane ruffling, which results in uptake of the bacteria (Cornelis et al 2006; Figure 4).

After being engulfed by the host, *Salmonella* survives within a membrane-bound vacuole called the *Salmonella*-containing vacuole (SCV) (Beuzón et al 2002). However, defects on the vacuole allow for bacteria release, leading to cytosolic *Salmonella* (Malik-Kale et al 2012; Figure 4). *Salmonella* only allows a single bacterium per SCV (Eswarappa et al 2010), therefore every time it divides, so does the vacuole (Lahiri et al 2010). The bacterium remains there for a lag period of replication before causing the vacuole to burst (Creasey and Isberg et al 2014, Lahiri et al 2010).

The success of *Salmonella* lies in its ability to avoid the lysosomal degradation pathway, therefore avoiding termination by the host (Bakowski et al 2008). Several hours after invasion, *Salmonella* ejects its second injectisome, the SPI-2 (T3SS), and delivers more than 30 effectors across the SCV. These effectors are the ones responsible for remodelling and positioning of the SCV in the perinuclear region, very close to the Golgi apparatus (Schleker et al 2012). It is also known that *Salmonella* does not need the SCV to survive and replicate as during infection there is a group of cytosolic bacteria adapted to survive and replicate in the cytosol. Studies have revealed that these bacteria can replicate 20-100 fold after 6 hours; whereas SCV bacteria can replicate 3-6 fold after 9 hours (Malik-Kale et al 2012). Also, work carried out in SifA mutants has confirmed that cytosolic *Salmonella* is capable of hyper-replication this is not possible in the macrophage cytosol due to the resistance from the host immune system (Beuzón et al 2000, Knodler et al 2014). These bacteria are transcriptionally different from intravacuolar *Salmonella* as they are induced by the invasion-associated type III secretion system; therefore, they are designed for invasion (Malik-Kale et al 2012). Even when is not clear why there is cytosolic *Salmonella*, some studies have established a possible vacuolar defect as the cause for a small percentage of *Salmonella* to escape the vacuole and adapt to the cytosol (Creasey and Isberg et al 2014, Martínez-Lorenzo et al 2001).

Because of the nutrient-rich cytosol, *Salmonella* manages to hyper-replicate and reprograms virulence gene expression toward invasion. The host senses cytosolic

Salmonella and automatically triggers inflammatory cell death and extrusion (Sebastiani et al 2002). If well in this circumstance *Salmonella* is vulnerable to the immune system, this is also exploited and the ready to infect *Salmonella* is released into the lumen of the gastrointestinal and biliary tracts by extrusion, which in turn allows *Salmonella* to infect secondary cells rapidly (Knodler et al 2010).

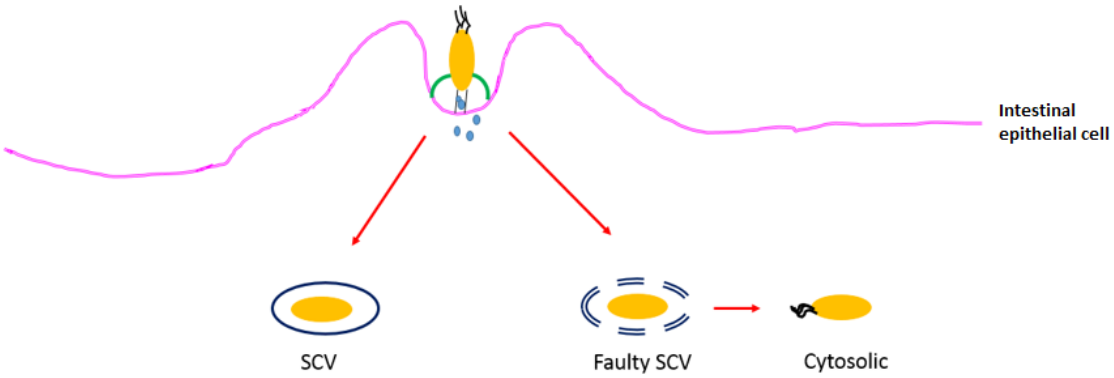

Figure 3. *Salmonella* host invasion. Typically *Salmonella* makes its way to the intestines and through unknown mechanisms recognizes binding sites. Upon attachment *Salmonella* injects effectors (toxins) that will encourage membrane ruffling and engulfment of the bacteria. Salmonella resides in the *Salmonella*-containing vacuole (SCV) but defects in the vacuole cause release of the bacteria into the cytosol. These are flagellated, ready to infect and capable of replication. Adapted from Boumart et al (2014).

1.5 Relevant bacteria-host interactions

1.5.1 Salmonella-Containing Vacuole (SCV) and the endosomal pathway

Endocytosis is one of the cell's forms of active transport in which molecules, such as proteins, are transported into the cell by engulfment (Doherty and McMahon et al 2009). The pathway is divided into four categories, phagocytosis, caveolae, micropinocytosis and clathrin-mediated endocytosis (Gruenberg and Van der Goot et al 2006).

Pathogens have exploited these pathways in order to gain entrance to the cell and use their lysosomal machinery to their benefit (Medina-Kauwe et al 2007). The most studied pathway is clathrin-mediated endocytosis (Bonazzi and Cossart et al 2006, Grove and Marsh et al 2011, Veiga and Cossart et al 2006). After entering the host-cell, pathogens will encounter themselves in the cytosol, to be more specific, the early endosome (Alix et al 2011). In here, they are transported further down to the endocytic pathway to late endosomes and lysosomes for their destruction (Ibarra and Steele-Mortimer et al 2009).

Salmonella has developed strategies to escape lysosomal degradation (Eswarappa et al 2010). At this point of infection, the bacterium is protected end encased in a membranous vacuole made from the host's membrane, called the SCV (Steele-Mortimer et al 2008). It has been reported that *Salmonella* uses the host's endocytic regulators, GTPase, Rab5, Rab11 and Rab7 to re-direct the SCV towards the perinuclear position of the cell (Brumell and Grinstein et al 2004). Intracellular positioning is vital to escape lysosomal degradation and for SCV based replication (Bakowski et al 2008). It is speculated that intravacuolar bacterial replication depends on spatiotemporal regulated interactions with host cell vesicular compartments (Ramsden et al 2007). This is possibly because the position facilitates bacterial requirements for membranes and nutrients vital to maintain its SCV and keep evading the immune system (Wasylnka et al 2008). Moreover, functional studies have identified the SCV has lysosomal-like characteristics by having an acidic lumen and being surrounded by lysosomal glycoproteins (Roark and Haldar et al 2008). Studies have localized the SCV close to the lysosomal pathway and in close proximity to the nucleus, Endoplasmic Reticulum (ER) and Golgi Complex (Deiwick et al 2006, Müller et al 2012).

As the SCVs mature, these are displaced along microtubules, towards the MT-organizing center (MOTC) and eventually also within the Golgi region and *Salmonella*-induced filaments (Sifs) (Brumell et al 2002, Mostowy and Shenoy et al 2015). These are tubular structures which result from the elongation of the SCV itself and are assembled from lysosomal glycoproteins (Brumell et al 2002).

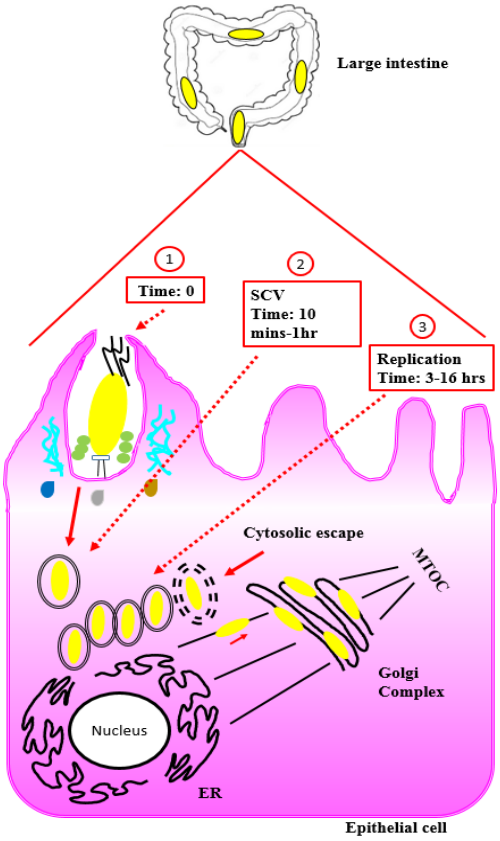

Figure 4. *Salmonella's* infection process and positioning. (1) Infection starts from the moment *Salmonella* attaches itself to the cell and effectors are injected into the host. **(2)** Between 10 mins – 1 hr the bacteria is encased in a membrane called the SCV. **(3)** Replication starts 3-16 hrs after infection. Defects in the vacuole can cause early release of *Salmonella* into the cytosol. *Salmonella* positions itself close the nucleus, ER and Golgi Complex. Positioning in the microtubules at late stages of maturation. Adapted from Schroeder et al (2011).

1.5.2 Bacterial inhibition of Apoptosis

Bacterial pathogens have developed several strategies to inhibit apoptosis during the infection process. By preventing apoptosis, these can thrive and multiply in the cytosol by using the host's resources, until re-activation of apoptosis become convenient for the bacteria (DeLeo et al 2004). It has been documented that bacteria can protect the mitochondria to avoid cytochrome *c* release (Fan et al 1998). Apoptosis can also be inhibited by blocking caspase activation or activating cell survival pathways (Faherty and Maurelli et al 2008). A few examples of these are, *Chlamydia sp*., known for inhibiting and degrading pro-apoptotic proteins (Fischer et al 2004). *Neisseria sp*., prevents cytochrome *c* release (Massari et al 2000), *Shigella flexneri* inhibits caspase-3 activation despite cytochrome *c* release (Clark and Maurelli et al 2007). *Listeria monocytogens* also shows this feature by activating the PI3/Akt and NF –κB pathways (Hashino et al 2015).

Apoptosis is a type of programmed cell death (PCD) leading to chromatin condensation, cytoplasmic shrinkage, DNA fragmentation culminating in cell death without damaging any neighbour cells, so in a way it is self-contained (Qi and Liu et al 2006). Studies carried out by Rajalingam et al. (2001) show how epithelial cells infected by *Chlamydophila pneumoniae* are resistant to staurosporine and TNF-α induced apoptosis. There have also been reports that probiotic bacteria, such as, *Lactobacillus rhamnosus* GG, prevents apoptosis by activating the anti-apoptotic Akt/protein kinase B (Yan and Polk et al 2002). It has also been observed, in the rat's small intestine, that *Salmonella* exploits the host's cell survival pathway in order to inhibit apoptosis by activating the PI3K/Akt pathway, which will prevent cytochrome *c* release and as a result block the activation of the caspase cascade (Huang et al 2005). Another strategy of *Salmonella* in the epithelial cells is to induce apoptosis in murine Bone Marrow-derived Macrophages (BMDM). This is achieved by injecting SipB macrophages where SipB interacts with casp-1, leading to apoptosis (Brennan and Cookson et al 2000, Lai et al 2015).

1.5.3 Innate immune response to *Salmonella*

The innate immune response is the first line of defence against pathogens by recognizing them in a generic, non-long-lasting way (Mogensen et al 2009). In mammals it recruits immune cells to the site of infection and triggers the complement system response, a part of the immune system, to upregulate the ability of phagocytic cells and antibodies (Buchmann et al 2015, Dunkelberger and Song et al 2010). If this fails, the adaptive immune system is activated, where a series of pathogen-specific responses are triggered to provide the host with long-lasting protection (Den Haan et al 2014, Getz et al 2005).

These responses are extremely important to maintain the gastrointestinal tract health. This is a challenge for the host as the guts are the key place to uptake and process nutrients, therefore any disproportionate immune response could lead to an imbalance in the digestive system (Arranz et al 2013, Round and Mazmanian et al 2009). Because of this the gastrointestinal epithelial cells are rich in lymphoid tissue and immune cells (Peterson and Artis et al 2014). The first line of defence is the layer of epithelial cells that secrete mucus with antimicrobial peptides (Liévin-Le Moal and Servin et al 2006). The second layer is the gut-associated lymphoid tissue (GALT) which underlays the epithelial cell. GALT contains up to 70% of the body's immunocytes and is composed of lymphoid follicles, lymphocytes, neutrophils, macrophages and dendritic cells forming the Peyer's patch (PP) (McGhee and Fujihashi et al 2012, Spahn and Kucharzik et al 2004). The PPs are composed of aggregated lymphoid follicles surrounded by the follicle-associated

epithelium (FAE) that contains microfold cells (M cells) (Jung et al 2010, Sipos and Muzes et al 2011). The role of the M cells is to transport luminal antigens and bacteria toward the underlying immune cells that will modulate the immune response (Mabbott et al 2013).

Salmonella has evolved to overcome the antimicrobial peptides barrier by activating the PhoP-PhoQ signal transduction pathway, where *Phop* is the response regulator and *PhoQ* the environmental sensor kinase (Broz et al 2012, Rosenfeld and Shai et al 2006). Work in bacteria has shown this two-component regulatory system controls transcription of virulence-associated genes that will respond to the environmental signals (Miller et al 1991, Tang et al 2013). Studies have also revealed that the immune protein interleukin-22 (IL-22) increases the growth of *Salmonella* by suppressing the growth of its competitors (Perez-Lopez et al 2016). Mice lacking IL-22 showed and overgrowth of commensal *E. coli* that outcompeted *Salmonella* in the gut (Behnsen et al 2014).

Once inside the lumen, *Salmonella enterica* serovar Typhimurium has evolved to overcome the neutrophil release of calprotectin to overcome bacterial growth (Diaz-Ochoa et al 2015). Calprotectin is a protein that eliminates the essential micronutrients needed for enhanced microbial survival (Liu et al 2012). These are just a few of the most studied mechanisms used by *Salmonella* to escape the immune system and start proliferation.

1.6 The Saf fimbriae

The Saf fimbriae has been identified as vital for infection. These are a fibrous organelle found on the surface of *Salmonella* (Bakowski et al 2008; Figure 5). The fimbriae are not unique to *Salmonella* but most of their structure and function are conserved among highly infective gram-negative bacteria, which include *Chlamydia*, *Yersinia*, *Shigella*, *Escherichi*a and *Pseudomonas* (Akopyan et al 2011).

There are two types of fimbriae and these vary depending on the usher/chaperone used for their biogenesis. These chaperones are classified as FGL and FGS (Cai et al 2011), where FGL produce a linear polymer consisting of one or two subunits that act as adhesins. In contrast, FGS produce adhesion pili which are made of a single subunit (Zavialov et al 2007). Salmonella atypical fimbriae (Saf) is an FGL made fimbria mainly composed of several SafA subunits and a minor SafD unit at the tip of SafA (Zavialov et al 2007; Figure 5). Because of its location, SafD is presumed to be important for adhesion to the host and to encode an antigen which helps *Salmonella* recognize proteins in the eukaryotic

membrane for effective infection (Salih et al 2008). Moreover, SafD is conserved in all *S. enterica* subspecies, making its study appealing for the development of vaccines not only to immunize humans, but also for vertebrates.

The fimbriae are surface organelles that play an important role in motility, attachment to epithelial cells or biofilm formation (Strindelius et al 2004). The Saf fimbriae are assembled via the FGL chaperone/usher pathway and are formed of four subunits, of which SafB and SafC are intracellular and SafA and SafD are extracellular. SafB is a chaperone located in the cytoplasm and SafC a pore forming protein located in the membrane of *Salmonella*. SafA forms most of the external fimbriae structure and located at the tip a putative invasion adhesion SafD (Folkesson et al 1999).

Adhesins are cell surface bacterial proteins positioned at the tip of the fimbriae found in all gram-negative bacteria that bind specifically to sugars present in host tissues (Krachler and Orth et al 2013, Thorns et al 1995). The external proteins of the *Salmonella typhimurium* Saf fimbriae are SafA and SafD, with SafD being the adhesin (Rose et al 2008, Zav'yalov et al 2010, Zavialov et al 2007). The flexible body of the fimbriae is made of several SafA subunits. Even when SafD is meant to be an adhesin due to its location at the tip of the fimbria (and due to homolog studies) adhesins (Strindelius et al 2004) there is no current published work available on any SafD interacting partners. In this work it is hypothesised that SafD is not the only key element involved in adhesion. It is plausible that SafD needs SafA for adhesion (therefore SafA binds to the host at least in a transient manner) or perhaps SafA is an adhesin in its own right and the fimbria benefits more from having a number of SafA subunits than SafD.

To date, there is no structure available for SafD. Being at the tip of the fimbriae SafD is involved in the formation of biofilms and attachment to surfaces (Strindelius et al 2004). The first protein-protein interaction between *Salmonella* and the host happens when *Salmonella* anchors itself to the intestinal epithelial cells of the stomach, particularly M cells (Jepson and Clark et al 2001, Tahoun et al 2012). This first potein-protein interaction occurs through the Saf pilus, therefore the study of the assembly of the Saf fimbriae is vital in order to avoid *Salmonella* infection completely. The three dimensional structure of the Saf fimbriae has been made available (Salih et al 2008; Figure 6). It is known that most of the flexible body is made of a polymer of SafA subunits interlinked to each other through an N-terminal (Nte) extension of the incoming subunit (Sauer et al 2004, Vetsch et al 2006). At the very top of the polymer sits SafD, which based on similarities with

E.coli fimbriae proteins, it is distinguished as a major adhesin (Anderson et al 2004, Salih et al 2008).

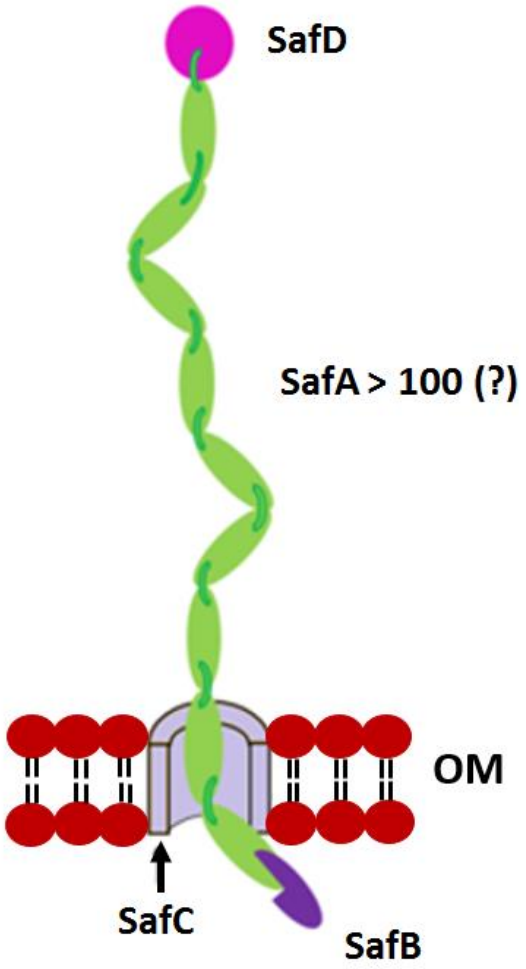

Figure 5. Schematic representation of Salmonella atypical fimbriae (Saf). From top to bottom: Based on structure it is hypothesised SafD sits at the tip of the fimbriae. The main flexible body is formed of SafA subunits linked through the N-terminal (Nte) extension of the incoming subunit. SafC is the fimbria usher and SafB the chaperone whose role is to complete SafA's IgG-like structure during biogenesis. Adapted from Salih et al (2008).

1.7 Structure of SafA monomer

The structure of SafA resembles that of immunoglobin (Ig) which consists of a pair of β-sheets linked by a disulfide bond and hydrophobic interactions (Bodelón et al 2013, Liu and May et al 2012). Nevertheless, SafA lacks the final β-strand which creates a hydrophobic cleft on the surface of the subunit, allowing for chaperone binding by donor strand complementation (DSC) (Zavialov et al 2002), and where each subunit docks to each other by donor strand exchange mechanism (DSE) (Remaut et al 2006).

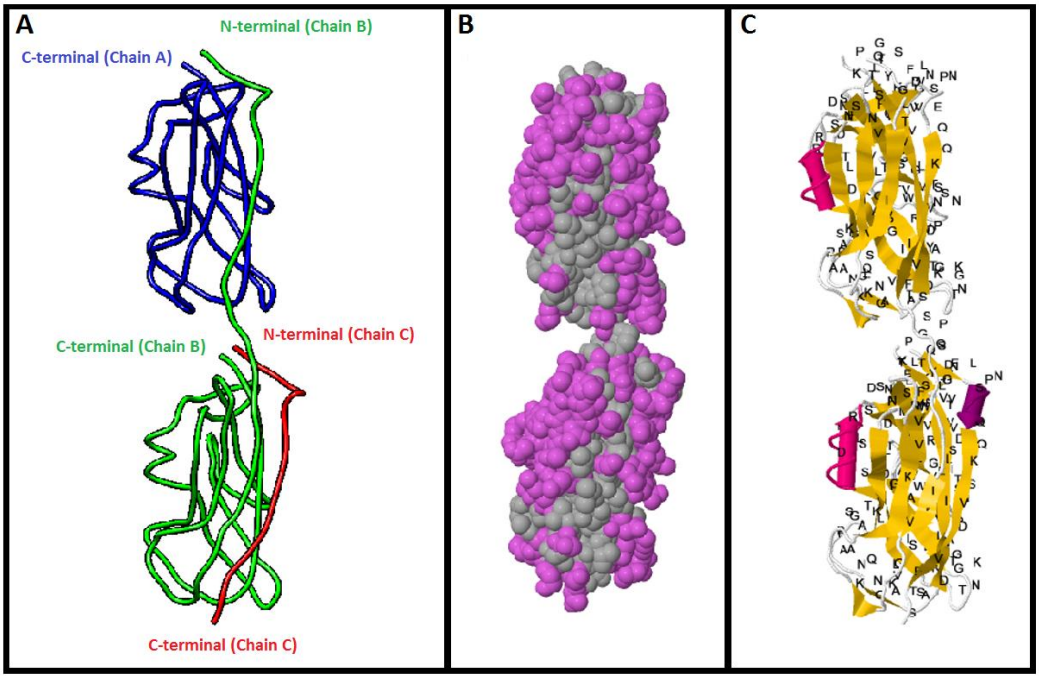

Figure 6. Electron Microscopy Model of the Saf fimbriae. (A) Rounded ribbon cartoon. Each chain is shown in a different colour with the N- and C- terminals for each chain labelled. **(B)** Hydrophobic amino acids are coloured grey and polar amino acids (charged or uncharged) are coloured purple. **(C)** Alpha helices are shown as rockets (6.6%), beta strands are shown as planks (49.7%). Random coils are white (43.7%). Adapted from Salih et al (2008).

The Saf fimbriae is synthesized through a mechanism called the chaperone-usher pathway (Sauer et al 2004). The first protein created is SafD, followed by the first SafA subunit of the polymer. Because of its position, it is hypothesized that SafD is created first and then interlinked to the first SafA subunit (Busch and Waksman et al 2012). The proteins then make their way to the plasma membrane where they are expelled out of the cell into the periplasm via the core complex SecYEG, which forms the protein channel (Pugsley et al 1993, Tziatzios et al 2004).

In the periplasm, chaperone SafB forms a chaperone-protein complex with SafA (Zavialov et al 2003). SafB have Ig-like folds, and binding between SafB and SafA occurs when SafB inserts its G_1 β-strand into SafA's cleft (Choudhury et al 1999, Zav'yalov et al 2010). Once the subunit is in the outer membrane the chaperone's G_1 β-strand is replaced by the β-strand from the Nte extension of the incoming subunit via the DSE, all this while the chaperone-protein complex still exists.

As postulated by the 'zip-in-zip-out' mechanism, the SafB chaperone will slowly be displaced as the Nte extension takes over (Rose et al 2008, Zavialov et al 2003). While this unzipping displacement is taking place, the chaperone-protein complex is making its

way to the outer membrane where pore making chaperone SafC is waiting to export the fimbria out of the membrane.

Therefore, for polymerization to occur DSE requires the formation of a tertiary complex formed of a subunit, the G_1 β -strand of the SafB chaperone and the Nte extension of the incoming subunit (Zavialov et al 2003). This process is totally dependent on the subunits hydrophobic groove. The product of the DSE is an Nte complex of interlinked subunits that now form a polymer. This complex varies from the chaperone-protein complex in that the new subunit's Ig domain is more compact and stable due to the addition of an extra hydrophobic pocket, P*, which prevents disassociation of the subunits (Remaut et al 2006, Zavialov et al 2003).

The 'zip-in-zip-out' mechanism states that all the processes of strand swap between chaperone and Nte extension are needed for proper subunit folding (Choudhury et al 1999, Rose et al 2008, Sauer et al 2002, Zavialov et al 2003). This concept contradicts Anfinsen's dogma which states the structure of a protein is determined solely by the protein's own amino acid sequence (Normark et al 2000). The Saf fimbriae clearly shows the structure and function of each subunit is dependent of chaperone's G_1 β -strand to obtain the C-terminal of their missing seventh strand (G) and of the N-terminal extension of the incoming subunit to maintain its acquired Ig-fold. Therefore, the Saf fimbriae is dependent on the other protein's sequence to complete its structure.

1.8 Protein selection: Fimbriae proteins SafA and SafD

Most of the current research targeting the fimbriae is aimed at developing vaccines (Remaut et al 2006). The study of SafA and SafD subunits would contribute to the understanding of *Salmonella*-host protein-protein interaction through the Saf fimbriae and take us a step closer to understand one of the mechanisms that contribute to *Salmonella* colonization of the host.

Whilst analysing the process of infection, two questions arise. If SafD is at the tip of the fimbriae, being considered a generic adhesin, and SafA's protein sequence is less conserved (and variable) (see Supplementary data for BLASTp results, Figures S63 and S64), it could indicate that SafA is the important factor in *Salmonella* to determine its host specificity. Therefore, in order for SafA to make this assessment it must make contact/attach itself to the host too (Figure 7).

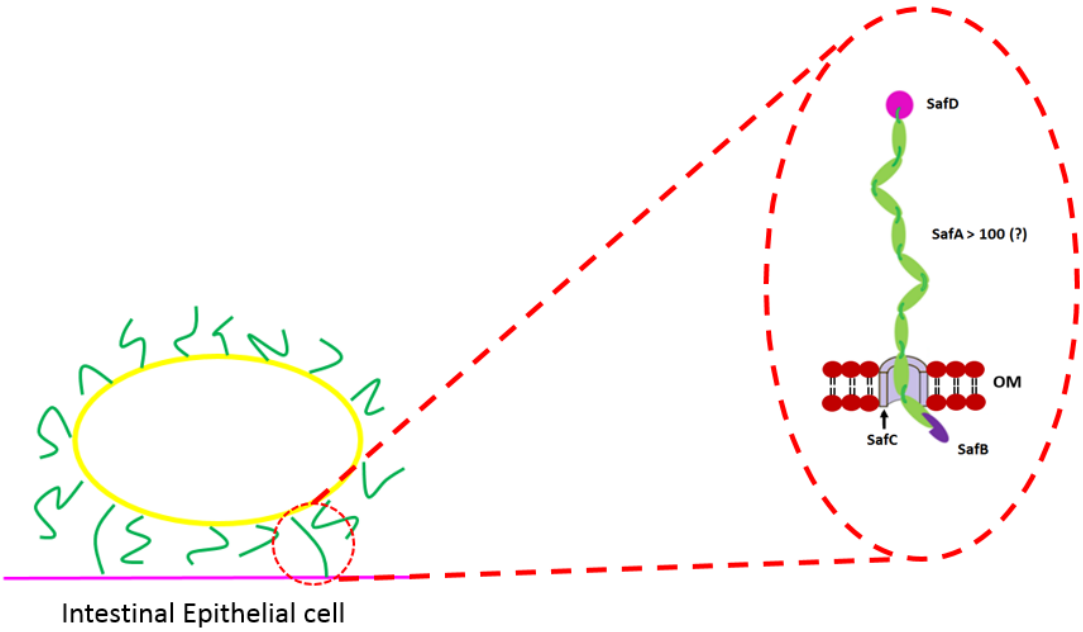

Figure 7. Schematic representation showing possible bacterial adhesion to a host cell by the Saf fimbriae. The bacteria attach to the host by bacteria-host protein interactions mediated by Saf fimbriae proteins SafA and SafD.

1.9 Aims and Objectives

The first protein-protein interaction between *Salmonella* and the host occurs during the attachment or just prior to it between SafA/SafD and host receptors localized at the host membrane. SafA forms most of the flexible body of the Saf pilus and has a sequence which is less conserved (and variable) within *Salmonella* strains (Folkesson et al 1999, Lauri et al 2011), whereas SafD is conserved (Protein BLASTp results for SafA and SafD available in Supplementary data, Figures S63 and S64). These observations indicate SafA is probably involved in recognising host specificity and SafD is a general adhesin.

Identifying protein binding partners for the Salmonella atypical fimbriae (Saf) and understanding the role of the fimbria in the *Salmonella* infection is imperative to develop alternative strategies for the treatment of *Salmonella Typhimurium* LT2, and potentially other *Salmonella enterica* strains.

The main aim of this work is to identify interacting partners for *Salmonella* fimbriae protein SafA in the mammalian digestion system and to propose a function for SafA based on its interacting partner(s) during mammalian infection.

The first objective is to rationally design SafA' (GST-SafA-6xHis) by isolating it from the polymer to obtain a stable recombinant protein capable of studying *Salmonella*-

mammalian host protein interactions. In addition, the construct will have to include tag (s) that will provide the means to immobilize the protein in different surfaces. Further to this, if required, the tag will be cleaved from the protein for assurance that any identified proteins binding to SafA' (GST-SafA-6xHis) are specific to the subunit and not to the tag. Therefore, recombinant SafA' (GST-SafA-6xHis) and its variants (SafA-6xHis, GST+SafA-6xHis and GST) will be subjected to circular dichroism (CD) studies to confirm that its secondary structure resembles that of the native crystal structure and to review whether the tag (s) influence the folding of the SafA' (GST-SafA-6xHis) subunit.

The second objective is to establish a robust affinity-enrichment system capable of providing support to capture specific host proteins binding to GST-SafA-6xHis and SafA-6xHis. It will be key to the success of this work to set up a system capable of immobilizing SafA' (GST-SafA-6xHis and/or SafA-6xHis) regardless of its tag.

The third objective is to identify unequivocally any SafA' (SafA-6xHis) interacting partners by LC-MS/MS. The fourth objective is to propose a biological role for SafA based on its interaction with the identified protein(s). Data for each identified protein will be retrieved through on-line tools and literature searches. Particular emphasis will be given to known bacterial interactions with these proteins during the host infection process.

1.10 Key results of the thesis

1) GST tag was successfully cleaved from the recombinant protein SafA' (GST-SafA-6xHis). Upon circular dichroism (CD) spectroscopy analysis, the secondary structure of cleaved SafA' (SafA-6xHis) resulted identical to the published crystal structure. Deconvolution of the data confirmed the subunit consists of 5% α-helices and 49% β-sheet which is a very close fit to the crystal structure of 4% α-helices and 49% β-sheet.

2) We present an alternative method to study protein-protein interactions by adapting Universal-BIND™ plates. A total of five systems using several technologies were trialled, with the Universal-BIND™ plates being the one that provided the most suitable platform for work with the mammalian intestine. Of all the systems, this one provided a format allowing for technical replicates, compatible with fluorescent detection (if required) and a non-porous surface that minimise the number of non-specific proteins present in the data analysis.

3) Putative functions, other than adhesion, are suggested for the Salmonella Atypical fimbriae (Saf). Based on the identification of proteins by LC-MS/MS and the comparison of these with other well-studied bacteria it can be suggested that SafA is involved in the intracellular survival of cytosolic *Salmonella*.

4) This work puts forward the importance of the little studied cytosolic *Salmonella*. The current work on *Salmonella* infection is carried out mainly by studying the *Salmonella*-containing vacuole (SCV), neglecting the importance of cytosolic *Salmonella*. Despite this, *Salmonella* replicates faster in the epithelial cytosol compared to the SCV and, at times, its hyper-replication can make up to half of the population free within the cytosol (Knodler et al 2014).

1.11 Methods used in this study to analyse protein-protein interactions (PPI)

Protein interactions can be stable or transient, and these can be classified widely as either strong or weak (La et al 2013). Because of the complexity of the task, a combination of techniques is necessary to identify and validate any protein interaction. Co-immunoprecipitation (Co-IP) is the prefered technique to study protein-protein interactions in vivo using antibodies against the proteins of interest. The principle behind this is the capture of the target protein through an antibody coupled to a matrix support like Sepharose beads through protein A or G (Kaboord and Perr et al 2008). Virtually, the captured protein is bound to the target antigen, which is bound by the antibody on the support. Immunoprecipitated proteins and their binding partners are then detected by sodium dodecyl sulphate-polyacrylamide gel electrophoresis (SDS-PAGE) and Western blot analysis (Hall et al 2005, Kaboord and Perr et al 2008).

Pull-down assays are a similar approach to Co-IP but the difference is that, instead of antibodies, a bait protein is immobilized on the beads to capture a binding protein (prey). This method is particularly useful in the study of novel protein interactions where the protein target is unknown as upon prey identification antibodies can be ordered and the findings confirmed by Western Blot (Brymora et al 2004, Nguyen and Goodrich et al 2006).

A way of studying transient protein interactions is using crosslinking. Transient interacting proteins are covalently crosslinked in an attempt to link the components of an interaction (Ozbabacan et al 2011). Detection methods for PPI include western and far

western blot analyses (Hunke and Müller et al 2012, MacPhee et al 2010). As these are fairly standard techniques they will only be referenced here.

1.12 Alternative Affinity tags that could have been used to immobilize SafA' (GST-SafA-6xHis)

Protein tags are peptide sequences that are attached to either N-terminus or C-terminus of proteins in order to facilitate purification and detection. Currently, there are a wide variety of protein tags and these can be classified into fluorescent tags, affinity tags and epitope tags (Zhao et al 2013). Affinity tags are used to facilitate the purification of proteins from crude cell lysates. The choice of the tag is usually dependent on the affinity resin used for purification. Among these we have, glutathione-S transferase (GST) which is used by inserting the GST DNA coding sequence next to the protein of interest. GST's strong affinity for GSH is used to capture the protein in GSH coated beads and in some cases it can also enhance the protein's solubilisation (Harper and Speicher et al 2011). The trouble with the GST tag is its ~26 kDa size and possibility of dimerization. Also, it is not suitable for protein studies as it might alter the native protein conformation.

The poly-histidine tag (His-tag) is constituted of 6-8 histidine residues. Histidine has a high affinity for metal ions, such as nickel, copper and zinc ions. Their small molecular weight, 840.40 Da, is an advantage and purification can be done under native or denaturing conditions (Bornhorst and Falke et al 2000). An alternative to His tag is Calmodulin Binding Protein (CBP), a 26 long peptide derived from the C-terminus of skeletal muscle myosin light chain kinase that binds specifically to calmodulin. With a small size of 4 kDa it allows the purification of proteins to take place in the presence of strong reducing agents. The tight binding to calmodulin allows for stringent washing conditions and is specifically advantageous for the purification of proteins in *E. coli* because of the absence of endogenous proteins that can interact with calmodulin (Gerace and Moazed et al 2015).

Maltose-binding protein (MBP) binds to amylase agarose and can increase the solubility of recombinant proteins expressed in *E. coli*. The downside of this tag is its large size of 43 kDa and in some cases it has been reported that upon cleavage of the tag the protein aggregates and becomes partially insoluble (Duong-Ly and Gabelli et al 2015).

On the other hand, we have epitope tags, which are small tags that recognize antibodies. Because of this these tags are usually used when the investigator wants to visualize a molecule such as in a gel or western blot. As a result of their small size, they have little

or no effect on the structure of the final fusion protein. In addition, these tags can be used when no antibody is known for the protein of interest as they are recognized by numerous commercial antibodies (Kimple et al 2013, Wood et al 2014).

One of the most popular epitope tags is the Myc tag, a synthetic peptide with a molecular weight of 1, 203 Da with a sequence of EQKLISEEDL corresponding to the C-terminal amino acids of human c-myc protein (Terpe et al 2003). Influenza Hemagglutinin (HA) is a synthetic peptide with an amino acid sequence of YPYDVPDYA. There is no evidence that shows HA interferes with the bioactivity of the recombinant protein and is recognizable by several commercial antibodies (Zhao et al 2013). Finally, FLAG tag is another short peptide tag, DYKDDDDK, which can be added to a protein using recombinant DNA technology. FLAG-tag is commonly used in assays where antibody recognition is required. Sometimes in the study of protein-protein interactions there are no known antibodies for a given protein and any antibody recognizing the FLAG sequence can be used. In addition to this, the FLAG-tag is more hydrophilic than other tags so they do not denature or modify the function of the proteins to which they are attached (Gerace and Moazed et al 2015).

A fluorescent tag is a molecule that is chemically attached to a protein in order to label it. A unique characteristic of all fluorescent proteins (FPs) is their ability to self-generate a visible wavelength chromophore from a sequence of three amino acids within their own sequence. They are non-toxic, and can therefore be used in fixed and in in-vivo studies. The most widely used protein is Green fluorescent protein (GFP) (Nagarkar-Jaiswal et al 2015).

The above is not an exhaustive list of the tags available to study PPI but some of them may be used in future studies to verify whether the addition of tags interfere with SafA specific interacting partners.

1.13 Affinity-enrichment Systems

The identification of new protein-protein interactions is a complex process. Currently, there are a variety of methods available which vary mainly in their level of sensitivity and specificity. One of the standard routes to study PPI is to capture a specific protein through co-immunoprecipitation (Co-IP); the eluate is separated in a SDS-PAGE gel and stained (Markham et al 2007). For this research we used a series of approaches for protein immobilization, detection and identification (see Chapter V and Table 1). The choice of surface used for the immobilization of the proteins was dependent on the tags present in

the recombinant protein and on the observations made whilst optimizing each system (Chapter III, section 3.4). We made use of Immobilized Metal Affinity Chromatography (IMAC) technology to immobilize proteins by their histidine tag (Chapter V, sections 5.3 and 5.4). Dynabeads® His-Tag Isolation & Pulldown (System 1, Chapter V, section 5.3) offered a non-porous surface to immobilize proteins through their histidine tag. Also, within IMAC technology, Nickel Affinity Gel (System 2, Chapter V, section 5.4) offered a porous surface with a high binding capacity for protein immobilization through their histidine tag. GSH-agarose (System 3, Chapter V, section 5.5) was used as a porous surface to immobilize proteins through their GST tag. Less conventional approaches, such as, nitrocellulose (System 4, Chapter V, section 5.6) were used to immobilize proteins through hydrophobic interactions. Another non-conventional approach was the adaptation of Universal-BIND™ plates (System 5, Chapter V, section 5.7) crosslink proteins via abstractable hydrogen bonding.

Multiple stability tests were performed prior to the affinity-enrichments using Horseradish peroxidase (HRP), which reacts with primary amines to form covalent amide bonds and provides with permanent conjugation (Veitch et al 2004). The selection of HRP for the preliminary tests was based on their high enzyme activity and long shelf-life as protein is stable for at least 12 months at -20^{o}C.

Instrument sensitivity is key for protein identification and any specific isolated proteins were identified by MALDI-TOF MS (Chapter VI, sections 6.3-6.6) and LC-MS/MS (Chapter VI, section 6.7-6.12). Mass spectrometry is a sensitive technique that measures mass-to-charge ratio (*m/z*) used to detect and identify molecules (Hale et al 2013). Most of the systematic analyses of proteomics have mass spectrometry as their central strategy. The development of electrospray ionization (ESI) and matrix assisted laser desorption/ionization (MALDI) allowed the progress of complex multi-stage instruments, such as, the quadrupole time-of-flight (Q-Q-ToF) and tandem time-of-flight (ToF-ToF) (Nagao et al 2010).

1.14 Relevant Immobilization Methods

1.14.1 IMAC technology: Dynabeads His-Tag Isolation & Pulldown and HIS-Select Nickel Affinity Gel

IMAC is one of the methods available to immobilize proteins due to the ability of the metal ions to reversibly interact with the different side chains and amino acids of the protein of interest (Cheung et al 2012).

The most relevant application of IMAC technology is for the purification of histidine-tagged recombinant proteins as it was originally designed as a separation method (Block et al 2009, Porath et al 1975). Divalent ions, such as, Cu^{2+}, Ni^{2+} Zn^{2+} and Co^{2+} are the preferred choice for His-tagged proteins purification, whereas, Fe^{3+}, Al^{3+} ,Ga^{+3} and Titanium are used for phosphopeptides and phosphoproteins capture (Fíla and Honys et al 2012). IMAC technology has developed greatly and nowadays is used for purification and immobilization of antibodies, His-tagged proteins and phosphorylated proteins. It is also used in proteomics for the study of protein-protein interactions and chip applications, such as, surface plasmon resonance (SPR) (Block et al 2009).

Dynabeads His-Tag Isolation & Pulldown (System 1, Chapter V, section 5.3) are magnetic bead surfaces designed for His-tagged protein isolation, which chemistry relies on the fixation of Cu^{+2} onto the beads with a tetradentate chelating ligand, in this way taking advantage of the known affinity of Cu^{2+} to histidine (Gaberc-Porekar and Menart et al 2001). It has a high selectivity for poly-histidine tags and this results in low background levels.

HIS-Select Nickel Affinity Gel (System 2, Chapter V, section 5.4) uses IMAC technology to immobilize His-tagged proteins but uses nickel as the metal ion. Its matrix is a 6% beaded agarose nickel, making it highly selective for recombinant proteins with a His-tag (Prasanna and Vijayalakshmi et al 2010). The technology and principle of immobilization resembles the one of Dyabeads, the matrix, except that the later one offers a higher binding capacity.

1.14.2 Beaded agarose and Transfer membrane: Glutathione (GSH)-Agarose and Nitrocellulose (NC)

Glutathione-Agarose (System 3, Chapter V, section 5.5) is an epoxy activated 4% cross-linked beaded agarose with glutathione attached to it through the sulfur (Yu et al 1989). The method relies on the immobilization of a GST fusion protein on glutathione sepharose agarose (Harper and Speicher et al 2011). Compared to IMAC technology (Systems 1 and 2, Chapter V, sections 5.3 and 5.4) no magnetic stand or special equipment is required, it has a high binding capacity and a lower background due to its porous nature. Its porous surface does increase washing steps as proteins can be trapped in the agarose, but with the proper washing procedures in place this is easily avoided.

Nitrocellulose (NC) (System 4, Chapter V, section 5.6) is a membrane highly used to immobilize proteins because of its non-specific affinity to amino acids (Larsen et al 2014).

NC is produced by treating cellulose with nitric acid and nitrocellulose membranes are made by dissolving the nitrocellulose in organic solvent and spreading the solution as a thin film on a smooth surface (Roman et al 2009). Because of this NC provides a good surface for immobilization due to its uniform high surface area. It has a high binding capacity and NC is also compatible with a wide range of methods, such as, fluorescent and colorimetric. NC is used as a solid-phase immobilization support for proteins, DNA and RNA (Bresser et al 1983, Yeretssian et al 2005). DNA microarrays exploit the use of NC and its ability to immobilize DNA in high quantities in a non-covalent irreversible manner to the membrane (Cretich et al 2010, Wang et al 2003). Successful binding of biomolecules to the NC slides coated by copoly (DMA-NAS-MAPS) has been tested by spotting an amino-modified oligonucleotide fluorescently labelled with Cy3 (Cretich et al 2010). In NC, proteins are immobilized through electrostatic and hydrophobic interactions (Kim and Herr et al 2013), offering an alternative to the conventional materials available for protein immobilization and affinity-enrichments. NC has also been used in the preparation of protein arrays (Snapyan et al 2003) and oligosaccharides microarrays (Fukui et al 2002, Hirabayashi et al 2003).

1.14.3 Universal-BIND™ plates (Sigma, CLS2504)

Universal-BIND™ plates (System 5**)** are 96 wells microplates made of polystyrene (Chapter II, section 2.13) (Gibbs and Kennebunk et al 2001). The surface covalently immobilizes biomolecules through covalent non-specific abstractable hydrogens (the hydrogen attached to aliphatic carbons) by UV illumination, resulting in a carbon-carbon bond (Lee et al 2016). Immobilization is not site oriented but the surface is useful for the immobilization of antigens of unknown structure, cell lysates and double stranded DNA (Vigueras-Santiago et al 2006). The use of this system to perform affinity-enrichments of mammalian proteins is not standard but was selected because protein could be immobilized regardless of orientation and the immobilization is not dependent on any tag, therefore making the system highly versatile.

Table 1. Comparison of systems established for this study.

System	Product	Main technical advantages	Main technical disadvantages
1	Dynabeads His-Tag Isolation & Pulldown (Invitrogen, 10103D)	- IMAC technology - Non-porous surface - Isolates Histidine tagged proteins - Easy to handle - Solid, uniform surface	- Low binding capacity - Non-specific binding due to amino acid residues
2	HIS-Select Nickel Affinity Gel (Sigma, P6611)	- IMAC technology - High binding capacity - Reduced background - Isolates Histidine tagged proteins - Easy to handle	- Porous surface - Longer washes required
3	Glutathione (GSH)-agarose (Sigma, G4510)	- High binding capacity - Reduced background - Isolated proteins containing GST	- Porous surface -Non-specific binding of proteins containing glutathione binding sequences - Longer washes required - Possible material loss during washes if column not used
4	Nitrocellulose (NC) Schleicer & Schuell, 401 191	- High binding capacity - Easy to handle - Compatible with fluorescent detection methods - Flat surface making it compatible with a wide range of scanners	- Porous surface - Non-specific binding of proteins through hydrophobic and electrostatic interactions - Long washes required

		- Immobilises proteins through hydrophobic and electrostatic interactions	
5	Universal-BIND™ plates Sigma, CLS2504	- 96-well format for replicas reproducibility - Easy to handle - Compatible with fluorescent detection - Non-porous surface - Covalent binding avoiding protein leak - Efficient blocking solutions available	- Limited binding capacity

In this work we systematically set up five systems (Chapter V). Briefly, IMAC technology (Systems 1 and 2, Chapter V, sections 5.3 and 5.4) was tested to immobilize the recombinant protein SafA' (GST-SafA-6xHis) through its histidine tag. GSH-agarose (System 3, Chapter V, section 5.5) was used to immobilize SafA' (GST-SafA-6xHis) through its GST tag. Least conventional methods were also tested: NC (System 4, Chapter V, section 5.6) and Universal-BIND™ plates (System 5, Chapter V, section 5.7) were used to immobilize SafA' (GST-SafA-6xHis). NC, SafA' (GST-SafA-6xHis) was immobilised by exploiting the likely hydrophobic interactions between the protein and membrane. In the case of the Universal-BIND™ plates, SafA' (GST-SafA-6xHis) was immobilised by utilizing its physico-chemical properties and by covalently cross-linking to the selected surfaces.

After trialling all the systems it was decided to use Universal-BIND™ plates (System 5, Chapter V, section 5.7) to immobilize the recombinant protein SafA' (GST-SafA-6xHis) and its variants: GST+SafA-6xHis (which corresponds to free GST present in a SafA-6xHis sample) and SafA-6xHis (which corresponds to SafA' in the absence of GST) to isolate mammalian interacting proteins. Together with BSA and GST as negative controls. The list of samples (positive and negative controls) used and protocols are in the materials and methods, Chapter II, section 2.13 and Chapter III, Figure 28. On balance, the

Universal-BIND™ plates (System, 5, Chapter V, section 5.7) reduced background protein even if it meant compromising on binding capacity and reduced yield.

1.15 Application of affinity purification techniques coupled with mass spectrometry methods

Mass spectrometry is a powerful tool for the identification of proteins (Baldwin et al 2004, Macht et al 2004, Pompach et al 2004). There are several ionization methods and the choice of the source will depend on the type of sample under investigation. Electrospray Ionization (ESI) and Matrix Assisted Laser Desorption Ionization (MALDI) are the most widely used because they are soft ionization techniques that allow ionization and measurement of whole molecules of large molecular weight, such as complete proteins. ESI works best ionizing polar molecules yielding a large mass range, whereas MALDI offers a very fast analysis and works best preferably with large molecules (Baldwin et al 2004, Cañas et al 2006).

The study of protein-protein interactions affinity purification coupled with mass spectrometry (AP-MS) is highly used (Dunham et al 2012, Gingras et al 2007, Morris et al 2014). This approach is popular in the study of host-pathogen's interactions (Greco et al 2014, Morris et al 2014). For instance, in the study of bacteria cell surface – host interactions, whole *Streptococcus gallolyticus* were incubated with epithelial cell lysates (HT-29) to allow for binding. Subsequently, any surface-exposed protein(s) were released from the bacterial surface and trypsinised to perform protein identification by LC-MS/MS. Finally, western blots were used to confirm any identified proteins. Their findings suggested protein CK8 binds to enolase, playing a key role in adhesion to the host (Boleij et al 2011).

Mass spectrometry has also been used for the identification of low-abundance bacterial adhesins. BabA adhesion protein in Helicobacter pylori was incubated with albumin-based photoprobe to BabA (a Lewis^b – binding adhesion) to which the Lewis^b saccharide and a biotinylated crosslinker structure had been coupled. The adhesin was tagged and extracted by sodium dodecyl sulphate (SDS) solubilisation of entire cells. In situ trypsinization was carried out and protein identification achieved by MALDI-TOF-MS (Larsson et al 2000).

1.16. Circular Dichroism (CD)

CD is a spectroscopic method that measures the difference in absorption between right and left circular polarized light and it can be measured only when a molecule contains

one or more chiral chromophores (Greenfield et al 2006, Kelly and Price et al 2000, Kelly et al 2005, Wallace et al 2003). CD spectroscopy is mainly used in the study of chiral molecules and it is particularly used in structural studies by analysing the secondary structure of proteins (Greenfield et al 2006, Hall et al 2014). Briefly, linearly polarized light is split into alternating left and right polarized light in a Photo Elastic Modulator (PEM) (Bürck et al 2015, Goldbeck et al 1997). When the two components pass through a solution containing a chiral chromophore these are absorbed unequally and the instrument quantifies the difference between the absorption of left and right handed circularly-polarized light (Kelly et al 2005, Louis-Jeune et al 2012).

CD is used widely to gather information on secondary structure content, although information on a protein's tertiary structure, for example when investigating the integrity of protein conformation following site directed mutagenesis can also be obtained (Picotti et al 2004). The technique is highly suitable to investigate a protein's stability, to assess the effect of environmental conditions on a protein and sometimes to detect conformational changes following protein-protein interactions following ligand binding (Greenfield et al 1999, Reed et al 2014, Siligardi et al 2014).

The far-UV spectral region of 180-240 nm is the spectral region used to determine protein secondary structure (Schmid et al 2001, Wallace and Janes et al 2001). These wavelengths cover the spectral region of the peptide bond. Each type of protein secondary structure such as alpha helix, beta sheet and random coil structures give rise to a unique spectrum. Thus it is possible to calculate the estimated fraction of each secondary structure element by analysing the protein's far-UV CD spectrum as a sum of the multiple fractions (Kelly et al 2005, Miles and Wallace et al 2016).

On the other hand, the near-UV spectral region of 250-350 nm can be used to determine information regarding a protein's tertiary structure (Kelly et al 2005, Lamazares et al 2015). This region relies on the aromatic acids as the chromophores. For example, tryptophan signals are detected between 280-290 nm, phenylalanine at 260 nm and tyrosine between 275-280 nm (Lamazares et al 2015, Nagatomo et al 2013).

CD spectroscopy offers several favourable properties, for instance, a small amount of material is needed, and provides rapid results with an established procedure for quantification (Greenfield et al 2006). Because the information that can be obtained is abundant, it is used in a wide range of applications. Secondary structure information can be gathered from the study of intact proteins, domains, constructs and natively unfolded

proteins (Martin and Bayley et al 2002). Conformational changes can be detected providing information in ligand and drug binding studies, macromolecular interactions and conformational states (Wallace et al 2003).

CD finds particularly frequent application in the study of the folding and unfolding of proteins and allows acquiring kinetic and folding pathway information. Other areas of application include the study of environmental effects on the protein, its thermal stability and identification of conditions suitable for crystallization (Kenney et al 2000); where it has been used to identify fidelity of folding, protein stabilization, domain structures, environmental effects and ligand binding (Page et al 2005). In the case of binding studies high throughput screening has been made possible and binding is often associated with a specific structural change that can be detected by CD (Hawe et al 2008). In some cases it is also possible to identify where in the sequence the change occurs and identify how large the structural change is (Ioannou et al 2015). The main disadvantages of CD are that the sample needs to be as pure as possible, not aggregated and the information that can be obtained is not at the atomic level (Lanucara et al 2014).

CHAPTER II – MATERIALS & METHODS

2.1 Chemicals

- Acetone (Sigma, #34850)
- Acrylamide/bis-Acrylamide/30% Solution (Sigma, #A3574)
- Ammonium persulphate 89+%, A.C.S. reagent (Sigma, #248614)
- 14.3 M (β-ME) β-mercaptoethanol (Sigma, #79F-0776)
- Bradford Reagent (Sigma, #B6916)
- Ethylenediaminetetraacetic acid solution, pH 8(Fluka, #03690)
- (TFA) Ttrifluoroacetic acid (WWR International Ltd., #151311 2E)
- Glycerol (Sigma, #G7757)
- Glycine (Sigma, #G7126)
- MALDI-Quality matrix solutions alpha-chc matrix solution (alpha-cyano-4-hydroxycinnamic acid) (Agilent Technologies, #G203AA)
- Methanol (WWR International Ltd., #20847.07)
- Micro Bio-Spin 6 Columns in SCC (BioRad#732-6200)
- Nitrocellulose 0.45µm, 200x200 mm, REF NO 401 191, LOT NO 2010/32020, Schleicer & Schuell.
- N,N,N',N'-Tetramethylethyl-enediamine (Sigma, #T-7024)
- (OG) *n*-octyl-β-D-glucoside (Sigma, #O8001)
- (PBS) Phosphate buffer saline (Composition: 0.01 M phosphate buffer, 0.0027 M potassium chloride and 0.137 M sodium chloride, pH 7.4) (Sigma, #P4417)
- Universal-BIND™ plates (Cornish#MFG0048340)
- Protease inhibitor (cOmplete, EDTA free-free) (Roche, #11873580001
- Protease inibitor Cocktail tablets, EDTA-free (Components: AEBSF, Bestatin, E-64, Pepstatin A, Phosphoramidon and Leupeptin, Aprotinin) (Sigma, #S8830)
- Sodium Carbonate (Fisons Scientific equipment, #S-2920)
- (SDS) Sodium Dodecyl Sulfate (ICN biomedicals Inc, #811034)
- Soft 96 well plastic plate [Titerek PVC 96 well microplate, Flow laboratories #77-173-05).
- Tris-Glycine-SDS buffer 10xConcentrate (Sigma, #T7777)
- Tris (hydroxymehyl) aminomethane (Sigma, #25285-9)
- (TMB) 3, 3', 5, 5'-Tetramethyl-benzine Liquid Substrate, Supersensitive, for ELISA (Sigma, #T4444)
- ZipTip$_{U\text{-}C18}$ (Millipore, #ZTC18M960)

2.2 Kits

- HiPPR^{TM} Detergent Removal Resin Column Kit, 54/pk (Thermo Scientific #88305)
- Trypsin Singles, Proteomics Grade (Sigma, #T7575)
- Quibit Q33211 (Thermo Scientific #Q33211)

2.3 Proteins & Antibodies

- (BSA) Bovine Serum Albumin (Sigma, #A2153)
- HRP/α-rabbit IgG (Sigma, #A9169)
- 3.4 mg/mL α-rabbit IgG (Sigma #0545).
- 10 mg/mL rabbit IgG (Sigma #I0825)
- SafA' (GST-SafA-6xHis) (AcroBiosystems)

2.4 Resins & Beads

- Dynabeads His-Tag Isolation & Pulldown (Invitrogen, 10103D)
- HIS-Select Nickel Affinity Gel (Sigma, P6611)
- Micro particles, magnetic, amino functionalized (Sigma, 53572)
- Glutathione (GSH)-agarose (G4510)
- Nitrocellulose (NC) (Schleicer & Schuell, 401 191)
- Universal-BIND™ plates (Sigma, CLS2504)

2.5 Binding and washing buffers

- B4 (4xPBS/0.02% OG): 100 µL of 10% OG was added to 50 mL of freshly prepared 4xPBS.
- B1 (1xPBS/0.02% OG): 40 µL of 10% OG was added to 20 mL of freshly prepared 1xPBS.
- 2xProtease inhibitor/2% OG: was prepared by adding 1 tablet of 1xProtease inhibitor to 4 mL of freshly prepared 1xPBS with 1 mL of 10% OG.

2.6 Elution buffers

- Dynabeads and HIS-Select Nickel Affinity Gel: A stock of 100 mM EDTA was prepared by adding 200 µL 0.5 M EDTA into 1000 µL diH_2O. Prior to use, 1 µL of 14.3 M β-ME was added to 15 µL of 100 mM EDTA.
- GSH-agarose: 4xloading buffer/β-mercaptoethanol was prepared by adding 17.5 µL of β-ME to 5 mL of 3x loading buffer [250 µL of 1 M Tris-HCl, pH 8.6, 3 mL of 30% Glycerol, 100 µL of 10% SDS, 6.65 mL diH_2O].

- Nitrocellulose (NC): 0.25x loading buffer/β-mercaptoethanol was prepared by diluting 4xloading buffer/β-ME 16 times in diH_2O.
- Magnetic micro particles, amino functionalized: A stock of 100 mM Glycine, pH2.5 was prepared by diluting 1M Glycine [3.75g of Glycine, 50 mL diH_2O] 10 times in diH_2O.
- Universal-BIND™ plates: A stock of 0.1% SDS/10 mM DTT was prepared by adding 10 μL of 10% SDS, 100 μL of 100 mM DTT and 890 μL diH_2O.

2.7 Protein extraction buffers

- Buffer P: 0.2M Sodium phosphate, pH 7.5/1x Protein inhibitor cocktail.
- Buffer PX: 0.2M Sodium phosphate, pH 7.5, 1xProtease inhibitor cocktail, 1% Triton X-100.
- 2xProtease inhibitor/2% OG: 1 tablet of 1xProtease inhibitor was added to 4 mL of freshly prepared 1xPBS with 1 mL of 10% OG.

2.8 Protein extractions

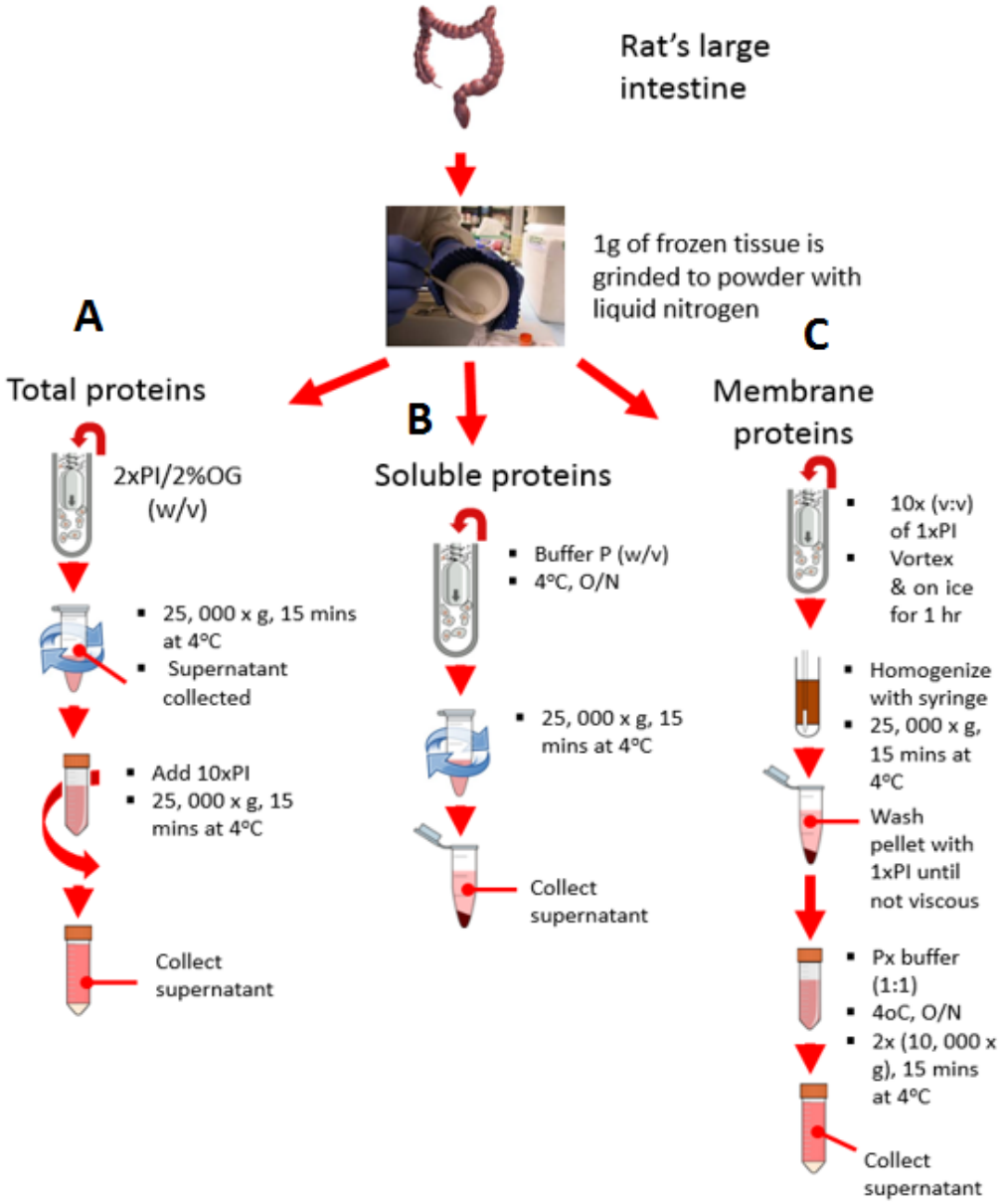

Figure 8. Workflow of the different protein extraction methods used Tissue was harvested and immediately frozen in liquid nitrogen. The amount required was grinded and treated as needed to extract different types of proteins. **(A)** Total proteins: tissue was homogenized with buffer containing protease inhibitors (PI) and Octyl glucoside (OG) (w/v). Slurry was transferred into an appropriate tube and spun down. Supernatant was collected and diluted 10x in 1xPI to later be centrifuged and collected. **(B)** Soluble proteins: tissue was homogenized with buffer P (w/v), followed by centrifugation where the supernatant containing the soluble proteins were collected. **(C)** Membrane proteins: tissue was homogenized with 1xPI (v:v), quickly vortexed followed by 1 hr incubation on ice. Further homogenization was achieved by using a syringe. Slurry was spun down and pellet washed a few times with 1xPI until it was not viscous. Buffer Px (1:1) was added and sample incubated overnight at 4°C. On the following day, slurry was centrifuged at least twice and supernatant collected.

2.9 Setting up of Dynabeads as an affinity-enrichment system

2.9.1 Binding capacity determination of Dynabeads His-Tag Isolation & Pulldown

Dynabeads are uniform, superparamagnetic beads of 1 μm diameter coupled with cobalt-based Immobilized Metal Affinity Chromatography (IMAC) chemistry. Dynabeads were supplied in 20% EtOH. The expected capacity is 40 μg of a 28 kDa histidine-tagged protein per 1mg beads. The gel was provided in 50% suspension in 30% ethanol. The expected binding capacity is of ≥15 mg of a 30 kDa histidine-tagged protein per 1 mL of gel.

The trial was performed to establish the amount of SafA' (GST-SafA-6xHis) protein needed to saturate the beads. Due to easier visualization during magnetic separation and to avoid loss during washes 5μL of beads was used per point. Expected saturation of beads with SafA' (GST-SafA-6xHis) was calculated by the following formula:

$$\frac{42\ \text{kDa (SafA)}}{2} = 21\ \mu\text{g of } 42\ \text{kDa (SafA}')\text{to saturate } 10\ \mu\text{L of Dynabeads}$$

Based on this, it was expected ~5 μg of SafA' (GST-SafA-6xHis) could be immobilized per 5 μL of Dynabeads. This was experimentally confirmed (data not shown).

2.9.2 SafA' (GST-SafA-6xHis) and bovine liver protein extracts affinity-extracts

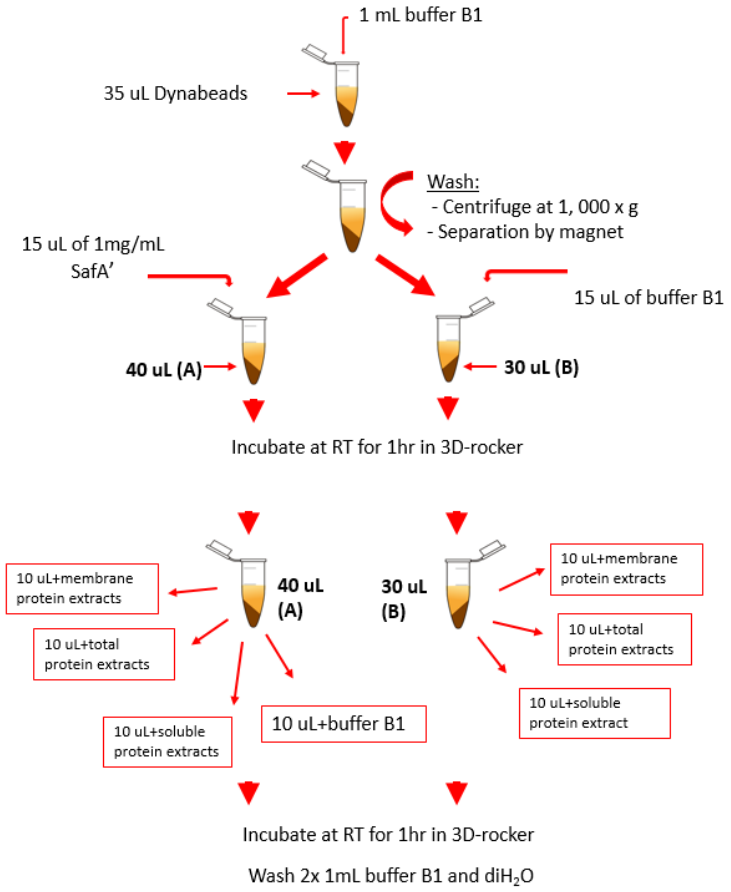

Figure 9. SafA' (GST-SafA-6xHis) affinity-enrichment with bovine liver protein extracts on Dynabeads workflow. Dynabeads were washed with buffer B1 and split into two aliquots of 40 µL **(A)** and 30 µL **(B)** each. SafA' (GST-SafA-6xHis) was added to batch A, whereas batch B was treated as the negative control. Both batches were incubated and washed. Batch A was divided into four aliquots and each incubated with different protein extracts. Batch B was divided into three aliquots and incubated with the same protein extracts as batch A. Any captured proteins were eluted by adding 15 µL 100 mM EDTA/1M β-mercaptoethanol and let to incubate at RT for 30 minutes. Subsequently, 5 µL of 5xloading buffer was added to each sample and let to incubate at RT for a further 30 minutes. Samples were placed in the magnet stand, supernatants heated for 5 minutes at 100 ºC in thermal blocker and separated in a 10% SDS-PAGE.

2.9.3 Depletion of non-specific binding proteins

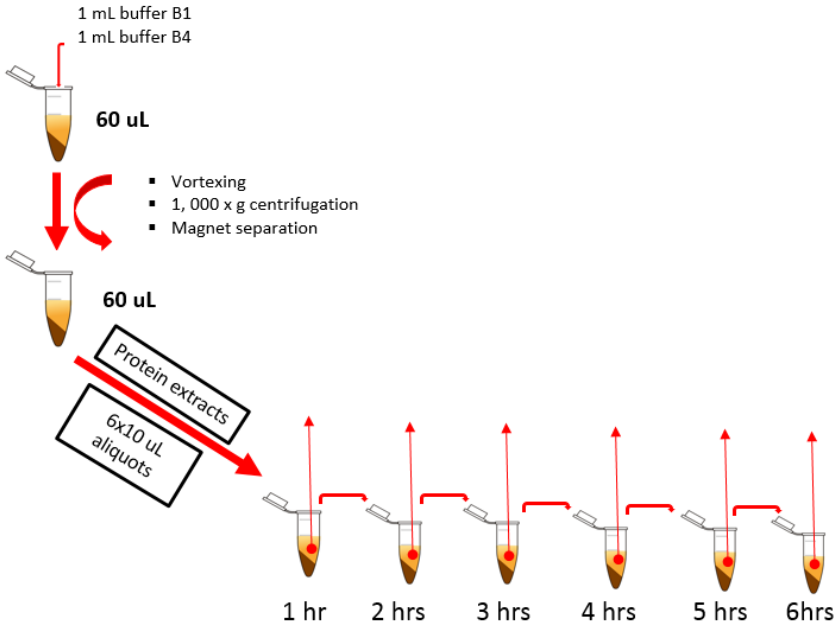

Figure 10. Workflow of non-specific proteins depletion by pre-incubation of protein extracts with Dynabeads. 60 µL of Dynabeads were washed with buffer B1 and B4. The batch was divided into six aliquots of 10 µL. The first aliquot was incubated for 1 hour at RT with 50 µL of bovine liver protein extracts. 1 µL of the supernatant was kept and the rest transferred into the next batch of fresh beads. This process was repeated six times whilst keeping all samples on ice at all times. Captured proteins from each of the five aliquots were eluted with 15 µL 10 mM EDTA/0.14 M β-ME. All these were mixed with 5 µL 5x LB/ β –ME, heated for 5 minutes at 100ºC and separated in a 10% SDS-PAGE gel.

2.9.4 Inhibition of non-specific proteins

In an attempt to disrupt the non-specific interactions between the non-specific proteins and beads, salt concentration in the proteins extracts was increased. 90 µL of Dynabeads were transferred into a 1.5 mL Eppendorf tube and washed in 1 mL buffer B4 and buffer B1 by vigorously vortexing, short centrifugation at 1,000 x g and magnet separation. The volume was made up to 90 µL with buffer B1; beads were distributed in 9 aliquots of 10 µL each and kept in ice until use. 100 µL of extracts was added per aliquot and 100 µL of each respective buffer was added to the corresponding tube, these were incubated for 1 hour on ice. Each buffered extract was collected from the beads by magnet and kept on ice until use. Beads were washed twice in 1 mL of buffer B1 and diH_2O. Elution was carried by incubating beads with 15 µL 10 mM EDTA/2.15 M β-ME for 30 minutes. 1 µL of each collected buffered extract and the captured non-specific protein were heated for 5 minutes at 100 ºC to later be separated in a 10% SDS-PAGE gel.

2.9.5 Identification of non-specific interactions between proteins and Dynabeads

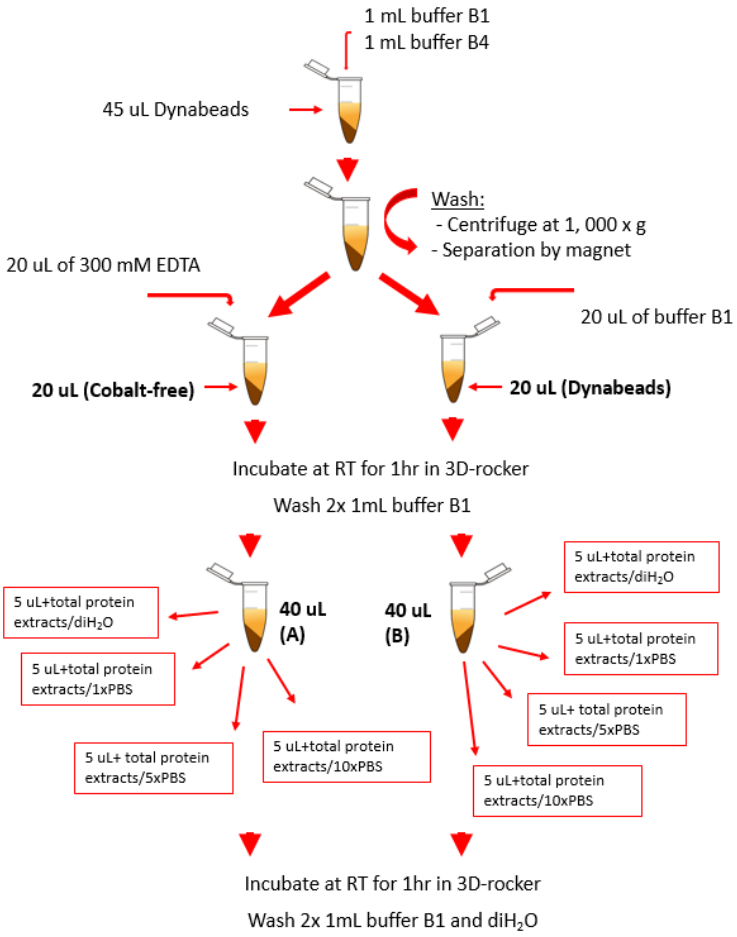

Figure 11. Investigation of non-specific protein interactions with Dynabeads workflow. Dynabeads were washed with buffer B1 and B4. The beads were split in two batches of 20 µL, being called cobalt free and Dynabeads respectively. 20 µL of 300 mM EDTA was added to the cobalt-free batch, whereas 20 µL of buffer B1 was added to the control (Dynabeads) batch. Each batch was distributed into four aliquots and incubated for 1 hr at RT in 3D-rocker with the different extracts. Any bound protein to the Cobalt-free beads and Dynabeads were eluted by incubation with 5xloading buffer at 100ºC. All the eluates and 1 µL of untreated extracts were heated for 5 minutes at 100 ºC and separated in a 10% SDS-PAGE gel.

2.10 Agarose Ni-based IMAC: His-select nickel affinity gel

The material is supplied as a 50% suspension in 30% ethanol. The expected binding capacity is >15 mg/mL of gel for a ~30 kDa histidine tagged protein (His-Select® Nickel Affinity Gel product information).

2.10.1 Protein Immobilization and Background Test

150 µL of gel was transferred into a 1.5 mL Eppendorf tube and washed 3x2 minutes with 1 mL of diH_2O by vigorous vortexing and centrifugation at 1,000 x g for 30 seconds. The

gel was washed twice more with 1 mL of buffer B1 and buffer B4 as per previous step. The beads were resuspended in 150 µL of buffer B1 and distributed in 3x50 µL aliquots. Afterwards, they were incubated for 1 hour at RT in 3D-rocker with 5 µg of SafA' (GST-SafA-6xHis), 20 µg of SafA' (GST-SafA-6xHis) and protein extracts respectively.

The unbound of each sample was collected and kept on ice. Samples were washed by adding 1 mL of buffer B1, incubating for 5 minutes at RT and centrifuging at 1,000 x g for 1 minute. This step was repeated 3 times. 600 µL of buffer B1 was added to the resuspended gel and transferred into a spin column. The gel/complex was centrifuged at 1,000 x g for 4 minutes and the flow through was discarded. 15 µL of 10 mM EDTA/2 M β-ME was added to each column and allowed to incubate for 30 minutes at RT. Subsequently, 5 µL of 5xloading buffer was added and allowed to incubate for a further 30 minutes at RT. Columns were spun down for 4 minutes at 1,000 x g flow through heated at 100^{o}C for 5 minutes and separated in a 10% SDS-PAGE gel.

2.10.2 Identification and inhibition of nickel binding proteins

450 µL of gel was transferred into a 1.5 mL Eppendorf tube and washed 3x2 minutes with 1 mL diH_2O, buffer B4 and buffer B1by fully resuspending and by centrifugation at 1,000 x g for 30 seconds. 500 µL of buffer B1 was added and the sample distributed in two aliquots of 250 µL each, called Nickel-free and Nickel. Tubes were marked and 250 µL of 200 mM EDTA was added to the Nickel-free aliquot, while 250 µL of buffer B1 was added to the Nickel aliquot. Both set of samples were incubated for 30 minutes at RT in 3D-rocker. Samples were centrifuged for 30 seconds at 1,000 x g and EDTA/buffer B1 were discarded, and samples were washed 3x2 minutes in 1 mL of buffer B4 by fully resuspending and 30 seconds centrifugation at 1,000 x g. The same wash was repeated with 1 mL of B1. The Nickel-free and Nickel samples were divided and incubated on ice for 1 hour with buffered extracts containing 0, 1x, 5x and 10x PBS respectively.

All samples were washed for 3x2 minutes with 1 mL of buffer B1 and diH_2O by fully resuspending and centrifugation at 1,000 x g. Samples were transferred into a column and diH_2O was allowed to go through. Columns were centrifuged at 1,000 x g for 30 seconds. 5 µL of 5xloading buffer was added to each aliquot and allowed to incubate for 30 minutes at RT. Columns were spun down for 4 minutes at 1,000 x g and the flow through heated at 100^{o}C for 5 minutes. Samples were allowed to cool down at RT and separated in a 10% SDS-PAGE gel.

2.11 GSH-agarose

2.11.1 Protein immobilization and background test

200 µL of GSH-agarose in glycerol was transferred into a 1.5 mL Eppendorf and washed 4x3 minutes in 1 mL of buffer B1. Agarose was resuspended with 200 µL of buffer B1 and divided into 4 aliquots. Aliquots were incubated for 2 hours at RT in 3D-rocker with 1 µg, 5 µg, 10 µg of SafA' (GST-SafA-6xHis) and 100 µL of bovine total protein extracts respectively.

Each sample was transferred into a separate fresh spin column and centrifuged at 1,000 x g for 30 seconds. The flow through (unbounds) were collected and kept on ice. Each column was washed 4x2 minutes in 1 mL of buffer B1 by fully resuspending and centrifugation at 1,000 x g. A final wash with diH_2O as per previous step was performed. 10 µL of 5xloading buffer/β-ME was added to each column and allowed to incubate for 30 minutes at RT. Columns were centrifuged at 1,000 x g for 30 seconds. Flow through was heated at 100^oC and allowed to cool down at RT before loading into 10% SDS-PAGE gel for separation.

2.11.2 Depletion of glutathione binding proteins

2.3 mL of GSH/glycerol was washed 4x3 minutes in 1 mL of buffer B1 by resuspending and centrifugation at 1,000 x g for 30 seconds. 300 µL of the resin was kept in ice and the rest was divided in two clean columns, resulting in 2 columns of 1 mL resin each. One of the columns was centrifuged at 1,000 x g for 2 minutes and flow though discarded, while the other was kept on ice. 0.5 mL of protein extracts was added into the column and allowed to incubate at RT for 2 hours, followed by centrifugation at 1,000 x g for 2 minutes. The flow though, which is now depleted extracts, was collected and kept on ice. The second column was centrifuged at 1,000 x g for 2 minutes and flow discarded, the previously collected depleted extracts were transferred to this fresh column and incubated at RT for 2 hours. Column was centrifuged at 1,000 x g for 3 minutes and depleted extracts collected. Both columns were washed with 600 µL diH_2O and spun at 1,000 x g for 30 seconds. Proteins captured by the columns were eluted by adding 10 µL of 5xloading buffer/β-ME and allowed to incubate for 30 minutes at RT. Columns were centrifuged at 1,000 x g for 2 minutes eluates were heated for 5 minutes at 100^oC and loaded into 10% SDS-PAGE gel for separation.

2.11.3 SafA' (GST-SafA-6xHis) affinity-enrichment with small intestine

2.3 mL of GSH/glycerol was washed 4x2 minutes in 1 mL of buffer B1, 1 mL 0.01% SDS and 1 mL of buffer B1 by resuspending and centrifugation at 1,000 x g for 30 seconds. The resin was split in two batches of 200 µL (A) and 100 µL (B). 20 µL of 1 mg/mL SafA' (GST-SafA-6xHis) was added to batch (A) and 20 µL of buffer B1 to batch (B). These were incubated at RT for 2 hours and centrifuged at 1,000 x g for 30 seconds and unbound kept on ice. Samples were washed 4x2 minutes in 1 mL of buffer B1 by resuspending and centrifugation. Batch A was divided in aliquots A1 and A2, whereas batch B was divided in aliquots B1 and B2. Aliquots A1 and B1 were incubated with 100 µL of buffer B1 and aliquots A2 and B2 with 100 µL of bovine total protein extracts. The incubations were overnight at 4ºC.

Samples were transferred into spin columns and extracts were allowed to pass through before centrifugation at 1,000 x g for 5 minutes. All extracts were kept on ice. Columns were washed 4x2 minutes in 600 µL of buffer B1 and diH_2O. 30 µL of 5x loading buffer/β-ME was added and incubated at RT for 30 minutes. To collect the eluates, columns were centrifuged at 1,000 x g for 5 minutes. Eluates were heated at 100ºC for 5 minutes, cooled at RT and separated by SDS-PAGE.

2.12 Nitrocellulose (NC)

2.12.1 Identification of Nitrocellulose binding capacity

Nitrocellulose (NC) was cut into nine pieces of approximately 0.5x0.5cm^2 and transferred into a non-binding 96 well plate. 50µL of 10µg/µL, 4µg/µL, 2µg/µL, 1µg/µL, 0.4µg/µL, 0.2µg/µL, 0.1µg/µL, 0.04µg/µL (w/v) Bovine Serum Albumin (BSA) in 10mM Na_2CO_3 pH7.5 (10% BSA in diH2O + 1M Na_2CO_3 pH7.5+ diH_2O), was added onto the different membranes and incubated overnight at ~4ºC. The unbound of each BSA sample was transferred to different tubes and kept in ice. Each membrane was transferred into a 2 mL tube and washed 3x5 minutes with 1mL of diH_2O. All water was aspirated and discarded and 25µL of 5xloading buffer/0.7M β-ME was added to each tube. Samples were incubated at 100ºC for 30 minutes. These were allowed to cool down at RT and separated in a 10% SDS PAGE gel. Unbound samples were also separated in a 10%SDS PAGE gel. Membranes were discarded.

2.12.2 Coating of nitrocellulose with BSA

NC was cut into long 0.5 cm wide strips. The strips were cut into identical 0.5x0.5 cm^2 square pieces. 1 mL of 1 µg/µL BSA was prepared and kept in ice until use. 20 NC pieces

were transferred into a 96 wells plate. 50 µL of the prepared 1 µg/µL BSA was added to each NC on the plate and incubated overnight at 4°C. The NC pieces were taken out of the plate by holding them by one corner with forceps. Each NC was rinsed separately in a Petri dish containing diH_2O. The pieces were air dried on filter paper and transferred into a Petri dish with the help of forceps. The Petri dish was then incubated for 10 minutes at 37°C. The NC pieces were stored into a clean sealed plastic box at 4°C.

2.12.3 Crosslinking of BSA

0.1% and 0.003% glutaraldehyde in 10 mM Na_2CO_3 were prepared and kept until needed. Three NC pieces were collected and each transferred into a separate 2 mL Eppendorf tube labeled: NC/SafA' (GSt-SafA-6xHis) +extract, NC/SafA' (GST-SafA-6xHis) + BSA and NC only. 50 µL of 0.003% glutaraldehyde was added to each tube and incubated overnight at RT. 35 µL of 25% glutaraldehyde was added to each sample and incubated for 1 hr at RT. The glutaraldehyde was aspirated and discarded. 1 mL of diH_2O was added to each tube, incubated for 5 minutes and diH_2O aspirated. The wash step was repeated three more times. Immobilization of the second layer of protein was performed immediately.

2.12.4 Blocking of membranes

Fifteen ~0.5x0.5cm^2 NC pieces were cut and transferred into 2mL tubes. To each group of 3 membranes 50µL of either reagent was added: 10 mM Na_2CO_3, 5% (w/v) milk (10 mL: 0.5 g dried milk (ASDA) +100µL of 1M Na_2CO_3 pH 9 +10 mL diH_2O), 1% (w/v) BSA (100 µL 10% BSA, 10 µL 1M Na_2CO_3 pH 7.5, 900 µL diH_2O), Buffer B1 or Buffer B4 and incubated overnight at +4°C. Buffers were aspirated and discarded; membranes were washed 5x3 minutes with 1 mL of diH_2O. Three more NC pieces were cut and 18 NC were incubated with 50 µL of 0.5 µg/µL labelled α-Rabbit IgG mixed with non-labelled Bovine IgG (50 µL 10 µg/µL (w/v) Bovine IgG, 1µL labelled α-Rabbit IgG, 10 µL 1M Na_2CO_3 pH7.5, 1mL diH_2O for 5 hours at +4°C. Membranes were washed 3x5 minutes with 1 mL of diH_2O. Membranes were kept on filter paper to air dry and then were transferred onto the microscopic slides for fluorescent intensity analysis.

2.12.5 Rabbit IgG Co-IP

Twelve ~0.5x0.5cm^2 NC pieces were cut and transferred into 2 mL tubes. Four groups of three membranes were prepared and the Co-IP's performed as per Table 2. Membranes were washed 3x5 minutes with 1 mL of buffer B1 and let to air dry on clean filter paper. These were transferred into a glass slide and analysed in BioChip imager.

Table 2. Preparation of NC membranes for α-rabbit IgG Co-IP.

ID	Positive Control	Negative Control 1	Negative Control 2	Negative Control 3
Rabbit IgG	+	-	-	-
Bovine IgG	-	+	-	-
Buffer B1	-	-	+	+
1% Milk	+	-	-	+
Fluorescent α-rabbit IgG	+	+	-	+

2.12.6 Identification and inhibition of NC binding proteins

Eight BSA/membrane (incubated with 50 µL of 1µg/µL BSA overnight, rinsed with diH_2O, air dried, incubated at 37^oC for 10 minutes, and stored dried at +4^oC) were transferred into 2 mL tubes, incubated with 50 µL of 0.003% glutaraldehyde for 2 hours at room temperature. Glutaraldehyde was aspirated and discarded, 100 µL of 1M Glycine was added to each tube and incubated for 20 minutes at RT. 100 µL of 10xTAE was added and incubated for another 20 minutes at RT. Blocking buffer was aspirated and discarded; membranes were washed with buffer B4 for 5 minutes, following a wash with buffer B1 for 5 minutes. 50 µL of liver extract was added to 50 µL of diH_2O, 0.5xPBS, 1xPBS, 2xPBS, 3xPBS, 4xPBS, 6xPBS and 10xPBS and then transferred to the membranes for overnight incubation at +4^oC. After incubation membranes were washed with 1 mL buffer B1 4x3 minutes on the 3D-rocker. Membranes were washed 5x3 minutes with 1 mL of diH_2O. 50 µL of 1xloading buffer/0.7M β-ME was added to each membrane and incubated for 30 minutes at 100^oC. All of the eluted samples were separated in a SDS-PAGE gel.

2.12.7 Affinity-enrichment of bovine liver protein extracts with Nitrocellulose (NC)

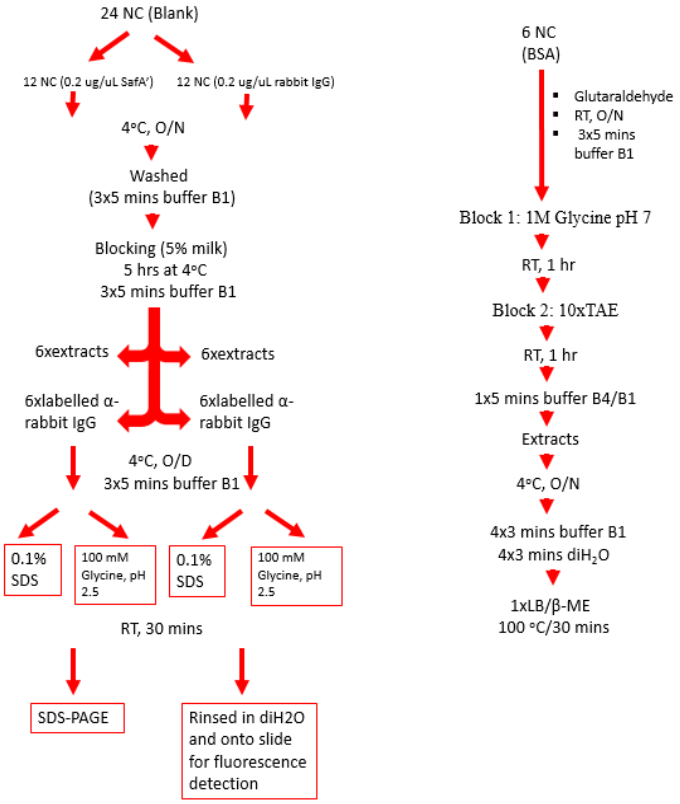

Figure 12. Workflow of method for Nitrocellulose (NC) based affinity-enrichment of SafA' (GST-SafA-6xHis) with bovine liver total protein extracts. Twelve NC pieces were incubated with SafA' (GST-SafA-6xHis) and twelve with rabbit IgG. After incubation, both sets were blocked with 5% milk. Each set of twelve was subsequently divided into sets of six. Six NC pieces in each set were incubated with total protein extracts and six NC pieces with labelled α- rabbit IgG. Following incubation and washing steps, three of the NC pieces incubated with extracts and three of the NC pieces incubated with labelled α-rabbit IgG were eluted with 0.1% SDS and the rest eluted with 100 mM Glycine, pH 2.5. NC pieces were incubated at RT and eluates separated in a SDS-PAGE or prepared for fluorescence detection. For the negative controls, six BSA/NC pieces were activated with glutaraldehyde, blocked twice with 100 mM Glycine, pH 2.5 and 10xTAE buffer. These were later incubated with protein extracts and eluates separated in a SDS-PAGE.

2.13 Universal-BIND™ plates

Universal-BIND™ plates are 96 wells microplates made of polystyrene. Proteins are immobilised on the plates as per any standard Enzyme-linked immunosorbent assay (ELISA) protocol and cross-linked to the plates with UV-light. The plate surface of the well is not large and the binding capacity is estimated to be around ~5 µg per well (Gibbs and Kennebunk et al 2001)

2.13.1 Testing of UV-light crosslinking efficiency

Initially, three solutions were prepared. Solution 1A (0.03 μg/μL of bovine IgG/HRP-α-rabbit IgG) by adding 35 μL of 10 mg/mL bovine IgG into 12 mL 10 mM Sodium Carbonate, pH 7.5. To this, 1 μL HRP/α-rabbit IgG was added and mixed well. Kept in ice until use. Solution 1B (0.03 μg/μL of bovine IgG) by adding 35 μL of 10 mg/mL bovine IgG into 12 mL 10 mM Sodium Carbonate, pH 7.5. Mixed well and kept in ice until use. Finally solution 1C (0.03 μg/μL BSA) was prepared by adding 35 μL of 1% BSA into 12 mL 10 mM Sodium Carbonate, pH 7.5. Mixed well and kept in ice until use.

Using these solutions, the samples were prepared as per Table 3.

Table 3. Preparation of solutions for plate coating.

ID	Solution (1.5 mL)	10% BSA (μL)
2A	1A	45
2B	1B	45
2C	1C	45

The solutions prepared in Table 3 were used to cover the wells of the plates as described in Figure 13.

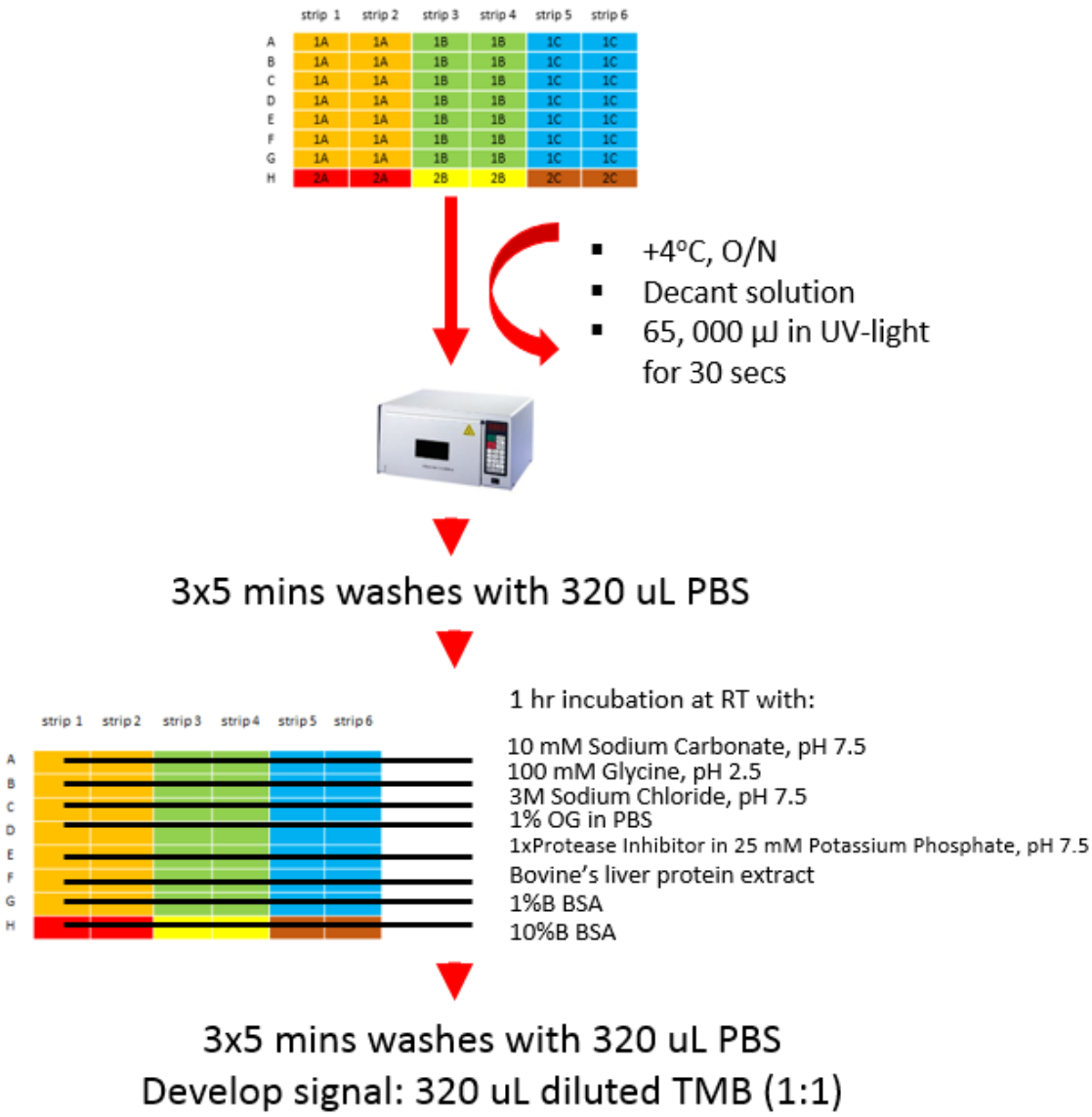

Figure 13. Experimental flowchart for UV-light crosslinking efficiency trial. Each respective well was incubated with their respective solution, as per Table 2. Plate was incubated overnight at 4ºC. Solutions were decanted and plate exposed to UV-light (65, 000 µJ) for 30 seconds. Plate was washed three times with PBS and each row was incubated with different solutions. Incubation was carried for 1 hour at RT. Plates were washed and signal developed with diluted TMB supersensitive and allowed to incubate for 5 minutes at RT. Absorbance was measured at 660 nm in the ELISA reader every 5, 10 and 15 minutes.

2.13.2 Binding capacity

A HRP/α-rabbit IgG dilution (of 1/10) was prepared by adding 10 µL of 10 mM Sodium Carbonate, pH 7.5 into a 1.5 mL Eppendorf tube, followed by the addition of 1 µL HRP/α-rabbit IgG. The sample was mixed well and used to prepare solutions in Table 4.

Table 4. Preparation of Bovine IgG/HRP serial dilutions.

ID	10 µg/µL bovine IgG (µL)	HRP/α-rabbit IgG (1/10) (µL)	10 µg/µL IgG/HRP (µL)	10mM Sodium Carbonate, pH 7.5 (µL)	Final concentration (µg/µL)
1H	15	1	-	1485	0.1
2H	-	-	500 µL of 1H	1000	0.033
3H	-	-	500 µL of 2H	1000	0.011
4H	-	-	500 µL of 3H	1000	0.0037
5H	-	-	500 µL of 4H	1000	0.0012
6H	-	-	500 µL of 5H	1000	4.1e-4
7H	-	-	500 µL of 6H	1000	1.4e-4
8H	-	-	-	1000	-

320 µL of each solution was added to strips 1, 2& 3 as per Figure 14 for overnight incubation at +4ºC.

	strip1	strip 2	strip 3
A	1H	1H	1H
B	2H	2H	2H
C	3H	3H	3H
D	4H	4H	4H
E	5H	5H	5H
F	6H	6H	6H
G	7H	7H	7H
H	8H	8H	8H

Figure 14. Coating of strips with bovine IgG/HRP dilutions.

Plate was decanted, placed in the UV light chamber and exposed to 65, 000 microjoules for 30 seconds, followed by a 5 minutes wash with 320 µL of diH_2O, 3x5 minutes with 320 µL of buffer B4 and 5 minutes wash with 320 µL PBS. Signal was developed by adding 320 µL of diluted TMB supersensitive in diH_2O (1:1) and let to incubate for 5 minutes ar RT. Pictures and readings were taken at 660 nm in the ELISA reader every 5, 10 and 15 minutes.

2.13.3 Binding buffer selection for protein immobilization

For this trial, a number of IgG/HRP serial dilutions were prepared in 10 mM Sodium Carbonate, pH 7.5, PBS, pH7.5, PBS (1/10), pH 7.5 and 500 m K_2HPO_4, pH 8.5. Table 5 shows an example as of how the samples were prepared.

Table 5. Preparation of bovine IgG/HRP serial dilutions in 10 mM Sodium Carbonate, pH 7.5.

ID	HRP (µL)	10mM Sodium Carbonate, pH 7.5 (µL)	HRP (1/20) (µL)	10 µg/µL bovine IgG (µL)	10 µg/µL IgG/HRP (µL)	Final concentration of bovine IgG (µg/µL)
0SC	1	20	-	-	-	-
1SC	-	1500	5	15	-	0.1
2SC	-	1000	-	-	500 µL of 1SC	0.033
3SC	-	1000	-	-	500 µL of 2SC	0.011
4SC	-	1000	-	-	500 µL of 3SC	0.0037
5SC	-	1000	-	-	500 µL of 4SC	0.0012
6SC	-	1000	-	-	500 µL of 5SC	4.1e-4
7SC	-	1000	-	-	500 µL of 6SC	1.4e-4
8SC	-	1000	-	-	-	-

Plates were covered with the different IgG/HRP serial dilutions in the different buffers by adding 320 µL of each solution as per Figure 15.

	10 mM Sodium Carbonate, pH 7.5			**PBS, pH 7.5**			**PBS (1/10), pH 7.5**			**500 mM K_2HPO_4, pH 8.5**			
Position	strip 1	strip 2	strip 3	strip 4	strip 5	strip 6	strip 7	strip 8	strip 9	strip 10	strip 11	strip 12	Protein concentrati

													on per well in each row (µg)
A	1H	1H	1H	1P	1P	1P	1PT	1PT	1PT	1D	1D	1D	~32
B	2H	2H	2H	2P	2P	2P	2PT	2PT	2PT	2D	2D	2D	~10.56
C	3H	3H	3H	3P	3P	3P	3PT	3PT	3PT	3D	3D	3D	~3.52
D	4H	4H	4H	4P	4P	4P	4PT	4PT	4PT	4D	4D	4D	~1.18
E	5H	5H	5H	5P	5P	5P	5PT	5PT	5PT	5D	5D	5D	~0.38
F	6H	6H	6H	6P	6P	6P	6PT	6PT	6PT	6D	6D	6D	~0.13
G	7H	7H	7H	7P	7P	7P	7PT	7PT	7PT	7D	7D	7D	~0.05
H	8H	8H	8H	8P	8P	8P	8PT	8PT	8PT	8D	8D	8D	0

Figure 15. Coating of wells with bovine IgG/HRP dilutions.

Plate was covered and incubated overnight at +4ºC. Protein was decanted from wells, plate placed in the UV-light chamber and exposed to 65, 000 microjoules for 30 seconds, followed by a 5 minutes wash with 320 µL diH_2O, 3x5 minutes with 320 µL buffer B4 and a 5 minutes final wash with 320 µL of PBS. Immediately after washing, signal was developed by adding 320 µL of diluted TMB supersensitive in diH_2O (1:1) and let to incubate for 5 minutes ar RT. Pictures and readings were taken at 660 nm in the ELISA reader every 5, 10 and 15 minutes.

2.13.4 Determination of optimal pH for protein immobilization

Phosphate buffer solutions at different pH were prepared as per Table 6.

Table 6. Preparation of Potassium Phosphate buffers.

ID	pH	Volume of 1 M K_2HPO_4, pH 9.0 (mL)	Volume of 1 M KH_2PO_4, pH 4.0 (mL)
A	**4.0**	-	10
B	**5.0**	2	8
C	**6.0**	1.32	8.68
D	**7.0**	6.15	3.85
E	**8.0**	9.4	0.6
F	**9.0**	10	-

10 µg/µL bovine IgG/HRP was prepared by adding 1 µL of HRP to 100 µL of 10 µg/µL bovine IgG in a 1.5 mL Eppendorf tube and diluted in the different buffers described in Table 6.

Following this, a range of IgG/HRP serial dilutions were prepared in all the buffers from Table 6. Below, Table 7 shows how the serial dilutions were prepared for Phosphate buffer, pH 4 (IgG/HRP was prepared in the same way in all the other buffers).

Table 7. Preparation of bovine IgG/HRP serial dilutions in Phosphate buffer, pH 4.

ID	Phosphate buffer, pH 4 (µL)	Bovine IgG/HRP (µL)	Final concentration of bovine IgG (µg/µL)
1A	1500	15 of 10 µg/µL	0.1
2A	1000	500 µL of 1A	0.033
3A	1000	500 µL of 2A	0.011
4A	1000	500 µL of 3A	0.0037
5A	1000	500 µL of 4A	0.0012
6A	1000	500 µL of 5A	$4.1e^{-4}$
7A	1000	500 µL of 6A	$1.4e^{-4}$
8A	1000		-

320 µL of each solution consisting of IgG/HRP in the different buffers was transferred to the plate as per Figure 16.

	strip 1	strip 2	strip 3	strip 4	strip 5	strip 6	strip 7	strip 8	strip 9	strip 10	strip 11	strip 12	Protein concentration per well (µg)
A	1A	1A	1B	1B	1C	1C	1D	1D	1E	1E	1F	1F	~32.00
B	2A	2A	2B	2B	2C	2C	2D	2D	2E	2E	2F	2F	~10.50
C	3A	3A	3B	3B	3C	3C	3D	3D	3E	3E	3F	3F	~3.52
D	4A	4A	4B	4B	4C	4C	4D	4D	4E	4E	4F	4F	~1.18
E	5A	5A	5B	5B	5C	5C	5D	5D	5E	5E	5F	5F	~0.38
F	6A	6A	6B	6B	6C	6C	6D	6D	6E	6E	6F	6F	~0.13
G	7A	7A	7B	7B	7C	7C	7D	7D	7E	7E	7F	7F	~0.04
H	8A	8A	8B	8B	8C	8C	8D	8D	8E	8E	8F	8F	0

Figure 16. Incubation of strips with 320 µL of protein in Potassium Phosphate at different pH ranges (for codes see Table 7).

Plate was covered and incubated overnight at +4ºC. Protein was decanted and plate washed 5 minutes with 320 µL of diH_2O, 3x5 minutes with 320 µL of buffer B4 and a 5 minutes final wash with 320 µL of PBS. Immediately after washing, signal was developed by adding 320 µL of diluted TMB supersensitive in diH_2O (1:1) and let to incubate for 5 minutes ar RT. Pictures and readings were taken at 660 nm in the ELISA reader every 5, 10 and 15 minutes.

2.13.5 Displacement of protein by BSA

0.01 µg/µL bovine IgG/HRP was prepared by transferring 5 mL 10 mM Sodium Carbonate, pH 7.5 into a 15 mL Falcon tube, followed by the addition of 5 µL 10 µg/µL bovine IgG and 1 µL of HRP/α-rabbit IgG. Solution was mixed well and used to prepare the samples in Table 8.

Table 8. Preparation of BSA serial dilutions.

ID	BSA (µL)	10mM Sodium Carbonate, pH 7.5 (µL)	Final BSA Concentration (%)
1B	500 µL of 10% BSA	-	10
2B	100 µL of 1B	900	1
3B	100 µL of 2B	900	0.1
4B	100 µL of 3B	900	0.01
5B	100 µL of 4B	900	0.001
6B	100 µL of 5B	900	0.0001
7B	100 µL of 6B	900	0.00001
8B	-	1000	0

Dilutions were kept in ice and used for the preparation of solutions in Table 9.

Table 9. Preparation of bovine IgG/HRP/BSA solutions.

ID	bovine IgG/HRP (µL)	BSA dilution (µL)	Final BSA concentration (%)
1	500	500 µL of 1B	10
2	500	500 µL of 2B	1
3	500	500 µL of 3B	0.1
4	500	500 µL of 4B	0.01

5	500	500 µL of 5B	0.001
6	500	500 µL of 6B	0.0001
7	500	500 µL of 7B	0.00001
8	500	500 µL of 8B	0

320 µL of each solution was added to strips 1, 2& 3 for overnight incubation at +4ºC. Protein was decanted from wells and plate exposed to 65, 000 microjoules in UV-light chamber for 30 seconds, followed by a 5 minutes wash with 320 µL of diH_2O, 3x5 minutes with 320 µL of buffer B4 and a 5 minutes final wash with 320 µL of PBS. Immediately after washing, signal was developed by adding 320 µL of diluted TMB supersensitive in diH_2O (1:1) and let to incubate for 5 minutes at RT. Pictures and readings were taken at 660 nm in the ELISA reader every 5, 10 and 15 minutes.

2.13.6 Blocking and Elution Trials

0.009 µg/µL bovine IgG/HRP was prepared by adding 5 µL of 10 mg/mL bovine IgG to 5.4 mL 100 mM potassium phosphate buffer, pH 6.5 in a 15 mL Falcon tube, followed by the addition of 10 µL of 1/50 HRP to the mixture. Solution was vortexed gently and kept on ice until use.

330 µL of bovine IgG/HRP was added to strips 1 and 2, whereas 100 mM potassium phosphate buffer, pH 6.5 was added to strips 3 and 4. Plate was covered and incubated overnight at 4ºC. Protein was decanted from wells, plate placed in UV-light chamber and exposed to 65, 000 microjoules for 30 seconds. Wells were washed 3x5 minutes with buffer B4 and a 5 minutes final wash with 100 mM Potassium Phosphate, pH 6.5 before and incubation for ~6 hours at +4ºC with the different working solutions as per Figure 17.

	strip1	strip2	strip3	strip4
A	100 mM potassium phosphate buffer, pH 6.5	100 mM potassium phosphate buffer, pH 6.5	100 mM potassium phosphate buffer, pH 6.5	100 mM potassium phosphate buffer, pH 6.5
B	1%BSA, pH6.5	1%BSA, pH6.5	1%BSA, pH6.5	1%BSA, pH6.5
C	1%OG, pH6.5	1%OG, pH6.5	1%OG, pH6.5	1%OG, pH6.5
D	1%Tween, pH6.5	1%Tween, pH6.5	1%Tween, pH6.5	1%Tween, pH6.5
E	1xPI, pH 7.5	1xPI, pH 7.5	1xPI, pH 7.5	1xPI, pH 7.5
F	extract	extract	extract	extract
G	100 mM Glycine, pH 2.5	100 mM Glycine, pH 2.5	100 mMGlycine, pH 2.5	100 mM Glycine, pH 2.5
H	3 M NaCl, pH ~7	3 M NaCl, pH ~7	3 M NaCl, pH ~7	3 M NaCl, pH ~7

Figure 17. Schematic diagram of a Universal-BIND™ plate showing the coating of wells with solutions for over day incubation.

0.009 μg/μL of bovine IgG/HRP was prepared by adding 5 μL of 10 mg/mL bovine IgG to 5.4 mL of 100 mM potassium phosphate buffer, pH 6.5 in a 15 mL Falcon tube, followed by the addition of 10 μL of 1/50 HRP to the mixture, vortexed gently and kept on ice until use, followed by a 5 minutes wash with diH_2O, 3x5 minutes with buffer B4 and a 5 minutes final wash with 330 μL of 100 mM potassium phosphate, pH 6.5. 330 μL of bovine/HRP was added to strips 3 and 4, whereas 100 mM potassium phosphate, pH 6.5 was added to strips 1 and 2. The plate was incubated over day for 5 hours at +4^oC.

Protein was decanted and plate washed 5 minutes with diH_2O, 3x5 minutes with buffer B4 and a 5 minutes final wash with PBS. Immediately after washing, signal was developed by adding diluted TMB supersensitive in diH_2O (1:1) and allowed to incubate for 5 minutes at RT. Pictures and readings were taken at 660 nm in the ELISA reader every 5, 10 and 15 minutes.

2.13.7 Anti-rabbit IgG Co-IP test established optimal conditions

0.01 μg/μL of bovine rabbit IgG and 0.01 μg/μL of rabbit IgG were prepared in phosphate buffer, pH 6.5. 0.01 μg/μL rabbit IgG was added to wells E and H of strip 1 and 0.01 ug/μL bovine rabbit IgG to wells G and H. The solutions were incubated overnight at 4^oC.

Quickly, without allowing wells to dry, protein was decanted from wells, plate placed in the UV-light chamber and exposed plate to 65, 000 microjoules for 30 seconds, followed by 3x5 mins wash with buffer B4 and a 5 minutes final wash with 100 mM Potassium Phosphate, pH 6.5. 1% BSA was added to each well and incubated over day at +4^oC for ~6hours. 15 μL of 1/50 HRP α-rabbit IgG was added to 50 μL of 1.5 mL mM phosphate buffer, pH 6.5 in a 1.5 mL Eppendorf tube. Quickly, without allowing wells to dry, decanted protein and washed 3x5 minutes with buffer B4 and a 5 minute final wash with 100 mM Potassium Phosphate, pH 6.5. Subsequently, 330 μL of α-rabbit IgG/HRP was added to wells E-F and incubated overnight at +4^oC.

Protein was decanted and plate washed 1x5 minutes with diH_2O, 3x5 minutes with buffer B4 and a 5 minutes final wash with PBS. Immediately after washing, signal was developed by adding diluted TMB supersensitive in diH_2O (1:1) and to incubate for 5 minutes at RT. Pictures and readings were taken at 660 nm in the ELISA reader every 5, 10 and 15 minutes.

2.13.8 Mammalian extracts affinity-enrichment in Universal-BIND™ plates

330 µL of 0.009 µg/µL BSA was added to the top 4 wells and 330 µL of 1mg/mL SafA' (GST-SafA-6xHis or variants GST+SafA-6xHis/SafA-6xHis as required) to the bottom 4 wells of the strip, subsequently the strip was incubated for 6 hrs at 4ºC. Protein was decanted from wells and without allowing wells to dry, strip was placed in UV-light chamber and exposed to 65, 000 microjoules for 30 seconds. Strip was washed for 3x3 minutes with buffer B4 and 1x3 minutes with 100 mM potassium phosphate, pH 6.5. 1% BSA was added to each well of the strip and incubated overnight at 4ºC. 330 µL of heart extracts were added to each well of the strip and incubated for 5 hours at 4ºC. Strip was washed for 3x3 minutes with buffer B1 and rinsed once with diH_2O. To elute 50 µL of 0.1% SDS was added to each well by rinsing all walls. 0.1% SDS was allowed to incubate at RT for 15 mins and transfered samples in 1.5 mL Eppendorf tubes. 20 µL of 100 mM DTT was added to each sample and incubated in ice for 30 minutes. Eluates from the first 4 wells were pooled together into a 1.5 mL Eppendorf tube and eluates from the bottom 4 wells were pooled into a separate 1.5 mL Eppendorf tube. Both sets of recovered eluates were divided in 3x15 µL aliquots designated for MALDI analysis and 3x50 µL aliquots designated for SDS-PAGE. 75 µL of 80% acetone was added to each MALDI aliquot and 250 µL to each SDS-PAGE aliquot. Samples were stored overnight at -20ºC before use.

2.14 Preparation of samples for Circular Dichroism (CD)

2.14.1 Cleaving of GST from GST-SafA-6xHis construct

HRV 3C Protease (ThermoFisher # 88947), a recombinant cysteine protease, was used to remove the GST fusion tag from the SafA' (GST-SafA-6xHis) construct. A mastermix was prepared as per Table 10.

Table 10. Preparation of cleavage reaction.

Component	A (µL)
HRV 3C Reaction buffer (10x)	30
1 mg/mL of SafA' (GST-SafA-6xHis)	260
HRV 3C Protease	13
Ultrapure water	-
Total	303

The reaction was incubated overnight or up to 2 days at 4ºC. The HRV 3C protease and now free GST tag were removed by incubating the mix with GSH-resin. ~400 µL of resin was transferred into a 1.5 mL Eppendorf tube and washed by application of 1 mL diH_2O

and vortexing followed by centrifuging at 1,000 x g for 2 minutes. This process was repeated twice. Subsequently, the agarose beads were washed three times by application of 500 μL HRV 3C buffer, vortexing and centrifuging as before. The agarose beads were transferred into a clean spin column and centrifuged for 2 minutes at 1,000 x g and the buffer was discarded. Immediately, ~300 mL of the cleaved sample mixture was added and let to incubate with the resin at RT for 30 minutes. The column was centrifuged as per the previous steps, and incubated again with fresh buffer for a further 30 minutes. The column was centrifuged for 2 minutes at 1,000 x g and the flow-through was collected. Cleaved SafA' (SafA-6xHis) was kept on ice until the next step (Figure 18).

2.14.2 Elution of GST tag from GSH-resin

300 μL of 20 mM reduced glutathione in 50 mM Tris-HCl, pH 7.00 was added to the GST/HRV 3C protease bound column. The column was gently vortexed and let to incubate at RT for 30 minutes. The flow-through was collected by centrifuging for 2 minutes at 1,000 x g. The sample was passed through the column again and allowed to incubate at RT for a further 30 minutes. The flow-through was collected and kept on ice until the next step (Figure 18).

2.14.3 Buffer exchange

Buffer exchange was carried out by using Zeba spin desalting columns, with a 7k molecular weight cut-off (ThermoFisher # 89891). The samples were in 50mM Tris-HCl pH 8 (Sections 2.14.1 and 2.14.2). They were exchanged into 10 mM Potassium Phosphate, pH 8.2 for analysis by CD. The storage solution was removed by 2 minutes centrifugation at 1,000 x g. 1 mL of 10 mM Potassium Phosphate, pH 8.2 was added and centrifuged for 2 minutes at 1,000 x g. This step was repeated three more times. The samples were added to the centre of the resin bed and centrifuged for 2 minutes at 1,000 x g. The flow-through containing the samples in 10 mM Potassium Phosphate, pH 8.2 were kept at -20^{o}C until use. 10 mL of the 10 mM Potassium Phosphate buffer, pH 8.2 was also kept to be used as a reference in the CD studies (Figure 18).

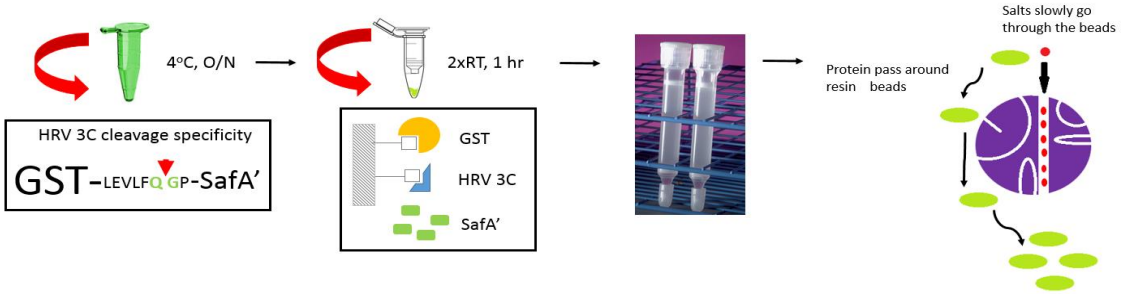

Figure 18. Workflow showing the cleaving process of the GST tag from the construct and buffer exchange of the resulting cleaved SafA' (SafA-6xHis). GST-SafA-6xHis was incubated overnight with HRV 3C protease (ThermoFisher # 88947). The mixture of cleaved SafA' (SafA-6xHis), GST and HRV 3C protease was passed through a GSH-column (Sigma # G4510) and the cleaved SafA' (SafA-6xHis) protein collected in the eluate. Buffer exchange from cleaving buffer to 10 mM Potassium Phosphate, pH 8.00 was performed by using Zeba spin desalting columns (ThermoFisher # 89891).

2.14.4 Denaturing polyacrylamide gel electrophoresis (SDS-PAGE)

Separation of proteins by SDS-PAGE was carried out by following the method of Laemmli (Laemmli et al 1970) in a PowerPac 200 electrophoresis unit (BioRad). The SDS-PAGE consisted of resolving gel 10-15% Acrylamide (Sigma), 0.375 M Tris-HCl pH 8.8, and 0.1% (w/v) SDS and stacking gel 4% Acrylamide (Sigma), 0.125 M Tris-HCl pH 6.8, and 0.1% (w/v) SDS . The polymerization of both solutions was carried out by adding 0.04% TEMED and 0.1% (w/v) ammonium persulphate. Prior to loading, the gel tank was filled with electrophoresis buffer 1x (10x=0.25 M Tris, 1.92 M glycine, 1% SDS). 1x volume of Laemmli sample buffer 4x concentrate was added to all samples, followed by incubation at 100°C for 5 min. The samples were centrifuged for 5 sec and then cooled on ice for 2 minutes. The gels were electrophoresed at a constant voltage of 60 mV until the protein entered the resolving gel and 120 mV thereafter. Proteins were then fixed and stained by incubating the gels in 35% methanol, 5% acetic acid, 0.25% Coomassie brilliant blue and microwaved for 3 minutes (avoiding boiling of gel). Gel was allowed to stain in shaker for 15 minutes before washing three times with water and left to destain overnight.

2.14.5 Non-denaturing gel (Native-PAGE)

Separation of proteins by Native-PAGE was carried out by following the same steps as the previous section (Section 2.14.4) but the SDS was not added in the preparation. Laemmli sample buffer without SDS was also prepared.

2.14.6 Western Blot

The separated proteins were transferred into the blotting membrane-nitrocellulose 0.2 µM (BioRad) according to the protocol described in (Matsudaira et al 1987). Nitrocellulose membranes were washed together with four pieces Whatman paper and 2 sponges in CAPS buffer pH 11 containing 10% methanol and 0.1% SDS. The sandwich was made by placing the gel and the nitrocellulose membrane between two layers of Whatman paper and the sponges. Proteins were electroblotted at a constant of 400 mA for 90 min.

Total proteins on membranes were detected using Ponceau red staining. All Western blotting procedures were carried out at room temperature with agitation except when stated otherwise. Membranes were blocked with 5% non-fat milk in TBST (20 mM Tris, 150 mM NaCl, containing 0.05% Tween-20, pH 7.4) for 60 minutes. Membranes were then incubated with primary antibodies in TBST 5% non-fat milk at 4°C overnight. Removal of excess primary antibody was carried out by washing the membranes in TBST three times for 5 minutes each. The secondary antibody (Goat (polyclonal) Anti-Rabbit IgG (H+L), Highly Cross Adsorbed, LI-COR, IRDye® 680LT) diluted 1:20, 000 was incubated with the membrane in TBST with 5% non-fat dry milk and 0.01% SDS/1% Tween-20 final for one hour at room temperature. Excess secondary antibody was removed by washing the membranes in TBST three times for 5 minutes each. Membranes were scanned in the Odyssey scanner (LI-COR) in the 700 nm channel.

2.15 Estimating Protein Concentration

2.15.1 Absorbance at 280nm

The concentration of the samples was determined by measuring absorbance at 280nm (A280) using a Perkin Elmer Lambda35 spectrophotometer. The extinction coefficient (ε280) was estimated using ProtParam (http://www.expasy.ch/tools/protparam.html), then used to derive the protein concentration using Lambert-Beer Law:

$$\text{Protein Concentration (M)} = A280/ (\varepsilon 280(M\text{-}1) \times \text{path length of cuvette (cm)})$$

All relevant protein information used, such as, molecular weight (MW), number of base pairs (BP), Isoelectric Point (pI) and extinction coefficient used in this study are shown in Chapter III, Table 12.

2.15.2 Qubit 2.0 Fluorometer

A Qubit benchtop fluorometer (ThermoFisher model Qubit 2.0) was used to detect protein concentrations as little as 12.5 µg/mL. Before use all the solutions were kept on the bench

for 15 minutes and readings were taken at RT. The Qubit instrument was calibrated using the three standard solutions provided by the manufacturer (10 µL of each standard was added to a 0.5 mL PCR tube with 190 µL Qubit working solution (ThermoFisher #Q33211). Simultaneously, each sample was prepared by adding 20 µL of the corresponding sample to 180 µL of Qubit working buffer. Standards and samples were gently vortexed and let to incubate for 15 minutes at RT. After calibration, samples were read and the concentrations recorded.

2.15.3 Quantitative Amino Acid Analysis (QAA)

QAA is the gold standard for accurate protein quantitation as long as the amino acid sequence is known. Samples were sent to the PNAC Facility at University of Cambridge for analysis. Samples were passed through a reversed-phase HPLC column for ion-exchange chromatography. The elute was hydrolysed, dried in a vacuum and dissolved in loading buffer, such as, 20 mM HCl and 0.2 M sodium borate, pH 8.8; 5 mM EDTA (Palace et al 1999). The HPLC instrument was calibrated by running a standard mixture of amino acids at different concentrations. The standard curve was generated by measuring the absorbance of samples containing a mixture of amino acids of known concentration (Rutherfurd and Dunn et al 2011). The samples were run and fitted into the standard curve. The relation between absorbance and concentration was used in order to calculate the concentration of the unknown sample.

2.16. Circular Dichroism studies (CD)

CD spectra were measured using SafA' (GST-SafA-6xHis) samples obtained before and after cleavage of the GST tag (Chapter IV). To enable comparability of spectra samples were treated as per Figure 18.

2.16.1 Far UV Circular Dichroism (CD)

Far UV CD spectra were recorded using a Jasco J-1500 spectropolarimeter (Jasco UK, Great Dunmow, UK) equipped with a Peltier thermally controlled cuvette holder and 1 mm path-length quartz cuvettes (Starna, Optiglass Ltd, Hainault, UK). All samples were measured undiluted but the cleaved SafA' (SafA-6xHis) sample was diluted 2.5-fold in 10 mM Potassium Phosphate buffer, ~pH 8.2. Data were recorded using a 0.1mm cuvette, in the range 260nm-190nm, using standard sensitivity (100 mdeg), a data pitch value of 0.2 nm, in continuous scanning mode with a scanning speed of 100 nm/min, response 1 sec, bandwidth 2nm, and an average of 16 scans. All data was corrected against a suitable buffer blank as indicated.

Data files were exported in text format and also saved in the file format JASCO 1.50 (with preview). The units selected were millidegrees, the initial wavelength 260 nm and final wavelength 190 nm, the wavelength step 0.5 nm. The lowest nm data point to use in the analysis depended on the selected method. The analysis programme and reference sets were selected (see below). The output units were selected as delta epsilon. Hence the data was submitted in millidegrees, plus Mean Residue Weight (MRW) in daltons [MRW=MW/ (number of residues – 1)], the protein concentration in mg/mL and the path length in cm.

The CD spectra were deconvoluted using two software programmes, CDPro (Sreerama and Woody et al 2000) and DichroWeb (Whitmore and Wallace et al 2008). For deconvolution in CDPro the mean residue was calculated using the following equation.

$$[\theta]mrw, \lambda = (MRW \times \theta\lambda) / (10 \times d \times c)$$

where MRW = M/(N-1) and M is the molecular mass of the polypeptide in Da. N is the number of amino acids in the chain $\theta\lambda$ is the observed ellipticity (degrees), d is the path length (nm) and c is the concentration (g/mL).

The CDPro software determines the secondary structure fractions by using the three programmes, SELCON3, CDSSTR and CONTINN and eight reference protein sets. A reference set consists of a group of proteins whose CD spectra and secondary structures are known. These are used to compare the CD spectra of the sample, therefore allowing predicting its secondary structure.

DichroWeb is an on-line based server for the determination of the secondary structure fractions. The server offers five analysis programmes, CONTINLL, SELCON3, CDSSTR, VARSLC and K2D. DichroWeb offers a choice of seven protein reference sets (Whitmore and Wallace et al 2004).

Both, CDPro and DichroWeb gave similar secondary structure predictions for the proteins (data not shown) but DichroWeb was preferred due to the availability of graphs and presentation of results in a more comprehensive manner. All deconvolution values presented in this thesis are therefore those obtained from DichroWeb.

2.16.2 Differential Scanning Fluorimetry (DSF)

Thermal melting curves were recorded for uncleaved SafA’ (GST-SafA-6xHis), undepleted cleaved SafA’ (GST+SafA-6xHis) and GST samples. Protein unfolding was monitored by adding the fluorescent dye Sypro orange (ThermoFisher). During the

unfolding process the dye binds to the exposed hydrophobic regions of the proteins, resulting in a large increase of fluorescence used to monitor the protein-unfolding transition. The reaction mixture consisted of 20 µL of the samples, 7.5 µL of 300x Sypro orange, 23 µL of diH_2O. Samples were added to wells on a 96-well thin-wall PC plate (BioRad). The plate was placed in iCycler iQ Real Time PCR Detection System (Bio-Rad). The temperature was increased from 10 to 95 °C in increments of 0.2 °C. The fluorescence intensity was measured in relative fluorescence units (RFU) using excitation/emission wavelengths of 490 and 453 nm, respectively. Each sample was ran in triplicate.

2.16.3 Analysis of Differential Scanning Fluorimetry (DSF) data

The data from the qPCR machine was exported into Excel. The instrument presented both, the raw fluorescence signal and the derivative of the fluorescence signal as a function of temperature. The average of the three replicates for the fluorescence signal was subtracted and the corrected average of the fluorescence signal as a function of temperature was plotted. The thermal melt (T_m) was calculated with Excel by calculating the V_{max}.

2.17 Matrix-assisted laser desorption-time of flight (MALDI TOF MS) mass spectrometry

All the spectra were manually acquired by using an Autoflex III TOF/TOF mass spectrometer and the FlexControl software (version 3.3) (Bruker Daltonik, GmbH). Among other features, the instrument is equipped with AnchorChip™ MALDI target technology for fast automation and long lifetime nitrogen laser with variable repetition rate. A nitrogen laser operating at 337 nm with a 3 ns pulse width was utilized in the 400 – 6000 Da range for the peptide mass fingerprinting. The instrument parameters consisted of a laser frequency of 100.0 Hz and a digitizer trigger level of 1000 mV. The detector gain voltage offset settings were 1300.00 V for linear and 1400.00 V for reflector. The laser attenuator offset 66% and the range 20% of the maximum.

As per Chapter V, Section 5.7, cleaved SafA' (GST-SafA-6xHis) was immobilized on the Universal-BIND™ plates (System 5) (over day at 4°C) by UV-light crosslinking and incubated with BSA blocking solution (overnight at 4°C). On the following day plates were washed three times with buffer B1 (Sections 2.5 and 2.13) and incubated with total protein extracts (Section 2.8) for 5 hours. After washing three times samples were incubated with elution buffer and all technical replicates pooled together. Cold 100% acetone was added to each vial and stored at -20°C overnight. After washing with 70%

acetone, the pellet was reconstituted for MS analysis in 25 µL of 5 mM K_2HPO_4, pH 9.0, as this was the buffer initially used for the affinity-enrichment. To aid pellet solubilisation we added the same additives originally present in the sample previous to acetone precipitation. Therefore, 5 µL of 0.05% SDS/ 50 mM DTT in 5 mM K_2HPO_4, pH 9.0 was also added to the reconstituted pellet. The mixture was heated in dry heating block at 50ºC for 30 minutes. As per Figure 19, only for MALDI-TOF MS analysis (not LC-MS/MS) resuspended pellets were passed through HiPPR detergent removal spin columns to remove residues of detergent. The resin has a high affinity for most detergents and low affinity for proteins and peptides. It removes ionic, non-ionic and zwitterionic detergents, such as, SDS, Triton™ X-100, NP40 and CHAPS, at concentrations of 0.5-1%. This oligosaccharide-based resin has a small hydrophobic cavity which creates a microenvironment for detergent's nonpolar moiety to enter and form an inclusion complex (ThermoScientific, Instructions for HiPPR™ detergent removal resin).

While samples were allowed to cool down, the vial containing the stock of Thermo Scientific HiPPR Detergent Removal Resin was gently swirled until an even suspension was obtained. An aliquot of 25 µL of the resin slurry was added onto a spin column and this was centrifuged at 1,000 x g for 1 minute. The flow-through was discarded. To equilibrate the resin, 25 µL of 5 mM K_2HPO_4, pH 9.0 was added to the column, followed by another centrifugation at 1,000 x g for 1 minute and the flow-through was discarded. This step was repeated twice. The column was blocked on the lower end with a plug, to avoid liquid outflow, and the column was placed into a fresh 1.5 mL microfuge tube. The protein sample was applied slowly onto the compacted resin bed. The column containing sample and resin was capped and vortexed gently followed by a 10 min incubation at RT. Plug and cap were then removed and the column reverted to the 1.5 mL microfuge tube. The detergent-free samples were recovered as eluates by centrifugation at 1,000 x g for 2 minutes and collected. Samples were kept at RT for ~30 minutes until trypsinization.

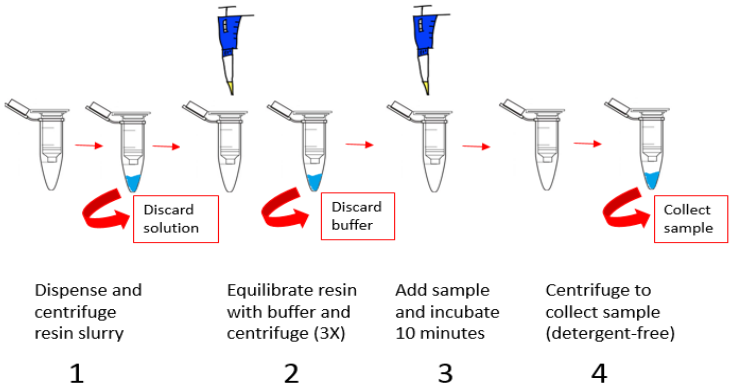

Figure 19. SDS removal procedure. 1) Detergent removal resin was added into the column and spun down at 1,000 x g to discard flow through. **2)** The column was washed 3x with equilibrium buffer. **3)** Detergent containing sample was added, mixed and incubated at RT for 10 minutes. **4)** Column was centrifuged at 1,000 x g for 2 minutes and detergent-free sample collected. Adapted from Thermo Scientific Instructions #88305.

2.17.1 Trypsination, ZipTip and spotting for MALDI-MS

Detergent free protein samples were digested as following: A ready to use vial containing 1 µg of Trypsin (Trypsin Singles, Proteomics Grade, Sigma) in 1 mM HCl was diluted in 50 µL of 20 mM NH_4HCO_3, pH 8.0. A total of 10 aliquots of 5 µL 0.02 µg/µL trypsin in 20 mM NH_4HCO_3, pH 8.0 were obtained and kept at -20ºC until needed. A 5 µL stock was added to the sample, mixed gently prior overnight incubation at 37ºC. The resultant peptide mixture was purified (desalted) and concentrated by using ZipTips with 0.2 µL C_{18} resin (Millipore). These 10 µL pipette tips with chromatography media (0.2 µL C_{18} resin) fixed at its end increase MALDI-TOF MS sensitivity and resolution, therefore were used prior to spotting. The peptide mixture was aspirated and dispensed though the ZipTip to bind, wash and elute.

The ZipTip was first equilibrated by pre-wetting with an automatic P10 pipette, pipetting10 µL 75% methanol in diH_2O (v:v) into tip. The wetting solution was dispensed to waste and the wetting of the ZipTip repeated 3 times. Peptides were loaded and bound to ZipTip's micro bed C18 reversed-phase resin. By pipetting up and down 10 times 10 µL of the sample (aspirated and dispensed in a fresh 1.5 mL Eppendorf tube), the last eluate was discarded. This cycle was repeated until the full volume of the sample (~30 µL) was loaded to the $ZipTip_{C18}$. Sample loading was followed by 3 washes with 0.1% TFA in ddH_2O (v:v) and eluted directly in 3 µL of MALDI matrix solution (saturated solution of α-cyano-4-hydroxycinnamic acid (Agilent Technologies) in 50% of

acetonitrile and 2.5% of trifluoroacetic acid). This was achieved by slowly aspirating and dispensing 10 times before spotting 3 µL onto the MALDI plate (MTP 384 Polished Steel TF Target, Bruker Daltonik GmbH).

2.17.2 MALDI-TOF MS Peptide criteria selection

A solution of BSA peptides was used to calibrate the system, according to manufacturer's instructions. The peak assignment tolerance selected was 50 ppm and the mode quadratic. To improve the quality of the spectra, each mass spectrum was generated from the data deriving from several single laser shots in 500-shot steps from different positions of the sample spot, acquiring only the spectra with an intensity ≥ 104 arbitrary units as suggested by the manufacturer. Finally, peak selection was performed using FlexAnalysis (version 3.3) (Bruker Daltonik GmbH) as described below.

Samples were spotted as per Figure 20 and after following the established criteria (as described below) specific peptides to SafA' (GST-SafA-6xHis) were selected. An example of a specific peak versus a non-specific (BSA specific) is presented in Figure 21.

Sample spotting and spectrum recording

1) Each set of affinity-enrichment consisted of a (GST-SafA'-6xHis) SafA'/large intestine affinity-enrichment (the GST-SafA' affinity-enrichment) and its corresponding negative control: a BSA/large intestine affinity-enrichment (the negative control). The samples were spotted as per Figure 20.

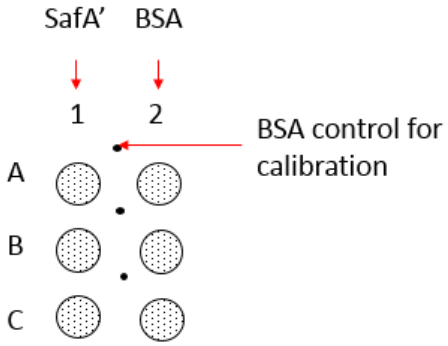

Figure 20. Positioning of SafA' (GST-SafA-6xHis) and negative control affinity enrichment samples spotted on the MALDI plate for MALDI-TOF MS analysis. GST-SafA'-6xHis affinity-enrichment eluents were spotted in column A and BSA negative control affinity- enrichment eluents were spotted in column B. BSA tryptic digests were spotted in-between columns for calibration purposes. Every sample had three spots.

2) Fifty spectra were acquired in each of 3 selected locations giving a good signal with well resolved peak over the whole MW range.

3) Three spectra were selected from the "GST-SafA-6xHis' " affinity enrichment and three spectrum were selected from the "control" affinity-enrichment. These six spectrum were overlaid using the Flex Analysis software (version 3.3) (Bruker Daltonik) and zoomed level to show ten mass units.

Background cut-off

4) The background threshold was manually set up by selecting 4 low intensity poorly resolved peaks. These were used to set the background. Usually, half of the peaks per window were above the threshold of the noise, and at least four peaks were required to setup the background.

Specific peaks rules

5) Where a peak was present in the SafA' (GST-SafA'-6xHis) affinity-enrichment only, the peak should be resolved at the isotopic level, e.g. with a well resolved isotopic partners, to be selected.

6) Intensity of any isotope had to be at least 2x background.

7) At least the peak intensity of one specific peak had to be ≥ 2x in comparison to highest non-specific peak.

8) After selection, all masses obtained from the 3 spectra were averaged and proteins were identified from the list of peaks as peptide mass fingerprint. These were searched with Mascot engine (Matrix Science, version 2.4.1) against a database of 546, 238 sequences derived from reference proteome of *Rattus norvegicus* (http://www.uniprot.org). The tryptic digestion setting was set up to two missed cleavages with no modifications allowed and the peptide tolerance ± 0.01% The list of masses was also searched with ProteinProspector against a database of 48, 573, 147 sequences also derived from the proteome of *Rattus norvegicus* (http://www.ncbi.nlm.nih.gov) and the same settings as above were applied.

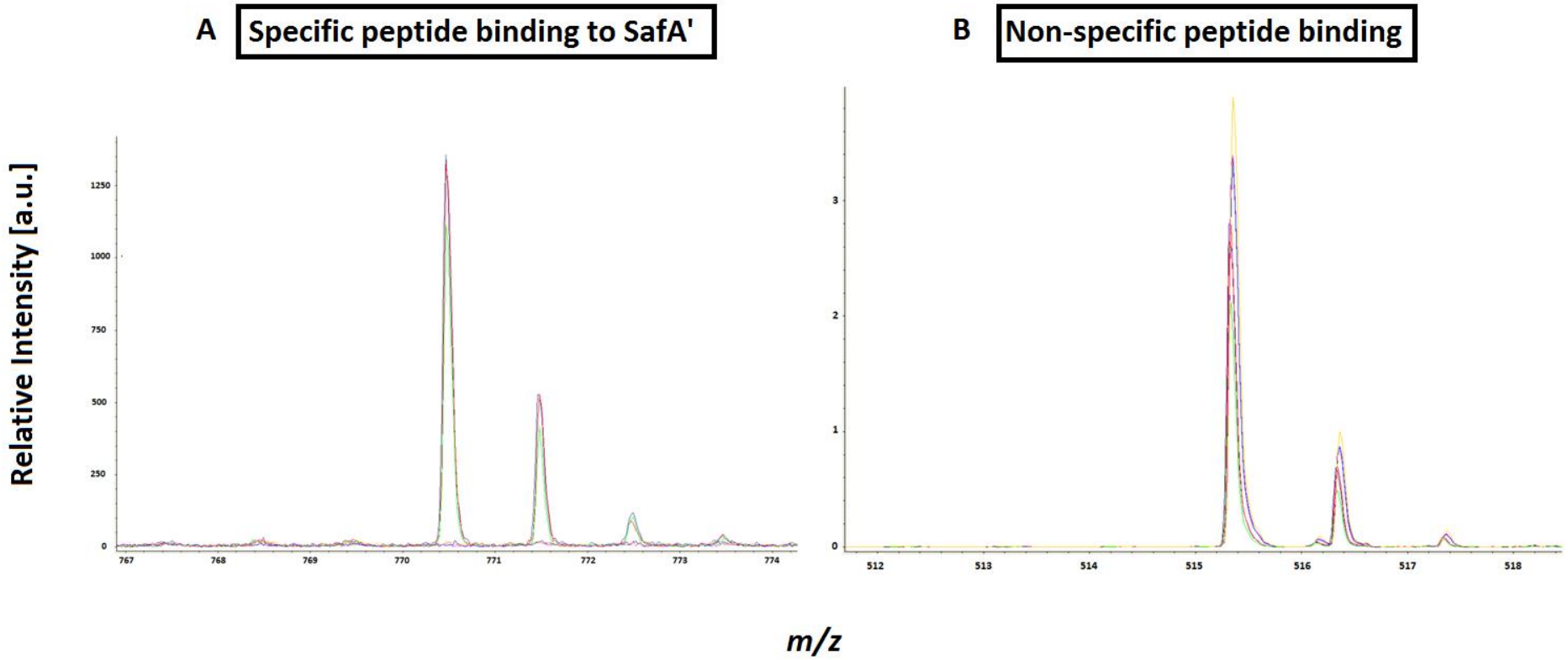

Figure 21. A representative image of peak selection by MALDI-TOF MS. Panel A gives an example of specific peptide binding to SafA' (GST-SafA-6xHis). Three spectra of GST-SafA-6xHis/heart (green, pink and dark blue) were overlaid together with three spectra of BSA/heart affinity-enrichment (yellow, red and light blue. Image shows the binding of a peptide exclusively to GST-SafA-6xHis as represented by the dark blue, green and pink peaks. Panel B gives an example of non-specific peptide binding to BSA (all six spectra indicate the same peak is present in the BSA affinity-enrichment). The six spectra were overlaid in the same way as previously. Image shows the peptide binds without a preference to either GST-SafA' or BSA. Image was taken using FlexAnalysis (version 3.3) (Bruker Daltonik GmbH).

2.18 nanoLC-ESI-MS/MS

Reversed phase chromatography was used to separate tryptic peptides prior to mass spectrometric analysis. Two columns were utilised, an Acclaim PepMap µ-precolumn cartridge 300 µm i.d. x 5 mm 5 µm 100 Å and an Acclaim PepMap RSLC 75 µm x 50 cm ^{2} µm 100 Å (Thermo Scientific). The columns were installed on an Ultimate 3000 RSLCnano system (Dionex). Mobile phase buffer A was composed of 0.1% aqueous formic acid and mobile phase B was composed of 80% acetonitrile containing 0.1% formic acid. Samples were loaded onto the µ-precolumn equilibrated in 2% aqueous acetonitrile containing 0.1% trifluoroacetic acid for 8 min at 10 µL min^{-1} after which peptides were eluted onto the analytical column at 250 nL min^{-1} by increasing the mobile phase B concentration from 3% B to 35% over 27 minutes then to 90% B over 5 minutes, followed by a 4 minutes wash at 90% B and a 12 minutes re-equilibration at 3% B.

Eluting peptides were converted to gas-phase ions by means of electrospray ionization and analysed on a Thermo Orbitrap Fusion (Q-OT-qIT, Thermo Scientific). Survey scans of peptide precursors from 350 to 1500 *m*/*z* were performed at 120K resolution (at 200 *m*/*z*) with a 4×10^5 ion count target. Tandem MS was performed by isolation at 1.6 Th using the quadrupole, HCD fragmentation with normalized collision energy of 35, and rapid scan MS analysis in the ion trap. The MS^2 ion count target was set to 10^4 and the max injection time was 200 ms. Precursors with charge state 2–7+ were selected and sampled for MS^2. The dynamic exclusion duration was set to 45 s with a 10 ppm tolerance around the selected precursor and its isotopes. Monoisotopic precursor selection was turned on. The instrument was run in top speed mode with 2 s cycles.

2.19 Data Analysis

The raw data was processed using MSConvert in ProteoWizard Toolkit (version 3.0.5759) (Kessner etl al 2008). MS^2 spectra were searched with Mascot engine (Matrix Science, version 2.4.1) against a database of 33,515 sequences derived from reference proteome of *Rattus norvegicus* and *Salmonella typhimurium* strain LT2 (http://www.uniprot.org/) and the common Repository of Adventitious Proteins Database (http://www.thegpm.org/cRAP/index.html). Peptides were generated from a tryptic digestion with up to two missed cleavages, carbamidomethylation of cysteines as fixed modifications, and oxidation of methionines as variable modifications. Precursor mass tolerance was 20 ppm and product ions were searched at 0.8 Da tolerances.

Scaffold (version Scaffold_4.3.2, Proteome Software Inc.) was used to validate MS/MS based peptide and protein identifications. Peptide identifications were accepted if they could be established at greater than 95.0% probability by the Scaffold Local FDR algorithm (Jones et al 2009). Protein identifications were accepted if they could be established at greater than 95.0% probability and contained at least 2 identified peptides. Protein probabilities were assigned by the ProteinProphet algorithm (Nesvizhskii et al 2003). Proteins that contained similar peptides and could not be differentiated based on MS/MS analysis alone were grouped to satisfy the principles of parsimony. Proteins sharing significant peptide evidence were grouped into clusters.

Further to this, all proteins identified based on the Scaffold FDR thresholds were curated for any contaminants coming from the user, such as, keratin from hair and skin. Contaminants introduced during the workflow, such as, trypsin and BSA powder were also removed from the list of identified proteins. At this point, a two-step analysis was carried where 1) any proteins identified from the negative controls (BSA or GST) were removed regardless if identification was due to the presence of one peptide. This reduced the list to 190 proteins that were identified in any of the undepleted cleaved SafA' (GST+SafA-6xHis) affinity-enrichments' only. 2) the list was reduced to a final 5 by dismissing any protein identified with any less than 2 peptides in both cleaved SafA' affinity enrichments.

CHAPTER III – CONSTRUCT DESIGN TO EXPRESS RECOMBINANT SAFA' (GST-SAFA-6XHIS)

3.1 Introduction and Rationale

Salmonella is a gram-negative bacterium and the exterior of their cell surface has flagelli, fimbriae and pili (Bardy et al 2003). These are distributed along the bacterium cell; Figure 22, Panel A shows a schematic difference in their structures. The flagellum is an appendage that holds a long rotating filament whose movement is used by the cell to push itself forward (Rossez et al 2015, Samatey et al 2004). Pili are hollow appendages used to transfer DNA to other cells and also function in cell adhesion (Melville and Craig et al 2013, Proft and Baker et al 2009, Ribet and Cossart et al 2015). Fimbriae are thin and hair-like structures that help in adhesion to surfaces and other cells (Kainulainen and Korhonen et al 2014, Proft and Baker et al 2009). These long flexible bodies are formed of protein polymers and are found on the surface of a number of gram-negative bacteria. Examples of these are *Escherichia coli* (Vizcarra et al 2016), *Neisseria gonorrhoeae* (Winther-Larsen et al 2001), *Streptococcus pyogenes* (Becherelli et al 2012), *Pseudomonas aeruginosa* (Ruer et al 2007) and *Sulfolobus acidocaldarius* (Henche et al 2012).

As in uropathogenic *E. coli* (UPEC) (Barnhart et al 2000) and Diffusely Adherent *E. coli* (DAEC), *Salmonella* has fibrous organelles that are present on its surface, they are referred to as Salmonella atypical fimbriae (Saf). The fimbriae are made of four subunits, SafA, SafD, SafC and SafB. SafC and SafB make up the intracellular region of the pilus while the main body is composed of a polymer of SafA subunits interlinked together by its N-terminal peptide with SafD located at the tip of the fimbriae, serving as a cap (Salih et al 2008).

The *Salmonella* fimbriae (Figure 22, Panel B) have been less studied than the ones in other bacteria but based on structural homology with the *E. coli* protein PapD (Ford et al 2012), Afa/Dr adhesins (Cota et al 2006) and *Yersinia pestis*, Caf1 protein (Zavialov et al 2005) it is thought that they function in cell adhesion (Humphries et al 2001, Remaut et al 2006). Each fimbria is formed of a polymer of more than 100 SafA monomers interlinked through an N-terminal peptide (Salih et al 2008).

The major goal of this thesis it to contribute to our understanding of SafA structure and function. For such studies it is desirable to work with a well-defined protein, rather than

a polymer. We therefore designed a construct that would encode a functional monomer of SafA. The design of the constructs to be used in this thesis are crucial for the success of the different experiments proposed. Therefore, in this chapter, we will delineate the details of the constructs of recombinant SafA' (GST-SafA-6xHis) used in this thesis. We will present the rationale behind the isolation of a stable monomeric SafA subunit from the Saf fimbriae (the flexible body of which is made of a chain of SafA subunits) and the choice of tags. The approach to design a monomer of SafA that is similar to the study of other bacterial fimbria proteins previously reported (Anderson et al 2004, Cota et al 2006).

3.2 Results: Construct design of *Salmonella* recombinant protein SafA' (GST-SafA-6xHis)

As the native form of SafA is a polymer made of several (>100) subunits, the only crystal structure available to date (Salih et al 2008) was used to understand the assembly of the fimbria (Figure 22, Panel A). It was imperative to assess the impact that the isolation of a single SafA subunit from a polymer would have in the folding and stability of the construct.

By using on-line molecular protein structure visualization and manipulation tools, such as Cn3D http://www.ncbi.nlm.nih.gov/Structure/CN3D/cn3d.shtml and JSmol http://jmol.sourceforge.net/) we inspected the crystal structure of each SafA subunit and how it is dependent on the structure of the previous SafA subunit (Salih et al 2008). Moreover, SafA has an Ig-like structure lacking the last (G) β strand of a typical seven-stranded immunoglobin fold (Berry et al 2014, Remaut et al 2006). By not having a complete structure, this leaves an exposed empty cleft between two of the β-sheets of the subunit. Therefore, SafA subunits are equipped with a short linker, denominated the N-terminal peptide, to embrace and create a chain (Salih et al 2008). To be technically accurate, their structure is completed by donor strand complementation (DSC) linked together when the N-terminal G_d of the previous subunit is inserted into the hydrophobic cleft (Rose et al 2008, Zavialov et al 2002).

As the native form of SafA is a polymer (Figure 23, Panel A), forming the fimbria, isolating a single SafA subunit would result in a hollow SafA monomer with an exposed hydrophobic empty cleft; and an N-terminal peptide sticking out of the structure trying to reach the previous subunit (Figure 23, Panel B). Based on these observations, it was decided to prepare a construct that includes the N-terminal peptide inserted into the empty cleft, creating a new N- and C-terminus, therefore closing the structure (Figure 23, Panel C). With affinity-enrichments planned, GST and 6xHistidine tags were added to the N-

and C-terminus respectively. The consultation of other published work supported the design of this study (Anderson et al 2004, Barnhart et al 2000, Cota et al 2006).

Initially, the goal of the thesis was not only to investigate SafA but also SafD. However, during the course of my study, published work (Cota et al 2006) showed that the experimental design to analyse SafD was flawed because we had designed an unstable SafD monomer by not completing its Ig fold-like structure. Unlike SafA' where we did complete the Ig fold-like structure by inserting the N-terminal peptide into the empty cleft. Because of this, all the work carried in SafD' has not been included in this thesis.

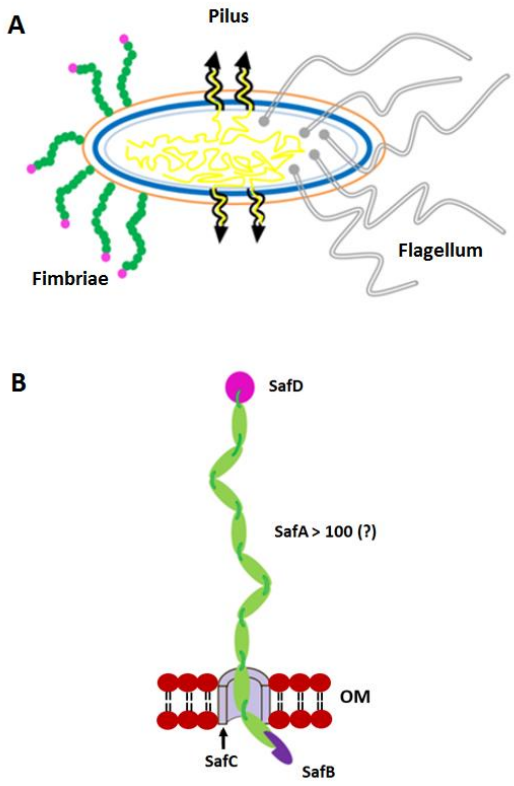

Figure 22. Salmonella's external structures. (A) Fimbriae are hairlike structures that help in adhesion to surfaces and to other cells. Pili are hollow appendages used mainly to transfer DNA to other cells. Flagella are appendages which specific function is to move and push the cell and provide motility. **(B) Schematic representation of the Saf Fimbriae.** The Saf fimbriae flexible body is mainly formed of a polymer of SafA subunits, it is hypothesized that SafD sits at the tip of this polymer, next to the most distal SafA subunit. SafB is the fimbria assembly chaperone and it transiently completes SafA's Ig fold-like structure during assembly. SafC is the outer membrane usher and together with SafB they are necessary for fimbriae biogenesis.

3.3 Engineering of *Salmonella* recombinant protein SafA' (GST-SafA-6xHis)

The only available crystal structure to date for SafA is that of a polymer (Figure 23, Panel A). The structure provided by Salih et al (2008) was inspected in Cn3D http://www.ncbi.nlm.nih.gov/Structure/CN3D/cn3d.shtml and JSmol http://jmol.sourceforge.net/. Figure 23 describes step by step the process leading to the design of the SafA' (GST-SafA-6xHis) monomer. Figure 23, Panel A shows the structure for two SafA subunits, which are actually three chains. Chain A belongs to a first SafA subunit, chain B belongs to a second SafA subunit and chain C to the "N-terminal peptide" belonging to a third SafA subunit, not depicted in the crystal image because it becomes then superimposable with the N-terminal peptide of the first chain (Chain A). The image presents SafA as a polymer where the structure of one subunit is dependent on the previous one by means of an N-terminal peptide donor strand. Figure 23, Panel B shows the structure of a single SafA subunit to be Ig-like (Salih et al 2008, Zavialov et al 2016) , with a missing G β-strand, which upon elimination of the N-terminal peptide (from the previous subunit, when the N-terminal peptide is missing, this exposes a hydrophobic empty cleft indicated by red dotted line in Figure 23, Panel B). The structure leaves a floating N-terminal peptide. Based on the above, it was decided to design a folded SafA monomer with the N-terminal peptide inserted into the empty cleft similarly to an Ig fold-like structure (Figure 23, Panel C). The presence of Immunoglobulin domains provides bacteria with well documented advantages during adhesion, the infection process and invasion (Barnhart et al 2000, Bodelón et al 2013, Holmgren and Bränden et al 1989).

The resulting engineered SafA was named SafA', which stands for the dual tagged construct GST-SafA-6xHis (Figure 24). To summarize, the design involved creating a monomeric version of SafA by shifting the N-terminal peptide (first 19 peptides of the mature sequence) inwards to fill in the empty cleft, thus, in this way creating a new C-terminus (Figure 23, Panel C). Placing the N-terminal peptide inside the empty cleft provided the missing beta strand to complete the protein's Ig fold-like structure. In addition, by closing and self-complementing the structure in this way we avoid any possible polymerization.

The predicted impact of each tag on the proteins' physical and chemical properties is shown in Table 11. The table lists the effects of adding each tag on molecular weight (MW), hydropathy (represented by GRAVY) and isoelectric point (pI) (Gasteiger et al 2005). The most notable effect was on the MW and hydrophathy, where native SafA is

~15 kDa and recombinant SafA' (GST-SafA-6xHis) is ~43 kDa, whereas the change in GRAVY (-0.124) signified the construct was less hydrophobic than native SafA. The pI was essentially unaffected. Finally, GST and Histidine fusion tags were placed at the new N- and C- terminus respectively.

Table 11. Physical and chemical properties of recombinant protein SafA' (GST-SafA-6xHis) and its constituents.

Protein	*MW (Da)	*GRAVY	*pI
GST	25700.8	-0.375	5.90
Poly-His	840.8	-3.200	7.21
SafA	15344.1	-0.219	6.16
SafA' (GST-SafA-6xHis)	43310.4	-0.343	6.19

*MW: molecular weight. *GRAVY: grand average of hydrophobicity.

*pI: isoelectric point

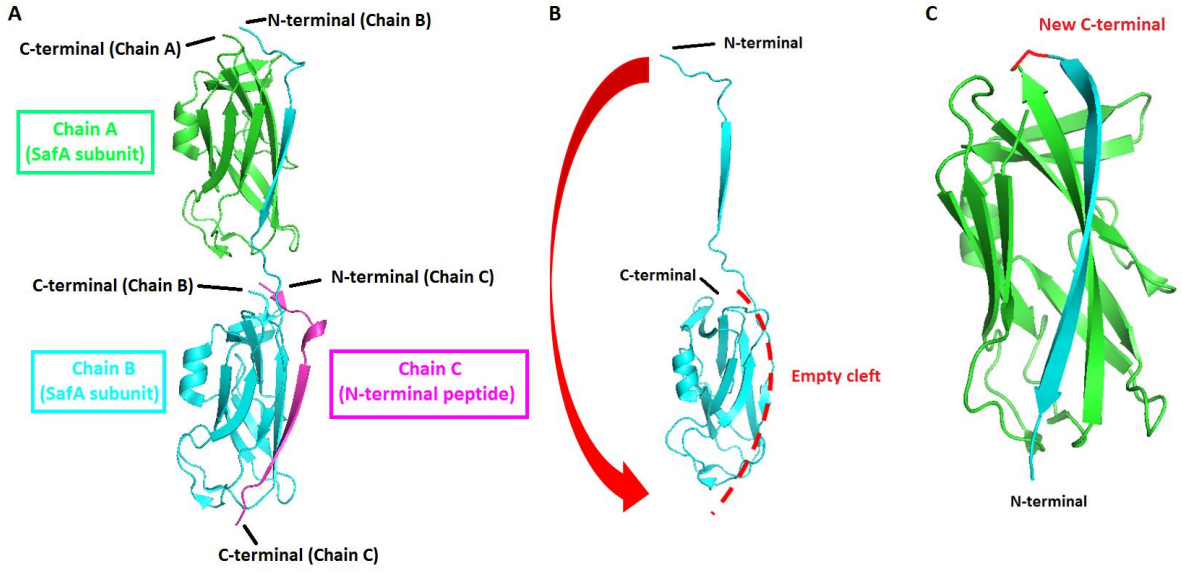

Figure 23. Engineering of recombinant SafA' (GST-SafA-6xHis). (A) SafA subunits forming a polymer. The previous subunit completes the following subunit's structure by providing its N-terminal peptide. **(B) Representation of an isolated SafA subunit.** The empty cleft at the centre of the protein indicates the structure of a SafA subunit is not complete if isolated. Each subunit is equipped with its own N-terminal peptide to link itself to the next subunit**. (C) Final SafA' (GST-SafA-6xHis) design.** A single subunit was isolated and the structure was stabilized by inserting the N-terminal peptide into the empty cleft. The figure was created using the SafA coordinates from PDB ID: 3CRE from the crystal structure proviuded by Salih et al (2008).

3.4 Choice of tags for SafA' (GST-SafA-6xHis) recombinant protein and its expression

To enable purification, GST and Histidine fusion tags were placed at the new N- and C-terminus respectively after insertion of the N-terminal sequence (Figure 24) (Anderson et al 2004, Cota et al 2006, Zavialov et al 2003, Zavialov et al 2005, Zavialov et al 2007). The purpose of the recombinant human rhinovirus (HRV 3C) sequence was to allow cleavage of the GST tag (Cordingley et al 1990, Ullah et al 2016). A four-residue linker (GSGS) was placed at the start and at the end of the SafA sequence in order to create adequate distance between the amino acid protein sequence and the fusion tags.

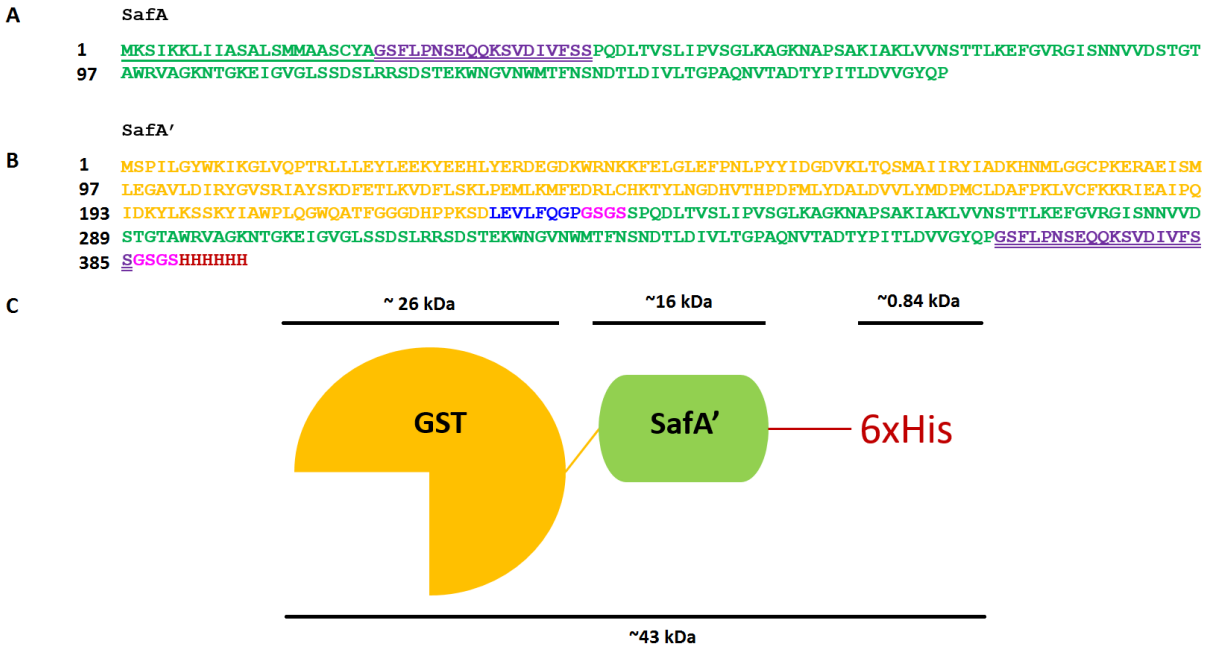

Figure 24. The SafA' (GST-SafA-6xHis) construct. (A) Amino acid sequence of SafA. Signal peptide formed of 22 amino acids (green and underlined), N-terminal peptide consisting of 19 amino acids (purple and double underlined). The rest of the sequence is in green. **(B) Amino acid sequence of the SafA' (GST-SafA-6xHis) construct.** For immobilization purposes GST tag was added to the N-terminal (yellow), the recombinant human rhinovirus (HRV 3C) site is shown in blue, $(GS)_n$ linkers at the beginning and at the end of SafA in pink. The signal peptide was not used for the design and the N-terminal peptide which is double underlined (purple) differs in position from the original sequence. The 6xHistidine tag was placed at the C-terminal as a second option for immobilization (red). **(C) Schematic description of the structure of SafA' (GST-SafA-6xHis).** Sequence, fusion tags, linkers and cleavage sites are represented in diagrams in matching colours to the full amino acid sequence construct. Image not to scale.

The described recombinant *Salmonella* SafA (SafA'/GST-SafA-6xHis) was produced in BL21(DE3) Competent E.*coli* cells by ACRObiosystems. The resulting SafA' (GST-SafA-6xHis) has a calculated MW of 43 kDa and the experimental results confirmed the expected MW (Figure 25).

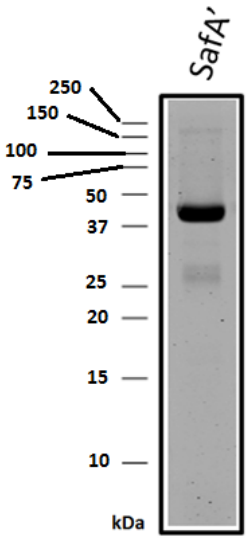

Figure 25. 15% SDS-PAGE analysis of recombinant SafA' (GST-SafA-6xHis) protein. 1 µg of SafA' (GST-SafA-6xHis) was reduced by adding a final concentration of 10 mM DTT. The sample was heated for 5 minutes at 95ºC and loaded into the gel. Image of the Coomassie stained gel was produced using Odyssey Infrared Imaging system.

3.5 HRV 3C protease cleaves SafA' (GST-SafA-6xHis) yielding a complex mixture

Where indicated, the GST tag was cleaved from GST-SafA-6xHis by using the HRV 3C protease (Chapter II, Section 2.14.1 and Chapter II, Figure 18). The protease recognizes the sequence Leu-Glu-Val-Leu-Phe-Gln-Gly-Pro between the Gln and Gly residues. It was important to determine the optimal ratio between HRV 3C protease and GST-SafA-6xHis in order to efficiently cleave GST, therefore 5 µg of GST-SafA-6xHis was incubated with different protease concentrations. Figure 26, Panel A shows the incubation of GST-SafA-6xHis with protease amounts added ranging from 0.25 µg to 8 µg. The results show the protease can cleave GST from GST-SafA-6xHis by using as little as 0.25 µg. The size of the protease is ~45 kDa and a band is visible on the gel. In total, there were three bands present in each sample. Based on the size of the bands these are suggested to be GST at ~26 kDa, cleaved SafA (SafA-6xHis) at ~16 kDa and the protease at ~43 kDa. As per Figure 26 (Panel A, Lane 1), a 1:20 protease to protein ratio was sufficient to cleave GST from SafA' (GST-SafA-6xHis). A low amount is desirable to minimize the abundance of the protease in the sample. Subsequently, the samples were depleted of GST and protease. Figure 26, Panel B shows incubation of the samples with GSH resin results in capturing most of the ~26 kDa species, indicating that the free GST present in the sample was removable by the resin. However, a small amount of free GST remained even after depletion as evidenced by the weak band at the size of GST in Figure

26, Panel B, Lane 3. All relevant physico-chemical properties of the different variants of the construct are provided for reference in Table 12.

Table 12. Wild type SafA, SafA' (GST-SafA-6xHis), cleaved SafA' (SafA-6xHis) and GST values calculated using on-line molecular tools. The Extinction coefficient used are the ones assuming all cysteines are reduced (bold).

	Wild type SafA (without signal peptide)	**Cleaved SafA' (SafA-6xHis)**	**GST**	**SafA' (GST-SafA-6xHis)**
MW (kD)	15.24784	16.88752	26.41344	43.28294
Bp	144	161	226	387
pI	6.43	7.20	5.73	6.19
Ext. coefficient	20970	19480	*43110 ****42860**	*62590 ****62340**

*Assuming all pairs of Cys residues form cysteines

** Assuming all Cys residues are reduced

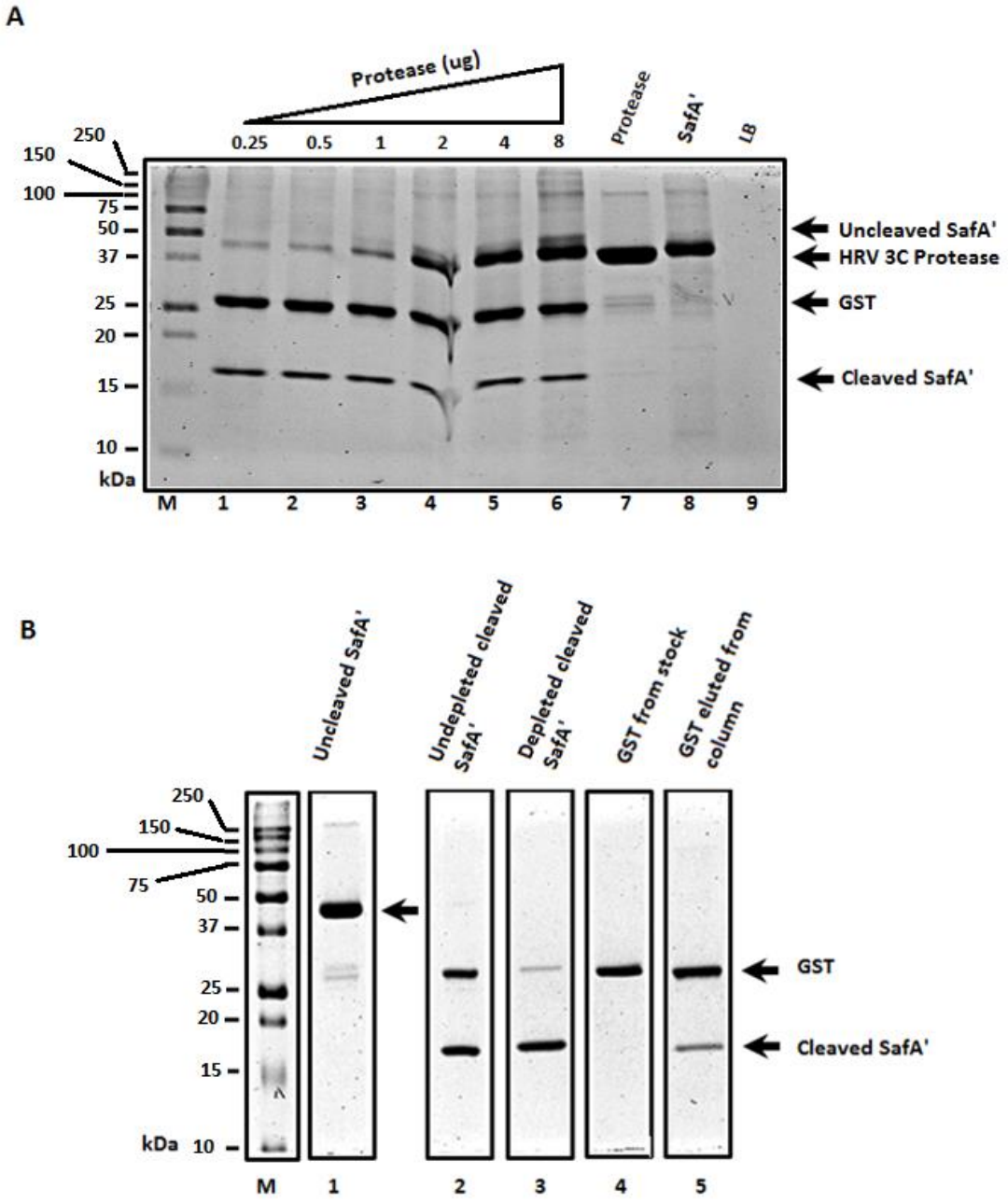

Figure 26. 15% SDS-PAGE gels of cleaved SafA' (SafA-6xHis/GST+SafA-6xHis) samples. Approximately 5 µg of total protein were loaded in each lane (both gels). Proteins were stained with Imperial Protein Stain (Coomassie dye R-250). All samples were heated at 100 ºC for 5 mins. MW, molecular mass marker in kDa. In both gels uncleaved SafA' (GST-SafA-6xHis) and HRV 3C protease migrate as a ~43 kDa polypeptide respectively. Cleaved SafA' (GST+SafA-6xHis) sample shows two bands of ~ 26 kDa and ~ 16 kDa. **(A)** Incubation of uncleaved SafA' (GST-SafA-6xHis) with different concentrations of HRV 3C protease, showing a 1:20 protease to protein ratio (0.25 µg: 5 µg) is sufficient to cleaved GST from GST-SafA-6xHis. **(B)** Depletion of the ~26 kDa (assumed to be GST) from the cleaved SafA' mix (GST+SafA-6xHis). GST was significantly depleted from the cleaved SafA' (GST+SafA-6xHis) sample (3) with apparent no significant cleaved SafA' (SafA-6xHis) loss. GST (4) matches the molecular weight of the observed ~ 26 kDa in the previous samples. The eluate from GSH-column (5) shows the meaningful capture of GST and also the presence of a detectable amount of cleaved SafA' (GST-6xHis). Cleaving of GST from SafA' (GST-SafA-6xHis) and depletion of GST from the cleaved SafA' (GST+SafA-6xHis) sample were successful. Image was taken using the Odyssey scanner.

3.6 Characterisation of cleaved SafA' (SafA-6xHis)

The purity of the samples is crucial for circular dichroism data (Kelly et al 2005). It is also important to know whether the obtained spectra reflect the structure of a monomer or polymer. Not knowing this would make it difficult to deconvolute the data. Because SafA exists as a polymer in nature, it was particularly important to verify whether - especially after cleaving GST - SafA' (GST-SafA-6xHis) was polymerizing. Native-PAGE, also known as non-denaturing gel electrophoresis (prepared in the absence of SDS) was used to investigate if there were polymers present. Whereas in SDS-PAGE gels proteins migrate according to their molecular mass, in Native-PAGE proteins migrate according to their charge and hydrodynamic size. Figure 27, Panel A shows neither uncleaved SafA' (GST-SafA-6xHis) or cleaved SafA' (GST+SafA-6xHis) show any evidence of polymers present. This is concluded based on the fact that only one band is observed in each lane at a position consistent with monomeric size.

Figure 26, Panel A had already indicated that the samples after GST cleavage represent a mixture of GST, cleaved SafA' (SafA-6xHis) and the HRV 3C protease. To further corroborate this conclusion, the samples were subjected to western blot analysis. Figure 27, Panels B-D show the western blot results of the cleaved SafA' (GST+SafA-6xHis) sample. The incubation of the cleaved SafA' (GST+SafA-6xHis) sample with anti-recombinant SafA' (GST-SafA-6xHis) (Figure 27, Panel B) recognized both bands, indicating they were both either GST, SafA-6xHis or a dimer of these. Anti-GST recognized the ~26 kDa band only (Figure 27, Panel C), in this way confirming the presence of, both, GST and cleaved SafA' (SafA-6xHis) in the mixture. Therefore, the bands present in Figure 27, Panel D, Lane 3 correspond to GST (~26 kDa) and cleaved SafA' (SafA-6xHis) (~16 kDa).

Based on these results we can ascertain that cleaving of GST from SafA' (GST-SafA-6xHis) was successful as it yielded a mixture of GST, cleaved SafA' (SafA-6xHis) and HRV 3C protease. Figure 28 summarizes all the SafA' (GST-SafA-6xHis) variants (GST+SafA-6xHis and SafA-6xHis) obtained and these will be used throughout the thesis. Moreover, it has been confirmed that the design of the SafA subunit does not polymerize at any stage and is suitable for CD studies. Finally, depletion of GST from the sample was mostly achieved, with the depleted cleaved SafA' (SafA-6xHis) sample containing only trace amounts of GST present and this has been taken into consideration during the analysis of CD data.

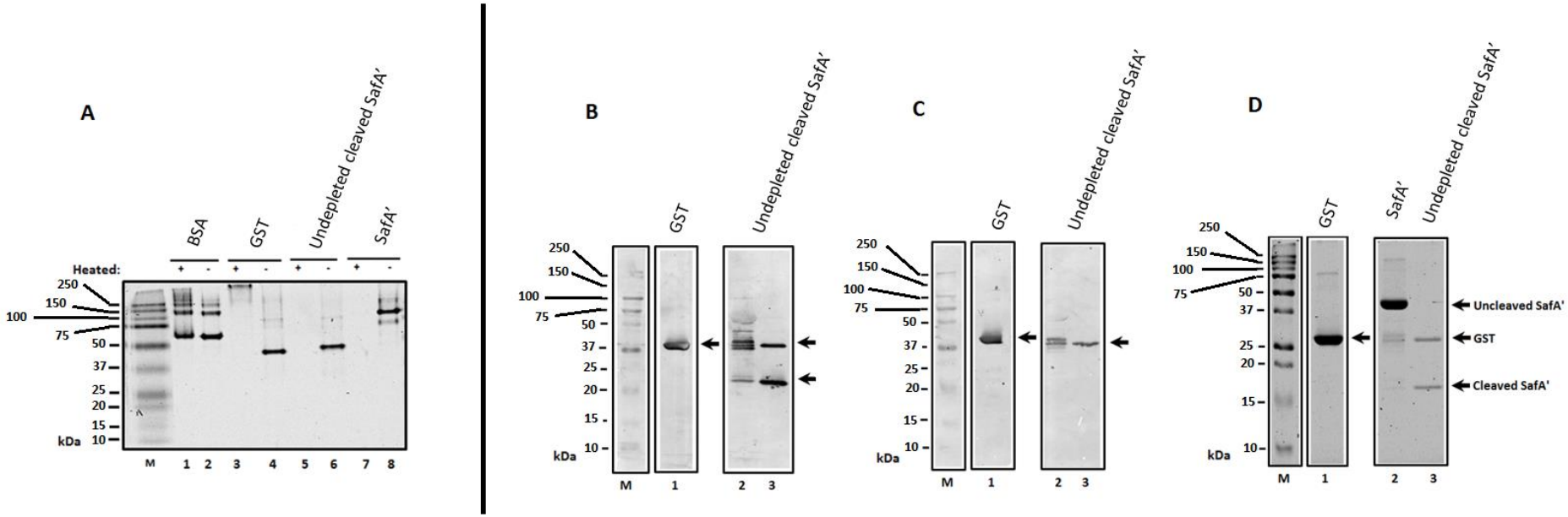

Figure 27. Analysis of observed bands in the cleaved SafA' (GST+SafA-6xHis) sample by Native-PAGE and Western blot. Approximately 5 µg of total protein was loaded in each lane. MW, molecular mass marker in kDa. Where applicable, proteins were stained with Imperial Protein Stain (Coomassie dye R-250). Images were taken using the Odyssey scanner from LI-COR. **(A) 15% Native-PAGE gel of cleaved SafA' (GST+SafA-6xHis).** Samples in lanes 1, 3, 5 and 7 were heated at 100 ºC for 5 minutes. BSA migrates regardless of being heated or not, whereas the rest of the samples cannot be visualized after heating. All proteins seem to migrate as monomers, therefore cleaved SafA' (GST+SafA-6xHis) does not polymerize. **(B-D) Western blot analysis of proteins present in the cleaved SafA' (GST+SafA-6xHis) mix.** The samples used throughout the three experiments belong to the same aliquot. All samples were heated at 100 ºC for 5 mins. **(B)** Incubation of GST (1) and undepleted cleaved SafA' (GST+SafA-6xHis) (2)(3) with anti-uncleaved SafA' (GST-SafA-6xHis). **(C)** Incubation of GST (1) and undepleted cleaved SafA' (GST+safA-6xHis) (2)(3) with anti-GST. **(D)** 15% SDS PAGE gel of GST (1) and undepleted cleaved SafA' (GST+safA-6xHis) (3) as used in the western blots, in addition to uncleaved SafA' (GST-SafA-6xHis) (2) for comparison purposes. Image was taken using the Odyssey scanner.

.

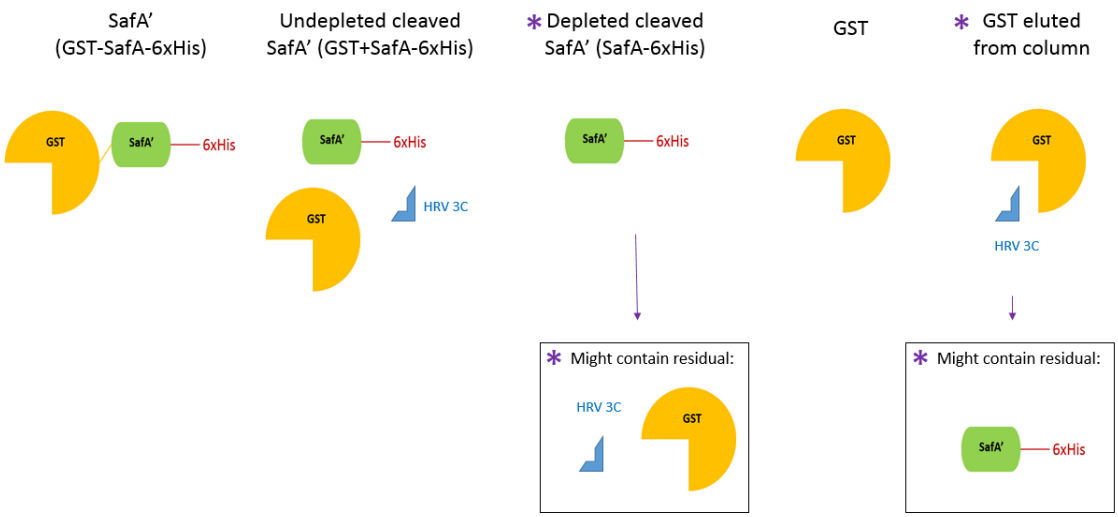

Figure 28. Representation of SafA' variants obtained after cleaving GST from construct. (A) Construct as designed. **(B)** Resulting mixture of proteins after GST cleavage from construct. **(C)** After Depletion of GST and HRV 3C protease from cleaved SafA' (GST+SafA-6xHis) mixture some residuals would still remain in the sample. **(D)** GST protein directly from stock. **(E)** GST protein eluted from column will also have HRV 3C protease in the mixture and possibly SafA-6xHis residuals.

3.7 Discussion

We designed an isolated recombinant version of the *Salmonella* fimbrial protein SafA based on its only crystal structure available (Salih et al 2008). SafA forms most of the external fimbria structure and based on its similarities with *E. coli* fimbria protein AfaE it is hypothesized to be an adhesin (Anderson et al 2004). In this study, SafA included a poly-His tag which was added to the new C-terminal and a GST tag added to the new N-terminal (Figure 24).

In nature SafA exists as a polymer and the structure of one subunit is dependent on the neighbouring unit through the N-terminal peptide (Rose et al 2008, Salih et al 2008). The disruption of the structure without taking into consideration SafA's Ig-like structure would have resulted in an unstable protein unlikely to be functional. The idea of inserting the N-terminal peptide into the empty cleft allowed completing the subunit's structure without compromising its stability. An analogous approach has been used to study the structure of other fimbria proteins (Anderson et al 2004, Cota et al 2006, Zav'yalov et al 2010). These monomers have not been used for affinity-enrichments or Co-IP's so far, but application of surface plasmon resonance (SPR) to quantify the binding of known protein-receptor interactions has been described (Berry et al 2014). The previous work further supports that our approach is appropriate and is expected to result in a stable and

functional monomer, competent to bind other proteins. However, while a monomeric form is required for handing and interpretation of biochemical and biophysical studies of the samples, it is not certain if the SafA monomer would interact with the host in the same manner as when a polymer because to date and to our knowledge, there is no published work where this has been attempted. Functional studies (Chapter VII, Section 7.5) carried out with adequate controls would be required to check whether the function of SafA is hindered by being isolated from the polymer.

For instance, the incubation of intestinal epithelial cell lines with the SafA' (ideally with both tags cleaved) monomer in comparison with the incubation of SafA-tagged *Salmonella* could highlight such potential differences. Further to this, SafA-SafA interactions and the kinetics on the assembly of the polymer could be studied. This would lead to the understanding of the fimbria and perhaps gather information that might lead to fimbria disruption. Such studies are beyond the scope of this thesis and represent interesting future directions of research in this area.

The addition of a tag may affect the folding and solubility of the recombinant protein and the choice also depends on downstream applications (Costa et al 2014, Young et al 2012). GST and poly-His tags were selected from the variety of resins/beads currently on the market for affinity-enrichments and the availability of commercial antibodies based on their proven success. The addition of a GST-tag (MW 26 kDa) may stabilize the recombinant protein and to protect against intracellular proteolysis (Kosobokova et al 2016, Terpe et al 2003). On the other hand, GST may create steric hindrance due to the relative large size with respect to SafA with the consequence of blocking interacting proteins (Hanson et al 2015, Wu and Oppermann et al 2003, Zhao et al 2013). It is worth mentioning that inconsistency was found in literature regarding the effects of GST on solubility. Some studies claimed negative effects (DelProposto et al 2009, Raran-Kurussi and Waugh et al 2012, Shen et al 2009), and improvements required adding detergents (Arnau et al 2006, Harper and Speicher et al 2011).

Polyamino acid constructs, such as, poly-His are widely used due to their small size (0.84 kDa) and low immunogenicity (Bornhorst and Falke et al 2000). Disadvantages are the protein's charge may be changed and this can affect the function of the protein (Wu and Filutowicz et al 1999). In general, having two tags may be advantageous to immobilize the recombinant proteins in two different orientations, the N-terminal by Poly-His tag and the C-terminal by GST-tag and allows potential two-step purification. These also gave

the option of selecting more than one affinity-enrichment system. For this reason, the impact of each tag in the proteins' physico-chemical properties was investigated (Table 11). The change in GRAVY (-0.124) indicated that in our particular case addition of a GST tag would improve solubility. Therefore, it was decided to use chimeric GST-SafA'-6xHis constructs for this study.

Overall, the recombinant protein design is similar to the earlier reported engineered AfaE and AfaD *E.coli* proteins (Anderson et al 2004). After searching for SafA homolog structures we found a particularly striking similarity between Afa/Dr fibrils and the Saf fimbria. Afa/Dr adhesins are produced by *Escherichia coli* strains which produce chronic diarrhea and recurrent urinary tract infections (Mansan-Almeida et al 2013). These fimbriae are also assembled via the chaperone/usher pathways and the AfaD protein caps the AfaE fibrils. Upon observation of the crystal structure of AfaD and AfaE docking we could see these fibrils are formed by a polymer of AfaE subunits and similarly to SafA this is linked to AfaD by an N-terminal strand.

In conclusion, the design of the construct was suitable for stability and function of the SafA protein as it was similar to previous studies of the analogous Afa/Dr adhesins. A stable SafA monomer was isolated from the fimbria by inserting the N-terminal peptide into the empty cleft to complete the proteins' Ig fold, and thus the work of this thesis opened the door to biophysical and biochemical studies of SafA.

CHAPTER IV - BIOPHYSICAL CHARACTERIZATION OF RECOMBINANT SAFA' (GST-SAFA-6XHIS) BY CIRCULAR DICHROISM (CD) AND DIFFERENTIAL SCANNING FLUORIMETRY (DSF)

4.1 Introduction and Rationale

We used circular dichroism (CD) spectroscopy to investigate secondary structure and stability of our GST-SafA-6xHis construct and also to compare the GST-fused construct with the protein after cleavage. The influence of the GST tag on SafA' (GST-SafA-6xHis) needed to be investigated to ensure that it does not interfere with the folding and stability of SafA' (GST-SafA-6xHis). GST is a ~26 kDa protein whereas SafA is a ~16 kDa protein and its native structure is a polymer, therefore it was plausible that such a tag might influence folding and/or stability of the protein. Moreover, to make the analysis well-founded we decided to cleave GST from the construct. This allows us to be absolutely certain that any captured proteins have exclusive affinity for SafA-6xHis. Thus, we investigated SafA' (GST-SafA-6xHis) secondary structure in the presence and absence of the GST. Fused GST was cleaved from the construct between Gln and Gly by using Human Rhinovirus 3C protease (HRV 3C Protease) (Ullah et al 2016) (see Chapter II, Section 2.14).

As described in the introduction (Chapter I, Section 1.16), the CD method is highly suitable for the purpose of structural comparison as it is a premier biophysical approach to determine the secondary structure of proteins (Miles and Wallace et al 2006). This technique is based on the fact that the left and right circularly polarised components of light are absorbed unequally when polarised light of appropriate wavelength passes through a solution of a chiral chromophore (Greenfield et al 2006). Thus, CD measures differences in absorption of left-handed and right-handed circularly polarized light arising from an optically active (chiral) molecule such as a protein (Greenfield et al 2006).

Exciton interactions between aligned amides in the backbone of a polypeptide chain produce characteristic changes to CD spectra (Greenfield et al 2006). This means that deconvolution of the CD spectra of proteins allows estimating the relative contribution of helices (α+PP2), β sheets/strands, turns and random coil structures. In practice, CD is used as an indicator for the foldedness of a protein, especially if the secondary structure composition of a protein is known. Additional complementary approaches to quantitation of secondary structure such as Fourier transform (FTIR) spectroscopy (Bramanti et al

1997, Kong and Yu et al 2007), and coherent two-dimensional infrared (2DIR) (Baiz et al 2012) can be used. For optimal results, the preparation of the sample is crucial with minimal presence of interfering agents such as NaCl, Tris, HEPES, glycerol and DTT/beta-mercaptoethanol and accurate protein concentration determination is vital due to the high sensitivity of the bands to concentration (Raussens et al 2003).

Because we were interested in the stability of the construct, we also carried out Differential Scanning Fluorimetry (DSF) (referred as thermofluor or thermal shift assay) investigation of the samples. In fluorescence melting denaturation, as the protein is subject to increasing temperature its structure will start to unfold and this transition can for example be followed by the addition of fluorescence dye (Johnson et al 2014). The midpoint (transition between the folded and unfolded state) is called the melting temperature (T_m). To complement the CD experiments, we also conducted fluorescence spectroscopy with Sypro® orange (ThermoFisher) (Chapter II, Section 2.16.2). This particular dye binds to hydrophobic surfaces exposed as the protein unfolds, making it an efficient tool to indicate temperature-induced changes (Vollrath et al 2014). For this purpose, reaction mixtures containing the selected protein and dye were prepared. Subsequently, the mixture was added to wells on a 96-well thin-wall PC plate (BioRad). As per materials and methods, Chapter II, Sections 2.16.2 and 2.16.3, the temperature was increased and the fluorescence intensity was measured in relative fluorescence units (RFU) (Goulas et al 2014).

In brief, the results described in this chapter confirm the secondary structure for the designed construct SafA' (GST-SafA-6xHis) is agreement with the published crystal structure in the absence of GST. This section also validates that fused GST does have an impact on the stability of the construct but SafA' (GST-SafA-6xHis) is stable even after cleaving GST.

4.2 Results: Secondary structure content of SafA' (GST-SafA-6xHis) constructs

During the purification process of samples (see Chapter III, Section 3.5), it was noted that the complete removal of GST from the cleaved SafA' (GST+SafA-6xHis) mixture was difficult and a minor band was still observed on the gel even after depletion (Figure 26, Panel B, Lane 3). This was taken into consideration when testing the mixtures by Far-UV CD. A total of five samples were prepared (Figure 28): SafA' (GST-SafA-6xHis), undepleted cleaved SafA' (GST + SafA-6xHis) (an approximate equimolar amount of GST and cleaved SafA'), depleted cleaved SafA' (SafA-6xHis) (mostly cleaved SafA'

with traces of GST), GST from stock and GST eluted from the column after cleavage. Because of the instrument's sensitivity to protein concentration it was imperative to be certain of the protein concentration in each sample. These were measured by absorbance at 280 nm, Qubit 2.0 and Quantitative Amino Acid Analysis (QAA) (see Chapter II, Section 2.15). The results are shown in Table 13.

Inaccurate concentration measurements are the most common source of error during analysis (Miles and Wallace et al 2016). In QAA a protein is hydrolysed into its amino acids, these are separated and quantified (Anders et al 2003, Daviter and Fronzes et al 2013). Currently, this is the most accurate method to obtain the true protein concentration in a sample. Therefore, the measurements produced by the latter were selected for the analysis.

Table 13. Protein concentration measurements of samples for CD studies. Three different methods were used to determine the protein concentration. Quantitative amino acid analysis (QAA) was the most sophisticated of the approaches and this was used for deconvolution of the data. All samples were in 10 mM Potassium Phosphate, pH 8.2 and the concentrations provided take any dilution made into account.

Protein	Absorbance at 280 nm (µg/µL)	Qubit 2.0 (µg/µL)	Quantitative Amino Acid Analysis (QAA) (µg/µL)
Uncleaved SafA' (GST-SafA-6xHis)	0.24	0.20	0.013
Undepleted cleaved SafA' (GST+SafA-6xHis)	*0.2	*0.20	*0.013
Depleted cleaved SafA' (SafA-6xHis)	0.10	0.14	0.083
GST eluted from column	0.1	0.20	0.071
GST stock	0.1	0.17	0.070

*As per SDS-PAGE gel (Figure 26, lane 2), the mixture appears to have an almost equimolar concentration of, both, GST and cleaved SafA' (SafA-6xHis). The QAA analysis only shows the concentration of cleaved SafA' (SafA-6xHis) but not GST, as this is a complex mixture any graphs for the undepleted cleaved SafA' (GST + safA-6xHis) samples has been produced as a reference only.

4.3 Cleaved SafA' (SafA-6xHis) secondary structure corresponds to published crystal structure

The secondary structure of uncleaved SafA' (GST-SafA-6xHis), undepleted cleaved SafA' (GST + SafA-6xHis), depleted cleaved SafA' (SafA-6xHis), GST (stock) and GST eluted from column (originally part of GST-SafA-6xHis) were analysed by far UV CD. It is important to note the undepleted cleaved SafA' (GST+ SafA-6xHis) sample has a significant amount of HRV 3C protease. Figure 29, Panel A; shows the overlaid spectra of all samples. As one can see, both of the GST samples (purchased GST stock and eluted from the GST column, also shown in direct comparison in Panel B) show a strong positive peak ~192 nm, a negative one at ~222 nm and a another negative peak at ~208 nm. These features are characteristic of the presence of significant amounts of helix in the samples (see deconvolution results in Table 14).

In contrast, the rest of the samples, namely uncleaved SafA' (GST-SafA-6xHis), undepleted cleaved SafA' (GST + SafA-6xHis) and depleted cleaved SafA' (SafA-6xHis) (Figure 29, Panel A) show a positive peak ~195 nm which is considerably smaller in size than the one present in the alpha helix rich GST protein samples. Panel C compares the spectra for depleted cleaved SafA' (SafA-6xHis) and undepleted cleaved SafA' (GST + SafA-6xHis) where the depleted cleaved SafA' (SafA-6xHis) shows a positive weak double peak of ~195 nm (note the change of scale in comparison with Panels A and B). The spectrum has a negative peak ~210 nm and a weak positive peak ~230 nm, characteristic of polyproline helices (PPII). Panel C shows a significant difference in spectra for the GST rich sample (undepleted cleaved SafA' in yellow) where only weak double peaks at ~192 nm (positive) and ~200-230 nm (negative) are detected. Clearly, the spectrum for depleted cleaved SafA' (SafA-6xHis) is consistent overall with a classical β sheets/strands spectrum. This result strongly supports the conclusion that the monomeric sample acquires the structure expected based on the crystal structure (see details in Table 14 for deconvolution results).

Panel D shows the comparison between uncleaved SafA' (GST-SafA-6xHis) and undepleted cleaved SafA' (GST + SafA-6xHis). The undepleted cleaved SafA' (GST+SafA-6xHis) mixture shows a peak at ~192 nm and the uncleaved SafA' (GST-SafA-6xHis) shows a peak ~198 nm. Both spectra show a negative peak ~208 nm. The graph shows a similar CD spectra whether GST is fused to SafA' (GST-SafA-6xHis) or free in the mixture (GST+SafA-6xHis), therefore having GST fused to SafA' (GST-SafA-6xHis) does influence its secondary structure.

As per crystal structure (PDB ID code 3CRE, (Salih et al 2008)), the expected secondary structure of SafA is 4% helical & 49% β sheet/strands; GST is 50% helical & 10% β sheet/strands (1A0F, (Nishida et al 1998)) and HRV 3C is 11% helical & 57% β sheet/strands (2B0F, (Bjorndahl et al 2007)). DichroWeb was used to deconvolute the CD spectra and to predict the secondary structure of the samples. Table 14 shows the total calculated percentages obtained. Depleted cleaved SafA' (SafA-6xHis) is predicted by the deconvolution of the CD data to be predominantly composed of β sheets and strands (5% alpha helices, 49% sheets). Undepleted cleaved SafA' (GST + SafA-6xHis) is conformed of 42% alpha helices, 29% β strands, consistent with the presence of GST.

Uncleaved SafA' (GST-SafA-6xHis) is estimated to consist of 44% alpha helices, 24% β strands. GST (stock) and eluted from column (with traces of cleaved SafA') include 40% helices (each) and 11% & 10% β sheets, respectively. The predictions were performed using the CDSSTR program using SET2 (Optimised for 178-260 nm) reference for depleted cleaved SafA' (SafA-6xHis), SET3 (Optimised for 185-240 nm) reference for undepleted cleaved SafA' (GST+SafA-6xHis) and uncleaved SafA' (GST-SafA-6xHis). Finally, SET5 (Optimised for 178-260 nm) was used for GST stock and GST eluted from column. However, the predictions include turns and unordered (random coil) structures (not shown).

Thus, in summary the secondary structure content predictions for the key samples (cleaved SafA' and GST) matched the expected ones as per the published crystal structures (Table 14). SafA is expected to consist of 4% helical helices and 49% beta sheet based on the crystal structure (PDB: 3CRE) and our predictions based on the CD spectra indeed estimated 5% helical helices and 49% beta sheet. GST, based on its crystal structure (PDB: 1A0F), is expected to consist of 50% helical and 10% beta sheet and our predictions estimated 40% alpha helices and 11% beta sheet. The other two samples (undepleted cleaved SafA' and uncleaved SafA') were both rich in alpha helices (~42%) and beta strands (~29%), which was expected due to the presence of both proteins. It is important to acknowledge that the undepleted cleaved SafA' (GST + SafA-6xHis) sample is a complex mixture and the QAA only determined the concentration for cleaved SafA' (SafA-6xHis), yet, is not as accurate as for the other samples.

In summary, the results confirm our design of the SafA subunit is in line with the known crystal structure.

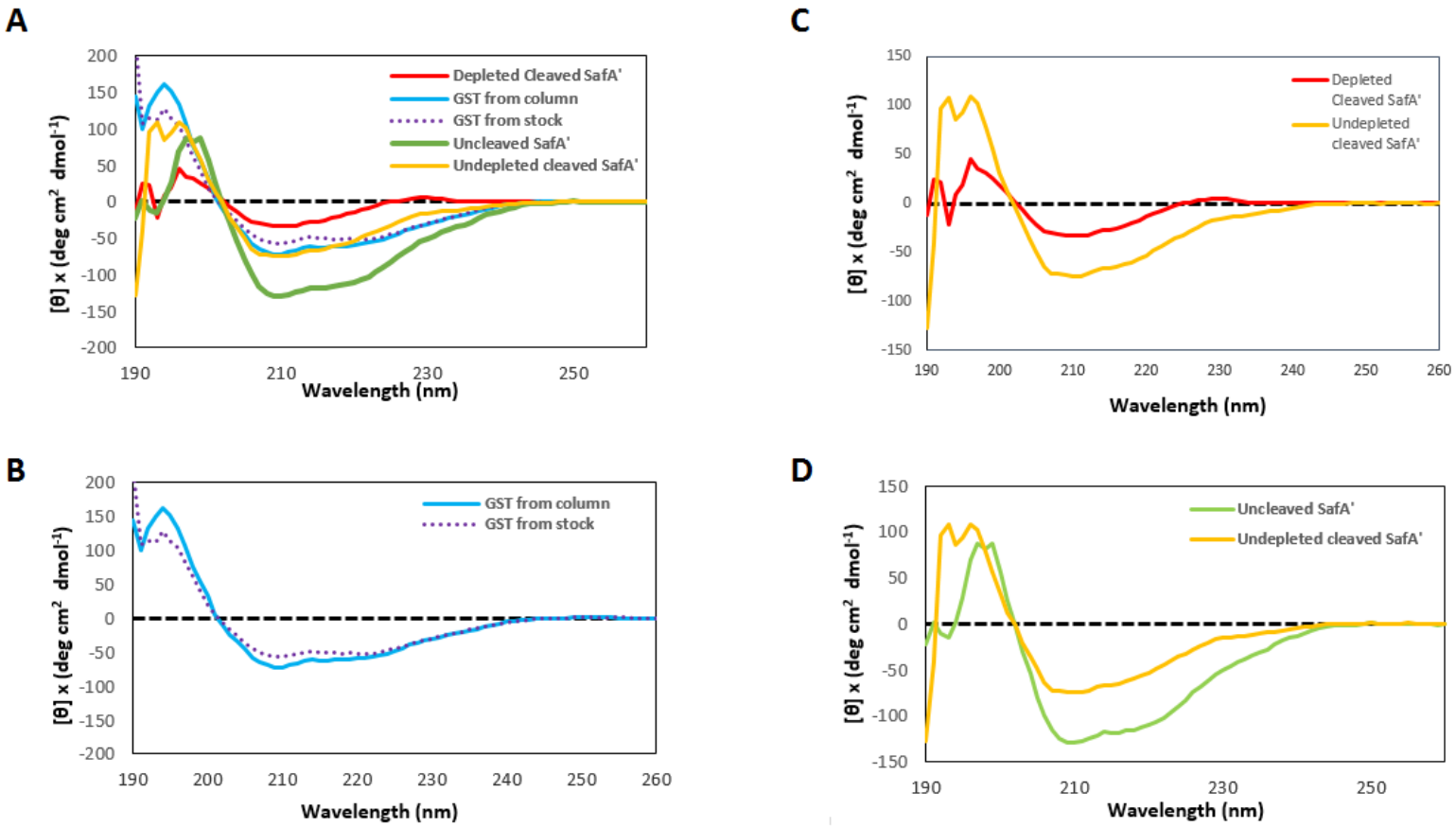

Figure 29. Circular Dichroism spectra of GST, SafA' and its variants. The Far-UV spectra were measured and graphs of the wavelength plotted against the mean residue elipcity (θ) are shown. Data were deconvoluted with the CDSSTR program on the DichroWeb server. **(A)** CD spectra of depleted cleaved SafA' (SafA-6xHis) (red), Undepleted cleaved SafA'(GST+SafA-6xHis) (mustard), uncleaved SafA'(GST-SafA-6xHis) (green), GST from column (sky-blue) and GST eluted from column (dotted purple). The graph shows the difference in structure between GST, GST-SafA-6xHis, GST+SafA-6xHis samples and cleaved SafA' (SafA-6xHis). **(B)** CD spectra of GST eluted from column (sky-blue) and GST from stock (dotted purple). Both samples show comparable structures with the minima at ~208 and ~222 nm. **(C)** CD spectra of depleted cleaved SafA' (SafA-6xHis) (red) and undepleted cleaved SafA' (GST+SafA-6xHis) (mustard). The graph shows the impact that having GST in the mixture has on the spectra. **(D)** CD spectra of uncleaved SafA'(GST-SafA-6xHis) (green) and undepleted cleaved SafA'(GST+SafA-6xHis) (mustard). The presence of GST in the sample regardless on whereas it is fused to the protein or as a free element results in identical spectra.

Table 14. Comparison of published SafA and GST secondary structures with CD predictions. The preditions were in accordance with the known crystal structures. NRMSD stands for normalized root mean square displacement, RMSE/data range).

	SafA crystal structure (%)	Depleted cleaved SafA' (SafA-6xHis)	Undepleted cleaved SafA' (GST+SafA-6xHis) (%)	Uncleaved SafA' (GST-SafA-6xHis) (%)	GST crystal structure (%)	GST stock (%)	GST from column (%)
α helices	4	5	42	44	50	40	40
β sheets/ strands	49 (sheets)	49 (sheet)	29 (strand)	29 (strand)	10 (sheet)	11 (sheet)	10 (sheet)
NRMSD	n/a	0.109	0	0.001	n/a	0.009	0.011

4.4 The fusion of the GST protein to the C-terminus of SafA' (GST-SafA-6xHis) does not affect the folding

To further investigate potential effects of GST on the SafA construct, the uncleaved SafA' (GST-SafA-6xHis), undepleted cleaved SafA' (GST + SafA-6xHis) and GST (eluted from the GSH-resin after cleaving) samples were subjected to thermal fluorescence denaturation studies (Khan et al 2007). This analysis allowed investigating the effect of the GST tag on the stability of SafA' (GST-SafA-6xHis). Figure 30 (Panels A, C and E) shows the thermal transition and calculated melting temperatures (T_m) (Panels B, D and G) for the three samples. With this analysis it is possible to calculate the temperature at which the proteins change their folding state (Naganathan et al 2007). A midpoint is calculated as an indicator of transition between folding and unfolding states (Khan et al 2007). The results indicated that the midpoints of the unfolding transition for uncleaved SafA' (GST-SafA-6xHis), (undepleted) cleaved SafA' (GST+SafA-6xHis) and GST are 59^{o}C, 55^{o}C and 62^{o}C, respectively. These results indicate the Tm for undepleted, cleaved SafA' (GST+SafA-6xHis) decreases with respect to those observed for the uncleaved SafA' (GST-SafA-6xHis) and GST samples.

From the graphs it is also noted that the Relative Fluorescence Intensity (RFU), indicating the rate of protein unfolding (Naganathan et al 2007), for the undepleted cleaved SafA' (GST+SafA-6xHis) sample is higher than that of GST alone. Therefore, it is possible that SafA is folded even in the absence of fused GST, affecting the readings.

The ThermoFluor assay (Section 4.4) results suggest that the fusion of the GST tag SafA positively affects the stability of the protein, based on previous observations that GST is a relatively stable protein and can help stabilize folding of recombinant proteins (Biotech et al 2000, Magdeldin and Moser et al 2012). Despite this, I have established that SafA' (GST-SafA-6xHis) is a folded protein also in the absence of fused GST, as indicated by Figure 30, Panels C and D where Panel C (of GST+SafA-6xHis) shows a graph of a sigmoidal shape (same as for GST-SafA-6xHis and GST, which are known to be folded) which is characteristic of the process of unfolding (Dyson and Wright et al 2005). Also, in Panel C, it can be noted the RFU counts for undepleted cleaved SafA' (GST+SafA-6xHis) are higher than for GST, indicating a higher concentration of unfolded protein present in the sample (Seabrook and Newman et al 2013). Finally, Panel D, shows the calculated Tm is less than uncleaved SafA' (GST-SafA-6xHis, fused GST) but higher than GST only, suggesting SafA-6xHis remains folded in the absence of the GST tag.

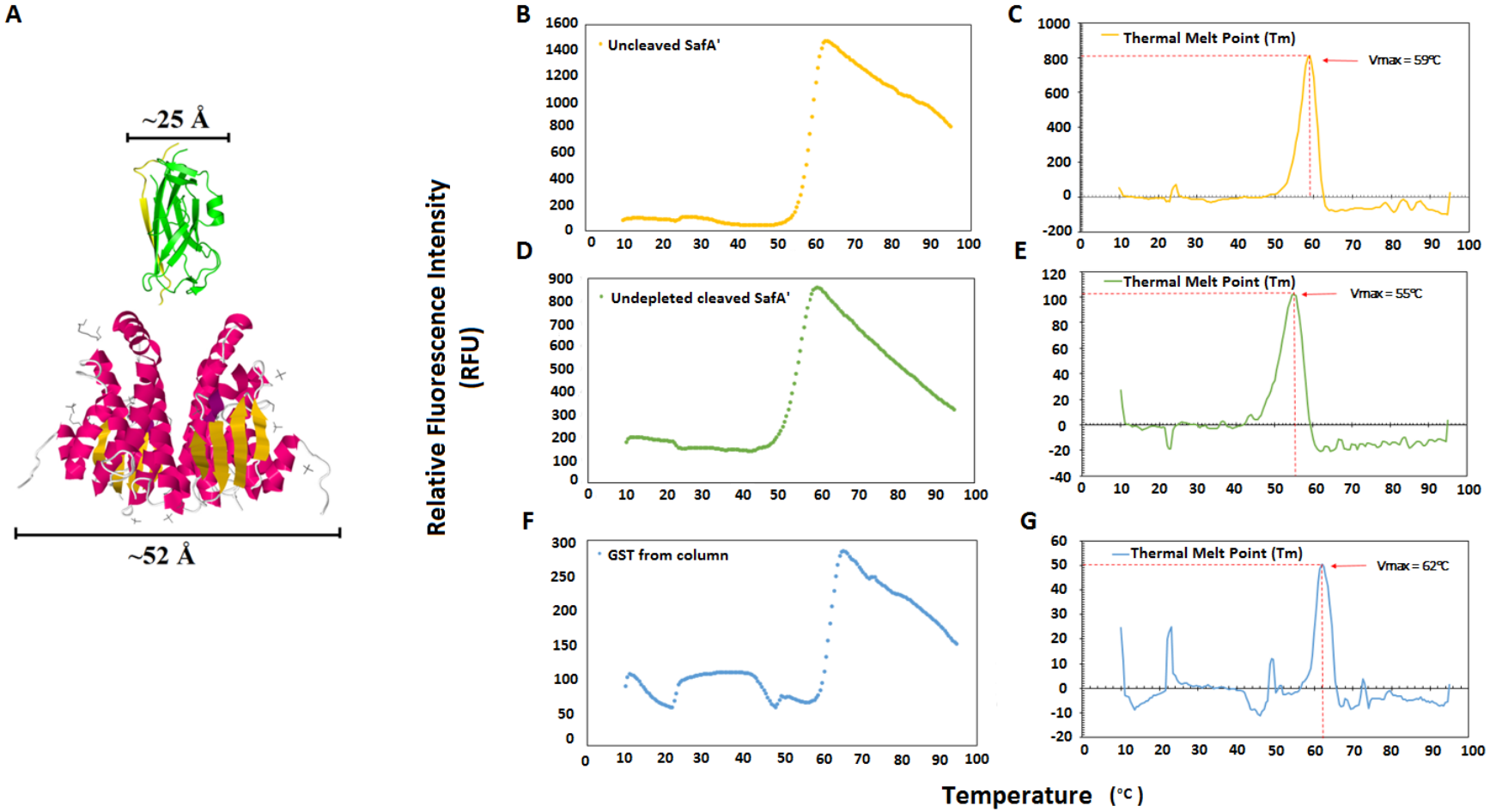

Figure 30. Temperature-induced denaturation of GST, uncleaved SafA' (GST-SafA-6xHis) and undepleted cleaved SafA (GST+SafA-6xHis) by Differential Scanning Fluorimetry (DSF). Graphs were obtained from the averaged values of three repetitions. **(A)** Crystal structure of GST and SafA **(B)(D)(F)** Recorded variation of the Relative Fluorescence Intensity (RFU) for uncleaved SafA' (GST-SafA-6xHis), undepleted cleaved SafA' (GST+SafA-6xHis) and GST showing the moment of transition between the folded and unfolded state. **(C)(E)(G)** Thermal Melt (T_m) or melting point of uncleaved SafA' (GST-SafA-6xHis), undepleted cleaved SafA' (GST+SafA-6xHis) and GST. The maximum value (V_{max}) was calculated giving a melting point of 59ºC, 55ºC and 62ºC respectively. Note difference in melting points and RFU counts for each sample. The Tm indicate fused GST stabilises SafA' (GST-SafA'6xHis) and the higher RFU counts over GST indicate SafA' (GST-SafA-6xHis) unfolds regardless of GST.

4.5 Discussion

Cleaving GST from the construct was required to eliminate any doubt regarding the structural integrity of SafA' (GST-SafA-6xHis) and thus the specificity of identified SafA' (GST-SafA-6xHis) binding proteins. Even though the design of SafA' (GST-SafA-6xHis) resembled a similar approach followed by Cota et al (2006) for a homologous protein, prior to this thesis it was not known whether the SafA protein was fully folded.

Circular dichroism (CD) spectroscopy revealed that the secondary structure of the designed subunit is consistent with the crystal structure (Table 14). Similarly, the GST control also showed CD spectra consistent with its crystal structure (Figure 29, Panel B and Table 14). During sample preparation it was noted that free GST could not be removed completely, therefore there are residual remains of approximately 1% GST and cleaved SafA' (SafA-6xHis) in each other samples. Regardless of this, the depleted cleaved SafA' (SafA-6xHis) and GST from column samples secondary structure content was in agreement their respective crystal structures. Table 14 represents a table of our predictions in comparison with the expected ones from the available crystal structures (PDB: 3CRE for SafA and PDB: 1A0F for GST).

Uncleaved SafA' (GST-SafA-6xHis) and undepleted cleaved SafA' (GST+SafA-6xHis) were shown to be rich in both α-helices and β-sheets (Figure 29, Panel C) as expected based on the combined crystal structures of GST and SafA. It is important to note the undepleted cleaved SafA' (GST+SafA-6xHis) sample also has HRV 3C protease in the mixture, and thus there are a total of three proteins present in these samples. Because of this, calculating the protein concentration was difficult and the QAA results provided a close estimate of SafA-6xHis in the undepleted cleaved SafA' (GST+SafA-6xHis) sample (Table 13). Nevertheless, as it can be appreciated from Figure 29, Panel D both spectra show the same shape but they do not overlap. This is possible because undepleted cleaved SafA' (GST+SafA-6xHis) also has HRV 3C protease in the mixture, therefore skewing the spectra and responsible for the lower wavelength features observed in some of the samples.

As well, thermofluor results might reflect that having GST-fused to the construct has an impact in the secondary structure in comparison to free GST (Terpe et al 2003) (Figure 30). The deconvolution analysis (Section 4.3) suggested that both, uncleaved SafA' (GST-SafA-6xHis) and undepleted cleaved SafA' (GST+SafA-6xHis) have a similar secondary structure, as indicated by Figure 29, Panel D and Table 14. Similar (yet not

identical) studies have been performed in the study of the secondary structure of uracil-DNA degrading protein (UDE) (Pukáncsik et al 2016). To conclude, the addition of GST confers stability, as expected by the relatively high stability of this protein (Tm 62ºC, Figure 30, Panels E and G). This figure is consistent with the thermal melt of GST reported to be approximately 60ºC (Lea and Simeonov et al 2012).

CHAPTER V - ESTABLISHING AN AFFINITY-ENRICHMENT SYSTEM TO ISOLATE SAFA INTERACTING PARTNERS IN THE MAMMALIAN LARGE INTESTINE

5.1 Introduction and Rationale

In proteomics the study of protein-protein interactions is highly dependent on choosing the right assay and detection method (Rao et al 2014, Srihari et al 2015, Stoilova-McPhie et al 2013). First, the selection of the right immobilization support is vital. The conventional way is to immobilize proteins through their fusion tag, such as, Glutathione S-transferase (GST) (Zalazar et al 2014), Histidine, among others (Kimple and Sondek et al 2004). Where glutathione agarose (Harper and Speicher et al 2011) and Immobilized Metal Affinity Chromatography (IMAC) technology (Block et al 2009, Cheung et al 2012) are among the most widely used. Immobilization by glutathione agarose is popular due to the strong but reversible affinity between the GST affinity tag and glutathione coupled to the sepharose matrix (Harper and Speicher et al 2011). On the other hand, the versatility of IMAC makes it attractive. The technology offers choice of metal ions, allowing for a variety of fusion tagged proteins to be immobilized (Block et al 2009, Cheung et al 2012).

Immobilization of a protein through a GST tag (Figure 36) is relatively cheap and the material can be obtained in the form of slurry or columns for convenience of work (Harper and Speicher et al 2011, Kimple et al 2013). On the other hand, IMAC technology offers the possibility of capturing protein through a Histidine tag (among others) (Block et al 2009). In comparison to GST, Histidine is small and can serve as a good alternative when facing the challenges of finding the right system. IMAC technology offers the choice of working with porous and non-porous surfaces. The advantage of the system relies in the ease of use and the limited loss that can occur during washes and transfers. This is because IMAC-based beads and agarose chemistry relies on the immobilization of a metal, such as $Cu^{+}2$ (Figure 32) and $Ni^{+}2$ (Figure 34), by a chelator (Block et al 2009, Kosobokova et al 2016).

A least conventional approach is the use of Nitrocellulose (NC) (Figure 38). The use of NC is commonly reserved to the one of transferring proteins from a polyacrylamide gel (Towbin et al 1979). To date the transfer mechanism is not fully understood but it is known to be through hydrophobic and electrostatic interactions (Low et al 2013, Matsumoto et al 2003). NC offers an attractive option to immobilize proteins regardless of their fusion tags; moreover the high binding capacity of the membrane combined with

the ease of use makes it a viable alternative. Finally, microwell plates have been extensively used for enzyme-linked immunosorbent assay (ELISA) (Karpinski et al 1990, Lequin et al 2005) (Universal-BIND^{TM}, Figures 39 and 40). The advantage of these is that the 96-well format is a good tool to prepare replicates and they also offer a solid support for protein which does not rely solely on fusion tags (Gibbs and Kennebunk et al 2001).

In this Chapter, the setup of five systems (1-5) to isolate target interacting proteins of SafA will be described. The work will focus on the results obtained in the large intestine affinity-enrichments but the systems were setup also with other tissues, such as, bovine liver and lamb's heart to compare whether any difficulties were tissue-based or system-based. In overall, each system was carefully studied to set up appropriate experimental conditions and establish a robust system capable of studying *Salmonella*-mammalian host protein-protein interactions.

5.2 Results: General considerations

The general approach (Figure 31) was to immobilize the bait protein on the selected surface, followed by blocking of any free active sites with Bovine Serum Albumin (BSA). The immobilized protein was then incubated with the selected protein extracts, and after an average of five hours incubation any captured proteins were eluted. The incubation time with the extracts was not arbitrary, but selected after experimental trials involving affinity-enrichments were performed by incubation at three, four, five, six hours and overnight. The results indicated incubation of the extracts with the immobilized protein for longer than five hours would result in high background and partial displacement of bait protein. Whereas, incubation times of less than four hours would result in clear gels showing no bands (data not shown).

Whole eluates were digested and, where possible, each sample was subject to MS comparative analysis and LC-MS/MS analysis for protein identification. SafA' (GST-SafA-6xHis) affinity-enrichments were performed in all systems and different sources of tissues were used. In some cases the system was not suitable to perform affinity-enrichment experiments with the large intestines but was for other tissues, such as, brain (images not shown). Nonetheless, all systems attempted but except the Universal-BIND™ plates (System 5) (Figure 41) yielded a strong background likely due to non-specific interactions. The reasons for the occurrence of non-specific binding were investigated (e.g. ionic binding to the beads surface) (Figure 33, Panels C and D; Figure

35, Panel B; Figure 37, Panel B and Figure 39, Panel E). For each system, the stringency was increased, rather unsuccessfully, using higher salt concentrations in the protein extracts (Peyser et al 2001, Shields and Farrah et al 1983, Zhang et al 2012). In the case of the GSH-resin, large quantities of a ~26 kDa protein seemed to be isolated (Figure 37, Panel A, Lane 8). Based in the size, affinity for GSH and previous publications (Hoensch et al 2002, Van Veld and Lee et al 1988); it was speculated to be glutathione S-transferase (an abundant protein in the guts tissue). Depletion of this protein from the extracts was also attempted. Protein extracts were incubated with fresh batches of GSH-resin prior to affinity-enrichments (Günther et al 2015, Millioni et al 2011, Polaskova et al 2010, Tu et al 2010), but this again failed to sufficiently decrease the background from the extracts (Figure 37, Panels B and C).

In conclusion, the Universal-BIND™ plates (System 5) provided the best platform to perform the isolation of SafA interacting proteins from the large intestine. The main limitation was due to small quantities of protein in comparison to the other systems, this was overcome by pooling proteins from several wells (technical replicates) together.

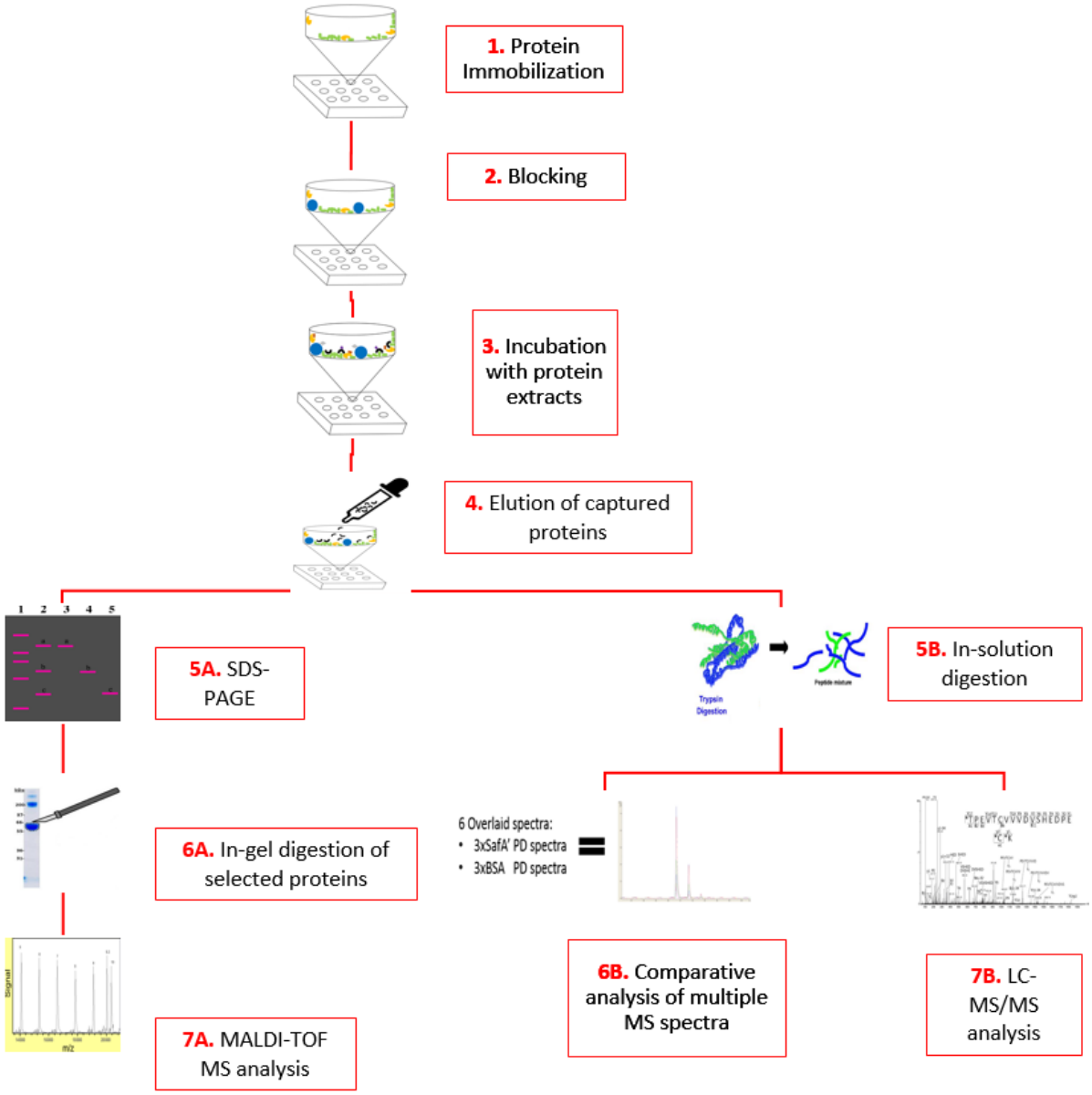

Figure 31. Flow chart of experimental approach. Bait proteins were immobilized on the desired surface **(1)** and any free reactive sites were blocked with BSA **(2)**. The immoblized proteins were incubated with protein extracts from selected tissues **(3)** and any captured proteins were eluted **(4)**. The first approach was to separate proteins by SDS-PAGE gels **(5A)** and perform in-gel digestion on selected bands **(6A)** for MALDI- TOF MS analysis **(7A)**. The second approach was to digest the whole eluates **(5B)** and analyse these using a comparative analysis of multiple MS spectra **(6B)**. The comparative analysis consisted in overlaying three affinity-enrichment spectra for the Salmonella bait protein against three affinity-enrichment spectra for their respective negative control. Unique peaks present solely in the *Salmonella* proteins affinity-enrichments and not in the negative controls were selected and considered as specific peptides to our recombinant proteins. Protein identification was achieved by LC-MS/MS analysis **(7B)**.

5.3 System 1. Superparamagnetic Cobalt-based IMAC: Dynabeads

To set up the magnetic isolation system, Dynabeads® His-Tag Isolation & Pulldown (Invitrogen) (System 1), was obtained. As per datasheet, Dynabeads are uniform, superparamagnetic beads of 1 µm diameter coupled with cobalt-based IMAC chemistry (Figure 32). The expected capacity is 40 µg of a 28 kDa histidine-tagged protein per 1mg beads (Benelmekki et al 2012).

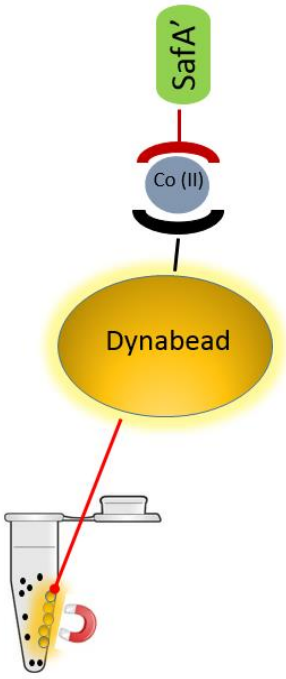

Figure 32. System 1: Immobilization of SafA' (GST-SafA-6xHis) on Dynabeads ®. Proteins are immobilized through their histidine tag by binding to the Cobalt present on the non-porous beads surface. Image is only a schematic representation and is not to scale.

5.3.1 SafA' (GST-SafA-6xHis) affinity-enrichment with bovine liver extracts

SafA' (GST-SafA-6xHis) affinity-enrichment trials were started with bovine liver extracts due to the high availability of the material. Other tissues, such as, lamb's heart and/rat intestine were also used to investigate whether complications with the systems was related to the source of tissue. In this section, unless otherwise stated, bovine liver was the tissue used. The initial (GST-SafA-6xHis) SafA'/bovine liver affinity enrichment identified the attachment of non-specific proteins to Dynabeads. It can be inferred from Figure 33, Panel A, lanes 3, 5 and 7 the presence of an unknown ~70 kDa protein to Dynabeads in the SafA' (GST-SafA-6xHis) sample. Lanes 4, 6 and 8 show the binding of the same protein to the negative control. The presence of the unidentified protein to both samples reveals the attachment of this ~ 70 kDa protein to SafA' (GST-SafA-6His) is non-specific. It is

possible to observe other non-specific proteins in the range of ~120 kDa to ~85 kDa in the soluble protein extracts affinity-enrichments, as per lanes 5 and 6. These same non-specific proteins are present in the total protein extracts affinity-enrichments, as per lanes 7 and 8. This was observed for all the negative controls, as per lanes 4, 6 and 8, with higher levels of the non-specific proteins in the absence of SafA' (GST-SafA-6His). The attraction of these proteins to the beads indicates the possibility of non-specific binding to the metal ion present on the beads. This first affinity-enrichment showed that protein immobilization was possible but the extracts were loaded also with non-specific proteins possibly binding to the cobalt on the beads. Based on this, the next step was to treat and deplete these non-specific binding proteins from the extracts previous to incubation with immobilized SafA' (GST-SafA-6His) on the beads.

5.3.2 Depletion of non-specific binding proteins

The non-specific proteins were depleted from total bovine liver protein extracts. The aim was to capture all or a sufficient amount of these non-specific proteins on beads to test whether in the resulting filtered extracts an interaction between any specific protein and SafA'(GST-SafA-6xHis) occurred. From this point onwards, any extracts used for Dynabeads affinity-enrichments were depleted prior to incubation. The liver extracts were depleted for six hours by transferring to a fresh batch of Dynabeads every hour (Chapter II, Section 2.9.3). Figure 33, Panel B show a series of consecutive depletions of the captured proteins. Lanes 1-6, show the capture of all non-specific proteins binding to Dynabeads by simple incubation of the extracts with beads. Figure 33, Panel B, Lane 1, shows the eluate of 50 µL liver extracts incubated for one hour with 10 µL of Dynabeads, exhibiting the isolation of two major unknown proteins as represented by two bands of ~70 kDa and ~45 kDa. After transferring the same 50 µL extract to a fresh 10 µL of Dynabeads, followed by another one hour incubation, is possible to see a total of six major bands in the range of ~120 kDa to ~35 kDa, as per Figure 33, Panel B. Lane 2 also shows the same pair of bands present in Lane 1 but with higher intensity, suggesting an increase on non-specific binding with time. The analysis of the results presented in Lane 1 also suggests that after the first step no other protein could be captured in one hour of incubation. After three hours of depletion, as shown in Lane 3, a total of seven unknown major proteins in the range of ~120 kDa and ~35 kDa were captured. After three hours not only more non-specific proteins seem to bind but the amount of captured protein seems to be increasing, as shown by the intensity of the bands. Lanes 8-10 confirm partial depletion of the proteins in the range of ~120 kDa – 40 kDa from the initial protein

extracts in Lane 7. Lane 7 shows all proteins present in the extract previous to any treatment and Lane 8 shows all proteins present in the extract after the six hours treatment. Upon comparison it seems as if all the proteins are still present but in lower amounts. Lane 9 shows the depleted extract after two hours and Lane 10 the depleted extract after four hours. This experiment shows full depletion of the non-specific proteins was not possible even after 6 hours treatment. At the time it was thought, levels of the non-specific proteins had decreased enough to permit any specific interaction between host proteins and SafA' (GST-SafA-6xHis) to occur. Unfortunately, this was not conclusive as the subsequent trials did not provide evidence of this.

5.3.3 Inhibition of non-specific protein binding by salt titration

Phosphate-buffered saline (PBS) studies were carried to determine the influence of salt concentration on the binding of non-specific proteins to Dynabeads. Extracts were buffered in a low to high salt concentration range (Chapter II, Section 2.9.4). Salt concentration in the extracts was gradually increased to reduce the strength of ionic binding proteins. Figure 33, Panel C, Lane 1, shows the presence of more abundant bands within a range of ~120 kDa to ~30 kDa binding to the beads. Lanes 1-9 shows the presence of two proteins in-between 60-70 kDa among others of lower intensity are as per Lane 2, after addition of 100 µL 0.5xPBS to 100 µL of extracts (final PBS concentration of 0.25xPBS in extracts), bands below ~60 kDa start to fade. After increasing the final PBS concentration twofold, Lane 3, the non-specific protein binding tend to increase as showed by the slight increase in intensity of the bands. Bands 4-9 show a gradual increase of protein binding which is directly proportional to the amount of salt added to the extracts. The extract run in lane 9 with a final concentration of 5xPBS shows the higher the salt concentration in the sample, the higher the binding of non-specific proteins to beads. The results show for this particular extract increasing the concentration of salt increases the ion exchange binding of the proteins to beads. It was not possible to reduce the amount of non-specific proteins binding to the beads. From the literature it is expected that ionic interactions would be reduced by the addition of salt as this would provide ions and compete for binding (Peyser et al 2001). Therefore, obtaining the opposite results would indicate, in this particular system, the interactions were perhaps of other nature. Further literature revealed that hydrophobic interactions are highly affected by the salt concentration in the sample as this can be heightened or reduced depending on the salt and volume of solute (Zangi et al 2007). With this in hindsight, it was possible the observed non-specific interactions were hydrophobic and not as previously speculated.

5.3.4 Identification of interactions between non-specific proteins and Dynabeads

In order to understand more on the non-specific binding of proteins to Dynabeads, a sample of beads was stripped off the cobalt ion (Biçak et al 1998, Tewari and Singh et al 1999, Zeng et al 2013); namely described here as 'non-cobalt beads'. The non-cobalt beads sample was tested in parallel with Dynabeads (control) for the non-specific binding of proteins. Each pair of samples was titrated with an increasing concentration of PBS to study the effect of salt in the binding of proteins to each set of beads. The control samples in Figure 33, Panel D shows bands corresponding to unknown proteins of ~50 kDa – 85 kDa eluted from the 'non-cobalt beads' (Lane 1) have a higher intensity than the same set of bands in Dynabeads (Lane 2), suggesting that the ionic exchange interaction between the proteins and the non-cobalt beads is stronger. Although displacement of all the non-specific binding proteins in both samples was not possible, we can observe the displacement of some proteins of low molecular weight but none of two major ones ~50-85 kDa. As a whole, the experiment shows for non-cobalt beads that the binding of non-specific proteins of low molecular weight can be reduced at its best by adding up to 10xPBS (Lane 7) and for Dynabeads up to 5xPBS (Lane 6).

5.3.5 SafA' (GST-SafA-6His) affinity-enrichment with lamb's heart protein extracts

A SafA' (GST-SafA-6His) affinity-enrichment with protein extracts from lamb's heart was performed in order to check whether the presence of non-specific proteins was a problem with other mammalian tissues. As per Figure 33, Panel E, Lanes 3, 5 and 7; there are no detectable specific protein interactions between SafA' (GST-SafA-6xHis) and lamb heart proteins, as their respective negative controls in Lanes, 4, 6 and 8 show the same bands. Following these results it was decided to abandon the use of Dynabeads.

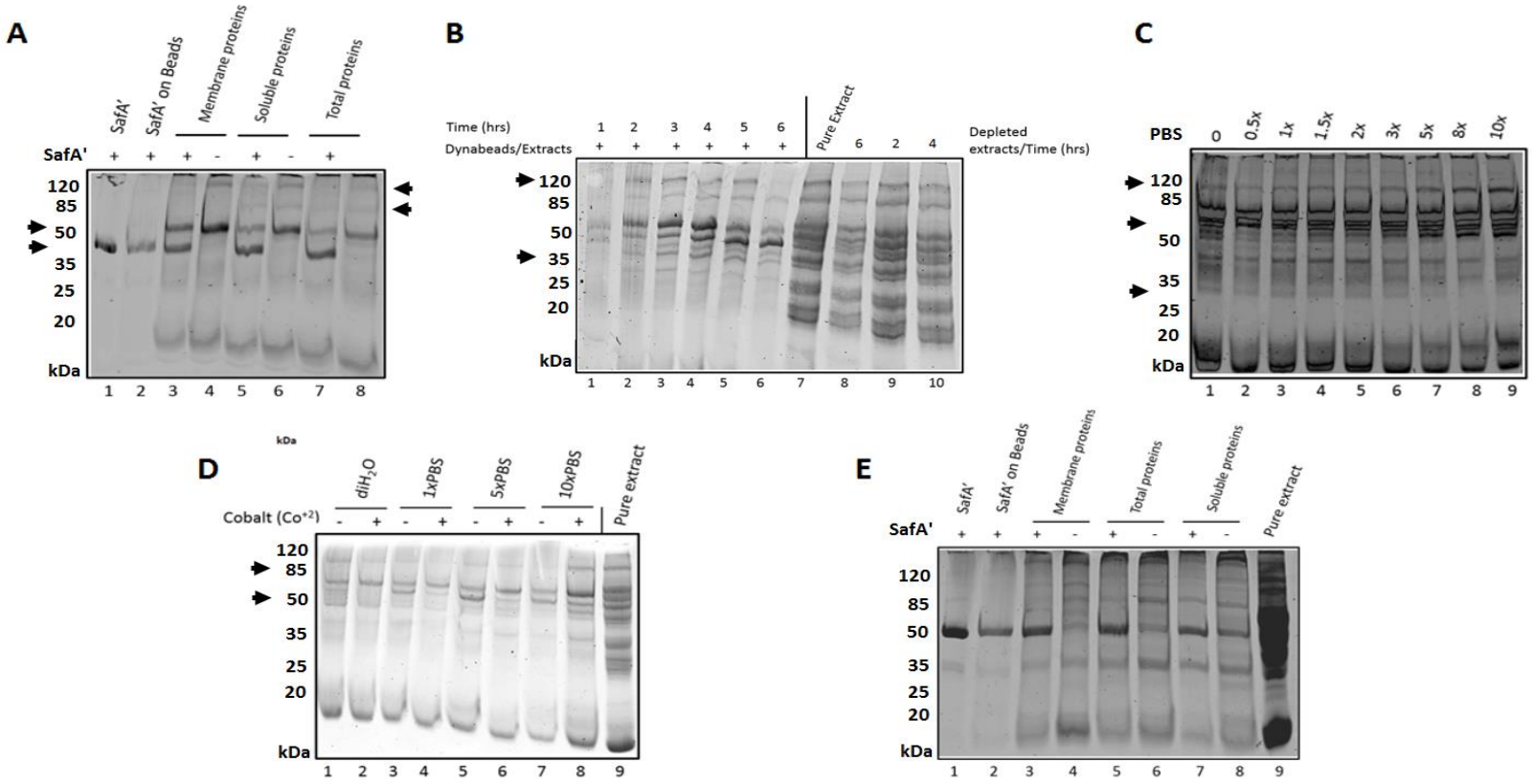

Figure 33. Setting up of Dynabeads as an affinity-enrichment system to study protein interactions in the mammalian host. (A) (GST-SafA-6xHis) SafA'/bovine liver affinity-enrichment. **(A) (GST-SafA-6xHis) SafA'/bovine liver affinity-enrichment.** (GST-SafA-6xHis) SafA'/Dynabeads were incubated with membrane, soluble and total protein extracts from bovine liver. The capture of high amounts of non-specific proteins is noted. **(B) Depletion trials.** Bovine liver protein extracts were incubated with Dynabeads and any non-specific proteins were captured. Depletion of these was partially achieved. **(C&D) Investigation of non-specific interactions. (C)** Extracts were incubated with different salt concentrations. This made no impact in the binding of proteins to the beads. **(D)** Dynabeds were stripped of their Cobalt ion to check whether proteins bind to the beads surface or the ion. At the same time these were incubated with different salt concentrations in an attempt to disrupt the non-specific interactions. No major change in the binding of the non-specific proteins was noted. **(E) SafA' (GST-SafA-6xHis) and lamb's heart affinity-enrichment.** (GST-SafA-6xHis) SafA'/Dynabeads were incubated with lamb's heart protein extracts. The tissue selection did not improve the systems capability of performing affinity-enrichments in the mammalian host with this particular system. All SDS-PAGE were 10% and stained with Coomassie blue. Samples were eluted in 5xLB/β-ME and heated for 5 minutess at 100ºC. Images were taken with the Odyssey Scanner

.

5.4 System 2: Agarose Ni-based IMAC: HIS-Select Nickel Affinity Gel

Following the lack of success with System 1 it was decided to test HIS-Select Nickel Affinity Gel (SIGMA) to immobilize SafA' (GST-SafA-6xHis) using a porous surface. As per data sheet, HIS-Select Nickel Affinity Gel uses IMAC and is a proprietary chelate on a beaded agarose charged with nickel (Figure 34). SafA' (GST-SafA-6xHis) was successfully immobilized on Ni-agarose and the presence of non-specific binding proteins was also tested (Figure 35, Panel A, Lane 7). Lane 8 shows a high amount of non-specific proteins binding to the agarose even after depletion (Lane 7).

5.4.1 Identification and inhibition of nickel binding proteins by salt titration

In order to find out whether the non-specific proteins bind to the nickel present on the agarose or to the agarose itself, a sample of nickel-agarose was stripped of the nickel ion (this will be referred as 'agarose only'). The 'agarose only' sample was tested in parallel with nickel-agarose (control) for the non-specific binding of proteins. Each pair of samples was titrated with buffered extracts containing increasing concentration of PBS to study the effect of salt in the binding of proteins. The results showed that agarose is not sufficient to isolate protein in absence of nickel ions (Figure 35, Panel B). It can be observed that Lane 6 has the lowest amount of binding proteins and Lane 4 has the highest. Therefore, to some extent, increasing the amount of salt aids the breakage of ionic interactions between proteins and nickel. However the presence of non-specific proteins lead to discard also System 2.

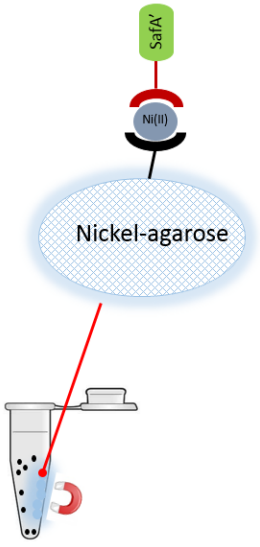

Figure 34. System 2: Immobilization of SafA' (GST-SafA-6xHis) on HIS-Select Nickel Affinity Gel. **Proteins** are immobilized through their histidine tag by binding to the Nickel present on the porous beads surface. Image is only a schematic representation and is not to scale.

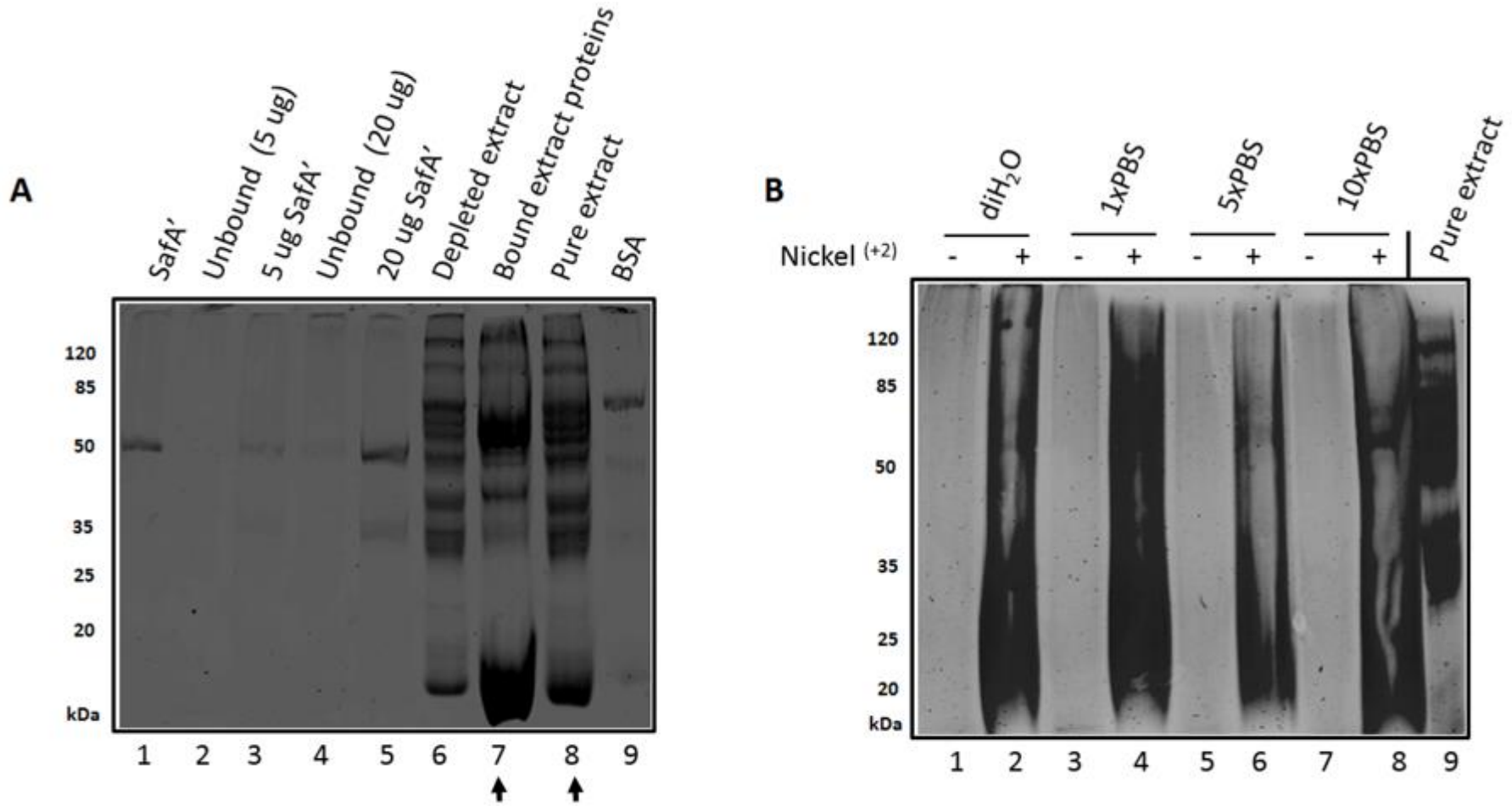

Figure 35. Setting up of HIS-Select Nickel Affinity Gel as an affinity-enrichment system to study protein interactions in the mammalian host. (A) Establishment of protein immobilization and non-specific background. SafA' (GST-SafA-6xHis) was immobilized in the gel but abundant non-specific proteins binding to the gel were observed. **(B) Investigation of non-specific interactions.** The gel was stripped of the Nickel ion and incubated with different salt concentrations. The gel free of nickel shows the non-specific proteins bind to the nickel in the gel. These interactions could not be disrupted with the increase of salt. All SDS-PAGEs were 10% and stained with Coomassie blue. Samples were eluted in 5xLB/β-ME and heated for 5 mins at 100ºC. Images were taken with the Odyssey Scanner.

5.5 System 3. GSH-agarose: Protein immobilization and background test

To immobilize SafA' (GST-SafA-6xHis) through its GST tag we used Glutathione-Agarose (SIGMA). As per datasheet, the material consists of glutathione attached through the sulfur to epoxy activated 4% cross-linked beaded agarose (Figure 36). The expected binding capacity is of ~5-10 mg glutathione S-transferase per mL resin.

SafA' (GST-SafA-6xHis) was successfully immobilized in GSH-agarose and a possible glutathione binding protein was also isolated. Figure 37, Panel A, Lane 3, represents 1 µg SafA' (GST-SafA-6xHis) immobilized on beads, Lane 4 shows 5 µg and lane 6 shows 20 µg of protein immobilized. As depicted by the smear in Lane 8, we observe that non-specific proteins with a higher molecular mass are more abundant in the extract despite some success in depleting the extract (Lanes 8 and 9). A similar systematic analysis performed for System 1 and 2 was carried out in order to find out whether this system is suitable for mammalian extracts affinity-enrichments.

5.5.1 Depletion of glutathione binding proteins

A trial was setup to identify the time and amount of material needed to fully deplete this protein prior to any affinity-enrichment. The extracts were depleted a total of two hours in 1 mL GSH-agarose columns (Chapter II, Section 2.11.2). The depletion consisted in the incubation of the protein extracts sample with GSH-agarose for one hour, this was performed twice. For instance, after the initial protein extract was incubated with the first batch of GSH-agarose, this was collected and immediately transferred into a second fresh batch of GSH-agarose for further depletion. Any bound proteins to the GSH-agarose were eluted and loaded into the gel. Figure 37, Panel B represents the capture of a ~26 kDa protein (Lanes 1 and 2). Lanes 3 and 4 show the impact of depletion in the proteome of the sample, where in comparison with Lane 4, lane 3 shows the absence of not only the targeted ~26 kDa protein but also of others.

5.5.2 (GST-SafA-6xHis) SafA'/rat small intestine affinity-enrichment

The screening of SafA' (GST-SafA-6xHis) with rat extracts from the small intestine indicated that SafA' (GST-SafA-6xHis) was being displaced by the amount of glutathione binding proteins in the extract. It was also observed depleting the extracts was creating a loss of total protein and not only the non-specific ones. Figure 37, Panel C, Lane 2 shows the presence of SafA' (GST-SafA-6xHis) previous incubation with the extracts and Lane

4 shows the displacement of SafA' (GST-SafA-6xHis) from the agarose after incubation with the extracts. These results confirm there is a high concentration of glutathione binding proteins in the small intestine which cannot be depleted. It also suggests the unsuitability of this system particularly for extracts from the whole digestive system. Affinity-enrichments with extracts from other tissues were performed (data not shown) and confirmed it was suitable for heart and brain where the ~26 kDa isolated protein (presumed to be intestinal glutathione) (Van Veld and Lee et al 1988) is not present. In conclusion, the system was not suitable as we needed a robust system to carry affinity-enrichments in all possible tissues.

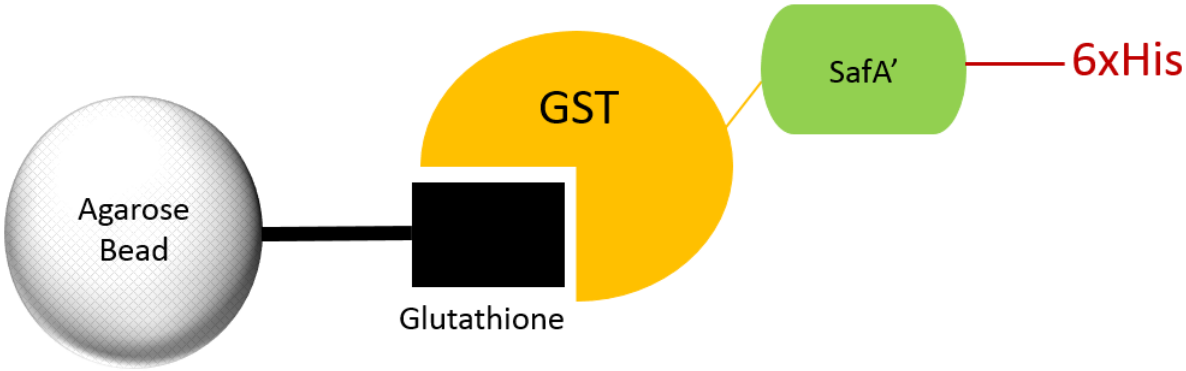

Figure 36. System 3: Immobilization of SafA' (GST-SafA-6xHis) on GSH-resin. Proteins are immobilized through their GST tag by binding to the glutathione present on the porous beads surface. Image is only a schematic representation and is not to scale.

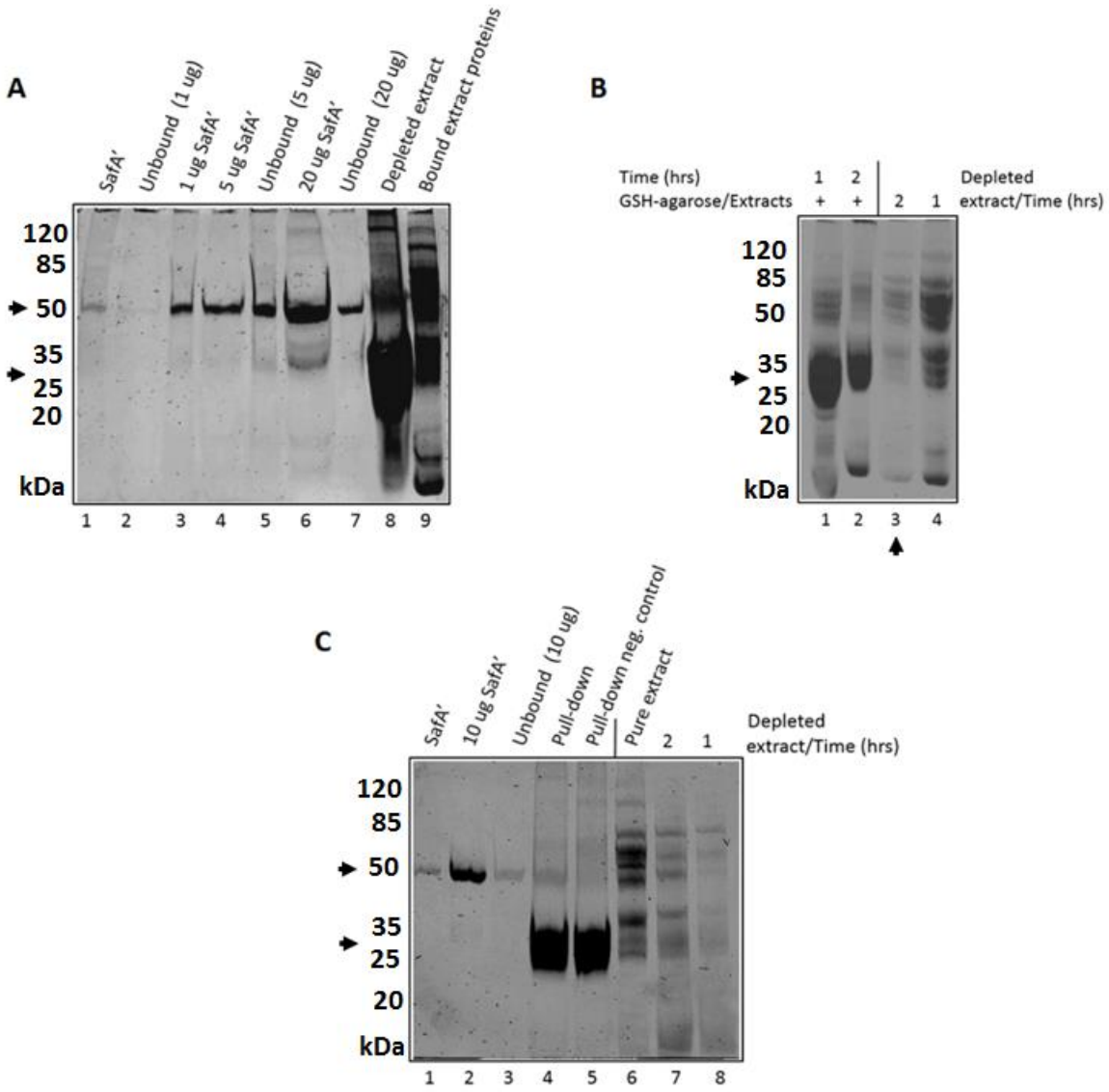

Figure 37. Setting up of GSH-agarose as an affinity-enrichment system to study protein interactions in the mammalian host. (A) Establishment of protein immobilization and non-specific background. SafA' (GST-SafA-6xHis) was immobilized on the agarose (Lanes 3, 4 and 8) but abundant non-specific proteins binding to the gel were observed (Lanes 8 and 9). **(B)** Depletion of non-specific proteins. Small intestine extracts were incubated with the agarose for one and two hours (Lanes 1 and 2). Non-specific proteins were significantly depleted (Lanes 3 and 4). **(C)** Affinity-enrichment of SafA' (GST-SafA-6xHis) with rat small intestine protein extracts. SafA' (GST-SafA-6xHis) was displaced from the agarose due to the high amounts of a ~35 kDa protein (Lane 4). The previous depletion step did not seem to have eliminated sufficient non-specific proteins (Lanes 7 and 8). All SDS-PAGE were 10% and stained with Coomassie blue. Samples were eluted in 5xLB/β-ME and heated for 5 minutes at 100ºC. Images were taken with the Odyssey Scanner.

5.6 System 4. Nitrocellulose (NC): Binding capacity and blocking

Because of the difficulties based above, it was opted to immobilize SafA' (GST-SafA-6xHis) by other than its fusion tags. NC was used as a non-conventional method for mammalian affinity-enrichments in which proteins were immobilized passive adsorption

(Figure 38) (Chutipongtanate et al 2015, Fridley et al 2013). To identify the binding capacity of a 0.5x0.5 cm^2 NC piece, 9x0.5x0.5 cm^2 NC pieces were prepared and incubated with a range of BSA from 0 μg-500 μg. After incubation the unbound BSA from each piece was kept in ice until use. Each of the NC pieces was eluted and separated in a 10% SDS-PAGE gel, the collected unbounds of each piece were loaded separately in a second 10% SDS-PAGE gel (Chapter II, Section 2.12.1). The first gel shows an increasing BSA gradient being eluted from the NC pieces (Figure 39, Panel A). The second gel with the collected BSA unbounds starts to show a small amount of BSA at 20 μg (Figure 39, Panel A). It was established that the binding capacity of a 0.5x0.5 cm^2 piece was ~20 μg.

Buffers B1 and B4 (Chapter II, Section 2.5) do not work as blocking agents, similarly to 10 mM Na_2CO_3. 1% BSA and 1% milk blocked the membrane, milk being the most efficient. The experiment was performed in triplicates and the intensity of each was averaged. After establishing binding capacity it was needed to identify the best blocking buffer in order to avoid non-specific interactions. Therefore, NC pieces were incubated with five different buffers before incubating with labeled α-rabbit IgG and measuring intensity of fluorescence (Figure 39, B). The experiment was performed in triplicates (for consistency and to level any defects that a NC might have) and the average fluorescence intensity of each NC piece taken. Fluorescence intensity, measured by arbitrary units (a.u.), was only detected where buffers did not block the NC piece, therefore leaving exposed active binding sites for labelled α-rabbit IgG to bind.

It was concluded 5% Milk with an average intensity of 3.3 a.u. was the best blocking agent, followed by 1% BSA with an average intensity of 22.8 a.u. Buffers B1 and B4 were also tested but they did not have blocking properties, neither did 10 mM Na_2CO_3. Due to the need of mass spectrometry as the downstream application, it was decided BSA was better suited as the blocking agent. The use of BSA would introduce solely one protein, which could be easily identified as a contaminant, whereas milk consists of a number of proteins, resulting in the introduction of unnecessary contaminants.

5.6.1 Fluorescent α-rabbit IgG affinity-enrichment

The system conditions was tested by selecting known binding partners rabbit IgG and α-rabbit IgG, together with bovine IgG and α-rabbit IgG as negative controls (Figure 39, Panel C). Fluorescent α-rabbit IgG was detected only in the NC piece with rabbit IgG, indicating a clear antigen-antibody affinity (as expected). The three NC pieces in the

negative control 1 showed no detectable signal, confirming bovine IgG does not interact with α- rabbit IgG due to the difference in species. None of the NC pieces in negative control 2 had protein or antibody present to monitor for protein contaminants in the experiment. Finally, all three NC pieces in control 3 confirmed the blocking solution (BSA) was adequate for the system as no labeled antibody bound.

5.6.2 SafA' (GST-SafA-6xHis) affinity-enrichment with bovine liver extracts

SafA' (GST-SafA-6xHis) was successfully immobilized to NC through crosslinking. The system also showed the binding of unknown binding proteins to BSA. First, NC was completely covered and crosslinked with BSA (Chapter II, Section 2.12.7). SafA' (GST-SafA-6xHis) was subsequently added onto the NC/BSA piece and any remaining reactive groups were blocked twice (Chapter II, Section 2.12.7) before incubation with extracts. As per Figure 39, Panel D; the presence of similar bands throughout all the samples regardless of whether they contained SafA' (GST-SafA-6xHis) or not indicated NC was suitable to perform affinity-enrichments in the mammalian host. To be consistent, we carried out the same systematic approach as in Dynabeads (System 1), nickel-agarose (System2) and GSH-agarose (System 3) to investigate whether the non-specific binding of proteins could be disrupted by increasing the concentration of salt in the extracts.

5.6.3 Identification and inhibition of NC binding proteins by salt titration

Rabbit IgG was immobilized on NC with buffered extracts ranging between 1x and 5x as described in Chapter II, Section 2.12.6. In Figure 39, Panel E all Lanes show the immobilization of rabbit-IgG still occurs regardless of high concentrations of salt present in the sample, showing high ionic binding of the protein to NC. Unfortunately, it was not possible to displace non-specific proteins by increasing the concentration of salt during crosslinking. Hence, it was concluded NC was not suited to study *Salmonella*-mammalian protein interactions.

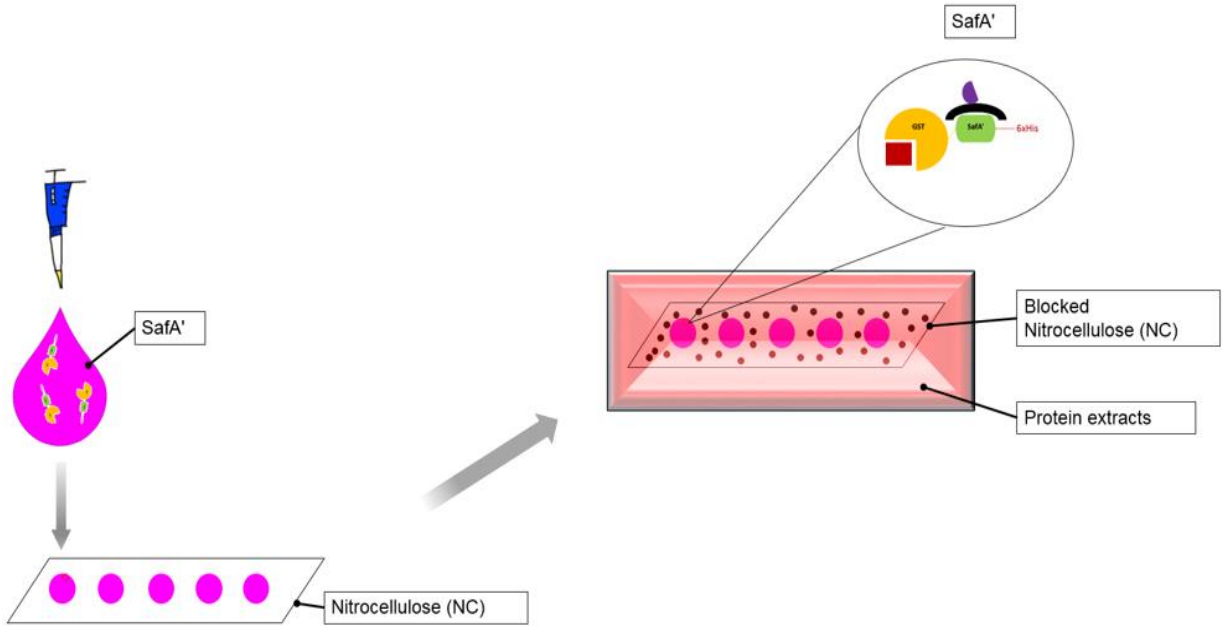

Figure 38. System 4: Immobilization of SafA' (GST-SafA-6xHis) on Nitrocellulose (NC). Proteins were immobilized through electrostatic interactions and hydrogen bonding. Image not to scale.

.

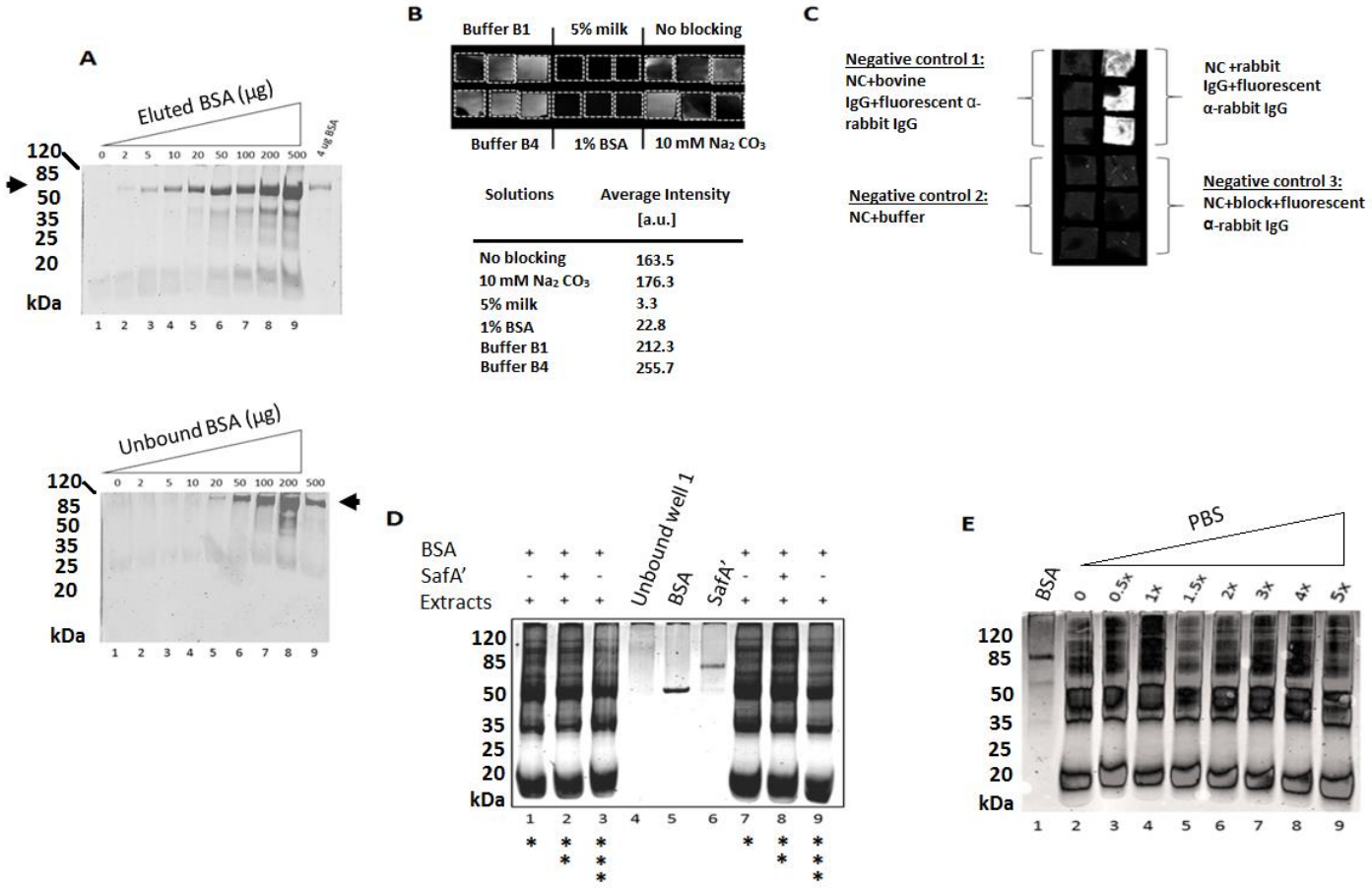

Figure 39. Setting up of Nitrocellulose (NC) as an affinity-enrichment system to study protein interactions in the mammalian host. (A) Establishment of binding capacity. Different concentrations of BSA were immobilised in 0.5x0.5cm^2 NC pieces. The unbound BSA for each piece was collected and the bound BSA for each piece was eluted. Both, eluted BSA and unbound BSA were separated by SDS-PAGE. **(B) Blocking trials.** NC pieces were incubated with different solutions prior incubation with labeled α-rabbit IgG. 5% milk and 1% BSA resulted the best blocking solutions. **(C) Fluorescent α-rabbit IgG Co-IP.** Fluorescent rabbit α-rabbit IgG successfully recognised rabbit IgG. The respective negative cotrols confirm the veracity of the results. **(D) Affinity-enrichment of (GST-SafA-6xHis) SafA'/bovine liver total protein extracts.** Non-specific binding present throughout all samples. **(E) Investigation of non-specific interactions.** Extracts were incubated with different salt concentrations. This made no impact in the binding of the non-specific proteins to NC. All SDS-PAGE were 10% and stained with Coomassie blue. Samples were eluted in 5xLB/β-ME and heated for 5 minutes at 100ºC. Images were taken with the Odyssey Scanner. Where relevant each piece was placed on a glass slide and scanned on the red channel using BioChip Imager (Packard). Experiment was performed in triplicates. Asterisks represent the samples were loaded in duplicates.

5.7 System 5: Setting up of Universal-BIND™ plates as an affinity-enrichment system to study protein-protein interactions in the mammalian large intestine

Finally, the fifth approach chosen was to crosslink proteins through abstractable hydrogen using UV light, which results in carbon-carbon binding by using Universal-BIND™ plates (Gibbs and Kennebunk et al 2001). This system produced reduced non-specific background in comparison with the previous systems (Figure 45), therefore it was decided to take it forward as the key method to isolate *Salmonella*-host interactors.

Figure 40, represent a workflow showing an overview of the experimental approach. After the tissues are harvested, total protein extracts from the large intestine are extracted. These proteins are added into a plate with UV-light crosslinked immobilized cleaved SafA' (GST-SafA-6xHis). Samples are eluted, precipitated and reconstituted. Whole eluates were digested and, where possible, each sample was subject to MS comparative analysis (Chapter VI, Section 6.4) and LC-MS/MS analysis for protein identification (Chapter VI, Section 6.7).

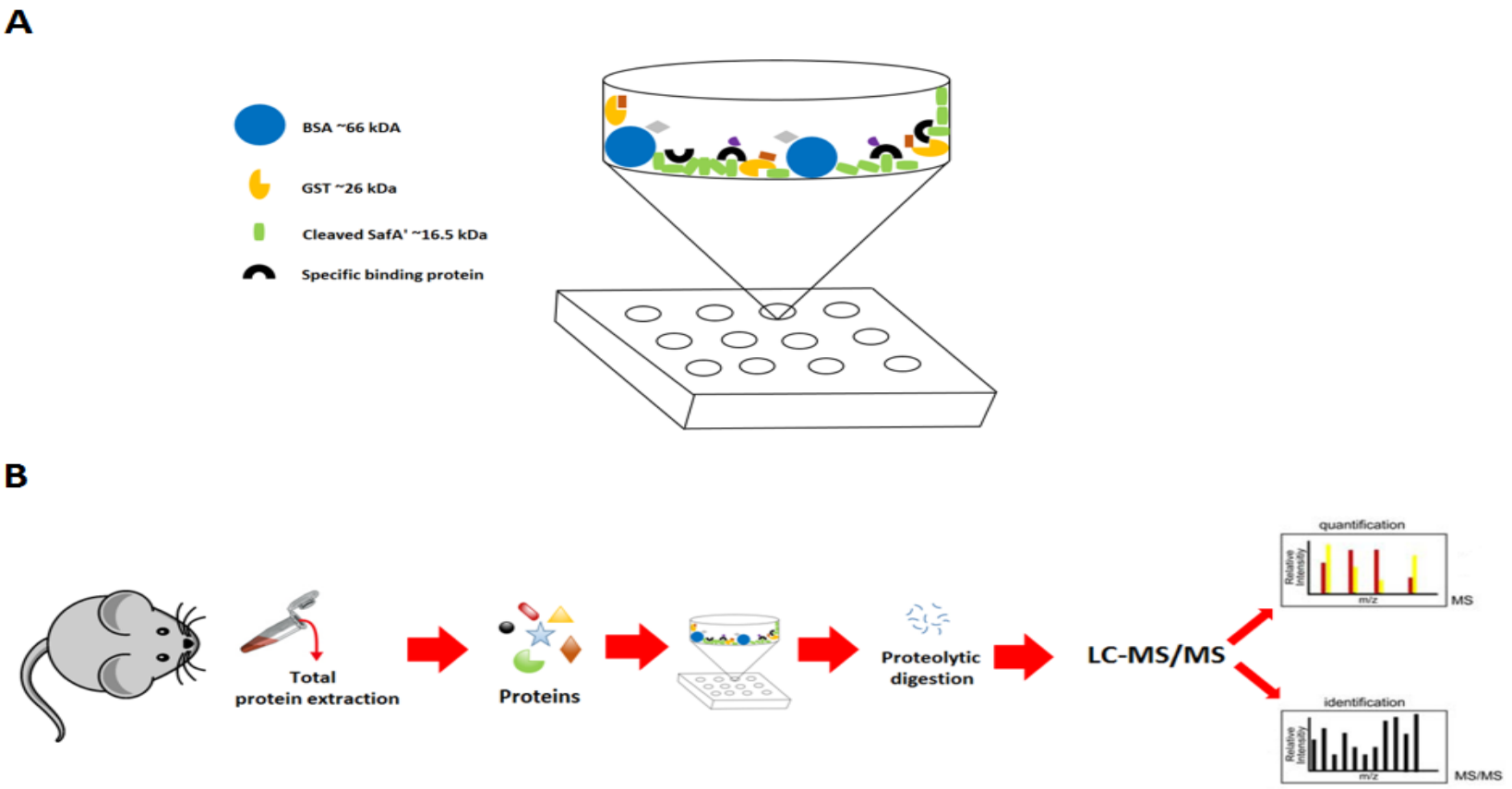

Figure 40. Schematic overview of the experimental approach. (A) System 5: Representation of Universal-BIND™ plates as an affinity-enrichment system. (GST-SafA-6xHis) Cleaved SafA'/bait protein is immobilized onto surface by UV-light crosslinking and any free active sites are blocked with BSA. **(B) Work-flow chart of experimental approach.** Large instestine tissues were harvested fom rat and total proteins were extracted. Bait protein was immobilized and any free reactive sites were blocked with BSA. The immoblized protein was incubated with total protein extracts from the large intestine. Any captured proteins were eluted. Finally, whole eluates were digested and analysed by LC-MS/MS. At this stage proteins are partially separated by HPLC, followed by the determinaton of their m/z values (MS) and finally the mass spectrometer proceeds to otbain the primary structure (sequence) information of the peptides (MS/MS).

Figure 41 shows an in detail workflow of the established affinity-enrichment system, were the bait is immobilized and incubated over day at 4ºC. Protein is crosslinked on plates by UV-light and immediately blocked overnight at 4ºC. After a washing step, wells are incubated with the selected tissue extracts for an average of five hours at 4ºC. Another washing step followed and samples were eluted from wells. All technical replicates were pooled into the one tube and incubated overnight at -20ºC with 100% Acetone for precipitation. Finally, samples were washed with 70% Acetone and pellet reconstituted for MS analysis. The next session will be dedicated to present technical background on the elaboration and optimization of our selected affinity-enrichment system.

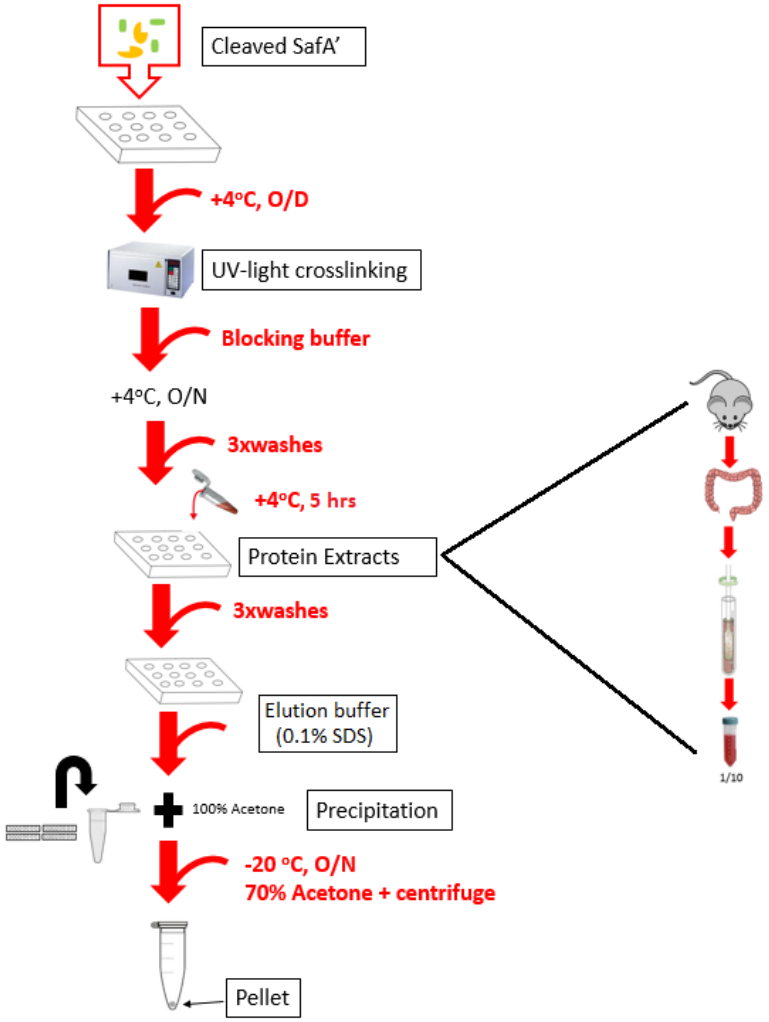

Figure 41. System 5: In-detail workflow showing adaptation of the Universal-BIND™ plates as an affinity-enrichment system. Cleaved SafA' (GST+SafA-6xHis) is immobilized on the plates (over day at 4ºC), UV-light crosslinked to the plates and incubated with blocking solution (overnight at 4ºC). On the following day plates are washed three times and incubated with total protein extracts for five hours. After washing three times samples were incubated with elution buffer and all technical replicates pooled together. 100% Acetone was added to each sample and stored at -20ºC overnight. After washing with 70% acetone, the pellet was reconstituted for MS analysis.

5.7.1 UV-light crosslinking enhances protein immobilization

It was important to establish whether crosslinking of the protein to the plates by UV-light had any advantage over immobilization by adsorption. Horseradish Peroxidase (HRP) was immobilized on the wells with and without using UV-light crosslinking (Figure 42). The experiments were carried out in parallel and both plates were incubated with all the solutions used in a typical affinity-enrichment with the aim to detect any possible HRP loss. Bovine IgG and BSA were used as controls because these were unlabelled proteins which would block the wells and if the samples were prepared correctly, no signal should develop as these were HRP free. As per results, the immobilization of HRP was successful on both plates as the HRP was detected; nevertheless, a significant higher signal was obtained from the UV-light cross-linked plate (Figure 42, Panel A).

In the non-crosslinked plate (Figure 42, Panel B), incubation of the HRP wells with elution buffers, such as, 100 mM Glycine, pH 2.5 and 3M NaCl, pH 9 did affect the amount of HRP but not as much as it does when incubated with 1% Octyl β-D-glucopyranoside (OG) in PBS. During affinity-enrichments the immobilized proteins are incubated with extracts containing protease inhibitors, therefore whether incubation with these would displace the immobilized protein on the wells was tested. It was noticed that these solutions would remove a non-significant but quantitative amount of HRP from the wells. Finally, it was observed incubation of the HRP wells with 10% BSA would displace most of the protein. In comparison, results of the crosslinked plates exhibited HRP would significantly remain on the wells but upon incubation with high BSA concentrations, the protein on the wells is as equally displaced as in the non-crosslinked plates. Thus, even though UV crosslinking strengthen immobilization of protein to the plates, this was not sufficient to retain the protein on the wells when incubated with high concentrations of BSA and OG.

In conclusion, for optimum protein immobilization on the Universal-BIND™ plates, crosslinking is recommended. In addition, 1% OG in PBS is too high and removes protein from the wells and it was decided not to use more than 0.02% OG in washing buffers. Incubation of HRP with elution buffer at low pH (100 mM Glycine, pH 2.5) and elution buffer with high salt concentration (3M NaCl, pH 9) indicated that these will succeed in dissociating most protein-protein interactions but the eluates could also have detectable amounts of bait protein. It was also noted that the use of 1x EDTA-free Protease inhibitors (Sigma) (see Chapter II, Section 2.1 for full components of tablets) and extracts can affect protein on the plates but with no great impact in the overall amount of protein present. To

be cautious, it was decided to dilute our protein extracts ten times to reduce the risk of protein displacement due to protease inhibitors and detergents. Lastly, it was observed that high concentrations of BSA would displace protein on the wells.

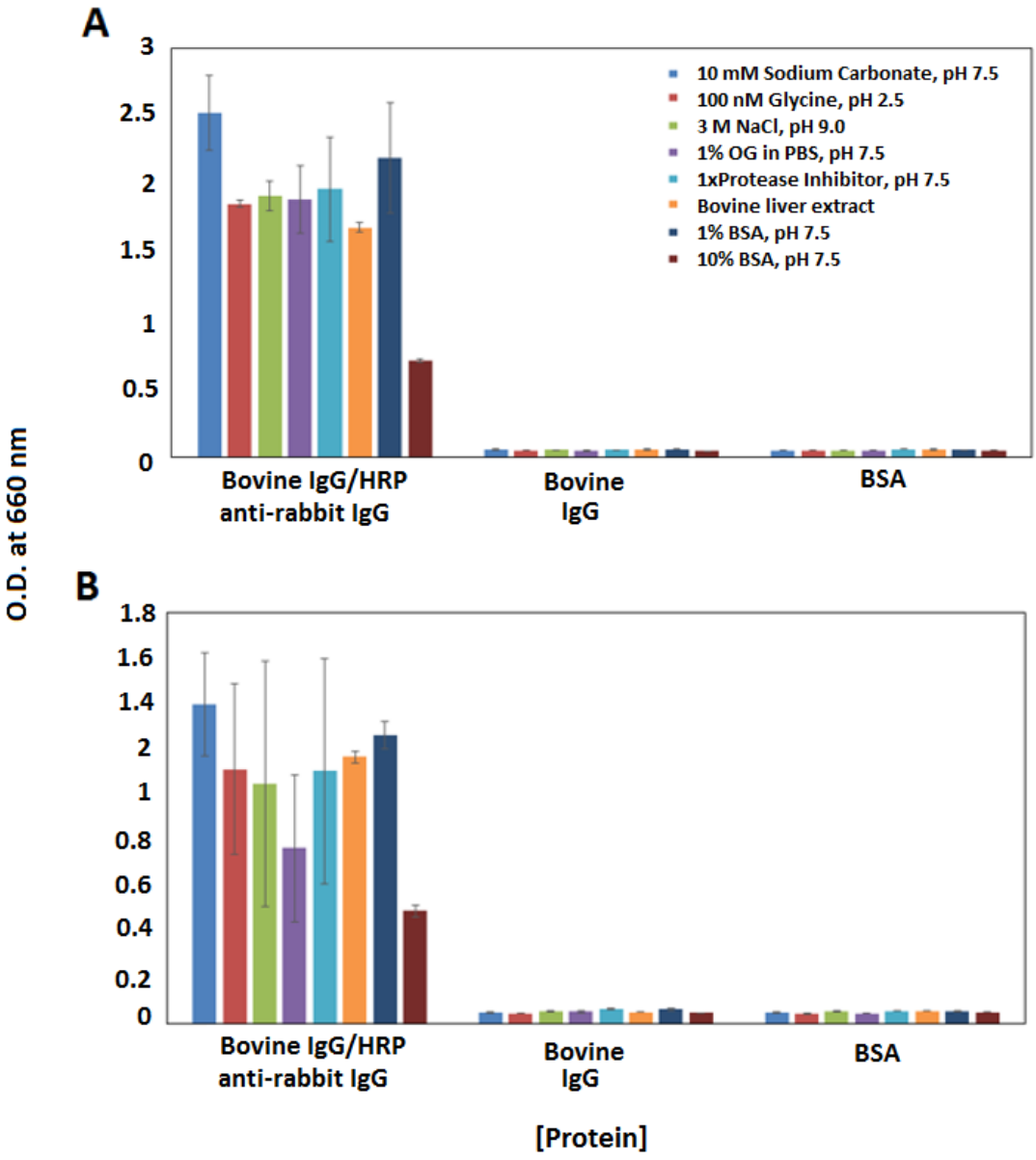

Figure 42. Impact of UV-light crosslinking on protein immobilization on the plates. The two panels illustrate the results from two plates **(A)** Samples subjected to UV-crosslinking and **(B)** not crosslinked. From left to right, HRP was immobilized and incubated with different reagents to test the displacement of immobilized protein. HRP was successfully immobilized on the plates with and without UV-crosslinking and the effect of the reagent was not significant. Signal developed after 15 minutes of adding diluted TMB supersensitive. Each sample had two replicates. Error bars were obtained by calculating the standard deviation (STDEVP). Absorbance was measured at 660 nm in the BioTek ELISA reader.

5.7.2 Binding capacity and binding buffer selection for protein immobilization

Protein-protein interactions are dependent not only in the availability of the prey protein present in the extracts but also of the amount of bait protein present for capture. Therefore, to understand the impact of this in the results, the binding capacity of the wells was estimated (Figure 43, Panel A). Three strips were covered with a range of bovine IgG/HRP between 0-~32 ug, eight points were prepared as threefold serial dilutions (Chapter II, Section 2.13.2). The graph shows a steep increase in signal between ~0.13 ug and ~0.384 ug with a second moderate but significant increase in signal between ~0.384 ug and ~1.18 ug. Thereafter there is a progressive signal increase but the difference between them is constant. Based on these results we estimated the binding capacity to be no more than ~1 ug.

After establishing the wells binding capacity it was required to identify the optimum binding buffer for protein immobilization. This was performed by preparing 12 strips with bovine IgG/HRP in a range of 0-~32 ug (Chapter II, Section 2.13.3). Eight points were prepared by a threefold serial dilution in four different binding buffers. Figure 43, Panel B shows a steep increase of signal until ~0.384 ug - ~1.18 ug. PBS, pH 7.5 presented the highest significant signal in comparison to the other buffers, whereas PBS (1/10), pH 7.5, 10 mM Sodium Carbonate, pH 7.5 and 500 mM K_2HPO_4, pH 8.5 also showed significant signal, the later one being poor in comparison to the others. It was concluded the most appropriate binding buffers for immobilization of bovine IgG/HRP were PBS, pH 7.5 and 500 mM K_2HPO_4, pH 8.5.

5.7.3 Determination of optimal pH for protein immobilization

Protein immobilization is dependent on many factors and finding the optimum pH for the buffer is pivotal. A threefold serial dilution of bovine IgG/HRP covering eight points between 0-~32 ug was prepared in a range of Phosphate buffers of pH 4-9 (Chapter II, Section 2.13.4). Figure 43, Panel C shows pH 4,5 and pH 8 emmit small detectable signals, whereas strong signals were detected at pH 6, 7 and 9. This trend was conserved through the whole range of protein concentrations. The experiment was repeated two more times and the data was reproducible. For all further experiments, immobilization of bovine IgG/HRP was kept at pH 6.5. Later, for SafA', 100 mM Potassium Phosphate buffer, pH 6.5 was used as the immobilisation buffer. The selection of buffer was because the mixture of monobasic and dibasic form solutions, depending on the desired pH.

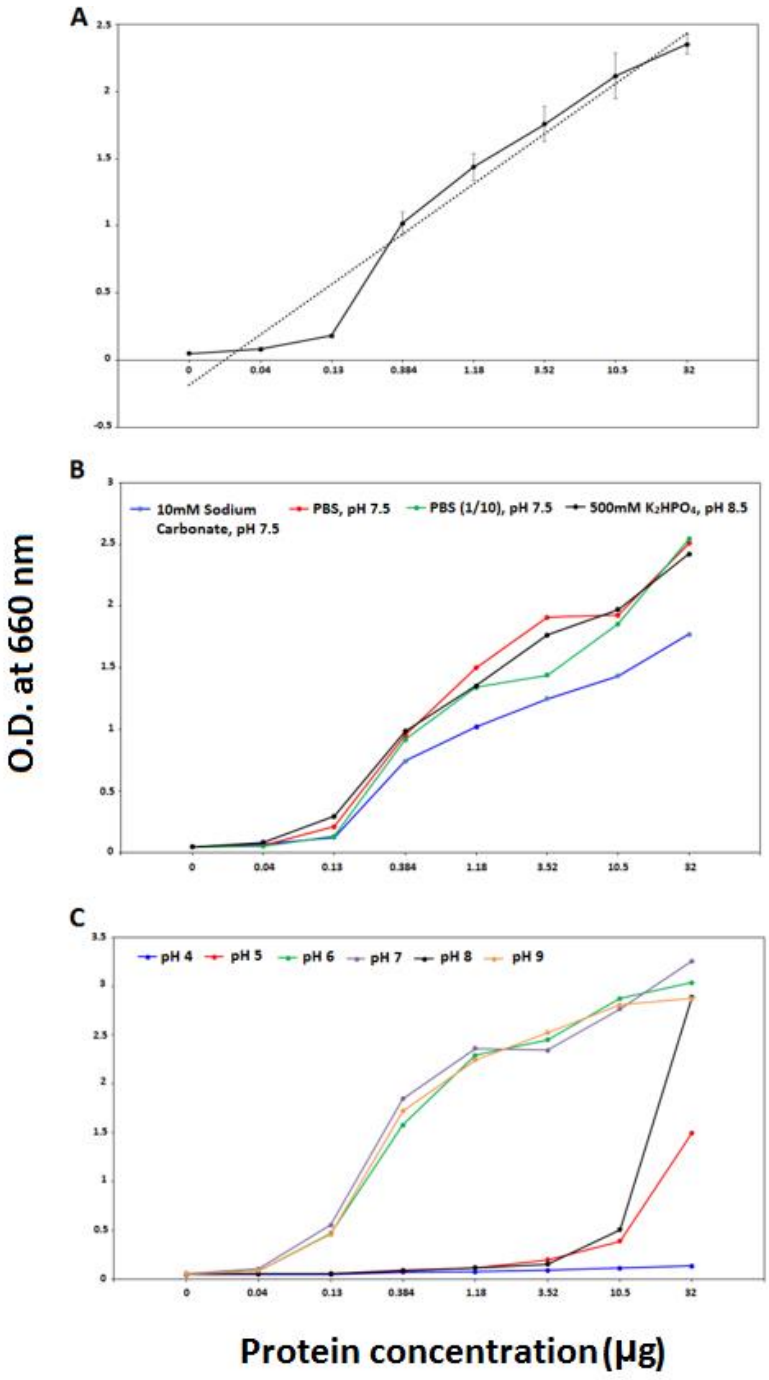

Figure 43. Setting up of Photo-reactive (Universal-BIND™) plate (System 5). (A) Binding capcity determination. Signal rapidly increases between ~0.384 µg and ~1.18 µg, therefore well saturation was established as ~1 µg. **(B) Determination of binding buffers for cross-linking bovine IgG/HRP.** Cross-linking of the maximum amount of protein (~1 ug) was achieved by PBS, pH 7.5. **(C) Optimization of pH in binding buffers for protein cross-linking.** Protein was immobilized on wells at different pH's using phosphate buffers. Immobilization of ~1 ug HRP (well saturation point) at pH 6, 7 and 9 give a strong signal, therefore an efficient immobilization. Signal developed after 15 minutes of adding diluted TMB supersensitive. Each sample had two replicates. Error bars were obtained by calculating stdevp. Plate was read at 660 nm in BioTek ELISA reader.

5.7.4 High concentrations of BSA in blocking buffer will displace immobilized protein

The previous trial indicated displacement of protein by high concentrations of BSA. In order to avoid non-specific proteins binding, blocking is however required. Therefore to determine the optimum concentration of BSA required to block the wells efficiently without displacing the bait protein, three strips were covered with a fixed concentration of bovine IgG/HRP. These were incubated with a range of BSA concentrations spiked with bovine IgG/HRP (Figure 44, Panel A). The rationale behind spiking BSA with bovine IgG/HRP was to find the point where protein was not displaced from the wells and the optimum concentration of BSA to achieve this without allowing the excess HRP to bind either. The range of BSA chosen had eight points between 0-10%; these were prepared using a tenfold dilution factor with an equal amount of bovine IgG/HRP in all of them (Chapter II, Section 2.13.6).

As per results, the range of BSA between 0-0.1% indicates these concentrations are too low by allowing excess HRP to bind, as indicated by the high signal. There is a significant drop in the signal between 0.1% and 1% which shows at this point the concentration of BSA is high enough to stop excess of HRP from binding and do not displace the HRP already on the wells. We also observe a signal drop between 1% and 10%, reflecting the absence of HRP in these samples. The results indicated 1% BSA is the ideal concentration for blocking as anything below will allow non-specific protein to bind and anything above will displace protein from the wells.This was taken into consideration for all affinity-enrichments.

5.7.5 Universal-BIND™ plates provide a strong platform to capture Salmonella-mammalian host interactions

Every affinity-enrichment performed involves a blocking step; therefore using the adequate blocking buffer to avoid non-specific binding like in the previous systems was crucial. Further to this, it was important to test whether solutions present in a typical affinity-enrichment would affect the balance of the protein on the wells. These tests were pivotal as consistency and reproducibility of results at this stage would allow us to be confident enough and take the system forward.

Two strips were incubated with bovine IgG/HRP and two strips were incubated with 100 mM phosphate buffer, pH 6.5 (control). After immobilization these strips were incubated with different blocking solutions, followed by incubation with α-rabbit IgG/HRP (Figure 44, Panel B). The first aim of the experiment was to test the suitability of different

solutions as blocking buffer, taking into consideration that these should block any free active sites but not displace the already immobilized protein. The second aim was to check if any of the solutions present in the protein extracts would wash away or displace the protein. The third and final aim of the experiment was to test the efficiency of 100 mM Glycine, pH 2.5 and 3 M NaCl, pH 8.00 as elution buffers.

The results (Figure 44, Panel B) indicate 1% BSA as the optimal blocking agent, 1% Tween washed away approximately half of the protein from the wells and is an inefficient blocking agent. 1% OG washed away protein and did not work as a blocking agent. The EDTA-free protease inhibitors (Sigma) (see Chapter II, Section 2.1 for tablet composition) used during the protein extraction were also tested (these were used to inhibit serine, cysteine, aspartic and metalloproteases). The results show these did not affect the stability of the protein on the wells but they can work as a blocking agent avoiding further HRP binding (Figure 44, Panel B). Incubation with bovine liver extracts did not show significant protein displacement but it is almost as efficient as BSA in blocking the wells. The experiment validated previous results and confirmed our ability to produce consistent data using the Universal-BIND™ plates.

After concluding the optimization of the system and finding the wells binding capacity to be ~1µg (Figure 43, Panel A), establishing the most appropriate blocking agent for the Universal-BIND™ plates to be 1% BSA; the system was ready to be tested with a pair of known interacting partners, such as, rabbit IgG and α-rabbit IgG. Other observations during the trials were also taken into consideration, such as, not using high amounts of OG in the washing buffers and the importance of crosslinking the plates under UV-light. The effect of each solution on immobilized proteins was also contemplated. Several buffer trials were also carried (Figure 43, Panels B and C) and it was considered appropriate to use 100 mM Potassium Phosphate, pH 6.5 as this is the pK_a of SafA' (GST-SafA-6xHis).

All the conditions were tested by immobilizing rabbit IgG on the wells, crosslinking protein to the plates by UV-light and blocking with 1% BSA before pulling down α-rabbit IgG. A negative control was prepared by immobilizing bovine IgG on the wells and treating it in the same way as the rabbit IgG Co-IP wells (Figure 44, Panel C). The results demonstrate the capture of α-rabbit IgG/HRP exclusively to the rabbit IgG wells. The negative control shows a signal of low significant value and therefore we concluded the system was successfully working.

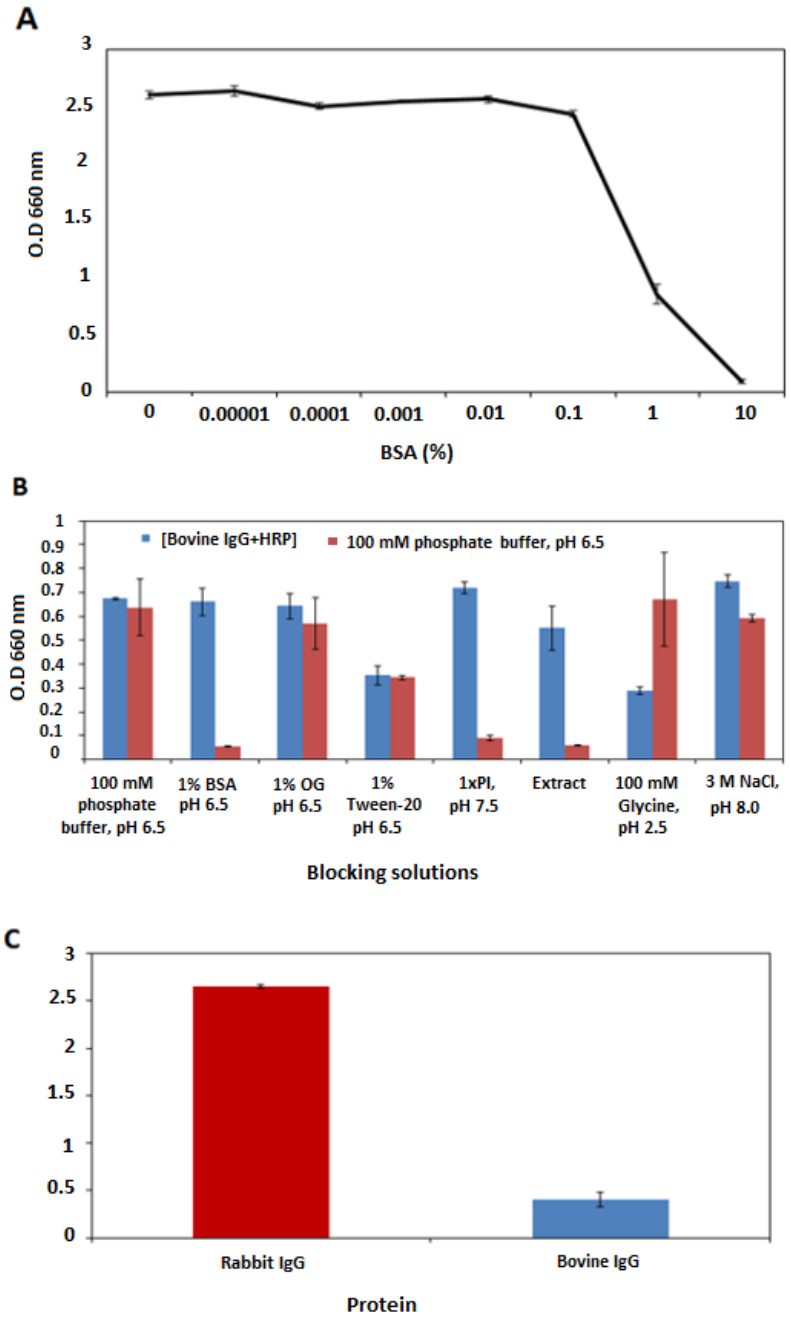

Figure 43. Optimization of Universal-BIND™ plates based affinity-enrichment system. Panels **(A)** and **(B)** show 1% BSA is an optimal blocking agent as it does not displace HRP from the wells and do not allow further binding of it either. **(A) Displacement of protein by bovine serum albumin (BSA).** BSA concentrations of 0-0.1% show no displacement of protein and did not block wells and 10% BSA displaced the protein and 1% was found to be optimal for blocking. **(B) Comparison of blocking and elution solutions.** 1% OG can wash protein away but does not work as a blocking agent. 1% Tween washes protein significantly from wells and can work as a blocking agent, yet not efficiently. 1xPI does not displace protein and blocks wells. Undiluted protein extracts can displace HRP and block wells. 100 mM Glycine, pH 2.5 can partially elute protein from wells but does not work as blocking agent. 3 M NaCl, pH 8 does not show any effect on the samples. **(C) α-rabbit IgG Co-IP.** Known binding partners were used to test the final working conditions. Each sample had two replicates. Signal developed after 15 minutes of adding diluted TMB supersensitive. Error bars were obtained by calculating the standard deviation (STDEVP). Absorbance was measured at 660 nm in the BioTek ELISA reader.

5.7.6. Affinity-enrichment results of Salmonella bait proteins SafA' (GST-SafA-6xHis) with rat extracts

After setting up and testing several systems, it was conclusive the system to take forward was the Photo-reactive (Universal-BIND™) plate. Nevertheless, the binding capacity of the wells being ~1 µg of bait protein imposed a limitation for the amount of any possible captured protein.

This section has a representative number of SDS-PAGE gels of affinity-enrichments between our recombinant *Salmonella* protein, SafA' (GST-SafA-6xHis), and proteins extracted from different tissues (Figures 44). Each affinity-enrichment was repeated at least three times (or less if tissue unavailable) in order to obtain consistent results. The work carried was extensive, we also carried affinity-enrichments between other recombinant *Salmonella* proteins supplied to us by our collaborators in Germany (data not presented). Nevertheless, these images are simply for the purposes of showing the versatility of the system and as an example of a combination of results.

5.7.7. SafA' (GST-SafA-6xHis) affinity-enrichment with proteins extracted from rat's small intestine, arge intestine and colon

SafA' (GST-SafA-6xHis) affinity-enrichments were performed using the Photo-reactive (Universal-BIND™) plates. Bait protein SafA' (GST-SafA-6xHis) was immobilized on plates with each of the mentioned extracts. Each affinity-enrichment had its respective negative control with BSA being immobilized on the respective surface and incubated with the same extracts (Figure 45, Panel A).

The SDS-PAGE gels for SafA' (GST-SafA-6xHis) affinity-enrichments with rat's small intestine and large intestine extracts performed in the Photo-reactive (Universal-BIND™) show no specific binding (Figure 45, Panel A, Lanes 4-6). Whereas there is a possible specific band of ~25 kDa in the colon extracts in the SafA' (GST-SafA-6xHis) affinity-enrichment (Figure 45, Panel A, Lane 1) (although this could potentially be leaking SafA' (GST-SafA-6xHis) as it resemebles one of the bands in Figure 45, Panel A, Lane 7). In most of the gels it is possible to observe BSA leaks from the system as reflected by bands of ~55-60 kDa. No SafA' (GST-SafA-6xHis) proteins were observed leaking from the system, at least in enough quantities for the gels to show. In Figure 45, Panel A, both BSA negative controls have a strong BSA band and at lower molecular weights it is possible to see the binding of some small proteins.

5.7.8. SafA' (GST-SafA-6xHis) affinity-enrichments with proteins extracted from rat's liver, heart and spleen

To continue with the systematically approach, affinity-enrichments with proteins extracted from rat's liver, heart and spleen were performed. Affinity-enrichments performed in the Photo-reactive (Universal-BIND™) plates did not reveal any specific protein to SafA' (GST-SafA-6xHis) (Figure 45, Panel B). Extract proteins were found to bind in an almost equal manner to all bait proteins. Even when bands can be observed, the gels point out that there are unresolved proteins which are present in each of the lanes, as represented by the smears.

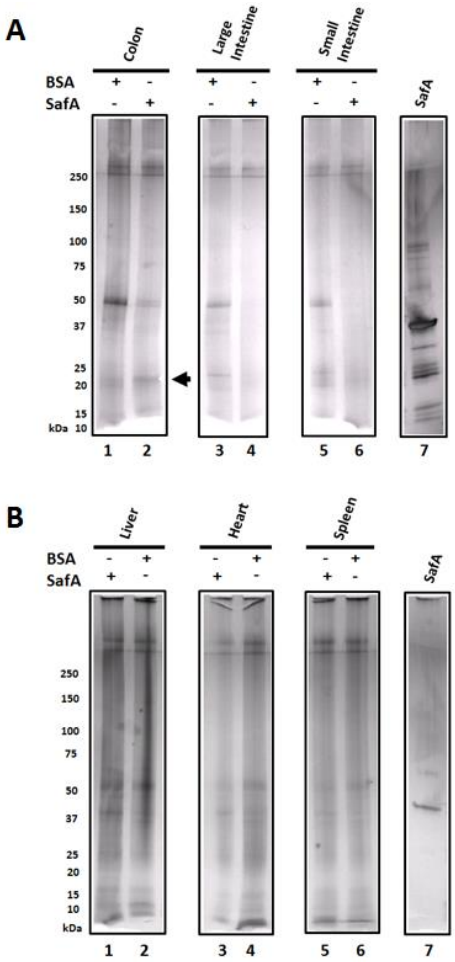

Figure 44. Silver stained 4-15% SDS-PAGE gels of diverse affinity-enrichments performed in Photo-reactive (Universal-BIND™) plates. (A) SafA' (GST-SafA-6xHis) affinity-enrichments with rat's colon, large intestine and small intestine extracts showing a possisble specific bands of ~25 kDa **(B)** SafA' (GST-SafA-6xHis) affinity-enrichments with rat's liver, heart and spleen extracts. **(C)** SafA' (GST-SafA-6xHis) affinity-enrichments with rat's liver and heart extracts. Image was taken in LI-COR Odyssey scanner. .

5.7.9 Discussion

There is not a single standard system that can be used to identify all protein-protein interaction (PPI); a number of different approaches have to be used. Yet, the general approach is to immobilize the bait on the selected surface, followed by blocking of any free active sites with agents, such as, BSA or milk. This is followed by incubation of a sample containing the protein/antibody of interest and elution or chemiluminescent detection (the exact procedure is determined by the selected protocol) (Arkin et al 2012, Buchwalow et al 2011, Hutsell et al 2010). Proteins were immobilized by using a repertoire of surfaces and chemistries, such as, superparamagnetic cobalt beads (IMAC technology) (System 1), agarose nickel beads (IMAC technology) (System 2), and GSH-agarose (System 3), Nitrocellulose (System 4) and Universal-BIND™ plates (System 5).

Of these, the IMAC technology-based systems are widely used for capture and purification of recombinant proteins (Block et al 2009) and are also a common approach for immunoprecipitation (Avila et al 2015, Elsaraj and Bhullar et al 2008, Gupta et al 2001, Khan and Lee et al 2014, Ma et al 2005, Rippa et al 2010, Sousa et al 2011, Sun et al 2012). In the case of NC, this is conventionally used for the electrophoretic transfer of proteins from gels (Towbin et al 1979), but as it is known for its binding capacity, it has also been used to enhance the binding capacity of microplates (Halim et al 2005). In regard to the Universal-BIND^{TM} plate (system 5), these have been extensively used for ELISA immunoassays (Gan and Patel et al 2013, de Matos et al 2010).

Several considerations can be made in the light of the experience gained by carrying out the different experimental techniques described in this Chapter. IMAC protein binding combined with magnetic capture and the non-porous nature of the beads improves experimental reproducibility. Dynabeads (System 1, Section 5.3) fall within this category. It offered a non-porous smooth surface for bait capture and handling of the samples during washing and the elution step was simplified by magnetic separation. The beads were tested with mammalian extracts from several tissues and they attract multiple non-specific proteins.

The use of IMAC technology for affinity-enrichments (Systems 1 and 2, Sections 5.3 and 5.4) was still an attractive option; therefore we decided to investigate whether using a different immobilization surface (agarose beads instead of magnetic beads System 2 and System 1) would resolve the issue of non-specific protein capture. HIS-Select Nickel Affinity Gel (System 2) had all the same advantages as the previously mentioned IMAC

system, but promised a much lower non-specific protein adsorption due to the nature of the bead material (agarose); and the opportunity to immobilize SafA' (GST-SafA-6xHis) through its Histidine tag by using a different ion ($Ni^{+}2$). Because this was an agarose-based system, it was possible to have longer washing times to eliminate any non-specific proteins binding to the mesh (Chapter I, Table 1).

To determine whether the non-specific protein binding was to the nickel ion or to the beads, Dynabeads (System 1) and Nickel-agarose (System 2) were stripped of their Cobalt and Nickel ions, followed by protein extracts incubation (Sections 5.3.4 and 5.4.1) .Further to this, in an attempt to disturb the possible ionic interaction between the beads and non-specific proteins, the extracts were buffered with different salt concentrations. The results did not show a measurable difference for Dynabeads but when the Nickel was stripped of the agarose, there were no visible non-specific proteins in the gel (Figure 35, Panel B).

Affinity-enrichments in GSH-agarose (System 3, Section 5.5) gave similar background results (Figure 37), with the difference that there was clearly the capture of a ~ 25-35 kDa protein. Similar levels of protein capture were achieved with empty agarose beads (no bait protein). This suggested that the proteins captured are likely to be endogenous GST present in the extracts (MW 25 kDa) (Figure 37, Panel A, Lane 8 and Panel B). Depletion of the extracts using glutathione resin was partially successful, although even after five consecutive rounds of depletion some ~25-35 kDa protein remained in the extract. A recorded difficulty of working with tissue extracts from GI tract is the presence of endogenous glutathione, an important endogenous antioxidant especially abundant in GI tract (Hayes et al 1989, Van Veld and Lee et al 1988). The realization of this ruled out the use of GSH-agarose as a potential system.

Having failed to establish a stable affinity-enrichment, two known systems were adapted. Nitrocellulose (NC) (System 3, Section 5.6), provides a high binding capacity and is a standard material for protein blotting. To prevent any free reactive sites, NC pieces were blocked with BSA. SafA' (GST-SafA-6xHis) was immobilized using crosslinking. This was done to ensure that NC was blocked and deterred non-specific binding. Unfortunately, the results showed that it made no difference and there was still high background (Figure 39, Panel D). As a final attempt to find a surface that would not capture non-specific proteins, Universal-BIND^{TM} plates (System 5, Section 5.7) were used. This would provide a non-porous surface, it was not dependent on any tag (advantageous as the

system could still be used once the GST tag was cleaved) and each well served as a technical replicate.

SafA’ (GST-SafA-6xHis) was finally immobilized on Universal-BIND™ plates (System 5) by hydrophobic protein sorption (passive adsorption). Further to this, the plates gave the option to crosslink proteins to the wells. The immobilization of the proteins by abstractable hydrogen bonding using UV-light illumination, resulted in a carbon-carbon bond (Aspholm et al 2006) (Gibbs and Kennebunk et al 2001) that would crosslink proteins to the surface and reduce any possible bait loss during the assay. After optimizing the system, the affinity-enrichments performed showed a reduction in background in comparison to the previous systems; and SafA’ (GST-SafA-6xHis) was not displaced. Therefore, after setting up a number of systems by exploiting the physio-chemical characteristics of SafA’ (GST-SafA-6xHis), this was concluded to be the most stable and robust system.

CHAPTER VI - MASS SPECTROMETRY ANALYSIS

6.1 Introduction

This Chapter will describe the experimental approach of both Mass Spectrometry (MS) analyses leading to the identification of host partners specific to fimbria protein SafA. The results presented in this section include the MALDI-TOF MS analysis of a series of tissues (heart, large intestine, small intestine and colon) that due to the complexity of the samples, led us to the use of the nanoLC-ESI-MS/MS. The latter, identifying five putative proteins binding solely to SafA-6xHis. Links to the putative biological function for *Salmonella* will be also presented.

MS based proteomics has become a vital tool in the study of protein-protein interactions (Eriksson et al 2000, Salzano and Crescenzi et al 2005, Sikdar et al 2016, Wang and Wilson et al 2013). Protein interaction studies can be performed by immobilizing a bait coupled to affinity tags on a surface, such as beads, on which the affinity ligand has been covalently bound. The ligand specifically and relatively strongly binds the affinity tag (McFedries et al 2013). The then immobilised protein can be incubated with lysates containing proteins of interest. Any non-specific binders are washed away and subsequently, any strongly specific interacting partners are eluted to be further analysed. For instance, by visualization on an SDS-PAGE and/or western blotting (if the putative prey is known) (Carneiro et al 2016, Nguyen and Goodrich et al 2006, Phizicky and Fields et al 1995, Rao et al 2014).

Alternatively, the whole eluates are trypsinized and analysed by mass spectrometry. The advantages of MS relies on its high sensitivity, capability of evaluating complex protein mixtures and detection of very low analyte concentrations without prior knowledge of the preys (Aichler and Walch et al 2015, McLafferty et al 2008). Protein identification is achieved by peptide based mass spectrometry. Because the proteome is so complex, there is no standard method for preparing the samples. Nonetheless, common practise is to digest proteins by endoproteinases. For example, trypsin, where the serine protease cleaves peptides at the carboxyl side of arginine and lysine (except when followed by proline) (Hustoft et al 2012, Olsen et al 2004). The absolute mass of the peptides present in the mixture is measured by a mass spectrometer and compared to a database containing

known protein sequences (Damodaran et al 2007, Henzel et al 2003, Marvin et al 2003, Thiede et al 2005).

There are two main methods of using peptide based MS to identify proteins, these are Peptide Mass Fingerprinting (PMF) and MS/MS. In PMF, after cleaving the proteins into small peptides, the mass-to-charge *(m/z)* values of the produced peptides are matched to in-silico protein databases, such as, SwissProt or NCBI. This is achieved by using specifically designed software search engines to identify proteins from the peptide sequence databases. An example of the most widely used mass spectrometry software are MASCOT (provided by Matrix Science Inc) (Cottrell and London et al 1999) and ProteinProspector (developed by UCSF) (Baker and Chalkley et al 2014). In the case of identification by MS/MS, peptide sequence information is acquired following peptide fragmentation in tandem mass spectrometry (MS/MS or MS2) (Cottrell et al 2011, Grebe and Singh et al 2011, Seidler et al 2010).

The different mass spectrometers can be described based on their ion sources and mass analysers. Basically, two types of ion sources are the most popular, the electrospray (ESI) and the Matrix Assisted Laser Desorption Ionization (MALDI) (Seymour et al 2010, Siuzdak et al 1999, Soeriyadi et al 2013). For proteomics research, three types of mass analysers are commonly used, quadrupole (Quad, Q), Ion Trap and Time-of-Flight (TOF). Further to this, both ion sources can be coupled with any of the mass analysers, for example, MALDI-TOF, ESI-Quad and the analysers can be combined with each other, such as, Q Trap, ESI-QQQ and MALDI QQ (Cañas et al 2006, El-Aneed et al 2009).

For MALDI the in-solution sample is mixed with a solid matrix. The sample/matrix crystals are vaporised by a UV laser pulse (Typical wavelengths are 337 nm and 355 nm) (Fuchs and Schiller et al 2013, Lu et al 2015) with a pulse duration between 0.5 and ~20 ns (Menzel et al 2002) where the sample molecules are ionized by photon transfer from matrix ($MH^+ + A \rightarrow M+AH^+$) (Knochenmuss et al 2000). The matrix absorbs the photon energy and converts it into thermal energy, causing an increase of temperature that will outset desorption and melt the sample between each UV laser pulse (Chu et al 2014, Menzel et al 2001). During the liquid phase (which is the interval between the laser pulse and desorption), molecules display high energy and they collide with each other (Lu et al 2015, Medzihradszky et al 2000). Once the molecules are desorbed from the plate's

surface, these are converted into a gas phase forming a plume of ions (Knochenmuss and Zenobi et al 2003, Zenobi and Knochenmuss et al 1998) (Figure 46, Panel A).

Electrospray ionisation (ESI) is usually used with ionic compounds of high polarity (Ghosh et al 2012, Tolstikov and Fiehn et al 2002). It consists of a fine needle and a series of skimmers. The in-solution sample is led on to the tip of a capillary tube where a high voltage (~3-~5 kV) is applied. The sample is nebulised and sprayed into the source of the chamber to form droplets (Freire and Wheeler et al 2008). As the charged particles (with the same polarity as the applied voltage) continue to move, the solvent is evaporated resulting in the increase of the electric field on the droplet surface. At some point, fission will occur and is through the repetition of this evaporation and fission cycle that the samples enter the gas phase (Cech and Enke et al 2001, Gaskell et al 1997, Hawkridge et al 2014, Ho et al 2003).

The basic principle of MS is ionization of analytes to convert them to a charged state. It is here where the two techniques divert as in PMF the ions are directly analysed based in their mass-to-charge ratio (*m/z*) (Jain and Wagner et al 2010). Whereas in peptide sequencing, the proteolytic digest is separated by high-pressure liquid chromatography (HPLC or RP-HPLC) (Kumar and Kumar et al 2012, Yamane et al 2002) and eluted into the ESI source. The sample is sprayed using an electric field towards a negatively charged plate, resulting in small charged droplets (Ho et al 2003). As the droplets start to evaporate they become smaller until the now charged ions are accelerated by the electric field and the mass-to-charge ratio (*m/z*) is measured (MS1) (Banerjee and Mazumdar et al 2012, Cech and Enke et al 2001). A list of ions with their absolute masses is obtained and the isolated peptides (or parent ions) are fragmented to be analysed by the second analyser (MS/MS) (Cañas et al 2006, Grebe and Singh et al 2011). Fragmentation occurs by higher-energy collisional gas dissociation (HCD) where the ions are allowed to collide with neutral molecules, such as, Argon, Helium or Nitrogen. The collision results in the bond breakage yielding peptide fragments (also called daughter ions) (Wells and McLuckey et al 2005) (Figure 46, Panel B). The resulting spectrum is the product of all fragment ions that derive from the isolated peptides (Medzihradszky and Chalkley et al 2015). Finally, the MS/MS spectra is matched against protein sequence databases (Aebersold and Mann et al 2003, Wang and Wilson et al 2013).

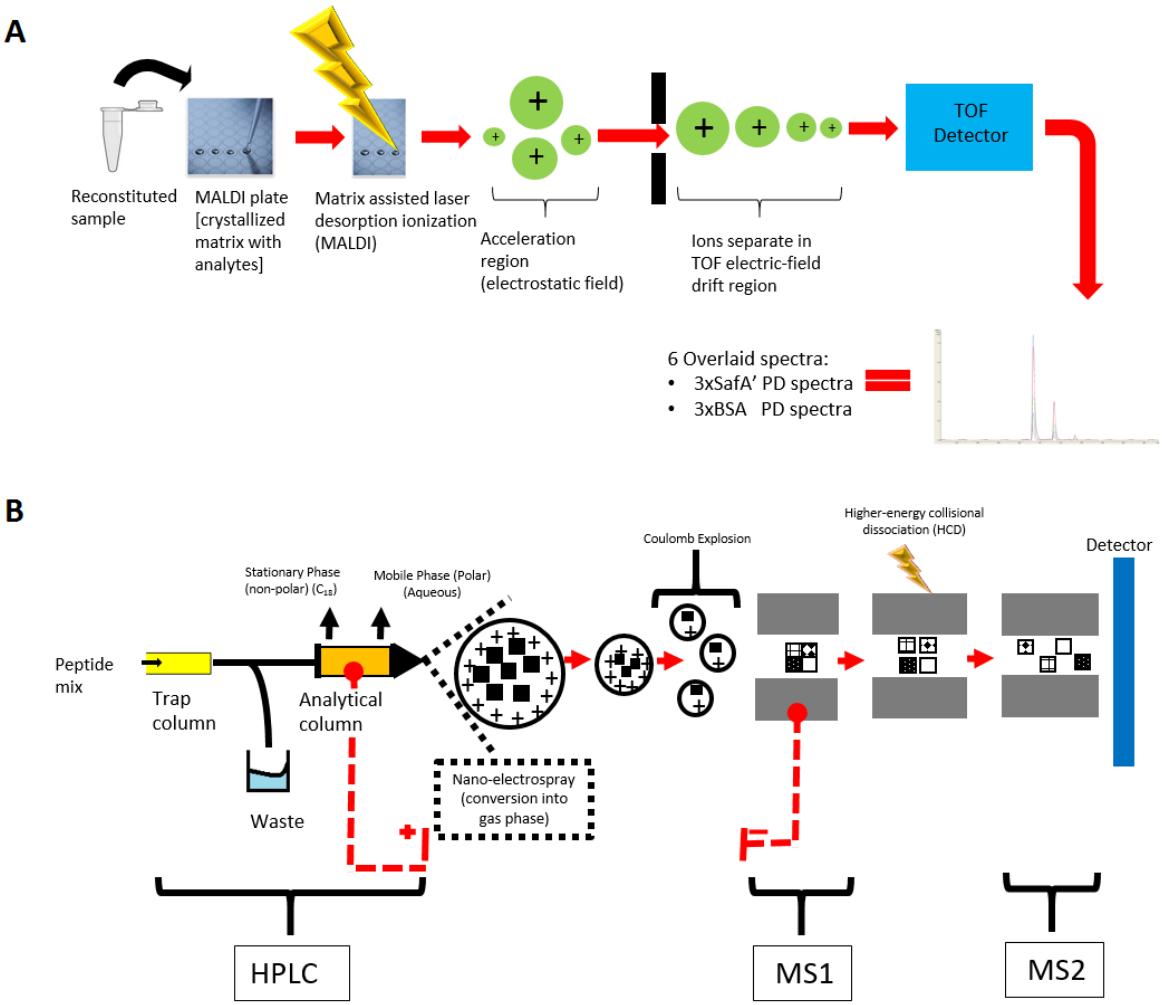

Figure 45. Workflow of the MALDI-TOF MS (MS1) comparative analysis and LC-MS/MS (MS2). **(A)** Samples are reconstituted and mixed with matrix for spotting on the MALDI plate. The now crystallized samples are vaporised by a UV-pulse for ionization. The molecules are desorbed from the plate's surface and are converted into the gas phase. They enter an electric field and subsequently the ions re separated by their mass-to- charge (*m/z*) ratio in the TOF. The lighter ions reach the TOF detector quicker and the heavier ones later. For analysis, three spectra for SafA' (GST-SafA-6xHis) affinity-enrichments and three spectra for the BSA affinity-enrichments are overlaid for peak selection. **(B)** The sample is injected and separated by HPLC before being eluted into the ESI source. The sample is nebulised and sprayed to form charged droplets. Eventually the ions are accelerated into the electric field and MS1 is performed to measure their mass-to-charge ratio (*m/z*). A list of ions with their absolute masses is obtained and the isolated peptides (or parent ions) are fragmented to be analysed by a second mass analyser (MS2). Fragmentation occurs by HCD. The collision yields peptide fragments ions that derive from the isolated peptides. Panel A adapted from Singhal et al (2015). Panel B adapted from Steen and Mann et al (2004).

6.1.1 MALDI-TOF MS

For PMF the protein sample was trypsinized, obtaining a peptide digest. The peptides were mixed with α-Cyano-4-hydroxycinnamic acid matrix (see Chapter II, Section 2.17.1). In the MS the analyte/matrix was vaporised by a series of UV-laser pulses causing ionisation and desorption. Subsequently, the molecules were in the gas phase and formed

a plume. High voltage was applied to the sample plate to accelerate ions out of the ion source into the flight tube where these would be separated according to their mass-to-charge ratios (*m/z*). For instance, the lighter ions travelled faster than the heavier ones reaching the detector first. Mass-to-charge (*m/z*) peptide values (usually MH^+) were converted to molecular weight (MW) and peptides of the same protein isoform were grouped into a protein by comparing to a relevant in silico digested reference protein database (NCBI, SwissProt and UniProt). The hits were ranked according to a probability scoring method reflecting that the candidate protein containing the highest number of proteolytic peptides with matching mass was given the highest score. Therefore, protein identification heavily relies in the score given to a protein (PMF) rather than for individual peptides as it is the case in MS/MS analysis, where peptide sequence information is retrieved.

6.1.2 nanoLC-ESI-MS/MS

Since whole eluates from affinity-enrichments were analysed, and thus are relatively complex protein mixtures, we used nLC-nESI-MS/MS as a better option. Peptides are first separated in time by reverse phase (RP) chromatography, a column with a hydrophobic stationary phase that adsorbs hydrophobic molecules in a polar mobile phase, allowing the hydrophilic molecules pass through (Mohammad and Jabeen et al 2003, Molíková and Jandera et al 2010, Uhl et al 2011). Therefore, the later ones are eluted first, whereas the hydrophobic molecules can be eluted by decreasing the polarity of the solution in the mobile phase (usually by adding more organic solvent) (Foster and Synovec et al 1996, Haggarty et al 2015). The advantages of using RP-chromatography, such as, C18 capillary columns is that it is stable and versatile, thus it can be used with water as a mobile phase, it allows for pH selectivity and can be applied to separate a range of molecules. (Kumar and Kumar et al 2012, Snyder et al 1997).

In brief, the NLC-nESI-MSMS workflow requires the digestion of proteins with a protease such as trypsin followed by nanoLC on C18 capillary columns in line with the MS instrument for direct analysis of the RP eluant. The eluate is desolvated and ionized in the ESI source to create an electrospray plume containing usually positively charged ionized peptides (Banerjee and Mazumdar et al 2012, Cox et al 2014). The peptides present in the spray travel down a voltage gradient in the mass spectrometer where they are separated by their mass-to-charge (*m/z*) ratio. At the next stage, the isolated peptide mass (*m/z*) is fragmented by HCD. The fragment ions broken at the level of the peptide

bond are recorded in the MS/MS giving amino acid information, based on mass differences of the b and y ions series (Hawkridge et al 2014, Jedrychowski et al 2011, Medzihradszky and Chalkley et al 2015, Scherl et al 2008, Shao et al 2014, Steen and Mann et al 2004).

PMF-related database searches are simpler than LC-MS/MS ones. Another advantage of MALDI-TOF MS is that it requires low amounts of analyte and it has high sensitivity (Chen et al 2013, Cobo et al 2013, Singhal et al 2015). On the contrary, it is known that MALDI-TOF MS requires pure samples and any contamination can be problematic, whereas LC-MS/MS is useful in the analysis of complex mixtures. LC-MS/MS also provides a higher confidence identification due to the sequence dependence of data obtained from the tandem mass spectrometry (El-Aneed et al 2009, Hird et al 2014, Tribalat et al 2006). For this study we used MALDI-TOF MS and nanoLC-ESI-MS/MS. (MALDI-TOF MS) was used for PMF (Gevaert and Vandekerckhove et al 2000, Thiede et al 2005) and nLC-nESI-MS/MS for peptide fragmentation (Biniossek and Schilling et al 2012, Sowell et al 2004, Williams and Tomer et al 2004).

6.2 Experimental Design

Initially different systems were tested to identify SafA' (GST-SafA-6xHis) interacting proteins using four different tissues (heart, colon, small and large intestine) in the MALDI-TOF MS (Figure 47). Nevertheless, *Salmonella's* main infection site is the digestive system (particularly the large and small intestine), therefore the nanoLC-ESI-MS/MS analysis was focused on identifying host interacting partners for SafA' (GST-SafA-6xHis) in the large intestine. Affinity-enrichments were performed as described in materials and methods (Chapter II, Section 2.13.8 and Chapter V, Figure 31). Figure 48 shows the number of biological and technical replicates analysed for the nanoLC-ESI-MS/MS. A total of seven affinity-enrichments were executed and five rats were used. The Universal-BIND^{TM} plate (system 5) was used, each well corresponding to a technical replicate. For analysis, these replicates were pooled together. Results for P1 and P2 are not presented due to lack of specific proteins binding to SafA' (GST-SafA-6xHis) only. Based on the previous observations, P3 was designed to have sixteen technical replicates and GST as an additional negative control. The use of more wells increased the amount of material available, allowing for a better analysis with more proteins. Therefore, for affinity-enrichments' P4-P7 the technical replicates were increased to a total of 32 wells. Affinity-enrichments' P1-P4 had SafA' (GST-SafA-6xHis) as a bait whereas affinity-enrichments'

P5-P7 had undepleted cleaved SafA’ (GST+SafA-6xHis). The undepleted cleaved SafA’ (GST+SafA-6xHis) affinity-enrichment was repeated twice and a third time without crosslinking the protein to the plates.

The work carried out for the MALDI-TOF MS analysis also used a Universal-BIND™ plate-based system and had only SafA’ (GST-SafA-6xHis) and BSA as baits with, initially, one replicate reconstituted in different volumes, such as, 50 µL and 15 µL (Figure 47). Due to limitation in the quantity of material available, technical replicates were pooled together. The MALDI-TOF MS analysis concluded with the pooling of two and sixteen technical replicates (Figure 47 and Table 15).

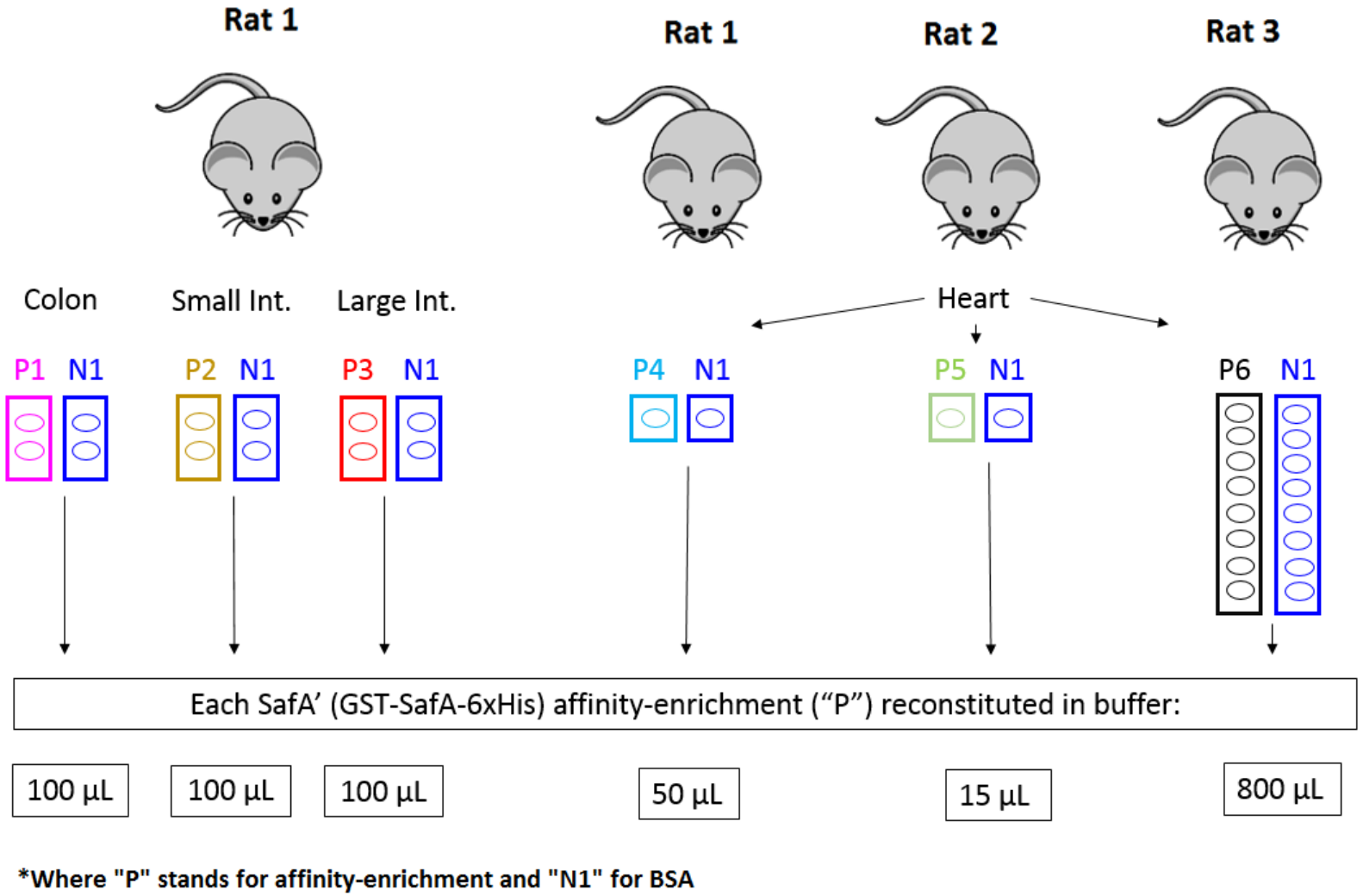

Figure 46. Experimental design used in the MS1 (MALDI-TOF MS) study. A total of three rats were used for the six affinity-enrichments (each rat represent a biological replicate) and each well a technical replicate. P1, P2 andP3 had two, P4 & P5 one and P6 eightwell as technical replicates. After elution, technical replicates were pooled together for analysis (see Chapter II, Section 2.13.8 and Chapter V, Figure 41 for the standard protocol used).

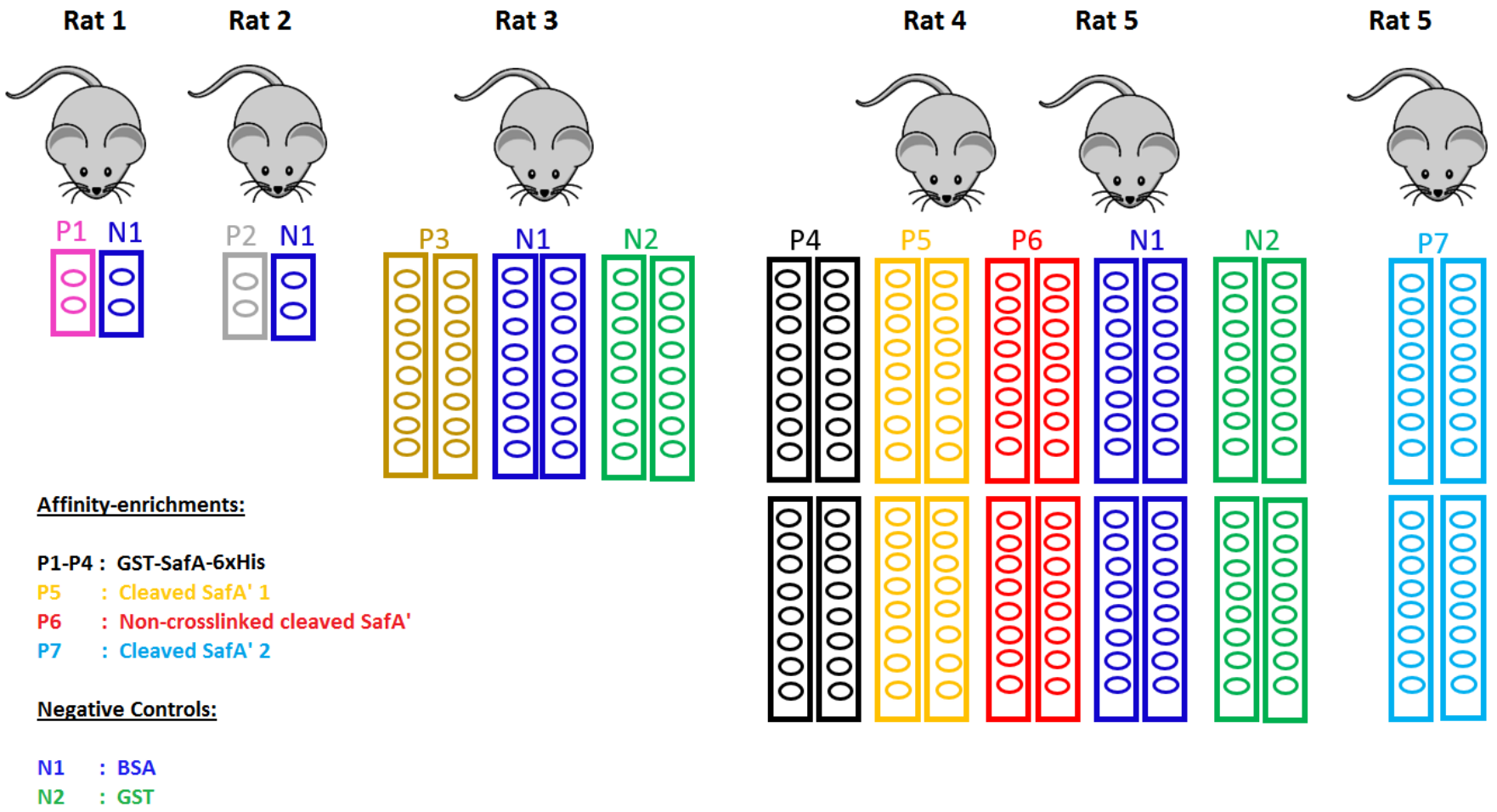

Figure 47. Experimental design used in the MS2 (LC-MS/MS) study. A total of five rats were used for the seven affinity-enrichments (each rat represent a biological replicate) and each well a technical replicate. P1&P2 (not to be presented or discussed) had two, P3 sixteen and P4-P7 thirty two wells as technical replicates. After elution, technical replicates were pooled together for analysis (see Chapter II, Section 2.13.8 and Chapter V, Figure 41 for the standard protocol used).

Affinity-enrichments were performed using the Universal-BIND™ plates (Chapter II, Section 2.13.8 and Chapter V, Section 5.7). These were used to isolate and identify mammalian proteins interacting with the SafA fimbria protein from *Salmonella enterica* serovar Typhimurium LT2. Initially, the affinity-enrichments' were performed with total protein extracts from different rat tissues ranging from kidney, brain, heart and the whole digestive system. These were then analysed by SDS-PAGE, where in some cases we could see some weak bands in the SafA' (GST-SafA-6xHis) samples only (Figure 45), but overall these did not show conclusive evidence on whether any specific interacting partners had been captured.

6.3 Results: MALDI-TOF MS Analysis

Affinity-enrichments from the heart and the intestine material were analysed by MALDI-TOF MS. The MALDI-TOF MS analysis was not successful to confidently identify any binding partner from the rat large intestine protein extract (the tissue of interest) that bound specifically to SafA' (GST-SafA6xHis). Spectra acquired for each affinity-enrichment (GST-SafA-6xHis' and their respective negative controls) were overlaid to manually check for any differential peaks (Figures 48-51). The detection of differential peaks in the SafA' (GST-SafA-6xHis) affinity enrichments' and the absence of these in the BSA negative controls suggested the presence of a protein(s) specifically binding to SafA' (GST-SafA-6xHis) (Table 15). From the peak list file generated from these differential peaks, the search performed with the MASCOT software identified a cyclin-dependent kinase-like 3 protein in the (GST-SafA-6xHis) SafA'/heart affinity-enrichment, absent in the BSA/heart affinity-enrichment (Figure 53). With the exception of the cyclin-dependent kinase-like 3 protein in the SafA' (GST-SafA-6xHis) affinity-enrichment sample, it was not possible to identify other differentially captured proteins from the heart and the intestine, more likely due to complexity of the samples, and the absence of LC separation prior MS analysis. Nevertheless, the observation of consistent differential peaks, absent in controls, gave us confidence to further investigate and identify specifically isolated proteins interacting with SafA' (GST-SafA-6xHis) with an alternative analytical workflow.

6.4 Comparative analysis of MALDI-TOF MS spectra indicated SafA' (GST-SafA-6xHis) affinity-enrichment's isolated peptides absent in the BSA negative controls

Based on SDS-PAGE gels it was indeed possible to identify if specific proteins were captured, nevertheless, these results were not conclusive as SDS page gels were not

sufficient to detect differential bands (Figure 45). Therefore, an alternative approach was undertaken. Whole eluates were prepared by removing the SDS to have detergent-free samples more suited for the downstream MALDI analysis. The proteins were digested and peptides applied on a MALDI target with an alpha-cyano-4-hydroxycinnamic acid matrix (Chapter II, Sections 2.17.1- 2.17.2) for MALDI-TOF MS and PMF analysis. Only a few affinity-enrichments were analysed by MALDI-TOF MS and this section describes how this analysis led us to seek for a more suitable method of analysis.

Samples were spotted, instrument calibrated and three different spectra were saved per affinity-enrichment. All samples were spotted next to their corresponding BSA negative control to later manually select any specific peaks (Chapter II, Section 2.17.2). The MS spectra obtained from the (GST-SafA-6xHis) SafA'/heart affinity-enrichment exhibited peptides specific to SafA' (GST-SafA-6xHis) in the range of ~1,000 - ~1,750 Da (Figures 49 and 50). These peptides are consistently present exclusively in the SafA' (GST-SafA-6xHis) affinity-enrichment in the three MS spectra taken and in none of the BSA control. The approach "comparative analysis" as 3x (GST-SafA6xHis) SafA'/heart and 3xBSA/heart MS spectra were overlaid resulting in a panel of 6x MS spectra. Three spots were used per affinity-enrichment and one MS spectra is the acquisition of several shots per spot (see Chapter II, Section 2.17.2).

Figures 49-52 show that the analysis revealed certain peptides (listed in Table 15) were unique to the SafA' (GST-SafA-6xHis) affinity-enrichment.

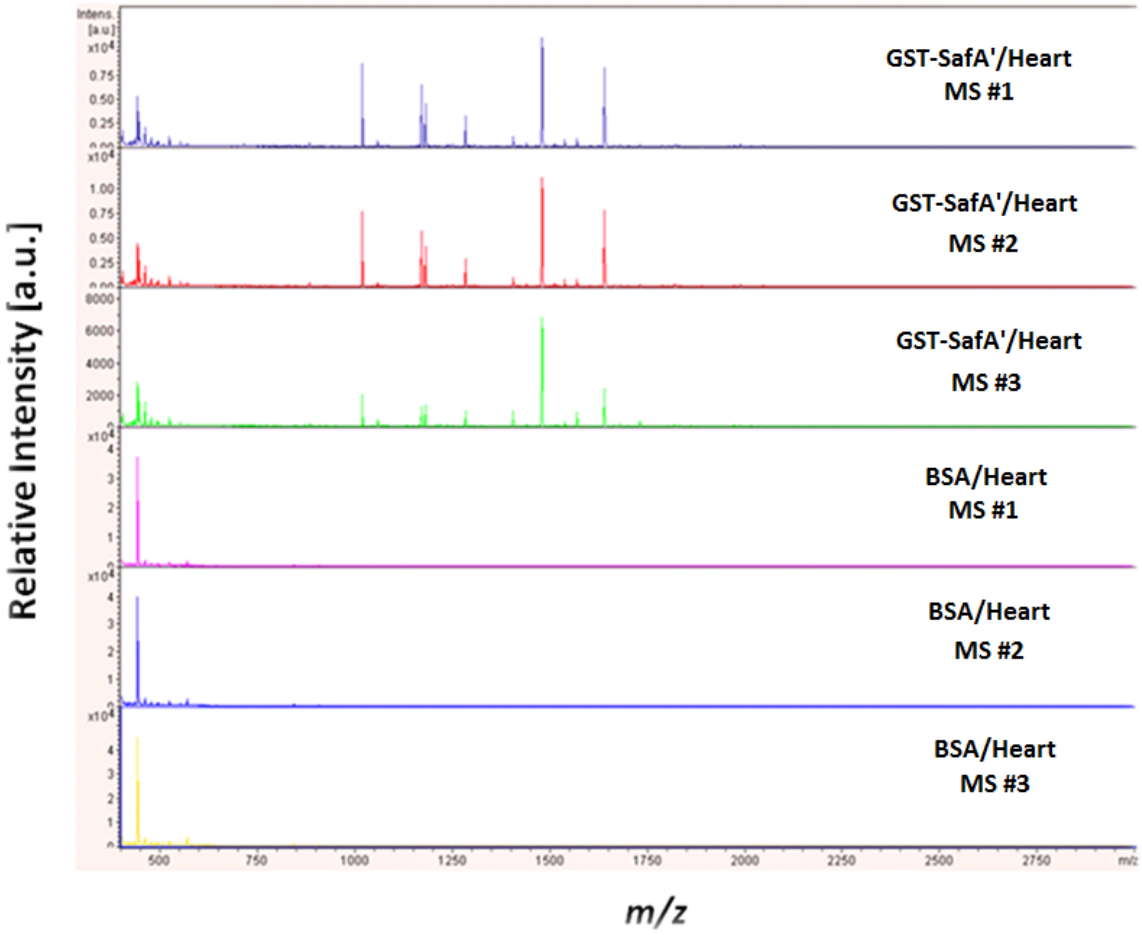

Figure 48. Comparison of (GST-SafA-6xHis) SafA'/heart and BSA/heart MS spectra showing an accumulation of peptides in the SafA' (GST-SafA-6xHis) affinity-enrichment. The top three (GST-SafA-6xHis) SafA'/heart MS spectra show a number of peaks not present in the negative control. These indicated the likelihood of a possible protein(s) specifically isolated by SafA' (GST-SafA-6xHis) from the heart protein extracts.

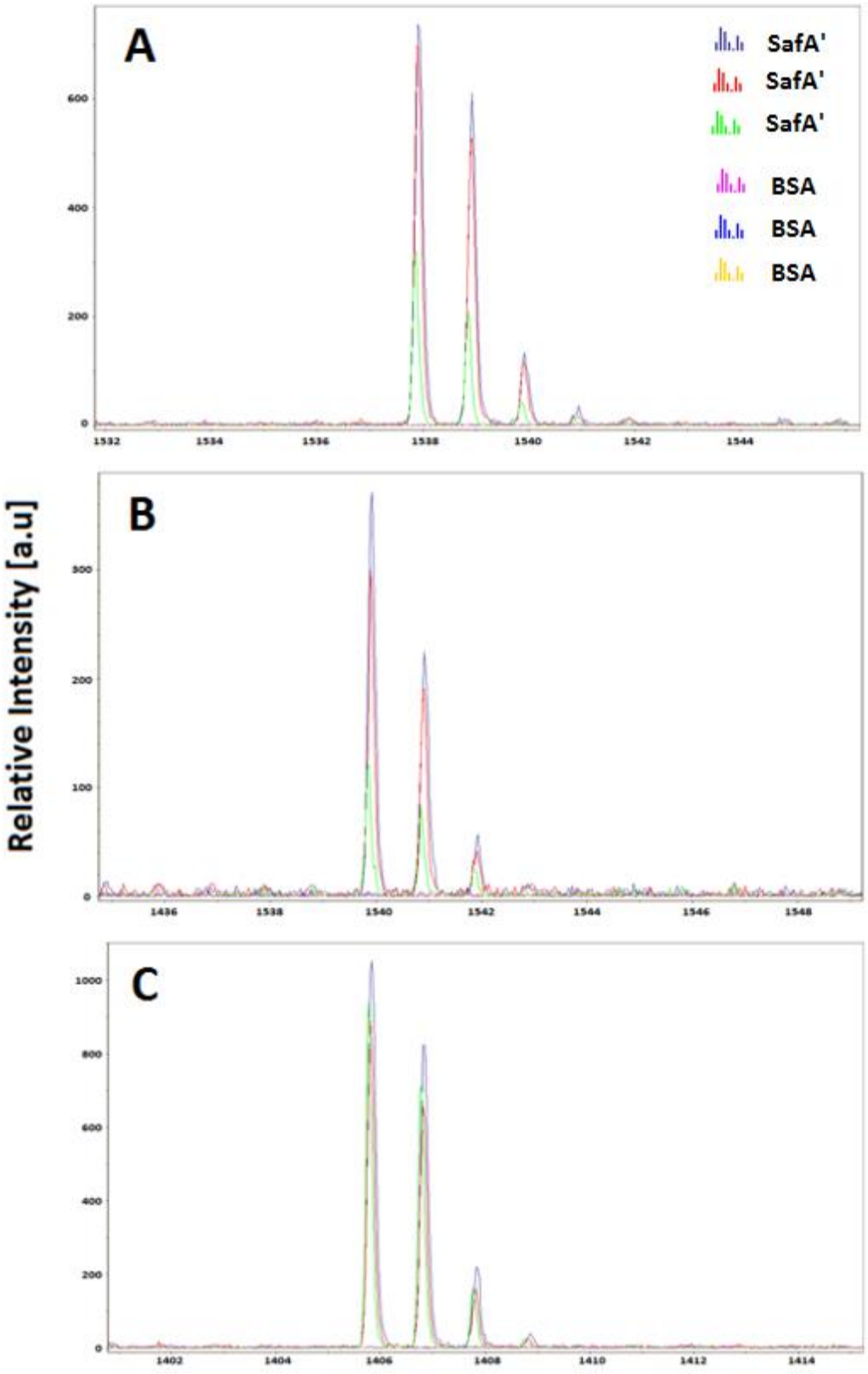

Figure 49. Details of a representative collection of well resolved specific peaks for SafA' (GST-SafA-6xHis)/heart. Three (GST-SafA-6xHis) SafA'/heart and three BSA/heart MS spectra were overlaid. The red, green and dark blue traces represent SafA' (GST-SafA-6xHis) spectra and pink, yellow and light blue traces represent the BSA/heart spectra (at the background level).

The same comparative analysis was performed for (GST-SafA-6xHis) SafA'/large intestine affinity-enrichment (Figure 51, Table 15). In this case the preliminary analysis showed from visual observation that no obvious differential peaks could be seen. Peak intensity were very low, thus the spectra needed to be zoomed in for further observation. Each peak was analysed manually and it was possible to identify a few specific signals unique to the (GST-SafA-6xHis) SafA'/large intestine (Figure 52). Affinity-enrichment of small intestine and (GST-SafA-6xHis) SafA'/colon yielded similar results (data not shown).

The arithmetic average was calculated for the mass of each peak present in the three spectra of this affinity-enrichment. This was also applied to all the previous ones as presented in Table 15. Among all the affinity-enrichments, (GST-SafA-6xHis) SafA'/colon did not yield enough specific peaks to identify the protein(s). The small and large intestine affinity-enrichments had longer peak lists yet these were not sufficient for protein identification. Finally the affinity-enrichments with heart yielded many more peaks which subsequently, were used to identify proteins in MASCOT and Protein Prospector using the PMF protocol. We also observed that some peak of identical *m/z* were shared between these lists, possibly indicating observation of the same peptide ions, a shared contaminant or perhaps arising from the same protein(s) being isolated in the heart and in the other tissues.

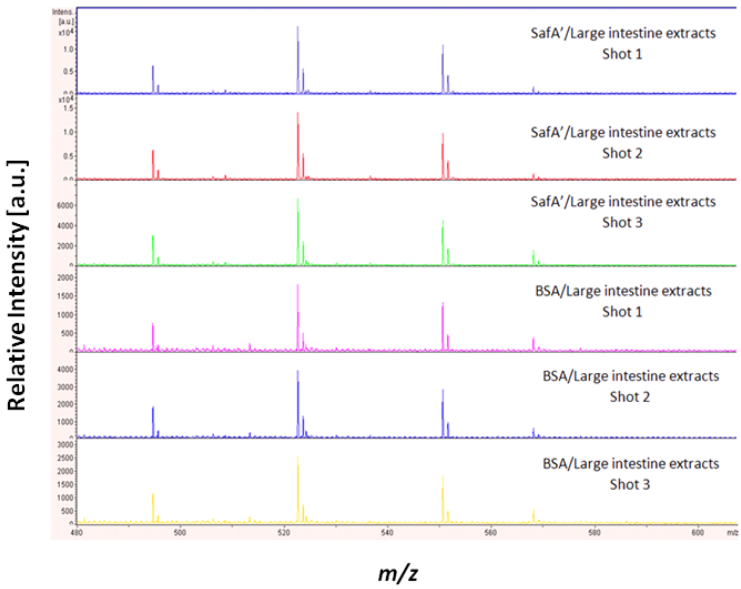

Figure 50. MS spectra of SafA' (GST-SafA-6xHis) affinity enrichment with rat's large intestine extracts. The image gives a representative example of the peaks observed in the three spectra of (GST-SafA-6xHis) SafA'/large intestine affinity-enrichment and the respective negative control in the form of three spectra of BSA/large intestine. From first visual inspection, none of the spectra show any specific peak exclusive to the SafA' (GST-SafA-6xHis) affinity-enrichment.

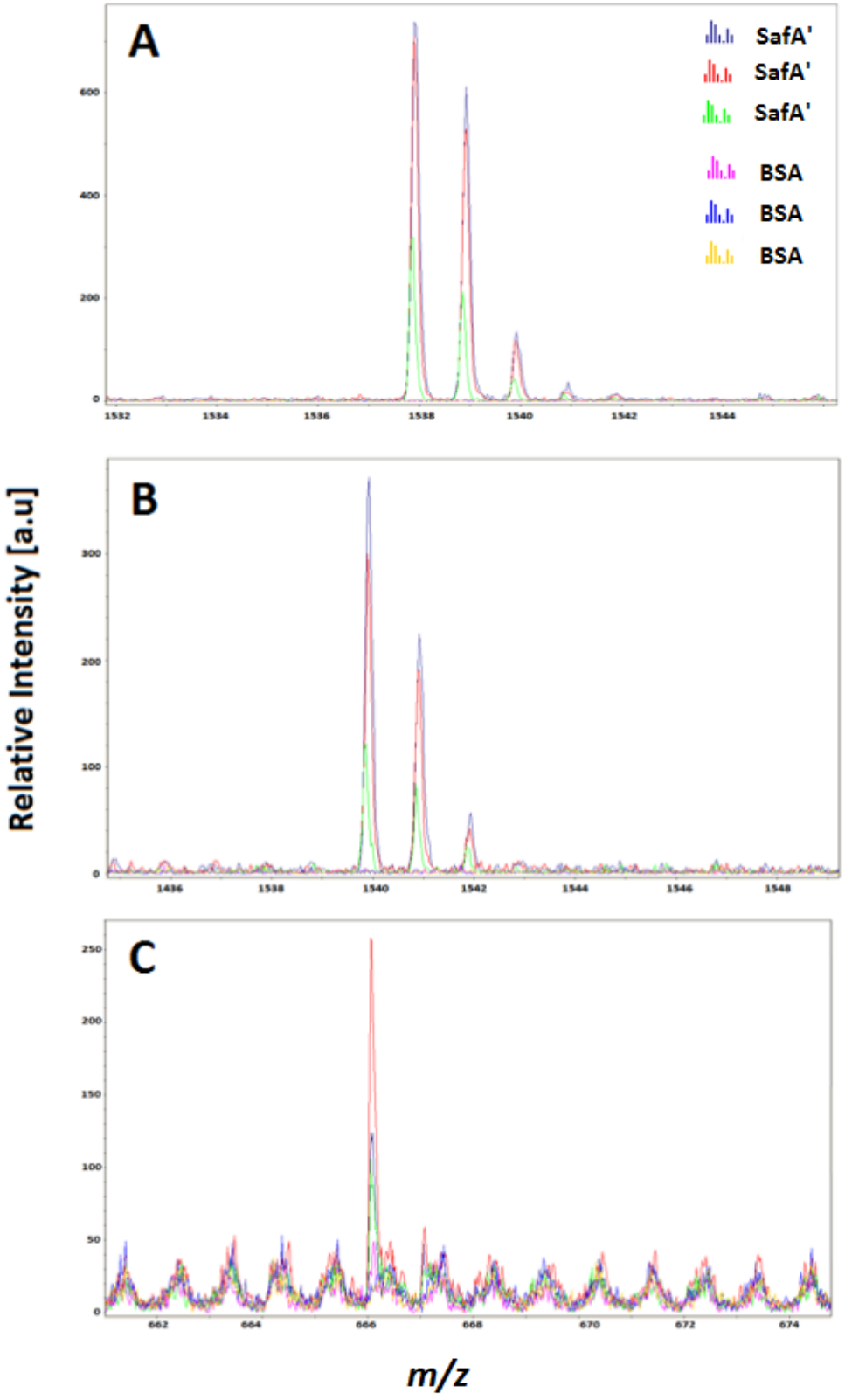

Figure 51. A representative collection of specific peaks for (GST-SafA-6xHis) SafA'/large intestine. Three (GST-SafA-6xHis) SafA'/large intestine and three BSA/large intestine MS spectra were overlaid. Red, green and dark blue traces represent SafA' (GST-SafA-6xHis) spectra and pink, yellow and light blue traces the BSA/large intestine spectra (at the background level).

6.5 MASCOT database search results identified cyclin-dependent kinase-like 3 protein in one of the (GST-SafA-6xHis) SafA'/heart affinity-enrichment's but resulted inconclusive for the intestines.

Using FlexAnalysis, three spectra were taken per affinity-enrichment and overlaid with their respective negative control; then each peak was manually selected as per the established criteria to create a differential peak list file (Chapter II, Section 2.17.2). Identical masses which appear in at least two affinity enrichments' were highlighted in bold. The masses were considered equal if the two values were within the root mean square (RMS) (MASCOT provides the RMS error of the set of matched mass values given in ppm) error calculated by MASCOT (0.05 Da) when fitting control albumin peptides whilst calibrating the plate (Table 15).

The interaction of *Salmonella* with cyclins has been studied. For instance, in the intestines, bacteria inhibit cyclins to promote virulence by injecting toxins (Bertsch et al 2009, Yao et al 2009). Also, it has been observed that 14 hours post-infection *Salmonella* induces binucleation of infected cells (Yao et al 2009). Cell containing two discrete nuclei are characteristic of cytokinesis failure (McMurray et al 2011), therefore it can be suggested *Salmonella* interferes with the cell cycle during infection (Santos et al 2016). Because of this, the identification of cyclin-dependent kinase-like 3 in any host tissue could indicate SafA plays a role in the arrest of the host cell-cycle. Regardless, cyclin-dependent kinase-like 3 was identified by PMF in one affinity-enrichment (with heart protein extracts) only and the bait used was SafA' (GST-SafA-6xHis). Thus, to be certain of identification the affinity-enrichments would need to be repeated at least twice more and with GST as an additional control (also, if possible with SafA-6xHis); as performed in the experiments to follow.

Table 15. List of masses (*m/z*) obtained from MALDI-TOF MS analysis for SafA' (GST-SafA-6xHis) affinity enrichment's with colon, small intestine, large intestine and heart. Identical masses which appear in at least two different tissue affinity-enrichments are highlighted in bold. Masses were within the RMS error calculated by MASCOT (0.05 Da) when fitting control albumin peptides whilst calibrating the plate. The volume (µL) of eluate used for each analysis varied. The masses highlighted in red are possible trypsin peaks. And the masses highlighted in blue were matched peptides to Cyclin-dependent kinase-like 3 for protein identification by PMF.

SafA' (GST-SafA-6xHis)					
2 wells (100 µL)			1 well (50 µL)	1 well (15 µL)	16 wells (800 µL)
Colon	Small int.	Large int.	Heart	Heart	*Heart
471.10	**417.05**	401.10	715.55	**423.00**	472.30
511.05	423.05	**409.15**	754.50	**430.35**	545.35
513.05	**439.00**	**417.05**	764.50	**439.00**	548.30
653.30	483.15	425.10	828.60	458.95	571.35
	485.15	**439.00**	882.50	**460.95**	581.35
	506.20	466.55	920.65	**464.05**	607.35
	530.10	**471.10**	927.60	488.35	672.45
	630.10	**506.20**	1017.65	**502.95**	689.40
	632.10	508.60	1057.70	504.35	**693.40**
	768.50	536.65	1068.60	**504.95**	733.45
	791.50	568.20	1075.70	515.35	**743.45**
	825.50	650.10	1080.55	571.40	**758.50**
	947.25	666.05	1163.70	628.40	770.50
	949.25	682.05	1170.70	**630.10**	779.45
	973.60	685.50	1180.75	**632.10**	**830.45**
	1093.60	907.30	1220.75	**758.50**	927.50
	1195.65	**947.25**	1234.80	775.45	**932.50**
	1220.80		1238.75	841.45	**973.55**
	1287.75		1249.70	**842.55**	1013.55
	1303.75		1278.75	881.30	1026.60
	1316.75		1283.80	903.40	1032.60
	1319.75		1292.70	904.45	1038.60

	1295.80	912.55	1090.55
	1305.80	947.20	**1126.55**
	1405.80	1025.65	**1232.65**
	1416.80	1044.60	**1234.70**
	1425.75	**1045.60**	**1274.75**
	1439.90	1064.60	1277.70
	1465.85	1068.55	1298.65
	1475.80	1075.55	**1316.75**
	1479.90	**1126.55**	**1320.60**
	1495.80	**1234.70**	1439.80
	1499.80	1278.70	1476.10
	1505.85	**1320.60**	**1479.80**
	1511.95	1357.75	1516.80
	1519.90	1476.75	1572.80
	1529.85	1493.80	**1576.80**
	1537.90	1612.90	1640.00
	1568.85	1766.90	**1716.90**
	1603.65	2284.60	
	1640.05		
	1667.90		
	1680.10		
	1700.95		
	1731.95		
	1804.00		
	1817.90		
	1820.00		
	1824.05		
	1833.95		
	1891.00		
	1960.10		
	1974.05		
	1990.10		
	2047.10		

The peak list shown in Table 15 were used for a PMF analysis with the MASCOT (http://www.matrixscience.com) and ProteinProspector (http://prospector.ucsf.edu/prospector/mshome.htm) search engines. The list of masses for the (GST-SafA-6xHis) SafA'/heart affinity-enrichment was run in MASCOT (Table 15); the software matched 10 masses to protein Cyclin-dependent kinase-like 3 with a significant score of 67 (Figure 53). The *Rattus norvegicus* database selected was NCBI nr and the peptide tolerance ±0.01%. The same list of masses was run in other software for confirmation; Protein Prospector (Figure 54) matched 11 masses to the same protein using NCBInr as database with total protein coverage of 18.5%, mean error of 1.04 ppm and MS error tolerance of 117 ppm. Both search engines identified predicted protein Cyclin-dependent kinase-like 3 as a possible binding partner of (GST-SafA-6xHis) SafA'/heart Affinity-enrichment. Regardless, it was considered that further analysis was required before claiming identification. To investigate this further, several peptides were fractionated by de novo sequencing with MALDI LIFT-TOF/TOF MS (LIFT function allows for analysis of ions generated by CID) (Suckau et al 2003). During the trials we could not identify peptides with amino acid information for Cyclin-dependent kinase-like 3. In addition to this, sixteen technical replicates for the (GST-SafA-6xHis) (SafA')/heart affinity-enrichment were pooled together and analysed by LC-MS/MS. The protein identified by PMF could not be identified by LC-MS/MS in a fresh affinity-enrichment. Due to limitation on resources, the investigation on the heart could not continue and it was decided to focus the analysis on intestines only.

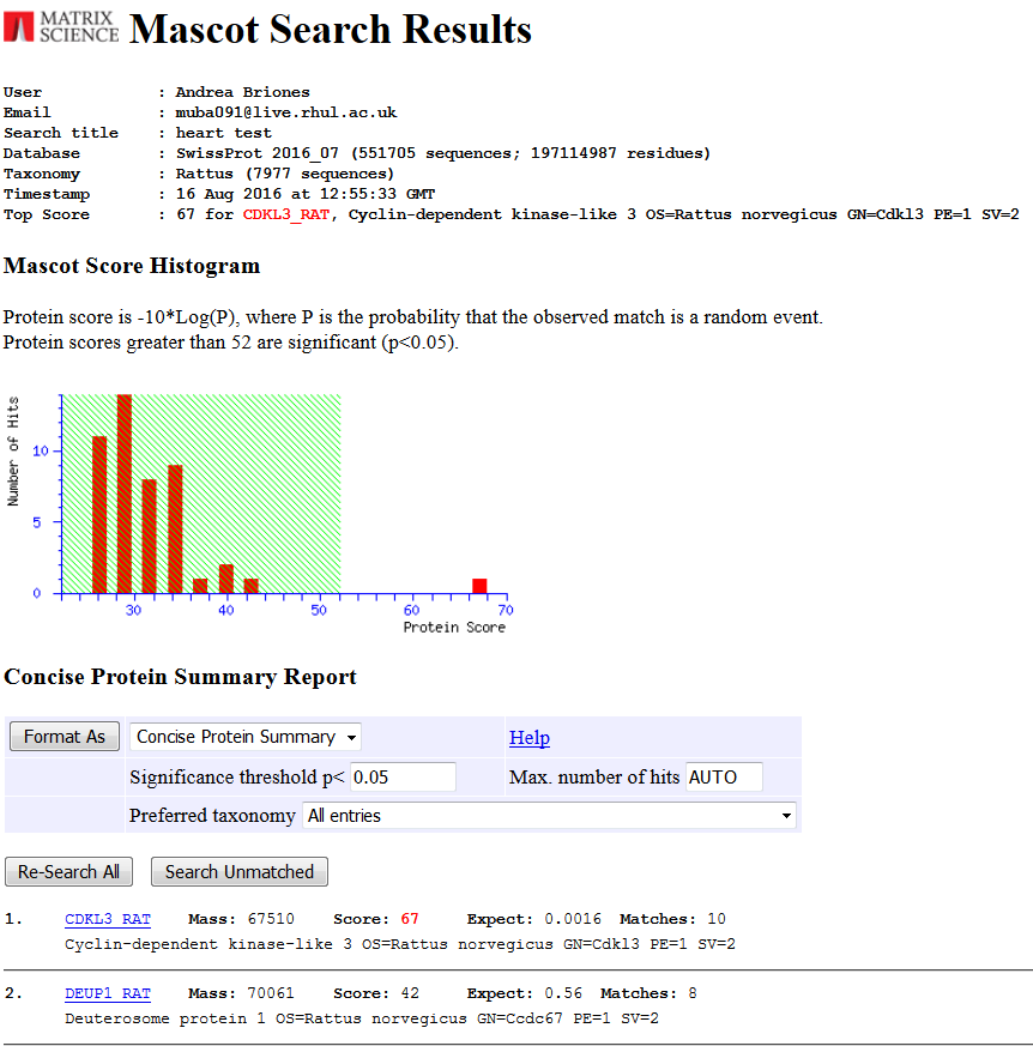

MATRIX SCIENCE **Mascot Search Results**

```
User            : Andrea Briones
Email           : muba091@live.rhul.ac.uk
Search title    : heart test
Database        : SwissProt 2016_07 (551705 sequences; 197114987 residues)
Taxonomy        : Rattus (7977 sequences)
Timestamp       : 16 Aug 2016 at 12:55:33 GMT
Top Score       : 67 for CDKL3_RAT, Cyclin-dependent kinase-like 3 OS=Rattus norvegicus GN=Cdkl3 PE=1 SV=2
```

Mascot Score Histogram

Protein score is -10*Log(P), where P is the probability that the observed match is a random event.
Protein scores greater than 52 are significant (p<0.05).

Concise Protein Summary Report

Format As | Concise Protein Summary | Help

Significance threshold p< 0.05 | Max. number of hits AUTO

Preferred taxonomy All entries

Re-Search All | Search Unmatched

1. CDKL3_RAT **Mass:** 67510 **Score:** 67 **Expect:** 0.0016 **Matches:** 10
Cyclin-dependent kinase-like 3 OS=Rattus norvegicus GN=Cdkl3 PE=1 SV=2

2. DEUP1_RAT **Mass:** 70061 **Score:** 42 **Expect:** 0.56 **Matches:** 8
Deuterosome protein 1 OS=Rattus norvegicus GN=Ccdc67 PE=1 SV=2

Figure 52. Peptide Mass Fingerprint (PMF) results performed by MASCOT search engine indicating the presence of protein Cyclin-dependent kinase-like 3 in the (GST-SafA-6xHis) SafA'/heart affinity-enrichment. The protein was identified with significant score of 67 by matching 10 out of 39 peptides using NCBInr database.

MS-Fit Search Results

[+] **Parameters**

[+] **Pre Search Results (NCBInr.2013.6.17)**

Fraction-Spot-Run ID: **1-1-1**
MS-Fit search selects **13743** entries (results displayed for top **5** matches).

[–] **Results Summary**

Protein Hit Number	MOWSE Score	# pep # mat % mat 39 pks	% Cov	% TIC	Mean Err ppm	Data Tol ppm	# Hom Prot	MS-Digest Index #	Protein MW (Da)/pI	Accession #		Species	Protein Name
1	3834	11/10/26	18.8	25.6	1.04	117	4	2997562	66471/9.3	149052527	M	RATTUS NORVEGICUS	cyclin-dependent kinase-like 3, isoform CRA_c

2997562	.	.	.	.	.	.	.	x	.	x	.	.	.	x	.	x	x	.	.	.	.	.	.	x	.	x	.	.	.	.	.	.	x	.	x	.	.	.	.	.	.	x	.	.	.	.	.	x	.	.	x	x

Similar Matches for Protein Hit 1

Protein Hit Number	MOWSE Score	# pep # mat % mat 39 pks	% Cov	% TIC	Mean Err ppm	Data Tol ppm	# Hom Prot	MS-Digest Index #	Protein MW (Da)/pI	Accession #		Species	Protein Name
1	3834	11/10/26	18.8	25.6	1.04	117	4	2997562	66471/9.3	149052527	M	RATTUS NORVEGICUS	cyclin-dependent kinase-like 3, isoform CRA_c

Protein Hit Number	MOWSE Score	# pep # mat % mat 39 pks	% Cov	% TIC	Mean Err ppm	Data Tol ppm	# Hom Pep	MS-Digest Index #	Protein MW (Da)/pI	Accession #		Species	Protein Name
2	3773	11/10/26	18.5	25.6	1.04	117	11	20355056	67553/9.4	82592668	M	RAT	RecName: Full=Cyclin-dependent kinase-like 3; AltName: Full=Serine/threonine protein kinase NKIATRE
3	3562	11/10/26	17.4	25.6	1.04	117	11	2998821	71608/9.2	149052529	M	RATTUS NORVEGICUS	cyclin-dependent kinase-like 3, isoform CRA_d
4	3502	11/10/26	17.0	25.6	1.04	117	11	2999755	72826/9.1	149052526		RATTUS NORVEGICUS	cyclin-dependent kinase-like 3, isoform CRA_b
5	1353	9/9/23	17.8	23.1	-1.67	125	9	21054572	57243/9.3	7001374		RATTUS NORVEGICUS	serine/threonine kinase NKIATRE alpha

Figure 53. Peptide Mass Fingerprint (PMF) results performed by ProteinProspector search engine indicating the presence of protein Cyclin-dependent kinase-like 3 in the (GST-SafA-6xHis) SafA'/heart affinity-enrichment. The protein was identified with significant MOWSE score of 3773 by matching 11 out of 39 peptides NCBInr database.

6.6 Discussion of MALDI data

Whole eluents were proteolytically digested and analysed directly rather than using pre-fractionation such as SDS-PAGE. Comparing MALDI-TOF MS spectra obtained for BSA (non-specific) vs SafA' (GST-SafA-6xHis) (specific) affinity-enrichments' yielded between 4 and 55 peptides depending of the tissue extract (Table 15). For example, a heart affinity-enrichment yielded 55 of peaks with *m/z* values present exclusively in SafA' (GST-SafA-6xHis) and missing in the negative control (BSA affinity-enrichment). For consistency, the decision on the presence or absence of each individual *m/z* peak was based on three separate MS spectra taken from each positive SafA' (GST-SafA'-6xHis) and negative (BSA) spotted digests. Each individual *m/z* peak in the range 1000 Da to 2000 Da was evaluated (Figure 49). A strict selection criteria was applied to each individual *m/z* peak (detailed in Chapter II, Section 2.17.2) to ensure consistency in selecting SafA' (GST-SafA-6xHis) specific peptides. The same analytical procedure was performed for the other tissue extract affinity-enrichments, i.e. the large intestine (Figures 50 and 51), small intestine and colon. Upon manual visualization of the peaks it was possible to select a few peak signals specific to SafA' (GST-SafA-6xHis) (Table 15). Some *m/z* values listed appeared in a number of SafA' (GST-SafA-6xHis) affinity-enrichments originated with extracts from different tissues.

The sets of generated *m/z* values were used for PMF using Mascot (Elias et al 2005, Stead et al 2006) and Protein Prospector (Baker et al 2010, Wang and Wilson et al 2013). The analyses yielded low MASCOT scores that did not meet the significance threshold of $p<0.05$ for all the series tested which precluded us from using the predictions made for protein identification. Combining a number of identical affinity-enrichments' to increase the total quantity of the protein did not improve the scores beyond the accepted threshold, except for one protein were both MASCOT and ProteinProspector identified cyclin-dependent kinase-like 3 present in the (GST-SafA-6xHis) SafA'/heart affinity-enrichment. MASCOT matched 10 out of 39 calculated peptide *m/z* with a significant score of 69 and total protein coverage of 16% from a 607 aa protein. The RMS error was of 51 ppm which was expected of the MALDI-TOF MS instrument used. It also satisfied the significance threshold $p<0.05$ (Figure 53).

ProteinProspector gave similar results by matching 11 out of 39 masses and with a mean error of 1.08 ppm (Figure 54). To further validate our results de novo sequencing with MALDI LIFT-TOF/TOF MS (LIFT function allows for analysis of ions generated by CID) was attempted. Whilst the control BSA digest could identify peptides with amino acid

information successfully from the acquired MS/MS data we could not identify by MS/MS the PMF identified cyclin-dependent kinase-like 3. This might be due to low amount of the corresponding protein available in the sample or to its complexity.

Ideally, if the time and resources would have allowed, further large scale (16 wells or more) (GST-SafA-6xHis) SafA'/heart affinity-enrichments should have been performed. Further to this it would still be difficult to identify whether the cyclin protein is specific to SafA or is binding to the GST tag. Therefore, having GST as a negative control and cleaving it from the construct would eliminate any doubts regarding its binding to SafA. Cyclins are a target of several bacteria during infection, such as, *E. coli*, *Salmonella*, *Yersinia*, among others (Jubelin et al 2009, 2010, Marchès et al 2003). Also, inhibition of the cell cycle in the intestinal epithelium could interfere with the constant cell renewal and probably benefit colonization (Nougayrède et al 2005). Cyclins were not found in the LC-MS/MS (large intestine) analysis (Section 6.7) as SafA interacting partners. The proteins were also absent from the GST or BSA negative controls. Based on this, it is possible, there is a strong specificity of heart cyclin-dependent kinase-like 3 for the construct.

The specificity that can be achieved by tandem mass spectrometry (MS/MS) makes the technique a better choice to unequivocally identify proteins. In this study, PMF was not sufficient. Even if acquisition of the fragment ion spectra had been obtained, by using the LIFT method, it would have not been able to identify peptides with the same amino acid composition but different sequences (Liu and Chen 2009, Le Maux et al 2015). In such case the peptides would have the same molecular weight and yield the same MS/MS spectra. Coupling LC with MS overcomes this problem by allowing for peptide separation (Wu et al 2009).

However, based on these results we felt optimistic that our affinity-enrichment protocol (Chapter II, Section 2.13.8 and Chapter V, Figure 41) is suitable for identifying proteins specifically interacting with SafA' (GST-SafA-6xHis) and decided to reanalyse our samples by nLC-nESI-MS/MS.

6.7 Results: nLC-nESI-MS/MS analysis

The MALDI-TOF MS analysis was not sufficient to confidently identify any specific proteins to SafA' (GST-SafA-6xHis). However, the comparison analysis showed the enrichment of peptides in the SafA' (GST-SafA-6xHis) affinity-enrichments' was higher than in the BSA negative control. Because of this, it was decided to use a more suitable

method to deal with complex mixtures. Further to this, we acknowledged the need to include new negative controls that would allow us to unequivocally identify interacting partners to SafA itself and not to the GST fused tag of the construct. As the analysis went along we also recognized the need to provide a higher amount of proteins, therefore we adjusted the experimental design (Figure 47). The MS/MS data was analysed using MASCOT and Scaffold, a bioinformatics grouping method that increases confidence in a protein identification report through the use of several statistical methods (Searle et al 2010). To enable Scaffold calculate the probability of correct protein identification we established fixed minimum requirements. The protein identification confidence threshold was setup to 99% and the peptide threshold to 95%. For protein identification to be accepted (minimum criteria for this study), at least two different peptide sequences need to be identified by the search algorithm (Bradshaw et al 2006, Omenn et al 2005), therefore it was part of the Scaffold criteria to reach 99% protein confidence identification (Figure 56). In 2 of the cleaved SafA' (GST-SafA' minus GST) affinity-enrichments.

For the previous MALDI-TOF MS analysis each affinity-enrichment had only BSA as a negative control and GST tagged SafA' (uncleaved SafA') as a positive. Three new controls were introduced in the Universal-BIND™ plates (System 5); undepleted cleaved SafA' (GST+SafA-6xHis) (without GST tag fused to the construct), non UV-light crosslinked undepleted cleaved SafA' (GST+SafA-6xHis) (immobilised protein by passive adsorption only) and GST protein (Figure 48). The addition of the controls was to differentiate between proteins binding to the GST tag and to SafA. The decision of not crosslinking undepleted cleaved SafA' (GST+SafA-6xHis) in System 5 was to determine whether UV-crosslinking stabilizes SafA' (cleaved/uncleaved) on the well polystyrene surface of the Universal-BIND™ plates (System 5), therefore enriching the mixture of bait protein. During the setup of the system, trials had showed the advantage of crosslinking protein to the plates prior incubation with the protein extracts of interest (Chapter V, Section 5.7.1), establishing that the bait protein, SafA' (GST-SafA-6xHis) still remain on the plates but without crosslinking protein loss would occur, as a result possibly affecting the binding of any specific protein. Having this control is not a proof of the above but it can indeed show the advantage of protein immobilization by UV-light crosslinking over passive adsorption.

The samples were subjected to LC-MS/MS analysis. For this, a total of seven SafA' (cleaved/uncleaved, crosslinked/non-crosslinked) affinity-enrichments were generated as detailed in Figure 48. Additional negative controls, using BSA and GST as baits were

included, and compared to affinity-enrichments performed with undepleted cleaved SafA' (GST+SafA-6xHis) vs uncleaved SafA' (GST-SafA-6xHis). All the baits, negative baits, undepleted cleaved SafA' (GST+SafA-6xHis) and uncleaved SafA' (GST-SafA-6xHis) were immobilised by crosslinking to the plates prior incubation with total protein extracts obtained from rat's large intestine. Undepleted cleaved SafA' (GST+SafA'-6xHis) with omission of its crosslinking to the plates was also included. For each affinity enrichment, samples were trypsinized and peptides from each digest were analysed by nLC-nESI-MS/MS according to the methods described in Chapter II, Section 2.18. The MS raw data was processed using MSConvert in ProteoWizard Toolkit (Kessner et al 2008). Subsequently, MS^2 spectra was performed in MASCOT by interrogating a database comprising of the combined reference proteomes of *Rattus norvegicus* (May 2014 database) and *Salmonella typhimurium* LT2 (May 2014 database) retrieved from the UniProt website (http://www.uniprot.org/). Finally, Scaffold was used to filter MS/MS based peptide and protein identifications as fully described in the methods, Chapter II, Section 2.19.

The data were analysed under stringent parameters in order to avoid false identification. For this, the retrieved data were scrutinised in Scaffold where the MASCOT search engine results are statistically interpreted using the PeptideProphet algorithm. In here the search engines scores are converted into probabilities of peptide identification. For instance, in identification MASCOT uses ion scores, identities and homology thresholds. PeptideProphet converts these into a single discriminant score developed using training data (Keller et al 2002). A histogram of the discriminant scores is created where the distribution of correct and incorrect matching data can be visualised. PeptideProphet considers the distributions as standard distributions where by using a curve-fitting depicts the correct and incorrect distributions (Nesvizhskii et al 2003). Following this, Bayesian statistics is used to calculate the probability of identification is correct (Nesvizhskii et al 2003). The software also incorporates information about the class label for the peptide identifications. For example, the peptides can be searched against decoy peptide sequences that are known for not being present in the organism If any of the MS/MS spectra matches the decoy peptides this assignment (which may lead to protein identification), would be incorrect (Ding et al 2008).

These probabilities are then used as threshold filters that allow the protein identifications to be viewed at different confidence levels (Searle et al 2010). Next, Protein Prophet

(Nesvizhskii et al 2003) groups all assigned peptides according to their corresponding proteins in the database. In here the assigned peptides corresponding to a specific protein and its probabilities are combined to compute a single protein confidence measure that is effective at distinguishing the correct from the incorrect protein identifications (Searle et al 2010), these probabilities are also used as threshold filters. Finally, Scaffold calculates the False Discovery Rate (FDR) for both peptides and proteins which in this case was "calculated by using the count of decoys against target identification hits" (©2016 Proteome SoftwareScaffold, version 4.0. User's Manual, Page 99).

The different MS2 samples described in Figure 48 were combined and as per methods, Chapter II, Section 2.19 filtered for proteins with protein identification confidence threshold to 99%, peptide threshold to 95% and protein FDR of 0.1%; and at least two peptides had to fulfil the criteria for protein identification as per minimum criteria defined in Chapter II, Section 2.19. We searched for the presence of SafA in the respective affinity-enrichment and BSA throughout. It was considered important to verify if proteins known to be present in the affinity-enrichments would be convincingly identified in their respective samples. For instance, absence of SafA in the *Salmonella* affinity-enrichment could have suggested the protein was lost throughout the experimental process, deeming any uniquely identified proteins in that particular sample non-specific. On the contrary, identification of SafA in the negative controls could have suggested a problem of cross-contamination inferring the affinity-enrichments analysed were not a reliable source of proteins. The identification of BSA was important because it was used as a blocking agent, thus purposely added in all samples and expected to be identified in all affinity-enrichments. Failure to consistently identify BSA would have meant appropriate identification was not being accomplished suggesting weakness on methodology.

An average of three SafA peptides with a 100% identification probability were found in the SafA' (cleaved/uncleaved) affinity-enrichment's (Supplementary data, Figure S65). During the affinity-enrichment's, BSA was used as a blocking agent and consistently used throughout, therefore expected to be present in all affinity-enrichments. An average of 30 BSA specific peptides were identified with 100% identification probability (Supplementary data, Figure S66). Of the 2, 119 identified proteins (Figure 55) only five fulfilled the minimum established criteria (Chapter II, Section 2.19) and have been identified as specific SafA' (SafA-6xHis) proteins. Several on-line molecular tools, such as, gene ontology, STRING and PubMed were used to retrieve as much biological

information from the identified putative proteins (Table 18). The successful identification of these proteins provide a much needed information on the intracellular life of cytosolic *Salmonella* and the function of the Saf fimbriae. Currently most of the studies are performed using the *Salmonella*-containing vacuole (SCV) and there is a lack of information on the fate of cytosolic *Salmonella*.

The identification of proteins, such as, TM9SF3, a transporter protein localised in the Golgi and plasma membrane. Serpinb1a, a known inhibitor of neutrophil elastase; MGST3-like protein (RGD1561381), a transmembrane protein located in the Endoplasmic Reticulum (ER) responsible for the catalysis of reduced glutathione (GSH) that leads to the activation of the inflammation response. Protein Bri3bp, also located at the ER/mitochondrion, involved in the modulation of the mitochondrial cell death response. Finally, hydrolase protein ABHD14B a positive regulator of RNA Polymerase II. All of these proteins have been scrutinised and there is evidence of their involvement in the host-pathogen response. In this section, the process of protein identification by LC-MS/MS is presented as well as their putative biological implications based on the current literature available.

6.8 Identification of total large intestine proteins captured by affinity-enrichments in Universal-BIND™ plates (System 5)

Affinity-enrichments' P3-P7 together with their respective negative controls yielded a total of 2,119 proteins identified based on the Scaffold FDR thresholds (Figure 55). These proteins included 1,797 contaminants (those not from the protein sample), coming from the user (e.g. keratin from skin and hair) or from reagents (e.g. BSA powder and trypsin). SafA was found only in the affinity-enrichments' where it was used as a bait, the identification of SafA in the SafA' (cleaved/uncleaved) affinity-enrichements' and not in the negative controls, indicated reliability in our methods. The remaining 322 proteins were those belonging to the protein samples, captured by the different baits used (GST-SafA-6xHis, GST+SafA-6xHis, BSA and GST). These were transferred from Scaffold to Excel where proteins with cleaved SafA' (SafA-6xHis) specificity were separated from BSA/GST binding proteins.

To identify which proteins bound specifically to cleaved SafA' (SafA-6xHis) we performed a two stage analysis. In stage 1 we subtracted from the list any proteins identified in the BSA or GST negatives control, even if it was 1 negative peptide against

a higher number of positive peptides (cleaved SafA' binding). The 190 proteins left were a mixture of identified proteins in one or both of the undepleted cleaved SafA' (GST+SafA-6xHis) affinity-enrichments with one peptide or more and not present in any of the negative controls. Stage 2 analysis involved the selection of proteins with 2 or more unique peptides in both of the undepleted cleaved SafA' (GST-SafA-6xHis) affinity enrichments. Following these stages we reduced the list down to five proteins that were present in undepleted cleaved SafA' (GST+SafA-6xHis) only. Figure 55 (all Scaffold data available in the supplementary electronic file) shows no protein was identified exclusively in the BSA or GST negative controls. 99 proteins were present simultaneously in the undepleted cleaved SafA' (GST+SafA-6xHis), BSA and GST affinity enrichment's. Only five proteins were shared between undepleted cleaved SafA' (GST+SafA-6xHis) and BSA, whereas 23 proteins were shared between undepleted cleaved SafA' (GST+SafA-6xHis) and GST.

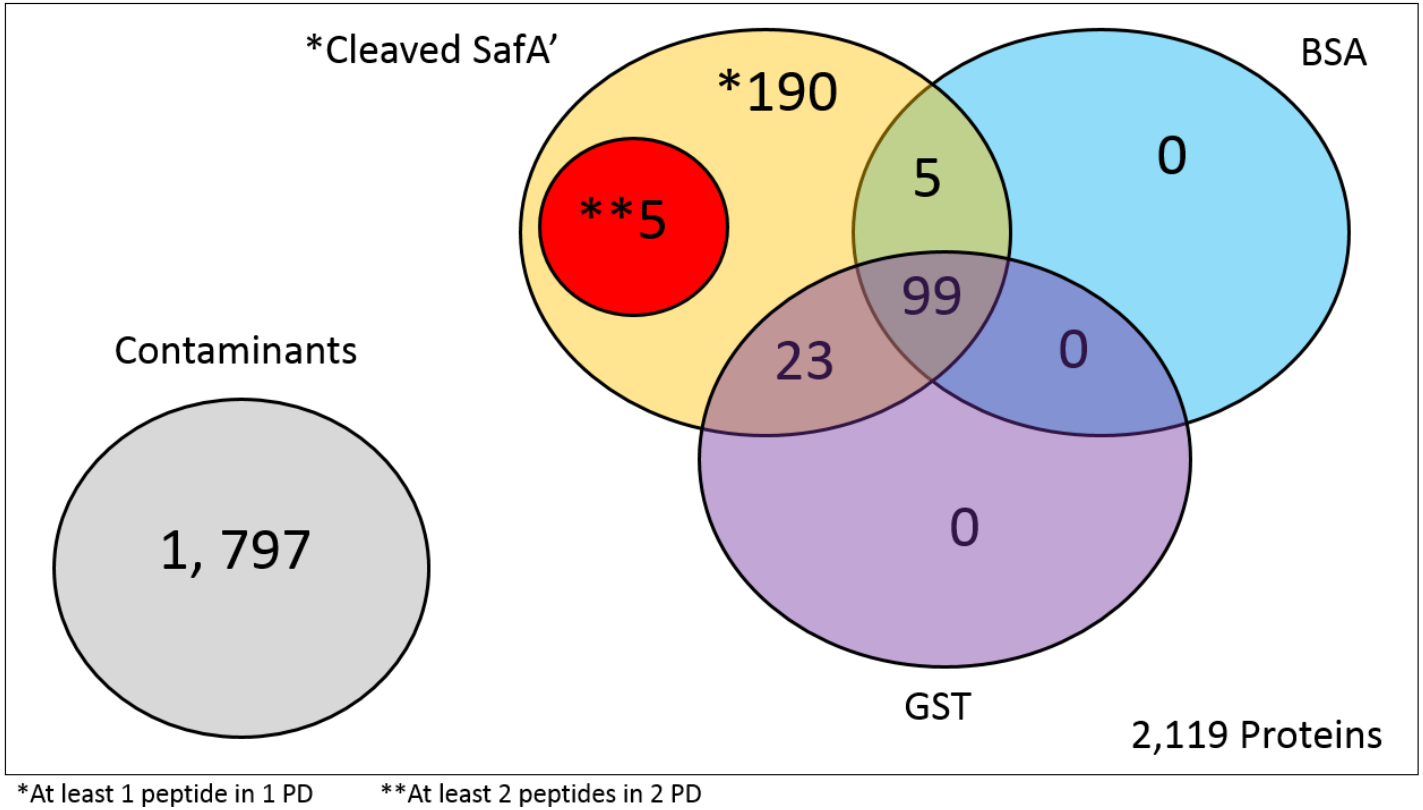

Figure 54. Venn diagram showing distribution of the proteins identified in affinity-enrichments P3-P7. Initially, a total of 2,119 proteins were identified based on the Scaffold FDR thresholds. These included 1,797 contaminants not from the protein sample but from the user (e.g. keratin from skin and hair) and from materials (e.g. BSA powder and trypsin). An exclusive **5 were identified with at least 2 peptides in both of the undepleted cleaved SafA' (GST+SafA-6xHis) affinity-enrichments' (these were absent from the GST and BSA negative controls and will be the only ones discussed from hereafter) and 190 proteins identified in the undepleted cleaved SafA' (GST+SafA-6xHis) affinity-enrichments' with no more than 1 peptide in one or both of the undepleted cleaved SafA' (GST+SafA-6xHis) affinity-enrichments'. No proteins were isolated solely in the negative controls, whereas 23 were shared between GST and undepleted cleaved SafA' (GST+SafA-6xHis), 5 shared between BSA and undepleted cleaved SafA' (GST+SafA-6xHis) and 99 shared present in all three affinity-enrichments.

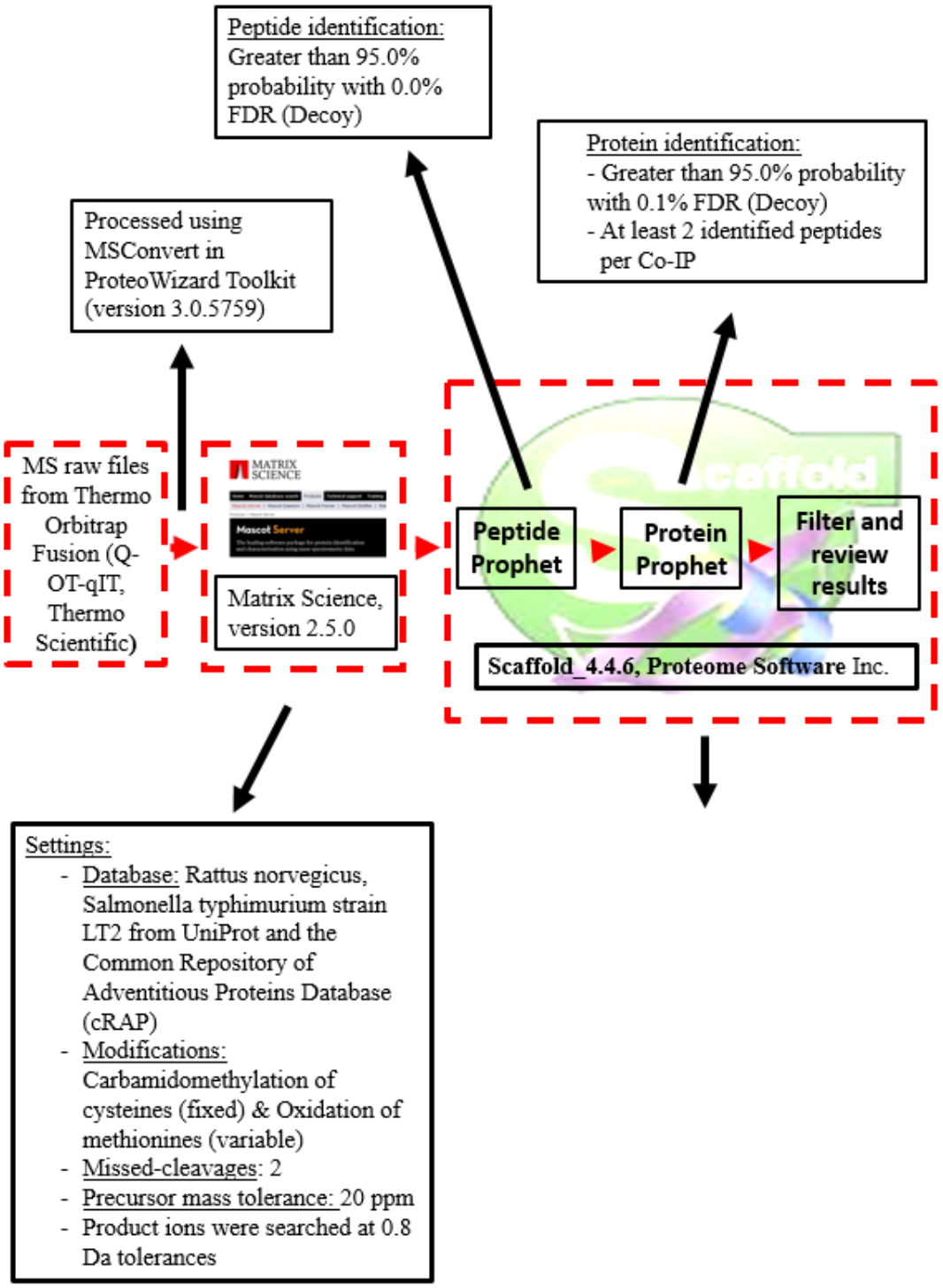

Figure 55. Workflow of data analysis. The raw files were processed using MSConvert in ProteoWizard Toolkit (version 3.0.5759) and the database performed in MASCOT (version 2.5.0). The results were statistically interpreted using Peptide Prophet algorithms. Next, Protein Prophet grouped all assigned peptides according to their corresponding proteins in the database. The False Discovery Rate (FDR) for both peptides and proteins by discriminant scoring using a Naïve Bayes classifier to try and classify correctly identified spectra from incorrectly identify spectra (decoy).

6.9 Identification of putative SafA interactors

Only five proteins were identified in both of the undepleted cleaved SafA' (GST+SafA-6xHis) affinity-enrichments' and in none of the negative controls (BSA and GST) with 2 peptides or more satisfying Peptide Prophet algorithm threshold of 95% and Protein Prophet algorithm threshold of 99% with a 0.1% FDR (decoy) (Table 16). It was found protein Bri3bp was also identified exclusively in the SafA' (GST-SafA-6xHis) affinity-enrichments. This may indicate the absence of protein identification in the non-crosslinked undepleted cleaved SafA' (GST+SafA-6xHis) samples is probably due to the lack of bait protein on the wells which was lost in the process.

Because of the limited quantities of protein captured by the system, it was necessary to pool together the technical replicates. Starting with 2, 16 and 34 wells pooled together. P1&P2 had two technical replicates, P3 sixteen and P3-P7 thirty two replicates; where P1&P2 did not yield any interactors (therefore these are mentioned but not discussed). Different rats were used for different affinity-enrichments', hence each affinity-enrichment is a biological replicate (Figure 48).

Table 16 provides information on the five identified proteins; its molecular weight (MW) in kDa and a breakdown on with how many peptides and in how many affinity-enrichment's these were identified.

Table 16. Putative SafA-6xHis interactors identified in the different affinity-enrichment (P3-P7) experiments. MS2 spectra were searched with MASCOT engine against sequences derived from reference proteome of Rattus norvegicus, *Salmonella* typhimurium strain LT2 (UniProt database) and the Common Repository of Adventitious Proteins (cRAP) Database. Each "P" column indicate the number of peptides for which a protein was identified only in the SafA' (cleaved/uncleaved) affinity-enrichment but not in any negative controls (No BSA or GST). The molecular weight (MW) is given in kDa.

Identified Protein	UniPrort (*Rattus Norvegicus*) Accession number	MW (kDa)	UV- crosslinked uncleaved SafA' (GST-SafA-6xHis)		UV-crosslinked cleaved SafA' (GST+SafA-6xHis)		Non UV-crosslinked cleaved SafA' (GST+SafA-6xHis)	Negative Controls	
			^P3	^O^P4	^O^P5	^O^P6	^O^P7	BSA (N1)	GST (N2)
Bri3 binding protein	Q5U3Z5	28	2	1	2	2	0	0	0
Tm9sf3	D3ZUD8	68	0	0	3	3	0	0	0
ABHD14B	Q6DGG1	23	0	0	2	2	0	0	0
Leukocyte elastase inhibitor A	Q4G075	43	0	0	2	2	0	0	0
RGD1561381	D3ZZQ8	17	0	0	2	2	0	0	0

^16 wells per Affinity-enrichment, ^O32 wells per Affinity-enrichment

Table 17 describes the percent coverage (%) (percentage of all the amino acids in the protein sequence that were detected in the sample), number of peptides identified that satisfy the algorithm criteria, peptide sequence and its relevant information as retrieved from Scaffold. Such as, MASCOT ion score, observed mass (*m/z*), charge state, delta mass, retention time and number of isoforms. Also, this is now shown in the table but all proteins had no isoforms.

Table 17. LC-MS/MS identified rat large intestine proteins binding specifically to SafA' (cleaved and uncleaved).

IDENTIFIED PROTEIN AND PERCENT COVERAGE (%)	AFFINITY-ENRICHMENT	PEPTIDE SEQUENCE	MASCOT ION SCORE	OBSERVED MASS *(M/Z)*	CHARGE STATE	DELTA MASS (DA)	RETENTION TIME (MIN)
BRI3 BINDING PROTEIN (Q5U3Z5)							
9.09%	^P3: Crosslinked Uncleaved SafA'						
		GSAGGLcSPSVEEK	19.9	689.32	2+	0.001739	40.94
		LEHLENQVR	25.38	569.300	2+	0.0003421	39.78
	^O^P4: Crosslinked Uncleaved SafA'						
		LEHLENQVR	30.4	569.3054	2+	0.002418	25.98
	^O^P5: Crosslinked Cleaved SafA' 1						
		GSAGGLcSPSVEEK	36.55	689.3203	2+	0.001739	31.50
		LEHLENQVR	35.58	569.3044	2+	0.0003421	26.20
	^O^P6: Crosslinked Cleaved SafA' 2						
		GSAGGLcSPSVEEK	57.45	689.3203	2+	0.001713	31.31
		LEHLENQVR	32.24	569.305	2+	0.001564	25.91
TM9SF3	^O^P5: Crosslinked Cleaved SafA' 1						

(D3ZUD8)							
5.28%		LEIGFNGNR	29.44	510.2674	2+	0.0005681	42.93
		YLDPSFFQHR	20.63	437.2157	3+	0.000006058	50.35
		VNAVPRPIPEKK	14.99	674.4087	2+	-0.0007399	25.88
	[O]P6: Crosslinked Cleaved SafA' 2						
		KLEIGFNGNR	38.16	574.315	2+	0.0007781	35.32
		KLEIGFNGNR	26.47	383.2123	3+	0.0004351	35.32
		LEIGFNGNR	21.33	510.2683	2+	0.00246	42.8
		YLDPSFFQHR	32.25	437.2161	3+	0.001194	50.13
ABHD14B	[O]P5: Crosslinked Cleaved SafA' 1						
(Q6DGG1)							
10%		FSVLLLHGIR	39.87	385.5736	3+	0.001819	57.50
		FSVLLLHGIR	26.62	385.5731	3+	0.0002621	57.50
		AVAIDLPGLGR	24.25	541.3207	2+	-0.002442	59.40
	[O]P6: Crosslinked Cleaved SafA' 2						
		FSVLLLHGIR	24.32	385.5739	3+	0.002644	56.84
		AVAIDLPGLGR	18.24	541.3221	2+	0.0003661	59.48
RGD1561381	[O]P5: Crosslinked Cleaved SafA' 1						
(D3ZZQ8)							
17.80%		IASGLGVAWIIGR	39.4	656.8918	2+	0.002548	71.38
		VLYAYGYYTGDPSK	35.71	798.8829	2+	0.0003261	52.09

	[O]P6: Crosslinked Cleaved SafA' 2						
		IASGLGVAWIIGR	37.64	656.8928	2+	0.004622	70.95
		VLYAYGYYTGDPSK	27.45	798.8825	2+	-0.0004219	52.11
LEUKOCYTE ELASTASE INHIBITOR A **Q4G075** **12.70%**							
	[O]P5: Crosslinked Cleaved SafA' 1						
		TFHFDSVEDVHSR	23.24	788.3644	2+	0.002878	39.78
		FQSLNAEVSK	22.36	561.7933	2+	0.0004481	35.09
		FQSLNAEVSKR	18.34	639.8448	2+	0.002376	30.41
		TYNFLPEFLTSTQK	27.68	844.9321	2+	0.003836	72.89
		ADLSGMSGSR	22.62	490.7274	2+	0.0008781	28.18
	[O]P6: Crosslinked Cleaved SafA' 2						
		IEESYILNSNLGR	21.09	754.3931	2+	0.00371	53.24
		LGLQDLFNSSK	40.27	611.3293	2+	0.003748	68.23

^16 wells per affinity-enrichment, [O]32 wells per affinity-enrichment

6.10 Initial prediticton of protein-protein interaction networks: STRING

STRING (http://string-db.org/) was initially used to predict whether the initial five proteins (Table 16) were part of a network. The database predicts direct and indirect interactions mainly by using previous knowledge from other databases or high-throughput experiments (Von Mering et al 2005). Based on the available evidence, the scores are indicators of confidence and how feasible STRING evaluates an interaction to be true. STRING could not find evidence relating any of the five proteins identified in the undepleted cleaved SafA' (GST+SafA-6xHis) affinity-enrichments, not even at the lowest confidence level of 0.150. Moreover, by relaxing the settings and allowing STRING to add more proteins within a network, the proteins did form part of other networks related to immune response and family of peptidases. As these results were inconclusive they will not be discussed further.

6.11 Gene Ontology

Gene ontology (GO) was also used in an attempt to retrieve organised terms regarding the characterisitics of gene products in the following three categories: protein class, molecular function and cellular component (Table 18). The results indicate that the predicted proteins belong to distinct classes and have different localization within the cell. This was also investigated by accessing databases, such as, UniProt (http://www.uniprot.org/) and NCBI (http://www.ncbi.nlm.nih.gov/) or by literature research as shown in Table 18. Their location varies between integral components of the membrane, Endoplasmic Reticulum (ER), cytoplasm, Golgi Complex and extracellular space. Furthermore, the molecular function shows the proteins play a role in catalytic activity, protein transport and serine-type endopeptidase inhibitors.

The information provided by GO allowed us to conclude that these proteins might be part of the mammalian host immune response and are either a target of *Salmonella* for its survival or on the opposite, these target *Salmonella* for its destruction. Regardless, the information obtained from GO and the literature research (Table 18) imply the involvement of these proteins either as a group(s) or indepently as enzyme regulators, transporters, immune system, response to stimulus, apoptosis, cellular adhesion, among others.

These proteins fall within biological and molecular categories that are plausible highly activated during infection. These results will be discussed by means of considering published literature based on similar bacterial protein-host interactions. Further to this, the possible biological relevance in the *Salmonella*-host infection process will be further discussed in the Discussion section.

Table 18. Gene Ontology (GO) terms and Biological information for the identified cleaved SafA' (SafA-6xHis) interactors. Panther and UniProt were used to retrieve GO terms. Descriptions were obtained from published data.

Identified Proteins	UniPrort Accession number	MW (kDa)	Gene Ontology			Short Description	Literature Reference
			Protein Class	Molecular Function	Cellular Component		
Bri3 binding protein	Q5U3Z5	28	No information available	No information available	Integral membrane (GO:0016021), mitochondrion (GO:0005739),membrane (GO:0016020)	Involved in apoptosis/drug induced apoptosis	Bauer et al 2010, Yamazaki et al 2007
Tm9sf3	D3ZUD8	68	Transporter	vesicle-mediated transport (GO:0006897)	Integral component of membrane (GO:0016021), membrane (GO:0016020)	Cellular adhesion and phagocytosis, control intracellular killing of bacteria, intramembrane cargo receptors	Benghezal et al 2003, Cornillon et al 2000, Perrin et al 2015
ABHD14B	Q6DGG1	23	Serine protease	Hydrolase activity (GO:0016787)	Cytoplasm (GO:0005737), extracellular exosome (GO:0070062), nucleus (GO:0005634)	Role in tumour suppression through limiting cell proliferation and cell cycling, immune system response, response to toxic substance	Brady et al 2011, Mol et al 2016, PANTHER (accessed on 15/05/2016)
Leukocyte elastase inhibitor A	Q4G075	43	Serine protease inhibitor	serine-type endopeptidase inhibitor activity (GO:0030414)	Cytoplasm (GO:0005737), extracellular space (GO:0005615)	Immune response, up-regulated during *Salmonella* infection	Gill et al 2012, Romero et al 2012)
RGD1561381	D3ZZQ8	17	Transferase	Antioxidant activity (GO:0016209), catalytic activity (GO:0016491)	Extracellular region (GO:0005576)	Similar to microsomal glutathione S-transferase 3	CAMP2.0 (accessed on 15/05/2016)

6.12 Discussion: A speculative discussion on the SafA interacting partners is presented here

6.12.1 Cytosolic *Salmonella* targets Endoplasmic Reticulum (ER) Bri3 binding protein (Bri3bp) to modulate apoptosis

The ER is an organelle which main function is to fold secreted, organelle and plasma membrane proteins (Stevens and Argon et al 1999). When homeostasis of the ER is disturbed, it results in the accumulation of misfolded or unfolded proteins that trigger the ER stress response. This signalling pathway is called the unfolded protein response (UPR) and has been widely studied in yeast (Ahner and Brodsky et al 2004, Denic et al 2006, Ruddock and Molinari et al 2006), mammals (Aridor and Hannan et al 2000, Foulquier et al 2002) and also observed in plants (Deng et al 2013, Hüttner and Strasser et al 2012, Vitale and Boston et al 2008). Subsequently, if the UPR response is not sufficient to re-establish balance, the next host response would be to start apoptosis (Fribley et al 2009, Kaufman et al 2002), carried out by the mitochondrial apoptosis pathway (Bravo-Sagua et al 2013, Hetz et al 2011).

Recent studies show that bacteria have evolved strategies to modulate different ER stress sensors to regulate the distinctive host cell responses (Celli and Tsolis et al 2015, Pillich et al 2016). The protein Bri3bp was consistently identified in four SafA' (cleaved/uncleaved) affinity-enrichments' with not a single peptide binding to any of the negative controls (Table 16). The role of Bri3bp is of binding to Bri3, a lysosomal protein involved in tumour factor-induced cell death (Wu et al 2003). Yamazaki et al (2007) has showed Bri3bp is involved in apoptosis, especially drug induced apoptosis. The work demonstrated the lack of Bri3bp had an impact in the decrease of apoptosis, whereas overexpression increased caspase-3 activity and mitochondrial cytochrome *c* release.

The consistent binding of Bri3bp protein to cleaved SafA' (SafA-6xHis) make it possible to suggest cytosolic *Salmonella* binds to Bri3bp to hijack the host's stress response and manipulate it to its benefit (Figure 57). It is known cytosolic *Salmonella* replicates ~20-30 fold in comparison to SCV-bound *Salmonella* (Knodler et al 2014, Malik-Kale et al 2012). Therefore the identification of Bri3bp suggests that cytosolic *Salmonella* targets apoptosis, using this as an advantage for hyper-replication, and possibly, the ability to re-activate apoptosis so that it can disseminate and spread to other cells when required.

To confirm this we would need to perform functional studies (which will be further elaborated in Chapter VII, Section 7.5), nevertheless, this has been extensively described

in other gram-negative bacteria. An example of this is *Anaplasma phagocytophilum* that inhibits neutrophil apoptosis by the transcriptional upregulation of bfl-1. It also inhibits mitochondria-mediated activation of caspase 3 (Ge et al 2005). In addition, studies in *Legionella pneumophila* (Banga et al 2007, Laguna et al 2006) and *Chlamydia trachomatis* (Dong et al 2005, Ying et al 2005) give further evidence of how bacteria use the host's immune system during the early stages of infection in order to facilitate their intracellular replication.

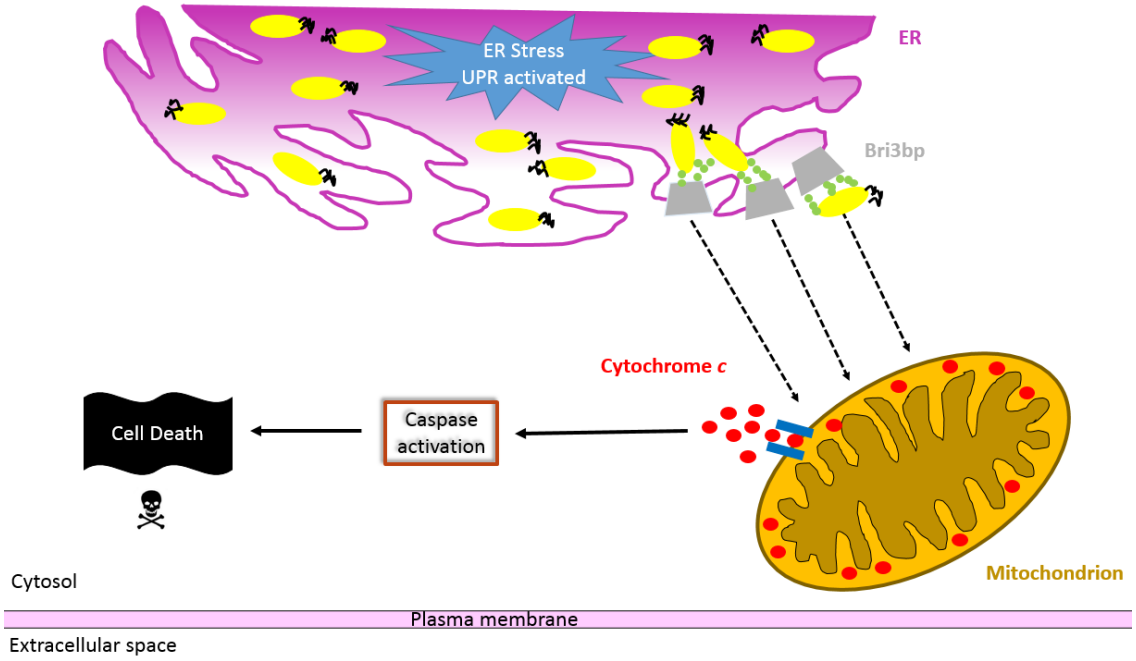

Figure 56. Hypothesised model showing *Salmonella* regulation of mitochondrial cell death. The host protects itself from the bacterium by activating its ER and UPR stress mechanisms. ER membrane protein Bri3bp activates mitochondrial cell death by encouraging the release of Cytochrome *c* which will lead to Caspase activation and ultimately cell death. Cytosolic *Salmonella* binds to Bri3bp to modulate apoptosis. It is possible it does this with duality and will either activate or block mitochondrial cell death if it needs further time to hyper replicate or if is advantageous to disseminate. Adapted from Sendoel and Hengartner et al (2014).

6.12.2 TM9SF3 protein transports cytosolic *Salmonella* through the Golgi complex to the cell surface

TM9 family proteins, also known as Phg1, play a role in the control of cell surface localization of membrane proteins (Benghezal et al 2003). The structure of the proteins is highly conserved with each other, presenting a large extracellular domain and nine putative transmembrane domains. This family is also present in several species, such as, *Dictyostelium discoideum*, *Saccharomyces cerevisae*, *Drosophila*, mice and human. TM9/Phg1 proteins were initially characterised in Dictyostelium, finding three members

of the family (Phg1A, Phg1B and Phg1C) (Benghezal et al 2003), three in *S. cerevisae* (TMN1, TMN2 and TMN3) (Froquet et al 2008), three in *Drosophila* (TM9SF2, TM9SF3 and TM9SF4) (Bergeret et al 2008, Perrin et al 2015) and four in human/mice (TM9SF1, TM9SF2, TM9SF3 and TM9SF4) (Chluba-de Tapia et al 1997, Schimmöller et al 1998).

Previous studies have confirmed these proteins act as intermembrane cargo receptors regulating exocytosis, cell surface localization of a subset of membrane proteins and cellular adhesion (Benghezal et al 2003, Bergeret et al 2008, Cornillon et al 2000, Froquet et al 2012). TM9 proteins are mainly present in the Golgi complex and can also be found in the plasma membrane (Cornillon et al 2000, Perrin et al 2015, Sugasawa et al 2001). Most of the studies have been carried in yeast and not in mammalian cells but work carried by Perrin et al (2015) showed TMSF4 transports glycine-rich TMD's through the Golgi Complex to the cell surface. Another relevant role of TM9 proteins was studied in mammalian cells where *phg1a* knockouts were incapable of killing *Klebsiella* bacteria. This was because the cells exhibited an unnatural high lysosomal pH, quite possibly impairing the cell to efficiently kill bacteria (Le Coadic et al 2013).

TM9SF3 was identified with three peptides in two of the cleaved SafA' (SafA-6xHis) affinity-enrichments' and absent in both of the negative controls (Table 16). As TM9 proteins and their functions are highly conserved within species, we propose cytosolic *Salmonella* binding to transmembrane protein TM9SF3 is to be transported from within the cell to the cell surface (Figure 58). This exit mechanism has not been previously described in any other bacterium and functional studies would be required to further characterise this. Regardless, the binding of TM9SF3 to cleaved SafA (SafA-6xHis) is undisputable, and is also plausible that as demonstrated in *Dictyostelium* and mammalian studies (Le Coadic et al 2013), cytosolic *Salmonella* binds to TM9SF3 and disrupts the production of functional lysosomes that would endanger its intracellular survival.

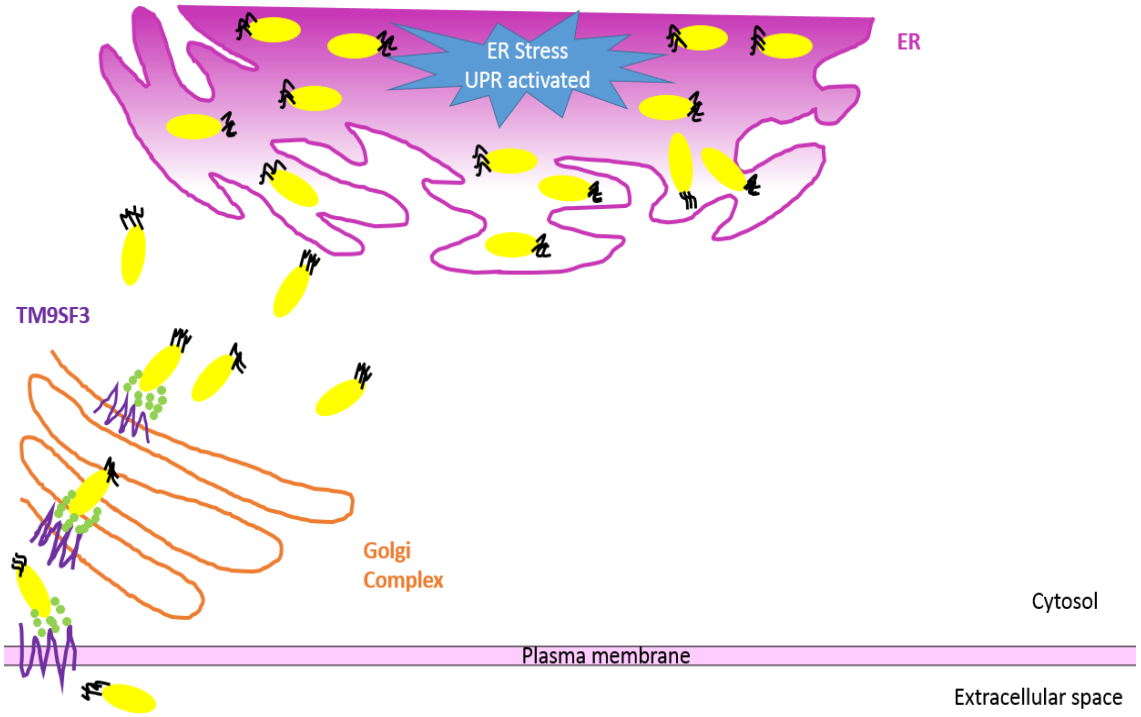

Figure 57. Hypothesised model depicting the exit of cytosolic *Salmonella* through transmembrane protein TM9SF3. During infection the ER stress response triggers the UPR and the bacteria is fighting a strong host response. Cytosolic *Salmonella* makes its way to the Golgi Complex and attaches itself to transmembrane protein TM9SF3. The bacteria is comfortably taken through the different layers of the Golgi Complex until is transported out of the cell. Figure adapted from Perrin et al (2015).

6.12.3 *Salmonella* induces transcriptional changes to modulate host's gene expression by ABHD14B binding

Protein ABHD14B was identified in two of the cleaved SafA' (SafA-6xHis) affinity-enrichments' and in none of the negative controls (Table 16). It belongs to the ABDH14 family and is found mainly in the cytosol, extracellular space and nucleus. It is categorised as a hydrolase and its role is of being a positive regulator of transcription from RNA polymerase II promoter (Strausberg et al 2002). There is no further literature available regarding this protein and neither of its interaction with *Salmonella* or any other bacterium.

There is evidence that bacterial pathogens can interfere with transcription by preventing trafficking of host transcription factors. During infection, host genes regulating the initial response to pathogens are targets of many bacteria (de Monerri and Kim et al 2014). A microarray-based analysis to investigate the host response to *Plasmodium* spp. showed the parasite uses the host's resources during infection (Albuquerque et al 2009). The studies were performed on infected hepatoma cells, showing a particular set of genes involved in ER stress response, receptor binding proteins, including transcriptional regulators to be distinctively expressed throughout infection.

Another example is the protozoan *Toxoplasma gondii*, it modulates cytokine-induced JAK/STAT signalling pathways and blocks IFNγ-mediated STAT1-dependent proinflammatory gene expression (Carey et al 2012, Leng et al 2009, Schneider et al 2013). Also, *Chlamydia trachomatis* is a human pathogen that lives and replicates within a vacuole called an inclusion. Studies carried by Soupene et al 2012) reported *Chlamydia* recruits several host proteins within its inclusion membrane. These proteins are acyl-CoA synthetase enzyme ACSL3, acyl-CoA binding protein ACBD6, nuclear protein ZNF23 (a pro-apoptosis factor), Acyl-CoA: lysophosphatidylcholine acyltransferase LPCAT1 (an ER protein), among others; possibly to inhibit several host cell responses. In addition, the protozoan genomes have identified histone modifying proteins and chromatin remodelers. The activity of these proteins is presumed but if correct, it would indicate their ability to affect the transcriptional profile of organisms (Croken et al 2012).

Finally, studies carried in *E.coli* infected human kidney cells have demonstrated this bacteria inhibits Pol II-dependent transcription. Their results showed a considerably reduction in gene expression was achieved by the stimulation of Pol II transcriptional repressors and by suppression of transcriptional activators/factors (Lutay et al 2013).

Based on the above, identification of ABDH14B in the affinity-enrichments' suggests cytosolic *Salmonella* binds to protein ABDH14B to inactivate transcription and the expression of certain genes that might favour *Salmonella's* intracellular survival (Figure 59). Without functional studies we cannot suggest which host genes, but as per literature, it is possible to speculate these genes are involved in ER stress and inflammatory signals.

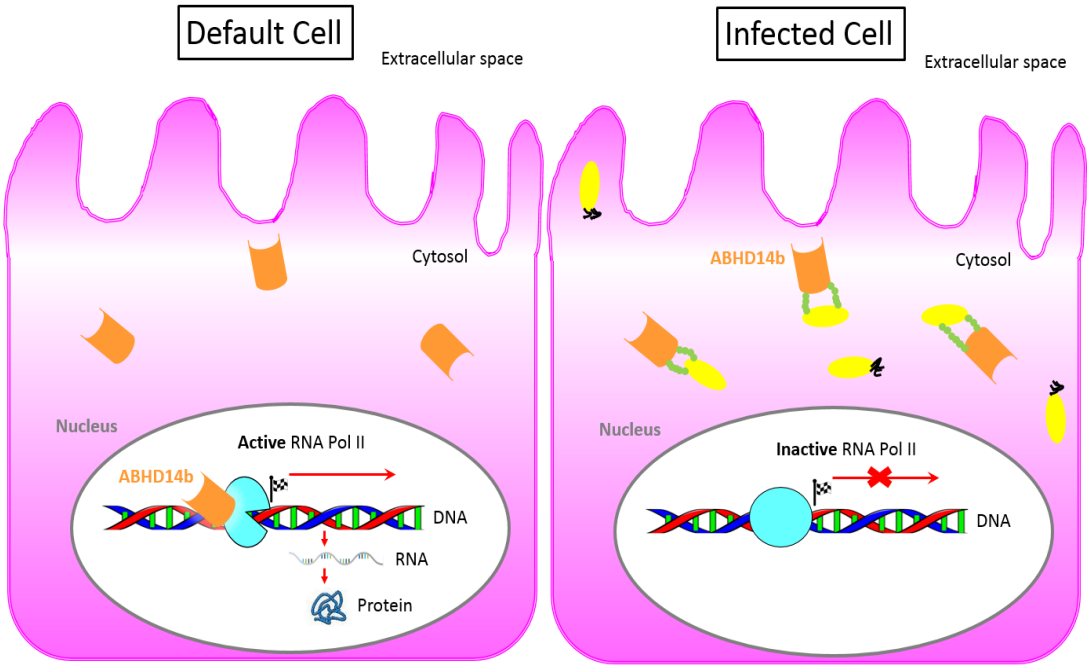

Figure 58. Hypothesised model of transcription inactivation by Salmonella. In an uninfected (default) cell ABHD14B binds to RNA polymerase II to activate transcription that will produce RNA and result in the synthesis of proteins. In the early stages (possibly) of infection *Salmonella* binds to cytosolic ABHD14B to halt the production of genes that might lead to its destruction. Adapted from Rolando and Buchrieser et al (2014).

6.12.4 SafA-mediated blocking of Serpinb1a exacerbates cell death leading to bacterial escape

Serpinb1a was identified with two peptides in two of the cleaved SafA' (SafA-6xHis) affinity-enrichments' (Table 16). The protein was not identified in any of the negative controls. Serpins are a large family of peptidase inhibitors involved in the modulation of homeostasis and thrombolysis (Silverman et al 2010). They are highly conserved and are abundant in the Archaea, Eukarya, bacteria and some viruses (Irving et al 2002, Ivanov et al 2006, Schell et al 2002, Silverman et al 2010). Serpinb1 proteins are known for inhibiting neutrophil elastase (NE) and cathespin G (CG). Mice lacking Serpinb1 have a reduced lifespan when infected with *Pseudomonas* (Baumann et al 2013). Two thirds of the Serpins are found extracellularly but unlike these Serpinb1a is located intracellularly, in the cytoplasm (Silverman et al 2010). In humans, B serpins or ov-serpins do not present a signal peptide and are located primarily in the cytosol. Because of their unique location among the Serpins and their function, it is thought these group of proteins play a role in the protection of the cell from overactive proteolytic activities (Aboud et al 2014, Williams et al 1999). Moreover, there are examples of Serpinb proteins playing a cytoprotective role from tumor necrosis factor-α (TNFα) induced apoptosis (Dickinson et al 1998).

Upon infection, bacteria interact with the immune system through their flagella, toxins and pili triggering host immune response. During acute inflammation, neutrophils are recruited at the site of damage where they secrete elastases, in response to this Serpins inhibit the elastases to protect the cell from further damage (Ruiz et al 2014). The primary role of Serpins is to modulate cell death, without it the cell would autodestruct whilst fighting bacteria. Moreover, it is documented many bacterium take advantage of this to exploit the inflammation response in their favour. Some bacterium will secrete their own elastase inhibitors, such is the case of *Bifidobacterium longum* which Serpin inhibits, both, pancreatic elastase and neutrophil elastase (Ivanov et al 2006). Human pathogen *Staphylococcus aureus* secretes a family of neutrophil serine inhibitors to block the host's neutrophil elastase, cahespin G and proteinase 3 (Stapels et al 2014). Finally, in a study aimed to identify proteins secreted by *lactobacillus rhamnosus* (a probiotic bacterium), a leukocyte elastase inhibitor was identified (Sánchez et al 2009).

A direct interaction between *Salmonella* and elastase inhibitors has not been reported so far. Nevertheless, as described above, there is some evidence in other bacteria to suggest cytosolic *Salmonella* can benefit from the inhibition of the host's elastases, in this way continue to hype replicate in the host cell (Figure 60). Further to this the inhibition of elastases seem so effective that some bacterium secrete the serpin-like proteins themselves. Functional studies (Chapter VII, Section 7.5) would be required in order to fully understand the biological implication of blocking Serpins but it is plausible to hypothesise that in the same way bacteria benefit from inhibiting the host's elastase, therefore avoiding cell death, it can also benefit from cell death. Bacterial induced apoptosis is strongly documented and is a means for *Salmonella* to escape the cell and re-infect other tissues (Grassmé et al 2001, Hausmann et al 2010, Kirschnek et al 2005, Lancellotti et al 2006, Weinrauch and Zychlinsky et al 1999).

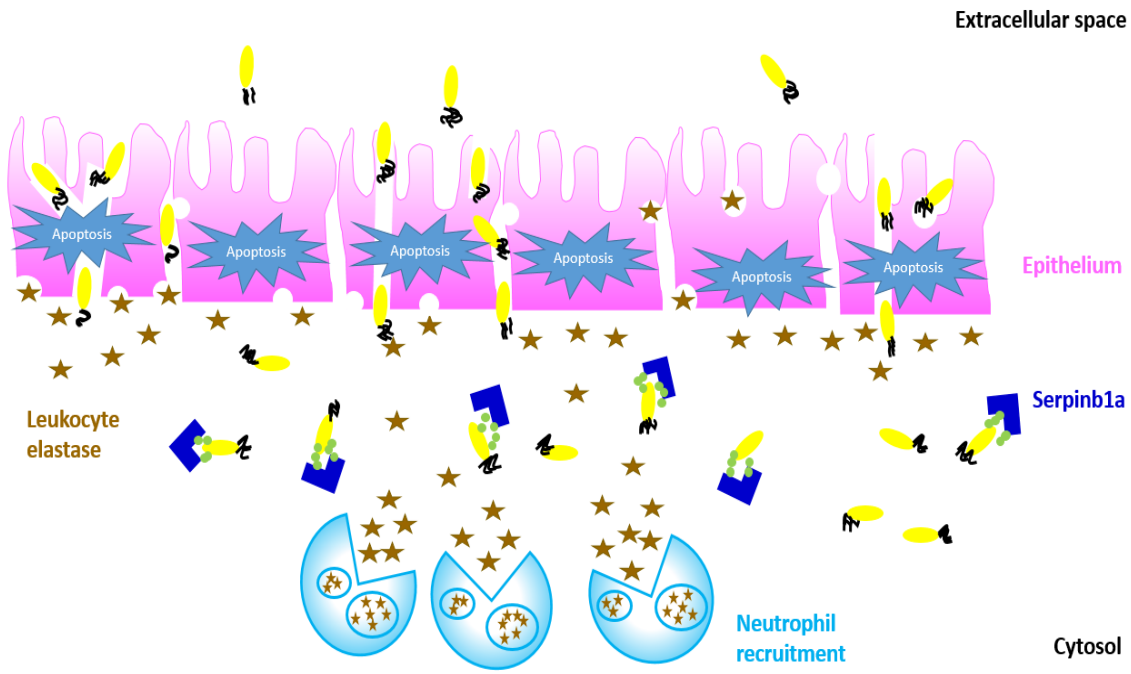

Figure 59. Hypothesised model of SafA-mediated blocking of Serpinb1a leading to cell death and *Salmonella* release to the extracellular space. Upon infection the cell recruits neutrophils to combat the bacteria. In return, these secrete leukocyte elastase that will result in apoptosis. To control an overactive reaction and unnecessary cell death, Serpins are released to bind leukocyte elastase and modulate apoptosis. Cytosolic *Salmonella* benefits from cell death so that it can escape the several host immune responses or perhaps it has hyper replicated and is ready to re-infect other tissues. Therefore, it binds to Serpinb1a, encouraging the cell to autodestruct. Adapted from Endo et al (2014).

6.12.5 Protein RGD1561381 inhibits Reactive Oxygen Species (ROS) for *Salmonella* intracellular survival

The identification of protein RGD156138 (a MGST3-like protein) in two of the cleaved SafA' affinity-enrichments', with two peptides in each, provides evidence on cytosolic *Salmonella* binding partners (Table 16). RGD1561381 is an uncharacterised protein with little information available but as per NCBI database (http://www.ncbi.nlm.nih.gov/gene/498340, accessed on 05/07/16) it is similar to microsomal glutathione S-transferase 3 (MGST3) and part of the membrane associated proteins in eicosanoid and glutathione metabolism (MAPEG). MAPEG members are categorised in six groups of microsomal glutathione transferases (MGST) (Bresell et al 2005, Jakobsson et al 2000). They are known for their role in the production of leukotrienes and prostaglandin E and for being key mediators of inflammation (Byrum et al 1997, Molina et al 2008, Samuelsson et al 2007). Microsomal proteins are mainly located in the Endoplasmic Reticulum (ER) but can also be found in the extracellular compartment (Sjögren et al 2013).

Studies and literature, particularly in MGST3, are scarce but the few reviews do confirm their location and roles in inflammation and ROS (Sherratt and Hayes et al 2001). MGSTs catalyse conjugation of leukotriene A4 and reduced glutathione (GSH) into leukotriene C4 which results in inflammation, leading to ER stress (Calmes et al 2015, Sherratt and Hayes et al 2001) which will induce a ROS response (Dvash et al 2015, Marí and Cederbaum et al 2001). Also, decrease of GSH has been related to increase of ROS (Armstrong et al 2002, Du et al 2009, Lushchak et al 2012, Salvemini et al 1999). Further information was retrieved from The International Mouse Phenotyping Consortium (IMPC) database (http://www.mousephenotype.org/data/genes/MGI:1913697 accessed on 05/07/2016) holding six images for gene MGI:1913697 where the expression of MGST3 was detected in the digestive system. It was found in the oesophagus, Peyer's patch, stomach, large intestine, gall bladder and the small intestine among other tissues.

There is evidence *Salmonella* thrives in the absence of ROS (Fang et al 2011, Umezawa et al 1995) but there is also evidence a percentage of *Salmonella* uses ROS to exponentially increase replication, disseminate and infect other tissues (Paiva and Bozza et al 2014). It has also been observed that *Salmonella* can take advantage of ROS production during acute inflammation (Stecher et al 2007). Most of the infection studies of *Salmonella* are in the SCV and there is a need to understand the intracellular survival of cytosolic *Salmonella*. Moreover, most of the known bacteria that exploit ROS are known to do not spend long times of their lifespan inside a mature phagosome (Bereswill et al 2010, Hanna et al 1994, Oberley-Deegan et al 2010, Sapra et al 2006), this is likely to be evidence that pathogens benefitting from ROS production are not fully exposed to direct oxidative damage (cytosolic *Salmonella*?).

Several studies have proven some pathogens indulge ROS as an indirect metabolic supplement. *Trypanosoma cruzi* epimastigotes multiply rapidly in axenic cultures supplied with H_2O_2 (Machado et al 2012, Paiva et al 2012). *Salmonella typhimurium* grows more actively in inflamed intestinal lumen when ROS is vigorously produced. In this case, intestinal ROS converts the thiosulfate produced by the microbiota into tetrathionate, which supports anaerobic growth, giving *Salmonella* the advantage required to respire and multiply (Winter et al 2010).

On the other hand, when vital, the cell contains ROS and tries to protect itself from tissue destruction by means of GSH, thioredoxin and catalase (Bhattacharyya et al 2014, Gómez-Pastor et al 2010, Kinnula et al 2005, Manfredini et al 2004).

Based on the results, we propose in response to ER stress the identified MGST3-like protein (RGD156138) catalyses GSH producing TC_4 which in consequence will activate inflammation signals (Figure 61). This response will feed back the initial ER stress and lead to imminent tissue destruction. In the midst of an overactive ROS response activated by the host immune system, cytosolic *Salmonella* binds to RGD156138, blocking the binding of GSH and setting it free to eliminate ROS. Studies do show at some point of infection *Salmonella* thrives during ROS, nevertheless, it has a bigger advantage over the host in the absence of it. Because of this, the binding of cleaved SafA' (SafA-6xHis) to RGD156138 indicates one of the many strategies used for intracellular survival is to control ROS and gives initial evidence on the behaviour of cytosolic *Salmonella*.

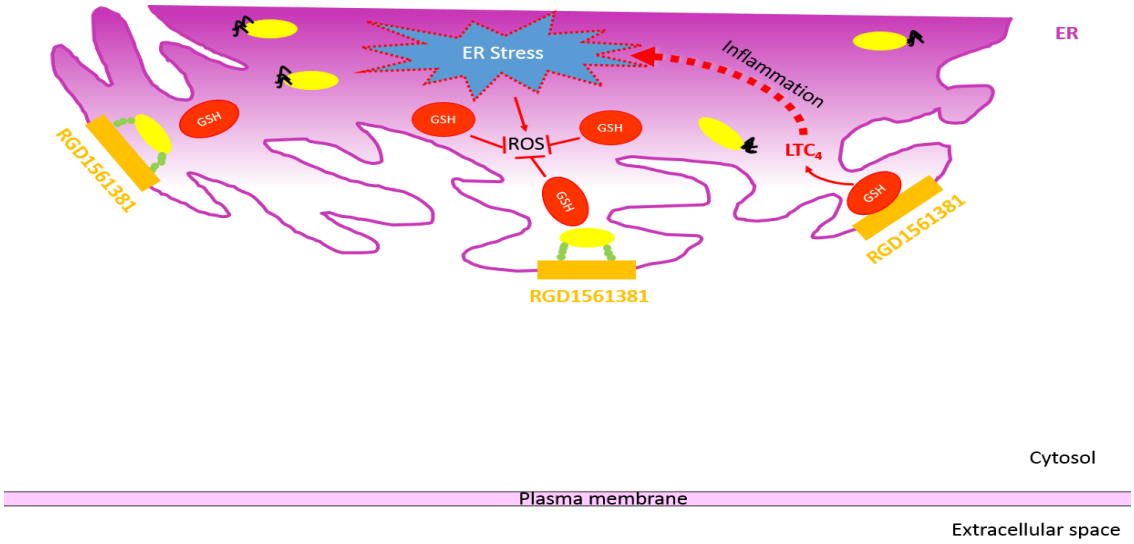

Figure 60. Hypothesized model of ROS inhibition by *Salmonella*. During infection the ER stress signal is activated. As a response, MGST3-like protein (RGD1561381) binds to reduced glutathione (GSH). This reaction will lead to the production of LTC_4 that will emit an inflammation signal and increase the ER stress. Under the increased stress ROS are produced and *Salmonella* are highly threatened. It is here where cytosolic *Salmonella* binds to RGD1561381 to release GSH and control overactive ROS.

CHAPTER VII - DISCUSSION

7.1 Lessons learned from the comparison of currently available methods for capturing protein-protein interactions

Five affinity-enrichment systems were set up to study protein-protein interactions between *Salmonella* and protein extracts from the mammalian large intestine (Chapter V). Widely used and commercially available technology was carefully tested against different binding conditions and a repertoire of lysates (protein extracts) provided from a variety of rat tissues.

Coupling of SafA' (GST-SafA-6xHis) to Dynabeads (System 1) through the histidine tag was achieved as expected (Chapter V, Section 5.3, Figure 32). The main outcome of the first affinity-enrichment was the overwhelming binding of non-specific proteins (Chapter V, Section 5.3, Figure 33). This was addressed by attempting to deplete the protein extracts by pre-incubating the extracts with empty Dynabeads (Chapter V, Section 5.3, Figure 33, Panel B). It is not rare that an affinity-enrichment presents background, non-specific binding has been reported for IMAC systems (Cheung et al 2012). The likely reason for this is the presence of Histidines and Cysteines in the lysates (Terpe et al 2003). Further to this, proteins may bind non-specifically through ionic interactions regardless of the IMAC chemistry on the surface (Bornhorst and Falke et al 2000). It was attempted, however unsuccessfully, to address this problem by increasing the ionic strength (salt concentration) in the extracts (Chapter V, Section 5.3, Figure 33, Panel C).

It was also investigated whether these non-specific proteins bind to the metal ion (Cu^{+2}) or the polymer covering the beads (Chapter V, Section 5.3, Figure 33, Panel D). Studies have been carried out were the efficiency of different ions favour the isolation of certain proteins over others (Liang et al 2007) but a particular study where beads have been stripped of their ion to study the interactions have not been (to our knowledge) reported. The increasing amount of salt in the extracts aided the removal of the lower molecular weight proteins only (Chapter V, Section 5.3, Figure 33, Panel D). This problem has also been reported in previous IMAC work (Jiang and Hearn et al 1996). Affinity-enrichments were also tested with extracts from lamb's heart (Chapter V, Section 5.3, Figure 33, Panel E), however with similar results, confirming further the unsuitability of this system for the study.

Thus, System 2, the second IMAC product was selected (Nickel Affinity Gel) where agarose was used instead of beads (Chapter V, Section 5.4, Figure 34) The Nickel Affinity Gel relies on the use of nitrilotriacetic acid (NTA) which is charged with Ni^{+2} ions, and shows affinity to His-tagged proteins (Crowe et al 1996, Magdeldin and Moser et al 2012). This system also provided higher binding capacity which increases the amount of immobilized bait protein or the use of less resin (to reduce elution volumes) (Ueda et al 2003). One key disadvantage of this material is its porous nature, and therefore the need of longer washing times to ensure complete diffusion of any non-specific proteins from the agarose mesh. Coupling of bait protein to agarose was achieved, however as per System 2, despite repeated depletion steps (Chapter V, Section 5.4, Figure 35, Panel A, Lane 6) and testing different extracts (Chapter V, Section 5.4, Figure 35, Panel B), elevated background due to the binding on non-specific proteins to the agarose matrix was evident. These results led to exclusion of this system for the study.

As a consequence of the above described lack of success using matrices recognizing the Histidine tag, it was decided to exploit GSH-mediated capture (System 3, Chapter V, Section 5.5, Figure 36). This system is widely used for the immobilization of GSH fusion protein on glutathione sepharose beads and widely used for pull-downs, affinity-enrichment experiments and Co-immunoprecipitation (Co-IP) experiments. Also, there is a number of reviews available (Luo et al 2014, Ren et al 2003, Yang et al 2008). SafA' (GST-SafA-6xHis) was successfully immobilised through the GST tag but after incubation of GSH-agarose with total protein extracts, a large quantity of a protein with MW of ~ 25-35 kDa was also captured despite repeated depletion (Chapter V, Section 5.5, Figure 37, Panel A, Lane 8). This is in line with literature reporting a difficulty of working with tissue extracts from GI tract tissues due to the presence of endogenous glutathione - an important endogenous antioxidant especially abundant in GI tract (Hayes et al 1989, Van Veld and Lee et al 1988).

Having tested protein capture through both His and GST tags present in our SafA' (GST-SafA-6xHis) construct we reverted to the use of tag-independent protein capture. Proteins were therefore immobilized onto NC through passive sorption and the binding capacity was determined (Chapter V, Section 5.6, Figure 38). Despite generally succeeding in crosslinking proteins (Chapter V, Section 5.6, Figure 39, Panel A), the use of this approach, as above, did not reduce the level of non-specific protein capture sufficiently to justify its use in this study (Chapter V, Section 5.6, Figure 39, Panel D).

It was then opted to test the adaptability of Universal-BIND™ plates (System 5) (Chapter V, Section 5.7, Figure 40), a 96 plate well-like system that met several of the conditions that were deemed essential for this study. The polystyrene microwell plates, are non-porous and allow for hydrophobic protein sorption, yet provide means for covalent crosslinking. Recombinant SafA' (GST-SafA-6xHis) was immobilized via abstractable hydrogen (the hydrogen attached to aliphatic carbons) bonding using UV-light illumination, resulting in a carbon-carbon bond (Leea et al 2016). Except for the covalent crosslinking, the plates are not different from traditional microwell plates used in ELISA and hence a large body of literature exist on optimizing protein immobilization (Biesiadecki and Jin et al 2011, Karaszkiewicz et al 2005, Woo et al 2011). This system provided a non-porous leak resistant surface with covalent bond crosslinking for strong protein immobilization allowing for harsh washes to eliminate background. The only disadvantage of this system was the limited binding capacity (Gibbs and Kennebunk et al 2001).

UV-light crosslinking over standard ELISA protein immobilization through adsorption was successfully tested with reduced protein loss (Chapter V, Section 5.7, Figure 42). Binding capacity and buffer optimisation for immobilisation was also tested (Figure 43). The occurrence of protein displacement and elution was also successfully tested in various experimental conditions (OG, PIs, BSA-blocking, elution buffers) (Chapter V, Section 5.7, Figure 44, Panel B). It is common practise to use milk as a blocking agent; nevertheless blocking trials were performed just with BSA due to its known efficiency for blocking excess protein-binding sites (Xiao and Isaacs et al 2012). The reason for choosing BSA as a blocking agent also relied in the fact that BSA is a single protein that can be easily identified in eluates. Setting up of System 5 continued by testing detergents, as well as any other solution used in the experimental conditions. The suitability of 1% BSA as a blocking agent was confirmed together with the superior performance of OG over Tween-20 (Chapter V, Section 5.7, Figure 44, Panels A and B). Finally, the final assay conditions were optimised by testing two known interactors, where anti-rabbit IgG was successfully isolated from rabbit IgG (Chapter V, Section 5.7, Figure 44, Panel C).

Further to this, it was decided 0.1% SDS was to be used as the elution buffer over 100 mM Glycine, pH 2.5 and 3 M, NaCl, pH 8 allowing reduced incubation time and presenting no limitation for subsequent analyses (trypsin digestion and MS analysis). Precipitation by acetone is a common method used to purify proteins from contaminants.

Adding this extra step allowed us to eliminate SDS from the samples but it also gave us the flexibility concentrate the eluates from as many wells as needed. Other methods, such as, precipitation by Trichloroacetic acid (TCA) and a combination of TCA/Acetone precipitation were tried, yet none was as successful as acetone precipitation (results not shown).

After setting up a variety of systems it was decided to adapt the Universal-BIND™ plates (System 5) for affinity-enrichments and for the identification of SafA (SafA-6xHis) putative interacting protein partners. To identify interacting proteins in the large intestine is problematic due to the concentration of unprocessed food, possibly other bacteria, toxins and faecal residuals. The number of proteins present in the large intestine which are not necessarily part of the intestines and can potentially "stick" to any given surface is an issue.

In conclusion, the exhausting comparison of the systems described to isolate the recombinant GST-SafA-6xHis has been pivotal in indicating that a non-porous, non-ionic surface and an efficient blocking alongside with crosslinking was to be preferred.

7.2 Mass spectrometry analysis was central to the identification of SafA-large intestine protein-protein interactions

Initially, affinity-enrichments of SafA' (GST-SafA-6xHis) with different tissues, such as, heart, colon, small intestine and large intestine (Chapter VI, Sections 6.2 and 6.3) were analysed by PMF. The approach consisted of overlaying 3xSafA' (GST-SafA-6xHis) and 3xBSA affinity-enrichment spectra (from the same tissue) and manually selecting the peaks present only in the SafA' (GST-SafA-6xHis) affinity-enrichments (Chapter VI, Section 6.4). Subsequently, the identity of the peptides was searched for using the MASCOT software search engine for protein identification (Chapter VI, Section 6.5, Figure 53).

From the spectra (data not shown), it was possible to identify peptides with an affinity for GST-SafA-6xHis. The identification of cyclin-dependent kinase-like 3 protein in the heart was achieved by PMF (Chapter VI, Section 6.5, Figures 48 and 49). Regardless, the identification would need to be confirmed with further replication. However, the bait used was uncleaved SafA' (GST-SafA-6xHis) and it could not be excluded that the binding is specific to SafA-6xHis or to GST. Moreover, in the study it was not possible to find evidence of *Salmonella* recombinant proteins binding to cyclin in any affinity-enrichment

other than in heart extracts. Albeit, there is published evidence that *Salmonella* interferes with the cell cycle of the host particularly in the intestines (Rosenberger et al 2000).

It is plausible that the complexity of the intestines tissue, contaminated with undigested food or faecal residues, resulted in missed identification of the abovementioned interaction with cyclins. It is also possible that the system of choice Universal-BIND™ plates (System 5) assay does not provide the right platform to study this particular interaction.

Due to the nature of *Salmonella* and its preference of tissue for infection, all subsequent analyses carried by LC-MS/MS were focused on the (GST-SafA-6xHis) SafA'/large intestine affinity-enrichments (Chapter VI, Section 6.2, Figure 51). In light of the 'MS1 results', the experimental design was redrawn (Chapter VI, Section 6.2, Figures 46 and 47) and several affinity-enrichments were performed with a variety of baits, such as, GST, BSA, GST-SafA-6xHis and GST+SafA-6xHis to aid the identification of specific SafA (SafA-6xHis) binding proteins.

A total of 2, 119 proteins were identified (Chapter VI, Section 6.8, figure 55). The data was analysed by systematically eliminating contaminants, such as human keratin, BSA, and trypsin. Stringent selection criteria were used whereby only proteins identified by no less than two peptides and in at least two undepleted cleaved SafA' (GST+SafA-6xHis) (satisfying the Scaffold filtering thresholds selected) were confidently considered as positive SafA-6xHis interactors. This approach reduced the list down to five proteins: Bri3bp binding protein, TM9SF3, ABDH14B, Leukocyte elastase inhibitor A and MGST3-like protein (RGD1561381) (Chapter VI, Section 6.9, Table 16).

Mass spectrometry is a reliable tool for protein identification, nevertheless, false protein identification is a frequent problem (Herrmann et al 2013). To avoid this, it is generally accepted to identify proteins with no less than two peptides and to apply filtering criteria with high thresholds (Carr et al 2004, Nielsen et al 2005). Due to time and resource constraints, the data supplied is not quantitative and further affinity-enrichments analysed by quantitave mass spectrometry would be required for this. Albeit, sufficient proof of identification could be obtained if western blots confirm the presence of the identified proteins in the affinity-enrichments. From the mass spectrometry data it can be concluded that System 5 is a reliable method capable of selecting proteins for identification by LC-MS/MS.

To date, there are no known interactors for any of the proteins forming the Saf fimbriae. The external proteins forming the flexible body are SafA and SafD. Due to its position at the tip of the fimbria, and its similarity with *E. coli* protein AfaD and *S. enteritidis* SefD (30% overall identity in both), SafD, is presumed to be an adhesin (Folkesson et al 1999). Studies on SafA and SafD homologues in *E. coli* have elucidated information on the role of each protein as a subunit and as a two subunit polymer. For instance, AfaE-III (SafA homologue) was observed to adhere to HeLa cells but was unable to internalize (Cota et al 2006, Jouve et al 1997, Tieng et al 2002), AfaD (SafD homologue) did not show a significant interaction with the cells and was also unable to be internalized. Whereas, AfaDE (A two subunit polymer formed of AfaE-III and AfaD) was observed to adhere itself to the HeLa cells and internalise (Cota et al 2006). Therefore, it cannot be excluded that biologically meaningful interactions could only be retrieved when SafA and SafD are used together and studied as a polymer that more closely represents the native fimbria. Comparative studies with infected tissues may also be carried out with tissues infected with *Salmonella* at different time points (Chapter I, Figure 4) to be able to distinguish between proteins that interact with SafA complex at the onset of the interaction with the host or during the establishment of the pathogen.

7.3 Putative functional SafA interacting proteins: hypotheses derived from literature and extended discussion

7.3.1 Regulation of Endoplasmic Reticulum (ER) stress sensors are key for cytosolic *Salmonella* intracellular survival

The searches indicate (Chapter VI, Section 6.9, Table 18 and Section 6.12) that cytosolic *Salmonella* inhibits mitochondrial apoptosis and ROS by binding to ER transmembrane proteins Bri3bp and RGD1561381 (MGST3-like protein). The Bri3bp protein plays a role in cell fate decision by modulating joint activities between the ER and mitochondria (Yamazaki et al 2007), and based on the conserved domain database, in apoptosis (Lin et al 2001). Most of the knowledge on Bri3bp has been provided by Yamazaki et al (2007), where Bri3bp was incubated with apoptosis inducers including ER stressors Tg (sarcoplasmic/endoplasmic Ca2+–ATPase inhibitor) and Tu (N-glycosylation inhibitor), together with the chemotherapy drug Etop (topoisomerase II inhibitor). It was concluded that abundance of Bri3bp left the cell vulnerable to pharmacological induced apoptosis, because of this Bri3bp must be involved in apoptosis-inducing signals emanating from the ER by increasing the sensitivity to Etop by upregulating the caspase cascade. In

addition, it was proved that overexpression of Bri3bp induced an increase in the of cytochrome *c*.

Further to this, upon exposure of the cell to Etop, the ER underwent morphological changes but these were not observed in cells with over-expressed Bri3bp. Therefore, it was established that the caspase-dependent facilitation of Etop-induced apoptosis by BRI3BP has an impact in ER morphology and that high levels of Bri3bp are responsible for mitochondrial cell-death. The current knowledge on Bri3bp is scarce. Nevertheless, it is feasible to hypothesise that *Salmonella* binds, through SafA, to Bri3bp protein in an attempt to block cytochrome *c* release and halt mitochondrial cell death (Chapter VI, Section 6.12.1, Figure 57). It is also possible that *Salmonella* would target Bri3bp in an effort to disturb the ER cisternae in an attempt to inactivate the ER and the many stress related signalling pathways activated by it, such as, inflammation and UPR. In addition, the cooperation between the ER and mitochondria has been highly studied (Banjerdpongchai et al 2010, Giorgi et al 2009, Lebiedzinska et al 2009, Malhotra and Kaufman et al 2011, Mueller and Reski et al 2015) and perhaps blocking Bri3bp has the ulterior aim of destroying the mitochondrion.

For instance, the proximity between the ER and mitochondrion influences one another and it has been shown how mitochondria is capable of accumulating Ca^{+2} by responding to microdomains of high Ca^{+2} that were generated in the ER (Csordás et al 2006, Hajnóczky et al 2014, Rizzuto et al 1998). Further evidence on the ER-mitochondria cooperation has been demonstrated by work on BAX and BAK. These multidomain proapoptotic proteins located in the ER can initiate mitochondrial dysfunction (Scorrano et al 2003). Moreover ER stress-induced mitochondrial dysfunction has been reported extensively in pancreatic beta cells (Lee et al 2010), hepatic cells (Egnatchik et al 2014), neuronal cell lines (Song et al 2016) and intestinal epithelial cells (Luo and Cao et al 2015), among others.

Studies carried out on BNAS1 (homolog of Bri3bp in yeast) (Katahira et al 2006) have placed Bri3bp as a regulator of antigen-receptor signal transmission in B cells. BNAS1 over-expression supressed the B cell receptor (BCR)-signalled transcriptional activation of Elk-1 through Jun N-terminal kinase (JNK) in DT40 chicken B cells. The BCR is a complex of membrane-bound immunoglobulin located at the surface of the B-cell, serving as a receptor for antigens (Rajewsky et al 1996, Rheingold et al 2003) that is known for its involvement in the regulation of apoptosis, differentiations, proliferation

and modulation of Ig gene recombination (Rheingold et al 2003). If homeostasis is disturbed and BCR is not tightly monitored, then this may cause immunodeficiency and autoimmunity (Cunningham-Rundles and Ponda et al 2005, Maródi and Notarangelo et al 2007).

Ag binding to the BCR is crucial for development and activation which will initiate a cascade of signalling events resulting in proliferation, differentiation or cell death (Liu et al 2010, Xu et al 2014). Because of this, bacteria target BCR as failure to produce mature B cells would weaken the humoral immune response (Mårtensson et al 2010). For instance, antibody deficiencies result in increased susceptibility to bacterial infections, such as, *H. influenzae* and *S. pneumoniae* (Duraisingham et al 2015, Fried and Bonilla et al 2009). Studies show that *Streptcoccus pyogenes* (IdeS) produces an IgG-degrading enzyme that cleaves IgG-BCR and blocks BCR signalling in response to receptor ligation, rendering it incapable of antigen (Ag) binding. This results in a loss of cellular events downstream of receptor ligation, particularly affecting MHC class II molecules (Järnum et al 2015).

On the other hand, interaction between *Salmonella* and the immune system has been recorded, for example, *Salmonella* spp are able to infect and survive within B lymphocytes (Kaur and Jain et al 2012, Rosales-Reyes et al 2005). Further to this, it has been proved binding to the BCR on the surface of B-cells triggers *Salmonella* uptake, resulting in an immediate antimicrobial humoral response. Regardless of this, *Salmonella* manages to survive within the B cells (García-Pérez et al 2012, Souwer et al 2009, De Wit et al 2010). In addition, after specific B cell receptor-mediated uptake SCV *Salmonella* remains dormant within B cells until it is slowly excreted (Souwer et al 2012). This would explain why infection starts in the intestines but later during infection can be found in the liver, spleen, lymph nodes and bone marrow (Vazquez-Torres et al 1999, Worley et al 2006).

In light of what has been described above, *Salmonella* uses the B-cell to gain entrance to the host and later transport itself to other tissues. BCR is not designed to uptake bacteria, yet *Salmonella* is a unique bacteria that facilitates its uptake to enter the host cell by using this unlikely receptor (Souwer et al 2009). As demonstrated in yeast by BNAS1 (Bri3bp homolog) (Katahira et al 2006), over-expression of Bri3bp would supress BCR, therefore if *Salmonella* binds to Bri3bp and blocks any Bri3bp-BCR signalling it would probably maintain the already present BCR or even enhance the number of BCR because regardless

of the humoral immune response emitted by it, it is of far greater advantage for *Salmonella* to increase its uptake in the host than remain dormant. After all, once inside the host-cell, infection can start given the adequate environment or it can be transported to any other cell by the B-cell.

RGD1561381 is a MGST3-like protein of ~17 kDa with amino acid identity to MGST2 (36%), LTC4 synthase (27%), MGST1 (22%) and FLAP (20%) part of the microsomal glutathione S-transferase superfamily (MAPEG) (Jakobsson et al 1997). These transferases are involved in the detoxification of xenobiotics, for example, environmental pollutants, antitumor agents and chemical carcinogens (Jakobsson et al 2000, Oakley et al 2011, Sherratt and Hayes et al 2001). They also play a role in the inactivation of secondary metabolites produced during ROS (Holm et al 2006). Even when in humans MGST3 is capable of detoxifying foreign molecules and synthesizing LTC4, in rats, the latter is not possible (Sherratt and Hayes et al 2001).

Glutathione S-transferases (GST) provide protection from membrane lipid peroxidation, usually initiated by ROS, such as OH·and HOO·to combine with hydrogen to produce water and fatty acid radicals (Marí and Cederbaum et al 2001, Vatansever et al 2013). Microsomal GSTs are transmembrane proteins located at the ER where detoxification of the cell by the cytochrome P450 occurs (family of isozymes responsible for biotransformation of drugs by oxidation) (Ogu and Maxa et al 2000). During infection, the bacterial pathogen Listeria monocytogenes produces pore-forming cytolysin listeriolysin O (LLO) and phospholipases C (PC-PLC and PI-PLC), the phospholipases C activate NADPH oxidase that might trigger ROS. To counteract this, LLO inhibits NADPH oxidase (Lam et al 2011).

There is evidence of how bacteria target ROS by obstructing the NADPH oxidase and mitochondrial-derived ROS modulation. Studies in *Francisella tularensis* have shown that they are rapidly ingested by neutrophils but are not eliminated. This is partially because it does not trigger a respiratory burst in human neutrophils by disrupting overall polymorphonuclear leukocytes (PMN) function and NADPH oxidative activity (McCaffrey and Allen et al 2006). The same has been observed in *Anaplasma phagocytophilum* (causes human granulocytic ehrlichiosis) where neutrophil NADPH oxidase is reduced (Carlyon et al 2004, IJdo and Mueller et al 2004).

There is no direct information on RGD1561381 in databases or literature. The databases description is of a MGST3-like protein. Therefore, we can speculate its function based on

the homolog proteins found in humans and rats. There is no literature available regarding the interaction of MGST3 protein with *Salmonella* or any other bacterium. Having said this, there is enough published evidence showing that bacteria would benefit from supressing ROS (Lam et al 2011, Paiva and Bozza et al 2014) and just a few are capable of doing so by means of injecting effectors (Hurley et al 2014, Moumene and Meyer et al 2016, Priller et al 2016). Therefore the binding of SafA to RGD1561381 could possibly be a novel way for cytosolic *Salmonella* of blocking GSH binding, a known antioxidant that acts directly with ROS and RNS (Reactive Nitrogen Species) (Kannan et al 2014, Lushchak et al 2012, Ou et al 2009). Maybe, hence some bacteria escape ROS by injecting effectors (McCaffrey and Allen et al 2006, Moumene and Meyer et al 2016), SafA is used as an adhesin for attaching to RGD1561381 and inject toxins that will bring transcriptional changes to the benefit of infection (Chapter VI, Section 6.12.5, Figure 61).

7.3.2 Cytosolic *Salmonella* keeps the host-cell from self-destruction

Serpins are a conserved family of proteins in prokaryotes (Ksiazek et al 2015, Law et al 2006) and eukaryotes involved in the regulation of protease-mediated processes (Ivanov et al 2006). These peptidase inhibitors can be split into excreted extracellular serpins, where these form ~10% of plasma proteins, and intracellular serpins which reside in the cytoplasm (Aboud et al 2014). Serpins inhibit proteases by inserting a bait peptide into the catalytic groove of the target protease (Korhonen et al 2015). Malfunction of serpins not only causes self-destruction, but also diseases like dementia, emphysema, hypersensitivity and changes in the immune system (Irving et al 2002, Seaborn et al 2014). The identification of Serpinb1a in our affinity-enrichments places *Salmonella* once more in the regulation of host cell death.

Serpins are pivotal for the host-defence functions and the innate immune systems in plants (Østergaard et al 2000, Fluhr et al 2012, Francis et al 2012, Roberts and Hejgaard et al 2008) and animals (Perera et al 2012, Roberts et al 2004, Wiedow and Meyer-Hoffert et al 2005, Yang et al 2016). In animals, Serpin6 (SRP-6) mutants (*srp-6*) demonstrated having a role of cell survival protection by blocking necrosis via neutralization of lysosomal peptidases (C1 family). This is achieved by the interruption of calpain-associated lysosomal lysis neutralization of lysosomal cysteine peptidases discharged from damaged organelles (Kirkegaard and Jäättelä et al 2009, Kolaczkowska and Kubes et al 2013, Luke et al 2007).

Polymorphonuclear neutrophil (PMN) granulocytes are fundamental elements of the immune response to infection (Kobayashi et al 2005, Kolaczkowska and Kubes et al 2013, Wright et al 2010). PMNs are produced daily in the bone marrow and have a short life-span of a few hours (Bekkering and Torensma et al 2013). Progressively these perish by caspase-dependent apoptosis (Koller et al 2004). PMNs carry in their interior neutrophil serine proteases (NSPs), elastases (NEs), cathepsin G (CG) and proteinase-3 (PE3) (Heinz et al 2012, Korkmaz et al 2010, Perera et al 2012). There is extensive evidence of the role of NSPs in response to pathogen stress and of Serpin's protective role in shielding the cell from damage, in *Pseudomonas aeruginosa* (Benarafa et al 2007), Influenza A (Gong et al 2011, Zhao et al 2014), *Mycobacterium bovis*, *Salmonella typhimurium*, *Listeria monocytogenes* (Hamerman et al 2002), among others. When wounding of tissue or inflammation occurs, neutrophils are swiftly recruited around the damaged tissue to release the antimicrobial factors within its cytosol (NSPs) together with ROS (Kessenbrock et al 2011, Miedel et al 2014).

Studies in mice have demonstrated Serpinb1a inhibits neutrophil secreted neutrophil elastase (NE) and cathespin G which are secreted during bacterial infection (Baumann et al 2013). Work carried out on Duchenne muscular dystrophy (DMD) showed that dystrophic muscle was enriched by serpinb1a, which was increased six-fold in comparison to wild type muscle, concluding that this is caused by the continuous influx of neutrophil in the chronically injured muscle (chronic inflammation) (Arecco et al 2016).

Finally, studies carried out on mice have shown that serpin protein Serpin 2a is induced in vitro in response to *Salmonella Typhimurium* (Hamerman et al 2002). There is enough knowledge and experimental evidence regarding the role of serpins, particularly serpinb1a (Arecco et al 2016, Silverman et al 2010, Zhao et al 2014). Further to this, there is also solid evidence of serpin upregulation of neutrophil serine proteases (NSPs) and of their importance in cell preservation (Baumann et al 2013, Roberts and Hejgaard et al 2008, Roberts et al 2004, Ye and Goldsmith et al 2001). Therefore, we propose that *Salmonella*, through SafA, binds to serpinb1a to block serpin1ba-NSP binding and allow the cell to self-destruct (Chapter VI, Section 6.12.4, Figure 60).

Alpha/beta hydrolase domain-containing protein 14B (ABHD14B), also known as CCG1-interacting factor B or CIB belongs to the AB hydrolase family and its role is of being a positive regulator of transcription from RNA polymerase II promoter (Marín-Buera et al 2015, Padmanabhan et al 2004). The core promoter is the adjacent DNA

sequence whose role is to initiate transcription by RNA polymerase II machinery (Kadonaga et al 2004, Nikolov and Burley et al 1997). Upon activation, RNA polymerase II catalyses the synthesis of mRNA from the DNA template. The core promoter is made up of several elements, the TATA box (not all core promoters have a TATA box), initiator, TCT, BRE, MTE and DPE motifs (Grünberg and Hahn et al 2013, Hampsey et al 1998). Having said this, the core promoters vary as different types of core promoters are transcribed by different transcription factors (Hahn et al 2004, Kadonaga et al 2012).

There is no documented interaction between *Salmonella* and ABDH14B or any other bacteria. Regardless, it is well documented that bacteria and viruses modulate transcription of host genes by targeting the RNA polymerase II promoter (Ashida and Sasakawa et al 2014, Berdygulova et al 2012, Georg and Hess et al 2011, Lutay et al 2013, de Monerri and Kim et al 2014, Samson et al 2013). Infections can result in the activation of genes related to host cell responses. Particularly affected genes are the ones associated with immune response or inflammation. For example, the parasite responsible for malaria, *Plasmodium* spp., induces transcriptional changes in more than 1000 hepatocyte genes (Albuquerque et al 2009). It has been demonstrated that early infection receptor-binding proteins production and stress-response genes were up-regulated, such as ER-stress response proteins, transcriptional regulators and signalling enzymes, but later during infections these were altered (Albuquerque et al 2009).

Toxoplasma gondii dysregulate the host cell cycle, causing arrest at the G2/M border (Brunet et al 2008, Molestina et al 2008). Further to this, microarray studies have shown more than 1000 genes were modified during infection. These genes encoded proteins involved in cell growth, differentiation, inflammation and apoptosis (Blader and Saeij et al 2009, Molestina et al 2008). Other bacteria have evolved to inhibit the proinflammatory transcriptional response where mitogen-activated protein kinases (MAPK) cascades activation and translocation of the nuclear factor κB (NF-κB) into the nucleus lead to the increase of a repertoire of immune molecules, among them, interleukin-1β (IL-1β) and IL-18 (Baxt et al 2013). *Shigella* spp (Ashida et al 2010, Li et al 2007), *Burkholderia pseudomallei* and pathogenic *E. coli* secrete proteins that will block the degradation of the inhibitor of NF-κB (IκBα) (Cui et al 2010). Another example can be found in *Chlamydia* spp., where zinc finger nuclear protein 23 (ZNF23) is captured and taken to its inclusion vacuole. ZNF23 is a proapoptotic transcription factor and repressor of cell division, therefore its sequestration is probably to halt apoptosis (Soupene et al 2012).

Studies carried in asymptomatic bacteriuria (ABU) strain *E. coli* 83972 revealed genes directly involved in the transcription of RNA polymerase II or its regulating pathways were strongly affected (Lutay et al 2013). Work carried out on Influenza has also highlighted the importance of polymerase II as a target to inhibit antiviral host response. For instance, it is thought binding of viral RNA polymerase to the C-terminal domain of the initiating form of RNA polymerase II might trigger events that are known to be activated during DNA damage, which would make the host degrade Pol II by ubiquitination (Chan et al 2006, Vreede et al 2010), in this way repressing antiviral host responses.

Interfering with transcription of DNA to RNA by RNA polymerase II has also been a target of bacteriophages in an attempt to hijack the host's transcription machinery and direct to serve their own needs (Chevallereau et al 2016, Tagami et al 2014). There is a clear advantage to re-programme the host's transcription by RNA polymerase II. We propose that *Salmonella* binds to ABDH14B, a positive regulator of transcription from RNA polymerase II promoter, in order to stop transcription of genes that are activated during infection and that will pose a threat to *Salmonella*. At this point it is possible to speculate but functional studies would be required to understand which genes are the ones being silenced or modulated by *Salmonella* (Chapter VI, Section 6.12.3, Figure 59).

7.3.3 Cytosolic *Salmonella's* exit mechanisms

A member of the transmembrane 9 superfamily (TM9SF) member, TM9SF3 was identified in this study. These proteins are highly conserved through evolution, where TM9SF1-TM9SF3 can be found in *Drosophila melanogaster*, *Saccharomyces cerevisiae* and *Dictyostelium discoideum* (Benghezal et al 2003, Bergeret et al 2008, Froquet et al 2008), whereas TM9SF1-TM9SF4 are found in mammals and in zebrafish TM9SF1-TM9SF5 (Pruvot et al 2010). Studies carried out in these organisms have shown that these proteins are key for adhesion and phagocytosis in immune response.

TM9SFs consist of a large-cytoplasmic domain and nine putative trans-membrane proteins (Chluba-de Tapia et al 1997). Work carried out in Drosophila shows the role of TM9SF4 in innate immunity, phagocytosis of pathogenic bacteria and adhesion (Bergeret et al 2008). In Dictyostelium and yeast, TM9SF4 (Phg1a) and TM9SF1 (Phg1b) homologs seem to co-regulate adhesion and phagocytosis of *Klebsiella pneumoniae* and *E. coli* (Benghezal et al 2003, 2006, Froquet et al 2012). Also, Drosophila studies have revealed that TM9SF4 is required for internalization of *Candida albicans* (Stroschein-

Stevenson et al 2005). According to further work, *Dictyostelium discoideum* placed phg1A (TM9SF4 homologue) and phg1B proteins as intracellular killers that control the required amount of Kil1 (protein required for efficient protein killing) (Le Coadic et al 2013). Because phg1a and phg1b are divergent members of the TM9 family, analysis of their functions can provide an overall view on the function of TM9 proteins only (Benghezal et al 2003).

Regardless of the above, the biological functions of TM9SF proteins remain largely unknown, especially, for TM9SF3. In cancer, TM9SF3 is overexpressed in chemotherapy-resistant breast cancer cell lines (Chang et al 2011) and in Scirrhous-type gastric cancer (Oo et al 2014). TM9SF4 is also highly expressed in human malignant melanoma cells deriving from metastatic lesions. On the other hand, studies in rat colon have suggested SMBP (TM9SF3's rat homolog) has a role in rat colon relaxation and eosinophil chemotaxis (Sugasawa et al 2001). Further to this, SMBP has been shown to be a unique member of the TM9SF family with functional ligand binding properties, suggesting that some of these integral membrane proteins may function as channels, small molecules transporters or receptors (Sugasawa et al 2001).

Work carried out by Perrin et al (2015) on TM9SF4 studied the mechanisms by which TM9 proteins control surface localization of membrane proteins. Her investigation reinforces the work carried out by Sugasawa et al (2001) in TM9SF3 in placing TM9 proteins as transporters. Without functional studies it is not possible to know what exactly the role of TM9SF3 is in *Salmonella* survival. Still, based on the evidence presented above, we hypothesise *Salmonella* binds to TM9SF3 in an attempt to be transported from the cytosol to the extracellular space (Chapter VI, Section 6.12.2, Figure 58).

7.4 Conclusions

Overall, it was identified in this study that SafA binds to five intracellular proteins from the rat's large intestine (Figure 62). Of these, Bri3bp and RGD1561381 (MGST3-like) are transmembrane proteins located in the endoplasmic reticulum (ER). I speculate that they are both a target of *Salmonella* to modulate mitochondria mediated cell-death and ROS. TM9SF3 is a transmembrane protein likely transporting cargos from the cytosol to the extracellular space (Bergeret et al 2008, Perrin et al 2015). I propose here that *Salmonella* can bind to this protein in order to escape from the cytosol to the extracellular space. Finally, ABDH14B is a cytosolic protein, playing a role in the positive regulation of the RNA polymerase II core promoter to possibly hijack the host and stop the

transcription of defence genes. Serpinb1a is also found in the cytosol and inhibits interleukin elastase to exacerbate neutrophil-mediated cell-death.

The current knowledge on *Salmonella's* intracellular survival is based on studies carried in the *Salmonella*-Containing Vacuole (SCV) (see also Chapter I, Sections 1.4 and 1.5) and little is known about the targets of cytosolic *Salmonella*. The identification of these five proteins advances the information on the intracellular life-style of cytosolic *Salmonella*. It also indicates that the Saf fimbriae might play a role during *Salmonella* infections other than being just an adhesin required for attachment prior to infection. Finally, the study of protein-protein interactions using intestinal proteins is challenging due to the number of contaminants and undigested food present. Therefore, I believe that the adaptation of Universal-BIND™ plates (System 5) capable of performing affinity-enrichments in such difficult lysates is nevertheless a technical achievement.

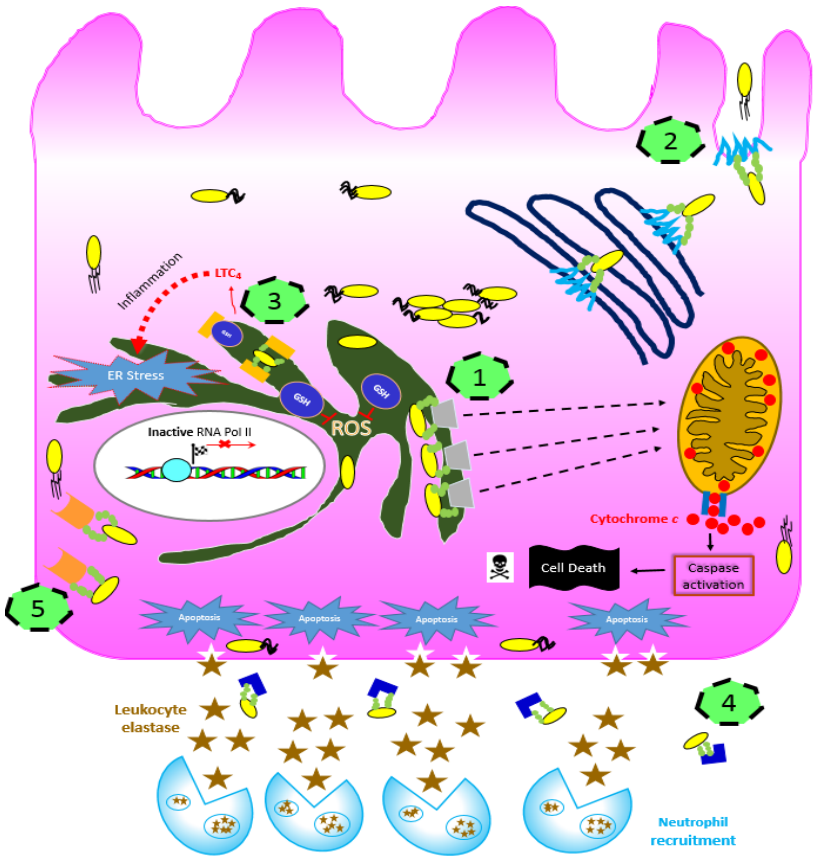

Figure 61. Hypothetical model showing the interaction of cytosolic *Salmonella* with the five identified proteins during its intracellular lifestyle. (1) *Salmonella* binds to Bri3 binding protein (Bri3bp) to modulate mitochondrial cell-death. **(2)** Protein TM9SF3 is used by the bacteria to be localised out of the cell. **(3)** Blocking of protein RGD1561381 by SafA releases GSH to mitigate ROS. **(4)** Leukocyte elastase inhibitors are neutralised by *Salmonella* to disturb the cell homeostasis and encourage host cell destruction by apoptosis. **(5)** Transcription of genes that will lead to bacteria destruction are blocked by sequestering transcriptional regulator ABHD14B protein.

7.5 Future Prospects

While the work carried out provides evidence of specific binding of a number of proteins to *Salmonella enterica Typhimurium* LT2 SafA, the impact of this during infection is not clear. It has been speculated on the putative functions, based on the literature available for other bacteria. Nevertheless, to evaluate this, further functional studies would be required.

Work needs to be done to characterise the pathways adopted by cytosolic *Salmonella* and its interaction(s) with the identified proteins. The first step would be to carry western blots for each of the identified proteins in order to detect the levels of protein present in the affinity-enrichments.

Functional studies would be performed in parallel by using large intestine epithelial cells and in-vivo by infecting animals. For these, both, wild type (WT) *Salmonella Typhimurium* LT2 and a mutant strain lacking the SafA gene would need to be obtained. Further to this, a GFP expression plasmid would be utilized to transform *Salmonella Typhimurium* LT2 for use in immunofluorescence microscopy, to visualize and follow *Salmonella* in live cells. Also, it would be considered that after infection *Salmonella* can remain in the *Salmonella*-Containing Vacuole (SCV) or found free in the cytosol (cytosolic *Salmonella*). Lysosomal membrane proteins 1 and 2 (LAMP1 and LAMP2) are recruited by the SCV and LAMP1 has been established as an SCV marker (Martínez-Lorenzo et al 2001, Roark and Haldar et al 2008). Consequently, we would perform the immunostain with the SCV marker LAMP1, to distinguish between the membrane-bound and cytosolic *Salmonella*.

An alternative to investigate the subcellular location of SafA, would be to transfect cells with plasmids encoding wild type SafA protein and immunostain. There would be a choice of primary antibodies, such as anti-GST-SafA', anti-histidine or anti-GST (although it is best to avoid the latter due to the elevated GSH present in the intestines). Finally, Alexa Fluor secondary antibodies would be used as the fluorescent dye for detection and the specimens examined by confocal microscopy. In addition to all these, it would also be beneficial to immunostain the cell with markers for different organelles to better visualise the compartments where the biological reactions take place.

It would be challenging to study the biological effects of *Salmonella* when binding to each of the identified proteins if all are present simultaneously in the cell. To address this, animal experiments would be advantageous to corroborate if the absence of any of the

identified proteins induces changes that could be observed between the infected mice and the controls. To elaborate further, each target gene would be mutated in embryonic stem cells to generate mutant mice (just one gene would be knocked out at the time). These would be observed throughout for any phenotypic changes or alterations during development, even though no changes are expected until infection. As the analysis progresses, we would decide whether it is deemed necessary to knock out more than one gene at once to fully understand the biological implications.

At present there are no specific studies on TM9SF3 but there are studies in TM9 proteins, such as TM9SF4. In *Dictyostelium*, knocking out of Phga1A (TM9SF4 homologue) has demonstrated the need for Phga1A and other two proteins (Phg1B and SadA) (Perrin et al 2015) for the surface localization of SibA, an integrin β homologue involved in cell adhesion (Cornillon et al 2006). TM9SF4 has also been placed in "tumour cell cannibalism", where the protein was found to play a role in a phagocytosis-based mechanism used by tumour cells to feed from neighbouring cells (Fais and Fauvarque et al 2012). Based on this, there is strong evidence to suggest any knockouts on TM9SF3 would probably affect the localization of receptors similar to integrin. It is my hypothesis that *Salmonella* could bind to TM9SF3 not to block localization of adhesins but to utilize the function of TM9SF3 as a transporter and exploit it to localize itself out of the cell. If the hypothesis is right, the silencing of TM9SF3 would not only decrease the presence of adhesins on the host cell surface but it would also lead to an overpopulation of intracellular *Salmonella* in comparison to suitable controls in WT cells or mutants were TM9SF3 is over-expressed.

As literature is scarce, the knocking out of hydrolase ABDH14B is difficult to predict. In retinal studies, the silencing of RasGRF1 caused transcriptomic modifications where ABDH14A had one of the highest levels of transcriptional inhibition (Fernández-Medarde et al 2009). Also, ABDH proteins have been considered important for lipid metabolism (Lord et al 2013). The function of ABDH14B is to activate transcription. As mentioned in the respective discussion (Chapter VI, Section 6.12.3), host transcription is a popular target for bacteria (Bierne et al 2012, Canonne and Rivas et al 2012). At this stage and with the lack of literature we cannot properly speculate on the effects of knocking out ABDH14B, but the absence of the protein would most likely result in the lack of production of certain bacteria-resistant genes (immune response based genes).

Serpinb1a is a serine protease inhibitor whose role is to maintain balance during the production of leukocyte elastase A released by the neutrophils (Silverman et al 2010). The binding of *Salmonella* to Serpinb1a is probably to break the cell's homeostasis/balance and let it destroy itself to escape. Therefore, the silencing of Serpinb1a would probably result in early cell destruction due to the lack of elastase inhibitor A.

RGD1561381 is a MGST3-like protein part of the MAPEG superfamily (MAPEG) (Jakobsson et al 1997). These transferases are involved in the detoxification of xenobiotics and play a role in the inactivation of secondary metabolites produced during ROS. I speculate that *Salmonella* binds to RGD1561381 to release GSH and mitigate ROS (Chapter VI, Section 6.12.5). Knocking out the protein would probably enhance *Salmonella* survival as we would expect a substantial decrease in ROS production by the host.

Finally, as discussed in Chapter VI, Section 6.12.1, Bri3 binding protein has been established to play a role in ER morphology and mitochondrial cell-death. I presented the hypothesis that *Salmonella* binds to Bri3bp protein in an attempt to block cytochrome *c* release and to halt mitochondrial cell-death of the host. It is also possible that *Salmonella* would target Bri3bp in an effort to disturb the ER cisternae to inactivate the ER and the many stress-related signalling pathways activated by it, such as inflammation and UPR. In addition, it has been proven that suppression of Bri3bp would lead to an overexpression of BCR, triggering the uptake of *Salmonella* by binding to the BCR present on the surface of B-cells, resulting in an immediate antimicrobial humoral response (see Chapter VII, Section 7.3.1). Based on this, knocking out Bri3bp could result in a non-functional ER due to the lack of properly folded cisternae and as a result the cell would probably accumulate toxins, unfolded protein and become an easier target for *Salmonella* infection due to its inability to cope. It is also a possibility that the lack of this protein would affect the expression of BCR (it would probably be up-regulated) and enhance the uptake of *Salmonella*. Because of this, such a knockout, would be easier to infect due to the increase uptake by the BCR.

SUPPLEMENTARY DATA

CHAPTER I – GENERAL INTRODUCTION

Table 19. Putative conserved domains retrieved from BLASTp for SafA and SafD proteins.

Homology (%)	Number of protein homologues retrieved through BLASTp	
	SafA	**SafD**
100	9	100
99.398-96.296	18	0
89.506-87.647	12	0
61.765-60	6	0
59.639-53.289	55	0
Total	100	100

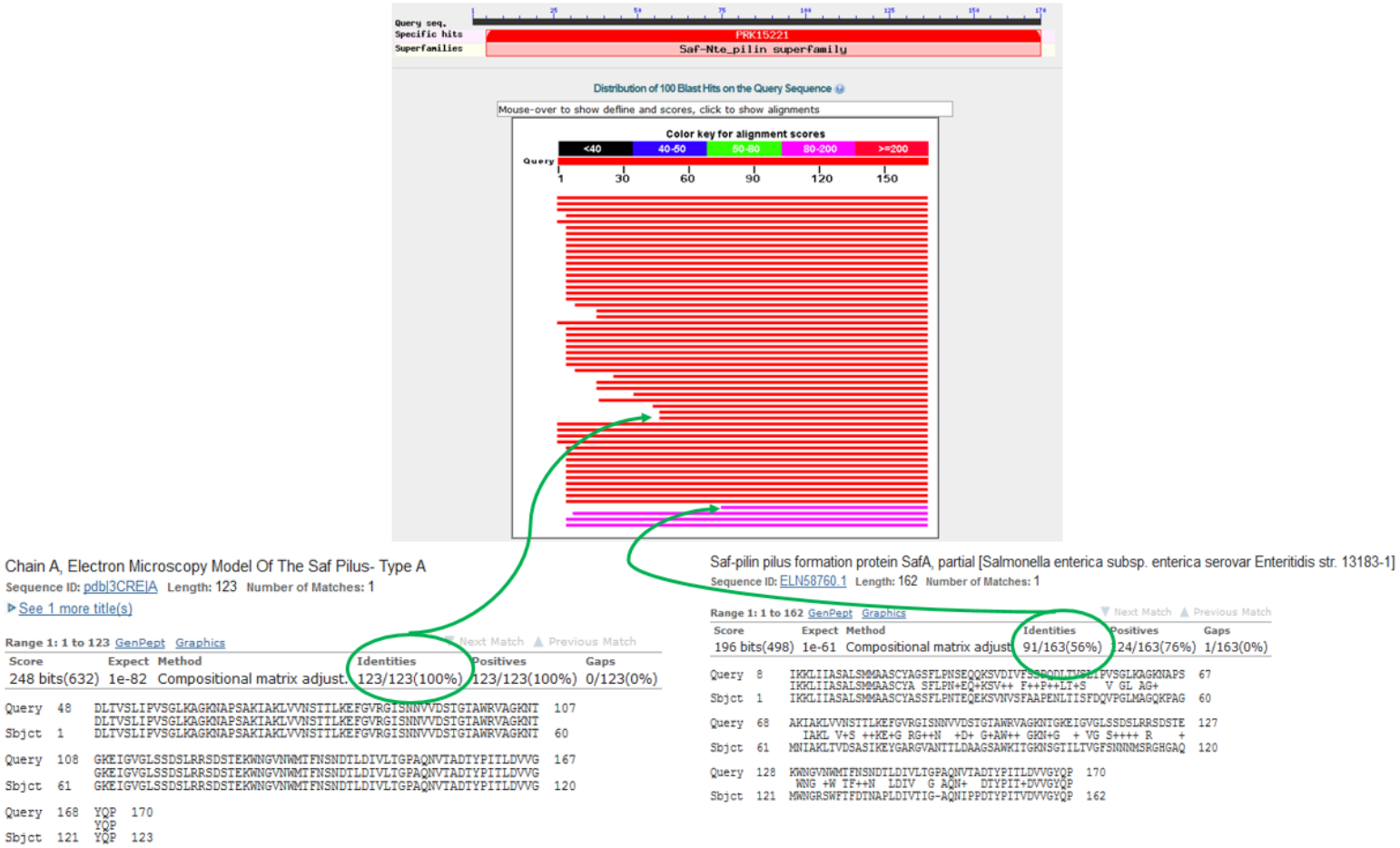

Figure S63. Graphic panel of the NCBI BLASTp results for SafA (UniProt ID Q8ZRK4). Query length is shown at the top of graphic. The colour key matches with the scores, where red representing the high scores, followed by pink, green, blue and black. Sequences found by BLASTp (matches) are presented as horizontal bars.

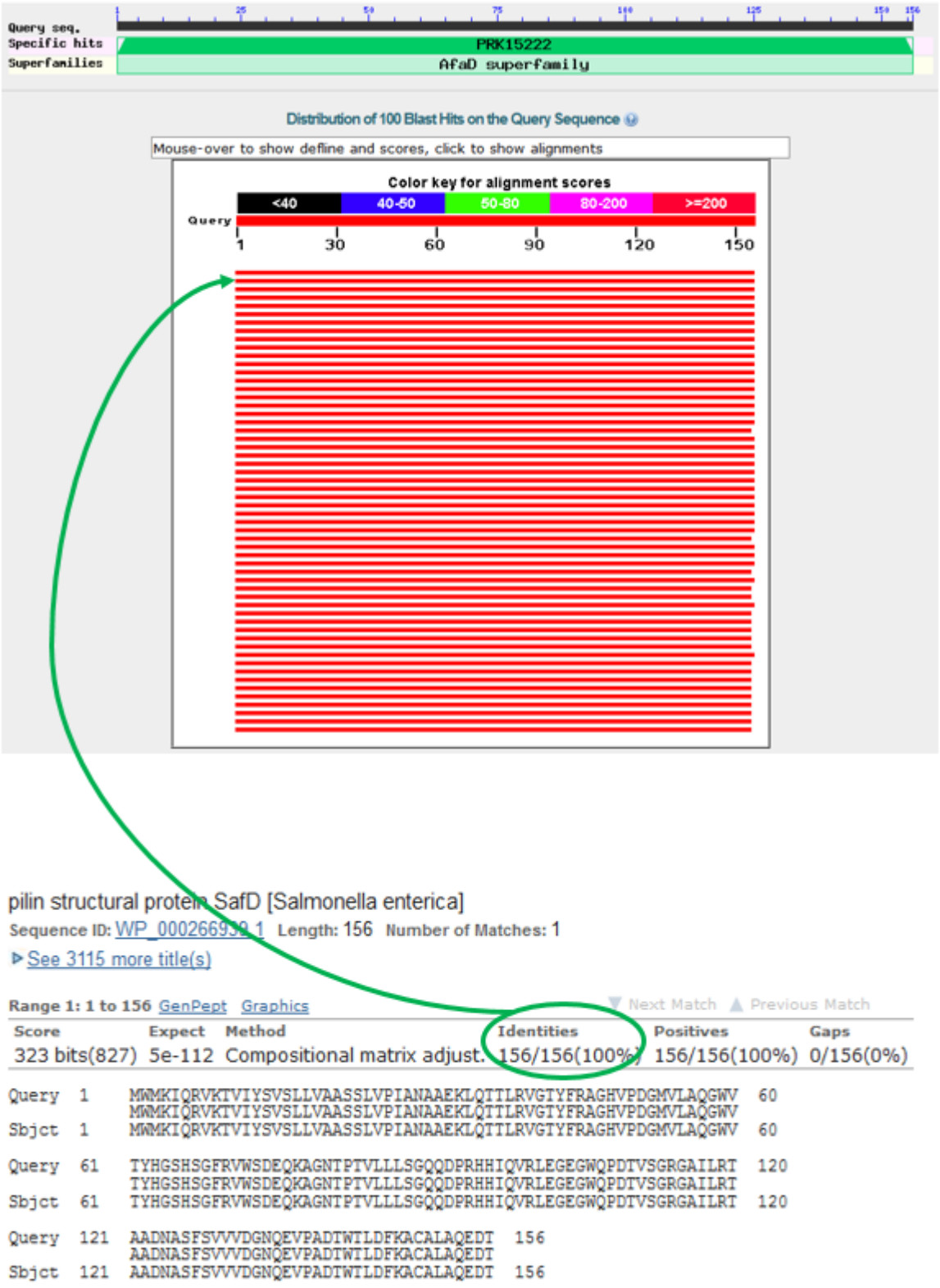

Figure S64.Graphic panel of the NCBI BLASTp results for SafD (UniProt ID Q7CR56). Query length is shown at the top of graphic. The colour key matches with the scores, where red representing the high scores, followed by pink, green, blue and black. Sequences found by BLASTp (matches) are presented as horizontal bars.

CHAPTER VI – MASS SPECTROMETRY ANALYSIS

6.7 Results: nLC-nESI-MS/MS analysis

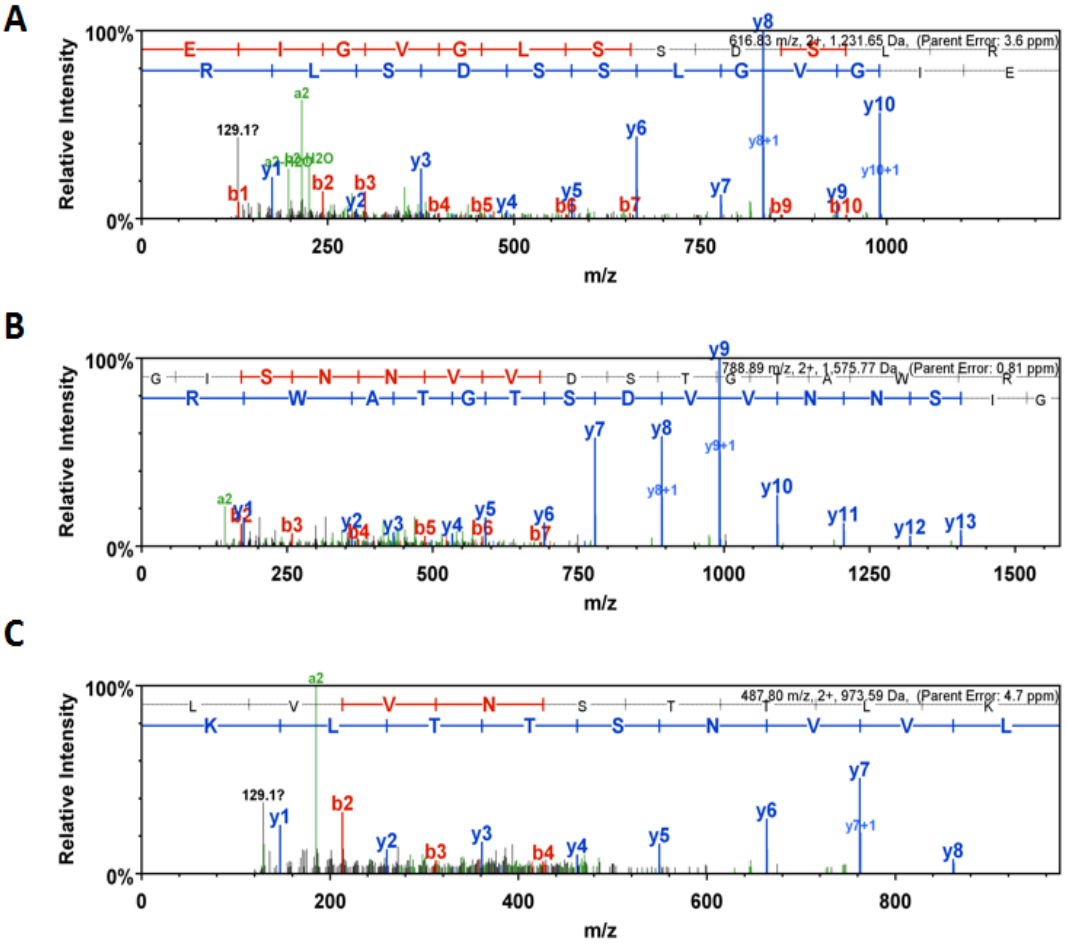

Figure S65. MS/MS spectrum of identified SafA peptides. Panels A-B represent the spectra of peptides identified at 100% to match SafA by Scaffold. All Scaffold data available in the electronic file.

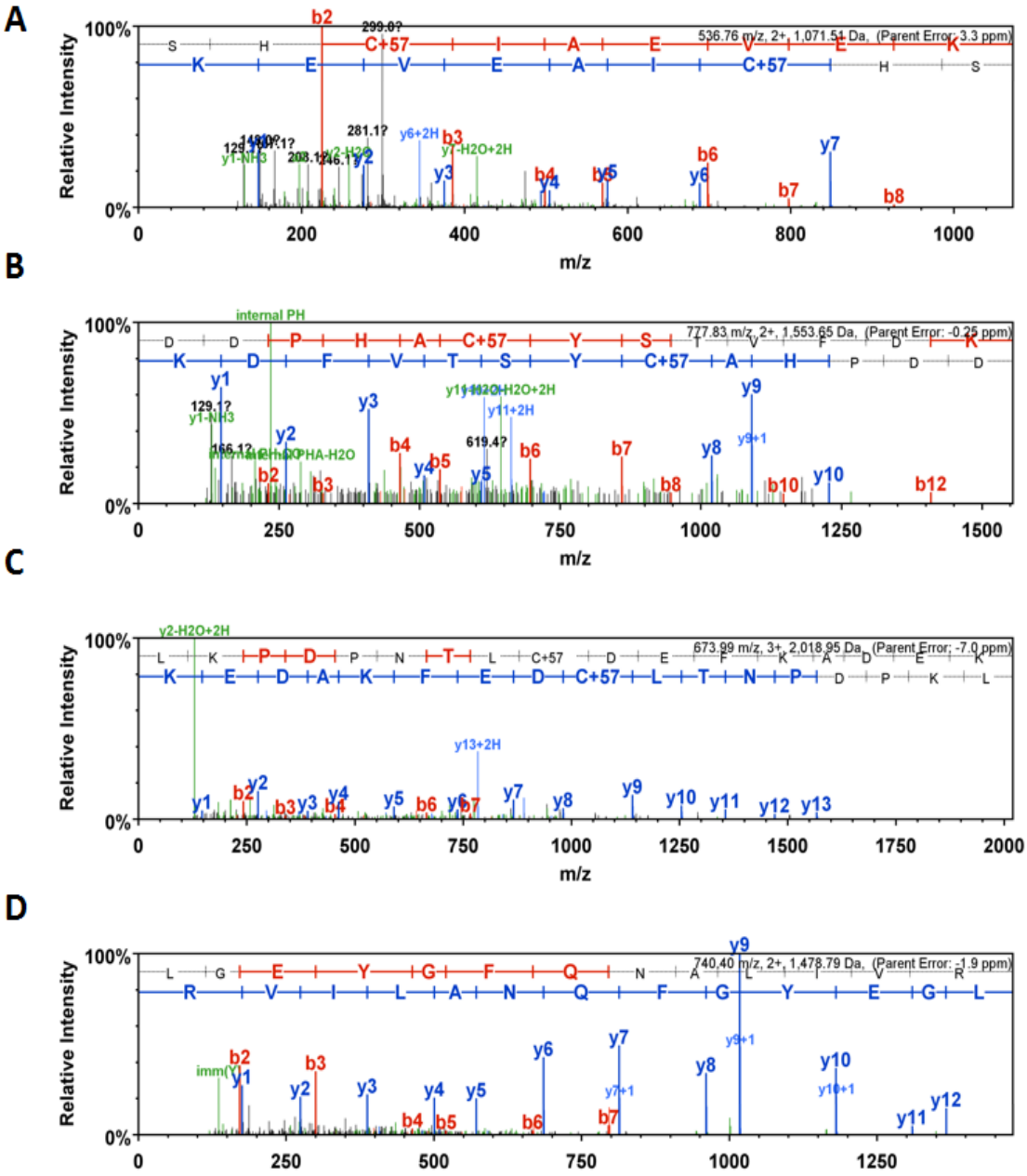

Figure S66. MS/MS spectrum of identified BSA peptides. Panels A-D represent some of the spectra of peptides identified at 100% to match SafA by Scaffold. All Scaffold data available in the electronic file.

References

Aboud L, Ball TB, Tjernlund A and Burgener A (2014) The role of serpin and cystatin antiproteases in mucosal innate immunity and their defense against HIV. *American journal of reproductive immunology (New York, N.Y. : 1989)* 71(1): 12–23.

Aebersold R and Mann M (2003) Mass spectrometry-based proteomics. *Nature*. Nature Publishing Group 422(6928): 198–207.

Ahner A and Brodsky JL (2004) Checkpoints in ER-associated degradation: excuse me, which way to the proteasome? *Trends in cell biology*. Elsevier 14(9): 474–478.

Aichler M and Walch A (2015) MALDI Imaging mass spectrometry: current frontiers and perspectives in pathology research and practice. *Laboratory Investigation*. Nature Publishing Group 95(4): 422–431.

Akopyan K, Edgren T, Wang-Edgren H, Rosqvist R, Fahlgren A, Wolf-Watz H and Fallman M (2011) Translocation of surface-localized effectors in type III secretion. *Proceedings of the National Academy of Sciences of the United States of America* 108(4): 1639–44.

Albuquerque SS, Carret C, Grosso AR, Tarun AS, Peng X, Kappe SH, Prudêncio M and Mota MM (2009) Host cell transcriptional profiling during malaria liver stage infection reveals a coordinated and sequential set of biological events. *BMC genomics*. BioMed Central 10(1): 1.

Alix E, Mukherjee S and Roy CR (2011) Subversion of membrane transport pathways by vacuolar pathogens. *The Journal of cell biology*. Rockefeller Univ Press 195(6): 943–952.

Amavisit P, Lightfoot D, Browning GF and Markham PF (2003) Variation between pathogenic serovars within Salmonella pathogenicity islands. *Journal of bacteriology* 185(12): 3624–35.

Anders JC, Parten BF, Petrie GE, Marlowe RL and McEntire JE (2003) Using amino acid analysis to determine absorptivity constants. *BioPharm International (February)* 2: 30–37.

Anderson KL, Billington J, Pettigrew D, Cota E, Simpson P, Roversi P, Chen HA, Urvil P, du Merle L, Barlow PN, Medof ME, Smith RAG, Nowicki B, Le Bouguénec C, Lea SM and Matthews S (2004) An atomic resolution model for assembly, architecture, and function of the Dr adhesins. *Molecular cell* 15(4): 647–57.

Anderson KL, Cota E, Simpson P, Chen HA, Du Merle L, Bouguénec CL and Matthews S (2004) Letter to the editor: complete resonance assignments of a “donor-strand complemented”AfaE: the afimbrial adhesin from diffusely adherent E. coli. *Journal of biomolecular NMR*. Springer 29(3): 409–410.

Arecco N, Clarke C, Jones F, Simpson D, Mason D, Beynon R and Pisconti A (2016) Elastase levels and activity are increased in dystrophic muscle and impair myoblast cell survival, proliferation and differentiation. *Scientific reports*. Nature Publishing Group 6: 24708.

Aridor M and Hannan LA (2000) Traffic jam: a compendium of human diseases that affect intracellular transport processes. *Traffic (Copenhagen, Denmark)* 1(11): 836–51.

Arkin MR, Glicksman MA, Fu H, Havel JJ and Du Y (2012) Inhibition of protein-protein interactions: non-cellular assay formats. Eli Lilly \& Company and the National Center for Advancing Translational Sciences.

Armstrong JS, Steinauer KK, Hornung B, Irish JM, Lecane P, Birrell GW, Peehl DM and Knox SJ (2002) Role of glutathione depletion and reactive oxygen species generation in apoptotic signaling in a human B lymphoma cell line. *Cell death and differentiation* 9(3): 252–63.

Arnau J, Lauritzen C, Petersen GE and Pedersen J (2006) Current strategies for the use of affinity tags and tag removal for the purification of recombinant proteins. *Protein expression and purification*. Elsevier 48(1): 1–13.

Arranz E, Pena A and Bernardo D (2013) Mediators of inflammation and immune responses in the human gastrointestinal tract. *Mediators Inflamm* 865638.

Ashida H, Kim M, Schmidt-Supprian M, Ma A, Ogawa M and Sasakawa C (2010) A bacterial E3 ubiquitin ligase IpaH9.8 targets NEMO/IKKgamma to dampen the host NF-kappaB-mediated inflammatory response. *Nature cell biology* 12(1): 66–73; sup pp 1–9.

Ashida H and Sasakawa C (2014) Shigella hacks host immune responses by reprogramming the host epigenome. *The EMBO journal*. EMBO Press 33(22): 2598–2600.

Aspholm M, Kalia A, Ruhl S, Schedin S, Arnqvist A, Lindén S, Sjöström R, Gerhard M, Semino-Mora C, Dubois A and others (2006) Helicobacter pylori adhesion to

carbohydrates. *Methods in enzymology*. Elsevier 417: 293–339.

Avila JR, Lee JS and Torii KU (2015) Co-immunoprecipitation of membrane-bound receptors. *The Arabidopsis book/American Society of Plant Biologists*. American Society of Plant Biologists 13.

Baiz CR, Peng CS, Reppert ME, Jones KC and Tokmakoff A (2012) Coherent two-dimensional infrared spectroscopy: quantitative analysis of protein secondary structure in solution. *The Analyst* 137(8): 1793–9.

Baker PR, Agard NJ, Burlingame AL and Chalkley RJ (2010) Quantitative Analysis on the Public Protein Prospector Web Site. *58th ASMS Conference of Mass Spectrometry and Allied Topics*.

Baker PR and Chalkley RJ (2014) MS-viewer: a web-based spectral viewer for proteomics results. *Molecular & Cellular Proteomics*. ASBMB 13(5): 1392–1396.

Bakowski MA, Braun V and Brumell JH (2008) *Salmonella*-containing vacuoles: directing traffic and nesting to grow. *Traffic (Copenhagen, Denmark)* 9(12): 2022–31.

Baldwin MA (2004) Protein identification by mass spectrometry issues to be considered. *Molecular \& Cellular Proteomics*. ASBMB 3(1): 1–9.

Banerjee S and Mazumdar S (2012) Electrospray ionization mass spectrometry: a technique to access the information beyond the molecular weight of the analyte. *International journal of analytical chemistry*. Hindawi Publishing Corporation 2012.

Banga S, Gao P, Shen X, Fiscus V, Zong W-X, Chen L and Luo Z-Q (2007) Legionella pneumophila inhibits macrophage apoptosis by targeting pro-death members of the Bcl2 protein family. *Proceedings of the National Academy of Sciences of the United States of America* 104(12): 5121–6.

Banjerdpongchai R, Kongtawelert P, Khantamat O, Srisomsap C, Chokchaichamnankit D, Subhasitanont P and Svasti J (2010) Mitochondrial and endoplasmic reticulum stress pathways cooperate in zearalenone-induced apoptosis of human leukemic cells. *Journal of hematology & oncology* 3: 50.

Barak JD and Liang AS (2008) Role of soil, crop debris, and a plant pathogen in *Salmonella enterica* contamination of tomato plants. *PloS one* 3(2): e1657.

Bardy SL, Ng SY and Jarrell KF (2003) Prokaryotic motility structures. *Microbiology*. Microbiology Society 149(2): 295–304.

Barnhart MM, Pinkner JS, Soto GE, Sauer FG, Langermann S, Waksman G, Frieden C and Hultgren SJ (2000) PapD-like chaperones provide the missing information for folding of pilin proteins. *Proceedings of the National Academy of Sciences of the United States of America* 97(14): 7709–14.

Barnhart MM, Pinkner JS, Soto GE, Sauer FG, Langermann S, Waksman G, Frieden C and Hultgren SJ (2000) PapD-like chaperones provide the missing information for folding of pilin proteins. *Proceedings of the National Academy of Sciences*. National Acad Sciences 97(14): 7709–7714.

Baumann M, Pham CTN and Benarafa C (2013) SerpinB1 is critical for neutrophil survival through cell-autonomous inhibition of cathepsin G. *Blood* 121(19): 3900–7, S1–6.

Bäumler AJ (1997) The record of horizontal gene transfer in *Salmonella*. *Trends in microbiology*. Elsevier 5(8): 318–322.

Baxt LA, Garza-Mayers AC and Goldberg MB (2013) Bacterial subversion of host innate immune pathways. *Science (New York, N.Y.)* 340(6133): 697–701.

Becherelli M, Manetti AG, Buccato S, Viciani E, Ciucchi L, Mollica G, Grandi G and Margarit I (2012) The ancillary protein 1 of Streptococcus pyogenes FCT-1 pili mediates cell adhesion and biofilm formation through heterophilic as well as homophilic interactions. *Molecular microbiology*. Wiley Online Library 83(5): 1035–1047.

Behnsen J, Jellbauer S, Wong CP, Edwards RA, George MD, Ouyang W and Raffatellu M (2014) The cytokine IL-22 promotes pathogen colonization by suppressing related commensal bacteria. *Immunity* 40(2): 262–73.

Bekkering S and Torensma R (2013) Another look at the life of a neutrophil. *World* 2: 005.

Benarafa C, Priebe GP and Remold-O'Donnell E (2007) The neutrophil serine protease inhibitor serpinb1 preserves lung defense functions in Pseudomonas aeruginosa infection. *The Journal of experimental medicine*. Rockefeller Univ Press 204(8): 1901–1909.

Benelmekki M, Xuriguera E, Caparros C, Rodr'\iguez-Carmona E, Mendoza R, Corchero J, Lanceros-Mendez S and Martinez LM (2012) Design and characterization of Ni 2+ and Co 2+ decorated Porous Magnetic Silica spheres synthesized by hydrothermal-assisted modified-Stöber method for His-tagged proteins separation. *Journal of colloid and interface science*. Elsevier 365(1): 156–162.

Benghezal M, Cornillon S, Gebbie L, Alibaud L, Brückert F, Letourneur F and Cosson P (2003) Synergistic control of cellular adhesion by transmembrane 9 proteins. *Molecular biology of the cell*. Am Soc Cell Biol 14(7): 2890–2899.

Benghezal M, Fauvarque M-O, Tournebize R, Froquet R, Marchetti A, Bergeret E, Lardy B, Klein G, Sansonetti P, Charette SJ and others (2006) Specific host genes required for the killing of Klebsiella bacteria by phagocytes. *Cellular microbiology*. Wiley Online Library 8(1): 139–148.

Berdygulova Z, Esyunina D, Miropolskaya N, Mukhamedyarov D, Kuznedelov K, Nickels BE, Severinov K, Kulbachinskiy A and Minakhin L (2012) A novel phage-encoded transcription antiterminator acts by suppressing bacterial RNA polymerase pausing. *Nucleic acids research* 40(9): 4052–63.

Bereswill S, Muñoz M, Fischer A, Plickert R, Haag L-M, Otto B, Kühl AA, Loddenkemper C, Göbel UB and Heimesaat MM (2010) Anti-inflammatory effects of resveratrol, curcumin and simvastatin in acute small intestinal inflammation. *PloS one*. Public Library of Science 5(12): e15099.

Bergeret E, Perrin J, Williams M, Grunwald D, Engel E, Thevenon D, Taillebourg E, Bruckert F, Cosson P and Fauvarque M-O (2008) TM9SF4 is required for Drosophila cellular immunity via cell adhesion and phagocytosis. *Journal of cell science*. The Company of Biologists Ltd 121(20): 3325–3334.

Berry AA, Yang Y, Pakharukova N, Garnett JA, Lee W, Cota E, Marchant J, Roy S, Tuittila M, Liu B and others (2014) Structural insight into host recognition by aggregative adherence fimbriae of enteroaggregative Escherichia coli. *PLoS Pathog*. Public Library of Science 10(9): e1004404.

Bertsch A, Leinenbach A, Pervukhin A, Lubeck M, Hartmer R, Baessmann C, Elnakady YA, Müller R, Böcker S, Huber CG and others (2009) De novo peptide sequencing by tandem MS using complementary CID and electron transfer dissociation. *Electrophoresis*. Wiley Online Library 30(21): 3736–3747.

Beuzón CR, Méresse S, Unsworth KE, Ruíz-Albert J, Garvis S, Waterman SR, Ryder TA, Boucrot E and Holden DW (2000) *Salmonella* maintains the integrity of its intracellular vacuole through the action of SifA. *The EMBO journal*. EMBO Press 19(13): 3235–3249.

Beuzón CR, Salcedo SP and Holden DW (2002) Growth and killing of a *Salmonella enterica* serovar Typhimurium sifA mutant strain in the cytosol of different host cell lines. *Microbiology*. Microbiology Society 148(9): 2705–2715.

Bhattacharyya A, Chattopadhyay R, Mitra S and Crowe SE (2014) Oxidative stress: an essential factor in the pathogenesis of gastrointestinal mucosal diseases. *Physiological reviews*. Am Physiological Soc 94(2): 329–354.

Biçak N, Senkal BF and Yarbas T (1998) Crosslinked poly (styrenesulfonamide) with iminoacetic acid chelating groups for hard-water treatment. *Macromolecular Chemistry and Physics* 199(12): 2731–2735.

Bierne H, Hamon M and Cossart P (2012) Epigenetics and bacterial infections. *Cold Spring Harbor perspectives in medicine*. Cold Spring Harbor Laboratory Press 2(12): a010272.

Biesiadecki BJ and Jin J-P (2011) A high-throughput solid-phase microplate protein-binding assay to investigate interactions between myofilament proteins. *BioMed Research International*. Hindawi Publishing Corporation 2011.

Biniossek ML and Schilling O (2012) Enhanced identification of peptides lacking basic residues by LC-ESI-MS/MS analysis of singly charged peptides. *Proteomics* 12(9): 1303–9.

Biotech AP (2000) The recombinant protein handbook: protein amplification and simple purification. *AA Edition, Amersham Pharmacia Biotech AB: Sweden*.

Bjorndahl TC, Andrew LC, Semenchenko V and Wishart DS (2007) NMR solution structures of the apo and peptide-inhibited human rhinovirus 3C protease (Serotype 14): structural and dynamic comparison. *Biochemistry*. ACS Publications 46(45): 12945–12958.

Blader IJ and Saeij JP (2009) Communication between Toxoplasma gondii and its host: impact on parasite growth, development, immune evasion, and virulence. *Apmis*. Wiley Online Library 117(5-6): 458–476.

Blanc-Potard AB, Solomon F, Kayser J and Groisman EA (1999) The SPI-3 pathogenicity island of *Salmonella enterica*. *Journal of bacteriology* 181(3): 998–1004.

Block H, Maertens B, Spriestersbach A, Brinker N, Kubicek J, Fabis R, Labahn J and Schäfer F (2009) Immobilized-metal affinity chromatography (IMAC): a review. *Methods in enzymology* 463: 439–73.

Blondel CJ, Jiménez JC, Contreras I and Santiviago CA (2009) Comparative genomic analysis uncovers 3 novel loci encoding type six secretion systems differentially distributed in *Salmonella* serotypes. *BMC genomics*. BioMed Central 10(1): 1.

Bodelón G, Palomino C and Fernández LÁ (2013) Immunoglobulin domains in Escherichia coli and other enterobacteria: from pathogenesis to applications in antibody technologies. *FEMS microbiology reviews*. The Oxford University Press 37(2): 204–250.

Boleij A, Laarakkers CM, Gloerich J, Swinkels DW and Tjalsma H (2011) Surface-affinity profiling to identify host-pathogen interactions. *Infection and immunity* 79(12): 4777–83.

Bonazzi M and Cossart P (2006) Bacterial entry into cells: a role for the endocytic machinery. *FEBS letters* 580(12): 2962–7.

Bornhorst JA and Falke JJ (2000) Purification of proteins using polyhistidine affinity tags. *Methods in enzymology* 326: 245–54.

Boumart Z, Velge P and Wiedemann A (2014) Multiple invasion mechanisms and different intracellular Behaviors: a new vision of *Salmonella*-host cell interaction. *FEMS microbiology letters*. The Oxford University Press 361(1): 1–7.

Bradshaw RA, Burlingame AL, Carr S and Aebersold R (2006) Reporting protein identification data the next generation of guidelines. *Molecular \& Cellular Proteomics*. ASBMB 5(5): 787–788.

Bramanti E, Benedetti E, Nicolini C, Berzina T, Erokhin V, D'Alessio A and Benedetti E (1997) Qualitative and quantitative analysis of the secondary structure of cytochrome C Langmuir-Blodgett films. *Biopolymers* 42(2): 227–37.

Bravo-Sagua R, Rodriguez AE, Kuzmicic J, Gutierrez T, Lopez-Crisosto C, Quiroga C, Díaz-Elizondo J, Chiong M, Gillette TG, Rothermel BA and Lavandero S (2013) Cell death and survival through the endoplasmic reticulum-mitochondrial axis. *Current molecular medicine* 13(2): 317–29.

Brennan MA and Cookson BT (2000) *Salmonella* induces macrophage death by caspase-1-dependent necrosis. *Molecular microbiology* 38(1): 31–40.

Brenner F, Villar R, Angulo F, Tauxe R and Swaminathan B (2000) *Salmonella* nomenclature. *Journal of clinical microbiology*. Am Soc Microbiol 38(7): 2465–2467.

Bresell A, Weinander R, Lundqvist G, Raza H, Shimoji M, Sun T-H, Balk L, Wiklund R, Eriksson J, Jansson C, Persson B, Jakobsson P-J and Morgenstern R (2005) Bioinformatic and enzymatic characterization of the MAPEG superfamily. *The FEBS journal* 272(7): 1688–703.

Bresser J, Hubbell HR and Gillespie D (1983) Biological activity of mRNA immobilized on nitrocellulose in NaI. *Proceedings of the National Academy of Sciences*. National Acad Sciences 80(21): 6523–6527.

Brown NF, Vallance BA, Coombes BK, Valdez Y, Coburn BA and Finlay BB (2005) *Salmonella* pathogenicity island 2 is expressed prior to penetrating the intestine. *PLoS Pathog*. Public Library of Science 1(3): e32.

Broz P, Ohlson MB and Monack DM (2012) Innate immune response to *Salmonella* typhimurium, a model enteric pathogen. *Gut microbes*. Taylor \& Francis 3(2): 62–70.

Brumell JH, Goosney DL and Finlay BB (2002) SifA, a Type III Secreted Effector of *Salmonella* typhimurium, Directs *Salmonella*-Induced Filament (Sif) Formation Along Microtubules. *Traffic*. Wiley Online Library 3(6): 407–415.

Brumell JH and Grinstein S (2004) *Salmonella* redirects phagosomal maturation. *Current opinion in microbiology*. Elsevier 7(1): 78–84.

Brunet J, Pfaff AW, Abidi A, Unoki M, Nakamura Y, Guinard M, Klein J-P, Candolfi E and Mousli M (2008) Toxoplasma gondii exploits UHRF1 and induces host cell cycle arrest at G2 to enable its proliferation. *Cellular microbiology* 10(4): 908–20.

Brymora A, Valova VA and Robinson PJ (2004) Protein-Protein Interactions Identified by Pull-Down Experiments and Mass Spectrometry. *Current protocols in cell biology*. Wiley Online Library 17–5.

Buchmann K (2015) Evolution of innate immunity: clues from invertebrates via fish to mammals. *M1/M2 Macrophages: The Arginine Fork in the Road to Health and Disease*. Frontiers Media SA 23.

Buchwalow I, Samoilova V, Boecker W and Tiemann M (2011) Non-specific binding of antibodies in immunohistochemistry: fallacies and facts. *Scientific reports*. Nature Publishing Group 1: 28.

Bürck J, Roth S, Windisch D, Wadhwani P, Moss D and Ulrich AS (2015) UV-CD12: synchrotron radiation circular dichroism beamline at ANKA. *Journal of synchrotron radiation*. International Union of Crystallography 22(3): 844–852.

Busch A and Waksman G (2012) Chaperone-usher pathways: diversity and pilus assembly mechanism. *Phil. Trans. R. Soc. B*. The Royal Society 367(1592): 1112–1122.

Büttner D (2012) Protein export according to schedule: architecture, assembly, and regulation of type III secretion systems from plant-and animal-pathogenic bacteria. *Microbiology and Molecular Biology Reviews*. Am Soc Microbiol 76(2): 262–310.

Byrum RS, Goulet JL, Griffiths RJ and Koller BH (1997) Role of the 5-lipoxygenase-activating protein (FLAP) in murine acute inflammatory responses. *The Journal of experimental medicine* 185(6): 1065–75.

Cai X, Wang R, Filloux A, Waksman G and Meng G (2011) Structural and functional characterization of Pseudomonas aeruginosa CupB chaperones. *PloS one*. Public Library of Science 6(1): e16583.

Calmes B, Morel-Rouhier M, Bataillé-Simoneau N, Gelhaye E, Guillemette T and Simoneau P (2015) Characterization of glutathione transferases involved in the pathogenicity of Alternaria brassicicola. *BMC microbiology*. BioMed Central Ltd 15(1): 123.

Cañas B, López-Ferrer D, Ramos-Fernández A, Camafeita E and Calvo E (2006) Mass spectrometry technologies for proteomics. *Briefings in functional genomics \& proteomics*. Oxford University Press 4(4): 295–320.

Canonne J and Rivas S (2012) Bacterial effectors target the plant cell nucleus to subvert host transcription. *Plant signaling \& behavior*. Taylor \& Francis 7(2): 217–221.

Cao G, Allard M, Strain E, Stones R, Zhao S, Brown E and Meng J (2014) Genetic diversity of *Salmonella* pathogenicity islands SPI-5 and SPI-6 in *Salmonella* Newport. *Foodborne pathogens and disease*. Mary Ann Liebert, Inc. 140 Huguenot Street, 3rd Floor New Rochelle, NY 10801 USA 11(10): 798–807.

Carey AJ, Tan CK and Ulett GC (2012) Infection-induced IL-10 and JAK-STAT: A review of the molecular circuitry controlling immune hyperactivity in response to pathogenic microbes. *JAK-STAT*. Taylor \& Francis 1(3): 159–167.

Carlyon JA, Latif DA, Pypaert M, Lacy P and Fikrig E (2004) Anaplasma phagocytophilum utilizes multiple host evasion mechanisms to thwart NADPH oxidase-mediated killing during neutrophil infection. *Infection and immunity*. Am Soc Microbiol 72(8): 4772–4783.

Carneiro DG, Clarke T, Davies CC and Bailey D (2016) Identifying novel protein interactions: Proteomic methods, optimisation approaches and data analysis pipelines. *Methods*. Elsevier 95: 46–54.

Carr S, Aebersold R, Baldwin M, Burlingame A, Clauser K and Nesvizhskii A (2004) The need for guidelines in publication of peptide and protein identification data working group on publication guidelines for peptide and protein identification data. *Molecular \& Cellular Proteomics*. ASBMB 3(6): 531–533.

Cascales E (2008) The type VI secretion toolkit. *EMBO reports*. EMBO Press 9(8): 735–741.

Cech NB and Enke CG (2001) Practical implications of some recent studies in electrospray ionization fundamentals. *Mass Spectrometry Reviews*. Wiley Online Library 20(6): 362–387.

Celli J and Tsolis RM (2015) Bacteria, the endoplasmic reticulum and the unfolded protein response: friends or foes? *Nature Reviews Microbiology*. Nature Publishing Group 13(2): 71–82.

Chan AY, Vreede FT, Smith M, Engelhardt OG and Fodor E (2006) Influenza virus inhibits RNA polymerase II elongation. *Virology* 351(1): 210–7.

Chang H, Jeung H-C, Jung JJ, Kim TS, Rha SY and Chung HC (2011) Identification of genes associated with chemosensitivity to SAHA/taxane combination treatment in taxane-resistant breast cancer cells. *Breast cancer research and treatment*. Springer 125(1): 55–63.

Chen JH, Yam W-C, Ngan AH, Fung AM, Woo W-L, Yan M-K, Choi GK, Ho P-L, Cheng VC and Yuen K-Y (2013) Advantages of using MALDI-TOF mass spectrometry as a rapid diagnostic tool for yeast and mycobacteria identification in clinical microbiological laboratory. *Journal of clinical microbiology*. Am Soc Microbiol JCM–01437.

Cheung RCF, Wong JH and Ng TB (2012a) Immobilized metal ion affinity chromatography: a review on its applications. *Applied microbiology and biotechnology* 96(6): 1411–20.

Cheung RCF, Wong JH and Ng TB (2012b) Immobilized metal ion affinity chromatography: a review on its applications. *Applied microbiology and biotechnology*. Springer 96(6): 1411–1420.

Chevallereau A, Blasdel BG, De Smet J, Monot M, Zimmermann M, Kogadeeva M, Sauer U, Jorth P, Whiteley M, Debarbieux L and others (2016) Next-Generation "-omics" Approaches Reveal a Massive Alteration of Host RNA Metabolism during Bacteriophage Infection of Pseudomonas aeruginosa. *PLoS Genet*. Public Library of Science 12(7): e1006134.

Chluba-de Tapia J, de Tapia M, Jäggin V and Eberle AN (1997) Cloning of a human multispanning membrane protein cDNA: evidence for a new protein family. *Gene* 197(1-2): 195–204.

Choudhury D, Thompson A, Stojanoff V, Langermann S, Pinkner J, Hultgren SJ and Knight SD (1999) X-ray structure of the FimC-FimH chaperone-adhesin complex from uropathogenic Escherichia coli. *Science*. American Association for the Advancement of Science 285(5430): 1061–1066.

Chu KY, Lee S, Tsai M-T, Lu I-C, Dyakov YA, Lai YH, Lee Y-T and Ni C-K (2014) Thermal proton transfer reactions in ultraviolet matrix-assisted laser desorption/ionization. *Journal of the American Society for Mass Spectrometry* 25(3): 310–8.

Chutipongtanate S, Changtong C, Weeraphan C, Hongeng S, Srisomsap C and Svasti J (2015) Syringe-push membrane absorption as a simple rapid method of urine preparation for clinical proteomics. *Clinical proteomics*. BioMed Central 12(1): 1.

Clark CS and Maurelli AT (2007) Shigella flexneri inhibits staurosporine-induced apoptosis in epithelial cells. *Infection and immunity*. Am Soc Microbiol 75(5): 2531–2539.

Le Coadic M, Froquet R, Lima WC, Dias M, Marchetti A and Cosson P (2013) Phg1/TM9 proteins control intracellular killing of bacteria by determining cellular levels of the Kil1 sulfotransferase in Dictyostelium. *PloS one*. Public Library of Science 8(1): e53259.

Cobo F (2013) Application of maldi-tof mass spectrometry in clinical virology: a review. *The open virology journal* 7(1).

Coburn B, Sekirov I and Finlay BB (2007) Type III secretion systems and disease. *Clinical microbiology reviews*. Am Soc Microbiol 20(4): 535–549.

Cordingley MG, Callahan PL, Sardana VV, Garsky VM and Colonno RJ (1990) Substrate requirements of human rhinovirus 3C protease for peptide cleavage in vitro. *The Journal of biological chemistry* 265(16): 9062–5.

Cornelis GR (2006) The type III secretion injectisome. *Nature Reviews Microbiology*. Nature Publishing Group 4(11): 811–825.

Cornillon S, Gebbie L, Benghezal M, Nair P, Keller S, Wehrle-Haller B, Charette SJ, Brückert F, Letourneur F and Cosson P (2006) An adhesion molecule in free-living Dictyostelium amoebae with integrin beta features. *EMBO reports*. EMBO Press 7(6): 617–621.

Cornillon S, Pech E, Benghezal M, Ravanel K, Gaynor E, Letourneur F, Brückert F and Cosson P (2000) Phg1p is a nine-transmembrane protein superfamily member involved in dictyostelium adhesion and phagocytosis. *The Journal of biological chemistry* 275(44): 34287–92.

Costa S, Almeida A, Castro A and Domingues L (2014) Fusion tags for protein solubility, purification, and immunogenicity in Escherichia coli: the novel Fh8 system. *Recombinant protein expression in microbial systems*. Frontiers E-books 24.

Cota E, Jones C, Simpson P, Altroff H, Anderson KL, du Merle L, Guignot J, Servin A, Le Bouguénec C, Mardon H and Matthews S (2006) The solution structure of the invasive tip complex from Afa/Dr fibrils. *Molecular microbiology* 62(2): 356–66.

Cottrell JS (2011) Protein identification using MS/MS data. *Journal of proteomics* 74(10): 1842–51.

Cottrell JS and London U (1999) Probability-based protein identification by searching sequence databases using mass spectrometry data. *electrophoresis* 20(18): 3551–3567.

Cox JT, Marginean I, Kelly RT, Smith RD and Tang K (2014) Improving the sensitivity of mass spectrometry by using a new sheath flow electrospray emitter array at subambient pressures. *Journal of The American Society for Mass Spectrometry*. Springer 25(12): 2028–2037.

Creasey EA and Isberg RR (2014) Maintenance of vacuole integrity by bacterial pathogens. *Current opinion in microbiology*. Elsevier 17: 46–52.

Cretich M, Sedini V, Damin F, Pelliccia M, Sola L and Chiari M (2010) Coating of nitrocellulose for colorimetric DNA microarrays. *Analytical biochemistry* 397(1): 84–8.

Croken MM, Nardelli SC and Kim K (2012) Chromatin modifications, epigenetics, and how protozoan parasites regulate their lives. *Trends in parasitology* 28(5): 202–13.

Crowe J, Masone BS and Ribbe J (1996) One-step purification of recombinant proteins with the 6xHis tag and Ni-NTA resin. *Basic DNA and RNA Protocols*. Springer 491–510.

Csordás G, Renken C, Várnai P, Walter L, Weaver D, Buttle KF, Balla T, Mannella CA and Hajnóczky G (2006) Structural and functional features and significance of the physical linkage between ER and mitochondria. *The Journal of cell biology*. Rockefeller Univ Press 174(7): 915–921.

Cui J, Yao Q, Li S, Ding X, Lu Q, Mao H, Liu L, Zheng N, Chen S and Shao F (2010) Glutamine deamidation and dysfunction of ubiquitin/NEDD8 induced by a bacterial effector family. *Science (New York, N.Y.)* 329(5996): 1215–8.

Cunningham-Rundles C and Ponda PP (2005) Molecular defects in T-and B-cell primary immunodeficiency diseases. *Nature reviews immunology*. Nature Publishing Group 5(11): 880–892.

Damodaran S, Wood TD, Nagarajan P and Rabin RA (2007) Evaluating peptide mass fingerprinting-based protein identification. *Genomics, proteomics & bioinformatics* 5(3-4): 152–7.

Daviter T and Fronzes R (2013) Protein sample characterization. *Protein-Ligand Interactions: Methods and Applications*. Springer 35–62.

Deiwick J, Salcedo SP, Boucrot E, Gilliland SM, Henry T, Petermann N, Waterman SR, Gorvel J-P, Holden DW and Méresse S (2006) The translocated *Salmonella* effector proteins SseF and SseG interact and are required to establish an intracellular replication niche. *Infection and immunity*. Am Soc Microbiol 74(12): 6965–6972.

DeLeo F (2004) Modulation of phagocyte apoptosis by bacterial pathogens. *Apoptosis*. Springer 9(4): 399–413.

DelProposto J, Majmudar CY, Smith JL and Brown WC (2009) Mocr: a novel fusion tag for enhancing solubility that is compatible with structural biology applications. *Protein expression and purification* 63(1): 40–9.

Deng Y, Srivastava R and Howell SH (2013) Endoplasmic Reticulum (ER) Stress Response and Its Physiological Roles in Plants. *International journal of molecular sciences* 14(4): 8188–212.

Denic V, Quan EM and Weissman JS (2006) A luminal surveillance complex that selects misfolded glycoproteins for ER-associated degradation. *Cell* 126(2): 349–59.

Dewoody RS, Merritt PM and Marketon MM (2014) Regulation of the Yersinia type III secretion system: traffic control. *The pathogenic Yersiniae-advances in the understanding of physiology and virulence*. Frontiers E-books 31.

Diaz-Ochoa VE, Jellbauer S, Klaus S and Raffatellu M (2015) Transition metal ions at the crossroads of mucosal immunity and microbial pathogenesis. *Metal economy in host-microbe interactions*. Frontiers Media SA 8.

Dickinson JL, Norris BJ, Jensen PH and Antalis TM (1998) The CD interhelical domain of the serpin plasminogen activator inhibitor-type 2 is required for protection from TNF- induced apoptosis. *Cell death and differentiation*. London: Edward Arnold, c1994- 5(2): 163–171.

Ding Y, Choi H and Nesvizhskii AI (2008) Adaptive discriminant function analysis and reranking of MS/MS database search results for improved peptide identification in shotgun proteomics. *Journal of proteome research*. ACS Publications 7(11): 4878–4889.

Doherty GJ and McMahon HT (2009) Mechanisms of endocytosis. *Annual review of biochemistry*. Annual Reviews 78: 857–902.

Dong F, Pirbhai M, Xiao Y, Zhong Y, Wu Y and Zhong G (2005) Degradation of the proapoptotic proteins Bik, Puma, and Bim with Bcl-2 domain 3 homology in Chlamydia trachomatis-infected cells. *Infection and immunity*. Am Soc Microbiol 73(3): 1861–1864.

Dong Geun Leea 1 So Young Anb 1 Min Seop Umd Woo Jin Choid Seung Man Nohc Hyun Wook Junga Jung Kwon Ohb (2016) Photo-induced thiol-ene crosslinked

polymethacrylate networks reinforced with Al2O3 nanoparticles. *Polymer*.

Du Z-X, Zhang H-Y, Meng X, Guan Y and Wang H-Q (2009) Role of oxidative stress and intracellular glutathione in the sensitivity to apoptosis induced by proteasome inhibitor in thyroid cancer cells. *BMC cancer*. BioMed Central 9(1): 1.

Dunham WH, Mullin M and Gingras A-C (2012) Affinity-purification coupled to mass spectrometry: basic principles and strategies. *Proteomics* 12(10): 1576–90.

Dunkelberger JR and Song W-C (2010) Complement and its role in innate and adaptive immune responses. *Cell research*. Nature Publishing Group 20(1): 34–50.

Duong-Ly KC and Gabelli SB (2015) Chapter Two-Affinity Purification of a Recombinant Protein Expressed as a Fusion with the Maltose-Binding Protein (MBP) Tag. *Methods in enzymology*. Elsevier 559: 17–26.

Duraisingham S, Manson A, Grigoriadou S, Buckland M, Tong C and Longhurst H (2015) Immune deficiency: changing spectrum of pathogens. *Clinical & Experimental Immunology*. Wiley Online Library 181(2): 267–274.

Dvash E, Har-Tal M, Barak S, Meir O and Rubinstein M (2015) Leukotriene C4 is the major trigger of stress-induced oxidative DNA damage. *Nature communications*. Nature Publishing Group 6.

Dyson HJ and Wright PE (2005) Intrinsically unstructured proteins and their functions. *Nature reviews Molecular cell biology*. Nature Publishing Group 6(3): 197–208.

Egnatchik RA, Leamy AK, Jacobson DA, Shiota M and Young JD (2014) ER calcium release promotes mitochondrial dysfunction and hepatic cell lipotoxicity in response to palmitate overload. *Molecular metabolism* 3(5): 544–53.

El-Aneed A, Cohen A and Banoub J (2009) Mass spectrometry, review of the basics: electrospray, MALDI, and commonly used mass analyzers. *Applied Spectroscopy Reviews*. Taylor & Francis 44(3): 210–230.

Elias JE, Haas W, Faherty BK and Gygi SP (2005) Comparative evaluation of mass spectrometry platforms used in large-scale proteomics investigations. *Nature methods* 2(9): 667–75.

Elsaraj SM and Bhullar RP (2008) Regulation of platelet Rac1 and Cdc42 activation through interaction with calmodulin. *Biochimica et Biophysica Acta (BBA)-Molecular Cell Research*. Elsevier 1783(5): 770–778.

Endo Y, Hirahara K, Yagi R, Tumes DJ and Nakayama T (2014) Pathogenic memory type Th2 cells in allergic inflammation. *Trends in immunology*. Elsevier 35(2): 69–78.

Eriksson J, Chait BT and Fenyö D (2000) A statistical basis for testing the significance of mass spectrometric protein identification results. *Analytical chemistry*. ACS Publications 72(5): 999–1005.

Eswarappa SM, Negi VD, Chakraborty S, Sagar BC and Chakravortty D (2010) Division of the *Salmonella*-containing vacuole and depletion of acidic lysosomes in *Salmonella*-infected host cells are novel strategies of *Salmonella enterica* to avoid lysosomes. *Infection and immunity*. Am Soc Microbiol 78(1): 68–79.

Faherty CS and Maurelli AT (2008) Staying alive: bacterial inhibition of apoptosis during infection. *Trends in microbiology* 16(4): 173–80.

Fais S and Fauvarque M-O (2012) TM9 and cannibalism: how to learn more about cancer by studying amoebae and invertebrates. *Trends in molecular medicine*. Elsevier 18(1): 4–5.

Fan T, Lu H, Hu H, Shi L, McClarty GA, Nance DM, Greenberg AH and Zhong G (1998) Inhibition of apoptosis in chlamydia-infected cells: blockade of mitochondrial cytochrome c release and caspase activation. *The Journal of experimental medicine* 187(4): 487–96.

Fang FC (2011) Antimicrobial actions of reactive oxygen species. *MBio*. American Society for Microbiology (ASM) 2(5): e00141–11.

Fernández-Medarde A, Barhoum R, Riquelme R, Porteros A, Núñez A, De Luis A, De Las Rivas J, De La Villa P, Varela-Nieto I and Santos E (2009) RasGRF1 disruption causes retinal photoreception defects and associated transcriptomic alterations. *Journal of neurochemistry*. Wiley Online Library 110(2): 641–652.

Fíla J and Honys D (2012) Enrichment techniques employed in phosphoproteomics. *Amino acids* 43(3): 1025–47.

Fischer SF, Vier J, Kirschnek S, Klos A, Hess S, Ying S and Häcker G (2004) Chlamydia inhibit host cell apoptosis by degradation of proapoptotic BH3-only proteins. *The Journal of experimental medicine*. Rockefeller Univ Press 200(7): 905–

916.

Fluhr R, Lampl N and Roberts TH (2012) Serpin protease inhibitors in plant biology. *Physiologia plantarum* 145(1): 95–102.

Foley S, Lynne A and Nayak R (2008) challenges: Prevalence in swine and poultry and potential pathogenicity of such isolates. *Journal of animal science*. American Society of Animal Science 86(14_suppl): E149–E162.

Folkesson A, Advani A, Sukupolvi S, Pfeifer JD, Normark S and Löfdahl S (1999) Multiple insertions of fimbrial operons correlate with the evolution of *Salmonella* serovars responsible for human disease. *Molecular microbiology* 33(3): 612–22.

Folkesson A, Advani A, Sukupolvi S, Pfeifer JD, Normark S and Löfdahl S (1999) Multiple insertions of fimbrial operons correlate with the evolution of *Salmonella* serovars responsible for human disease. *Molecular microbiology*. Wiley Online Library 33(3): 612–622.

Ford B, Verger D, Dodson K, Volkan E, Kostakioti M, Elam J, Pinkner J, Waksman G and Hultgren S (2012) The structure of the PapD-PapGII pilin complex reveals an open and flexible P5 pocket. *Journal of bacteriology*. Am Soc Microbiol 194(23): 6390–6397.

Foster MD and Synovec RE (1996) Reversed phase liquid chromatography of organic hydrocarbons with water as the mobile phase. *Analytical chemistry* 68(17): 2838–44.

Foulquier F, Harduin-Lepers A, Duvet S, Marchal I, Mir AM, Delannoy P, Chirat F and Cacan R (2002) The unfolded protein response in a dolichyl phosphate mannose-deficient Chinese hamster ovary cell line points out the key role of a demannosylation step in the quality-control mechanism of N-glycoproteins. *Biochemical Journal*. Portland Press Limited 362(2): 491–498.

Francis SE, Ersoy RA, Ahn J-W, Atwell BJ and Roberts TH (2012) Serpins in rice: protein sequence analysis, phylogeny and gene expression during development. *BMC genomics*. BioMed Central 13(1): 1.

Freire S and Wheeler AR (2008) Interfaces between Microfluidics and Mass Spectrometry. *Encyclopedia of Microfluidics and Nanofluidics*. Springer, 849–854.

Fribley A, Zhang K and Kaufman RJ (2009) Regulation of apoptosis by the unfolded protein response. *Methods in molecular biology (Clifton, N.J.)* 559: 191–204.

Fridley GE, Holstein CA, Oza SB and Yager P (2013) The evolution of nitrocellulose as a material for bioassays. *MRS bulletin*. Cambridge Univ Press 38(04): 326–330.

Fried AJ and Bonilla FA (2009) Pathogenesis, diagnosis, and management of primary antibody deficiencies and infections. *Clinical microbiology reviews* 22(3): 396–414.

Froquet R, Cherix N, Birke R, Benghezal M, Cameroni E, Letourneur F, Mösch H-U, De Virgilio C and Cosson P (2008) Control of cellular physiology by TM9 proteins in yeast and Dictyostelium. *Journal of Biological Chemistry*. ASBMB 283(11): 6764–6772.

Froquet R, le Coadic M, Perrin J, Cherix N, Cornillon S and Cosson P (2012) TM9/Phg1 and SadA proteins control surface expression and stability of SibA adhesion molecules in Dictyostelium. *Molecular biology of the cell* 23(4): 679–86.

Fuchs B and Schiller J (2013) MALDI-TOF MS: much more than only protein analysis. *J Glycomics Lipidomics* 3(1): E113.

Fukui S, Feizi T, Galustian C, Lawson AM and Chai W (2002) Oligosaccharide microarrays for high-throughput detection and specificity assignments of carbohydrate-protein interactions. *Nature biotechnology*. Nature Publishing Group 20(10): 1011–1017.

Gaberc-Porekar V and Menart V (2001) Perspectives of immobilized-metal affinity chromatography. *Journal of biochemical and biophysical methods*. Elsevier 49(1): 335–360.

Gal-Mor O, Boyle EC and Grassl GA (2014) Same species, different diseases: how and why typhoidal and non-typhoidal *Salmonella enterica* serovars differ. *Frontiers in microbiology*. Frontiers 5: 391.

Gan SD and Patel KR (2013) Enzyme immunoassay and enzyme-linked immunosorbent assay. *Journal of Investigative Dermatology*. Elsevier 133(9): 1–3.

García-Pérez BE, De la Cruz-López JJ, Castañeda-Sánchez JI, Muñóz-Duarte AR, Hernández-Pérez AD, Villegas-Castrejón H, García-Latorre E, Caamal-Ley A and Luna-Herrera J (2012) Macropinocytosis is responsible for the uptake of pathogenic and non-pathogenic mycobacteria by B lymphocytes (Raji cells). *BMC microbiology*. BioMed Central Ltd 12(1): 246.

Gaskell SJ (1997) Electrospray: principles and practice. *Journal of mass spectrometry*. Chichester, Sussex, England: John Wiley & Sons, c1995- 32(7): 677–688.

Gasteiger E, Hoogland C, Gattiker A, Duvaud S, Wilkins MR, Appel RD and Bairoch A (2005) *Protein identification and analysis tools on the ExPASy server*. Springer.

Ge Y, Yoshiie K, Kuribayashi F, Lin M and Rikihisa Y (2005) Anaplasma phagocytophilum inhibits human neutrophil apoptosis via upregulation of bfl-1, maintenance of mitochondrial membrane potential and prevention of caspase 3 activation. *Cellular microbiology*. Wiley Online Library 7(1): 29–38.

Georg J and Hess WR (2011) cis-antisense RNA, another level of gene regulation in bacteria. *Microbiology and Molecular Biology Reviews*. Am Soc Microbiol 75(2): 286–300.

Gerace E and Moazed D (2015) Chapter Four-Affinity Purification of Protein Complexes Using TAP Tags. *Methods in enzymology*. Elsevier 559: 37–52.

Gerlach RG, Jäckel D, Geymeier N and Hensel M (2007) *Salmonella* pathogenicity island 4-mediated adhesion is coregulated with invasion genes in *Salmonella enterica*. *Infection and immunity*. Am Soc Microbiol 75(10): 4697–4709.

Getz GS (2005) Bridging the innate and adaptive immune systems. *Journal of lipid research*. ASBMB 46(4): 619–622.

Gevaert K and Vandekerckhove J (2000) Protein identification methods in proteomics. *Electrophoresis* 21(6): 1145–54.

Ghosh C, Shinde CP and Chakraborty BS (2012) Ionization polarity as a cause of matrix effects, its removal and estimation in ESI-LC-MS/MS bio-analysis. *Journal of Analytical & Bioanalytical Techniques*. OMICS International 2010.

Gibbs J and Kennebunk M (2001) Immobilization Principles-Selecting the Surface. *ELISA Technical Bulletin* (1): 1–8.

Gingras A-C, Gstaiger M, Raught B and Aebersold R (2007) Analysis of protein complexes using mass spectrometry. *Nature reviews Molecular cell biology*. Nature Publishing Group 8(8): 645–654.

Giorgi C, De Stefani D, Bononi A, Rizzuto R and Pinton P (2009) Structural and functional link between the mitochondrial network and the endoplasmic reticulum.

The international journal of biochemistry \& cell biology. Elsevier 41(10): 1817–1827.

Goldbeck RA, Kim-Shapiro DB and Kliger DS (1997) Fast natural and magnetic circular dichroism spectroscopy. *Annual review of physical chemistry*. Annual Reviews 4139 El Camino Way, PO Box 10139, Palo Alto, CA 94303-0139, USA 48(1): 453–479.

Gómez-Aldapa CA, del Refugio Torres-Vitela M, Villarruel-López A and Castro-Rosas J (2012) The role of foods in *Salmonella* infections. *Salmonella-A Dangerous Foodborne Pathogen* 21–46.

Gómez-Pastor R, Pérez-Torrado R, Cabiscol E, Ros J and Matallana E (2010) Reduction of oxidative cellular damage by overexpression of the thioredoxin TRX2 gene improves yield and quality of wine yeast dry active biomass. *Microbial cell factories*. BioMed Central 9(1): 1.

Gong D, Farley K, White M, Hartshorn KL, Benarafa C and Remold-O'Donnell E (2011) Critical role of serpinB1 in regulating inflammatory responses in pulmonary influenza infection. *The Journal of infectious diseases* 204(4): 592–600.

Gophna U, Ron EZ and Graur D (2003) Bacterial type III secretion systems are ancient and evolved by multiple horizontal-transfer events. *Gene* 312: 151–63.

Goulas T, Garcia-Ferrer I, García-Piqué S, Sottrup-Jensen L and Gomis-Rüth FX (2014) Crystallization and preliminary X-ray diffraction analysis of eukaryotic alpha2-macroglobulin family members modified by methylamine, proteases and glycosidases. *Molecular oral microbiology*. Wiley Online Library 29(6): 354–364.

Grassmé H, Jendrossek V and Gulbins E (2001) Molecular mechanisms of bacteria induced apoptosis. *Apoptosis : an international journal on programmed cell death* 6(6): 441–5.

Grebe SK and Singh RJ (2011) LC-MS/MS in the clinical laboratory-where to from here? *The Clinical Biochemist Reviews*. The Australian Association of Clinical Biochemists 32(1): 5.

Greco TM, Diner BA and Cristea IM (2014) The impact of mass spectrometry-based proteomics on fundamental discoveries in virology. *Annual review of virology*. Annual Reviews 1: 581–604.

Greenfield NJ (1999) Applications of circular dichroism in protein and peptide analysis. *TrAC Trends in Analytical Chemistry*. Elsevier 18(4): 236–244.

Greenfield NJ (2006) Using circular dichroism spectra to estimate protein secondary structure. *Nature protocols* 1(6): 2876–90.

Grimont PA, Weill F-X and others (2007) Antigenic formulae of the *Salmonella* serovars. *WHO collaborating centre for reference and research on Salmonella*. Institute Pasteur Paris, France 9.

Grove J and Marsh M (2011) The cell biology of receptor-mediated virus entry. *The Journal of cell biology*. Rockefeller Univ Press 195(7): 1071–1082.

Gruenberg J and Van der Goot FG (2006) Mechanisms of pathogen entry through the endosomal compartments. *Nature reviews Molecular cell biology*. Nature Publishing Group 7(7): 495–504.

Grünberg S and Hahn S (2013) Structural insights into transcription initiation by RNA polymerase II. *Trends in biochemical sciences*. Elsevier 38(12): 603–611.

Günther R, Krause E, Schümann M, Blasig IE and Haseloff RF (2015) Depletion of highly abundant proteins from human cerebrospinal fluid: a cautionary note. *Molecular neurodegeneration*. BioMed Central 10(1): 1.

Gupta M, Kogut P, Davis FJ, Belaguli NS, Schwartz RJ and Gupta MP (2001) Physical interaction between the MADS box of serum response factor and the TEA/ATTS DNA-binding domain of transcription enhancer factor-1. *Journal of Biological Chemistry*. ASBMB 276(13): 10413–10422.

Den Haan JM, Arens R and van Zelm MC (2014) The activation of the adaptive immune system: cross-talk between antigen-presenting cells, T cells and B cells. *Immunology letters*. Elsevier 162(2): 103–112.

Haggarty J, Oppermann M, Dalby MJ, Burchmore RJ, Cook K, Weidt S and Burgess KE (2015) Serially coupling hydrophobic interaction and reversed-phase chromatography with simultaneous gradients provides greater coverage of the metabolome. *Metabolomics*. Springer 11(5): 1465–1470.

Hahn S (2004) Structure and mechanism of the RNA polymerase II transcription machinery. *Nature structural \& molecular biology*. NIH Public Access 11(5): 394.

Hajnóczky G, Booth D, Csordás G, Debattisti V, Golenár T, Naghdi S, Niknejad N, Paillard M, Seifert EL and Weaver D (2014) Reliance of ER-mitochondrial calcium signaling on mitochondrial EF-hand Ca 2+ binding proteins: Miros, MICUs, LETM1 and solute carriers. *Current opinion in cell biology*. Elsevier 29: 133–141.

Hale JE (2013) Advantageous uses of mass spectrometry for the quantification of proteins. *International journal of proteomics*. Hindawi Publishing Corporation 2013.

Halim ND, Joseph AW and Lipska BK (2005) A novel ELISA using PVDF microplates. *Journal of neuroscience methods*. Elsevier 143(2): 163–168.

Hall RA (2005) Co-immunoprecipitation as a strategy to evaluate receptor-receptor or receptor-protein interactions. *G protein coupled receptor-protein interactions. Wiley, New Jersey, USA* 165–178.

Hall V, Sklepari M and Rodger A (2014) Protein secondary structure prediction from circular dichroism spectra using a self-organizing map with concentration correction. *Chirality*. Wiley Online Library 26(9): 471–482.

Hamerman JA, Hayashi F, Schroeder LA, Gygi SP, Haas AL, Hampson L, Coughlin P, Aebersold R and Aderem A (2002) Serpin 2a is induced in activated macrophages and conjugates to a ubiquitin homolog. *The Journal of Immunology*. Am Assoc Immnol 168(5): 2415–2423.

Hampsey M (1998) Molecular genetics of the RNA polymerase II general transcriptional machinery. *Microbiology and Molecular Biology Reviews*. Am Soc Microbiol 62(2): 465–503.

Hanna PC, Kruskal BA, Ezekowitz RA, Bloom BR and Collier RJ (1994) Role of macrophage oxidative burst in the action of anthrax lethal toxin. *Molecular medicine (Cambridge, Mass.)* 1(1): 7–18.

Hanson BR, Slepenkin A, Peterson EM and Tan M (2015) Chlamydia trachomatis type III secretion proteins regulate transcription. *Journal of bacteriology*. Am Soc Microbiol 197(20): 3238–3244.

Hapfelmeier S, Stecher B, Barthel M, Kremer M, Müller AJ, Heikenwalder M, Stallmach T, Hensel M, Pfeffer K, Akira S and others (2005) The *Salmonella* pathogenicity island (SPI)-2 and SPI-1 type III secretion systems allow *Salmonella* serovar typhimurium to trigger colitis via MyD88-dependent and MyD88-independent mechanisms. *The Journal of Immunology*. Am Assoc Immnol 174(3): 1675–1685.

Harper S and Speicher DW (2011a) Purification of proteins fused to glutathione S-transferase. *Methods in molecular biology (Clifton, N.J.)* 681: 259–80.

Hashino M, Tachibana M, Nishida T, Hara H, Tsuchiya K, Mitsuyama M, Watanabe K, Shimizu T and Watarai M (2015) Inactivation of the MAPK signaling pathway by Listeria monocytogenes infection promotes trophoblast giant cell death. *Frontiers in microbiology*. Frontiers Media SA 6.

Hausmann M (2010) How bacteria-induced apoptosis of intestinal epithelial cells contributes to mucosal inflammation. *International journal of inflammation* 2010: 574568.

Hawe A, Sutter M and Jiskoot W (2008) Extrinsic fluorescent dyes as tools for protein characterization. *Pharmaceutical research* 25(7): 1487–99.

Hawkridge AM (2014) Practical considerations and current limitations in quantitative mass spectrometry-based proteomics. Royal Society of Chemistry.

Hayes P, Harrison D, Bouchier I, McLellan L and Hayes J (1989) Cytosolic and microsomal glutathione S-transferase isoenzymes in normal human liver and intestinal epithelium. *Gut*. BMJ Publishing Group Ltd and British Society of Gastroenterology 30(6): 854–859.

Heaton J and Jones K (2008) Microbial contamination of fruit and vegetables and the behaviour of enteropathogens in the phyllosphere: a review. *Journal of applied microbiology*. Wiley Online Library 104(3): 613–626.

Heinz A, Jung MC, Jahreis G, Rusciani A, Duca L, Debelle L, Weiss AS, Neubert RH and Schmelzer CE (2012) The action of neutrophil serine proteases on elastin and its precursor. *Biochimie*. Elsevier 94(1): 192–202.

Henche A-L, Ghosh A, Yu X, Jeske T, Egelman E and Albers S-V (2012) Structure and function of the adhesive type IV pilus of Sulfolobus acidocaldarius. *Environmental microbiology* 14(12): 3188–202.

Henzel WJ, Watanabe C and Stults JT (2003) Protein identification: the origins of peptide mass fingerprinting. *Journal of the American Society for Mass Spectrometry*. Elsevier 14(9): 931–942.

Herrmann AG, Searcy JL, Le Bihan T, McCulloch J and Deighton RF (2013) Total variance should drive data handling strategies in third generation proteomic studies. *Proteomics*. Wiley Online Library 13(22): 3251–3255.

Hetz C, Martinon F, Rodriguez D and Glimcher LH (2011) The unfolded protein response: integrating stress signals through the stress sensor IRE1α. *Physiological reviews* 91(4): 1219–43.

Hirabayashi J (2003) Oligosaccharide microarrays for glycomics. *TRENDS in Biotechnology*. Elsevier 21(4): 141–143.

Hird SJ, Lau BP-Y, Schuhmacher R and Krska R (2014) Liquid chromatography-mass spectrometry for the determination of chemical contaminants in food. *TrAC Trends in Analytical Chemistry*. Elsevier 59: 59–72.

Ho C, Lam C, Chan M, Cheung R, Law L, Lit L, Ng K, Suen M and Tai H (2003) Electrospray ionisation mass spectrometry: principles and clinical applications. *Clinical Biochemist Reviews*. AUSTRALIAN ASS OF CLINICAL BIOCHEMISTS INC 24(1): 3–12.

Hoensch H, Morgenstern I, Petereit G, Siepmann M, Peters WHM, Roelofs HMJ and Kirch W (2002) Influence of clinical factors, diet, and drugs on the human upper gastrointestinal glutathione system. *Gut* 50(2): 235–40.

Holm PJ, Bhakat P, Jegerschöld C, Gyobu N, Mitsuoka K, Fujiyoshi Y, Morgenstern R and Hebert H (2006) Structural basis for detoxification and oxidative stress protection in membranes. *Journal of molecular biology*. Elsevier 360(5): 934–945.

Holmgren A and Bränden C (1989) Crystal structure of chaperone protein PapD reveals an immunoglobulin fold. *Nature* 342(6247): 248.

Holt KE, Thomson NR, Wain J, Langridge GC, Hasan R, Bhutta ZA, Quail MA, Norbertczak H, Walker D, Simmonds M and others (2009) Pseudogene accumulation in the evolutionary histories of *Salmonella enterica* serovars Paratyphi A and Typhi. *BMC genomics*. BioMed Central 10(1): 1.

Huang F-C, Li Q and Cherayil BJ (2005) A phosphatidyl-inositol-3-kinase-dependent anti-inflammatory pathway activated by *Salmonella* in epithelial cells. *FEMS microbiology letters* 243(1): 265–70.

Hueck CJ (1998) Type III protein secretion systems in bacterial pathogens of animals and plants. *Microbiology and molecular biology reviews : MMBR* 62(2): 379–433.

Humphries AD, Townsend SM, Kingsley RA, Nicholson TL, Tsolis RM and Bäumler AJ (2001) Role of fimbriae as antigens and intestinal colonization factors of *Salmonella* serovars. *FEMS microbiology letters*. The Oxford University Press 201(2): 121–125.

Hunke S and Müller VS (2012) *Approaches to Analyze Protein-Protein Interactions of Membrane Proteins*. INTECH Open Access Publisher.

Hurley B, Lee D, Mott A, Wilton M, Liu J, Liu YC, Angers S, Coaker G, Guttman DS and Desveaux D (2014) The Pseudomonas syringae type III effector HopF2 suppresses Arabidopsis stomatal immunity. *PloS one*. Public Library of Science 9(12): e114921.

Hustoft HK, Malerod H, Wilson SR, Reubsaet L, Lundanes E and Greibrokk T (2012) A critical review of trypsin digestion for LC-MS based proteomics. *Integrative Proteomics*. InTech: Rijeka, Croatia 1: 73–82.

Hutsell SQ, Kimple RJ, Siderovski DP, Willard FS and Kimple AJ (2010) High-affinity immobilization of proteins using biotin-and GST-based coupling strategies. *Surface Plasmon Resonance: Methods and Protocols*. Springer 75–90.

Hüttner S and Strasser R (2012) Endoplasmic reticulum-associated degradation of glycoproteins in plants. *Frontiers in plant science* 3: 67.

Ibarra JA and Steele-Mortimer O (2009) *Salmonella*-the ultimate insider. *Salmonella* virulence factors that modulate intracellular survival. *Cellular microbiology*. Wiley Online Library 11(11): 1579–1586.

IJdo JW and Mueller AC (2004) Neutrophil NADPH oxidase is reduced at the Anaplasma phagocytophilum phagosome. *Infection and immunity* 72(9): 5392–401.

Inlow JK ((n.d.)) Immobilized Metal Affinity Chromatography (IMAC) of Mushroom Tyrosinase.

Ioannou J, Donald A and Tromp R (2015) Characterising the secondary structure changes occurring in high density systems of BLG dissolved in aqueous pH 3 buffer. *Food Hydrocolloids*. Elsevier 46: 216–225.

Irving JA, Steenbakkers PJM, Lesk AM, Op den Camp HJM, Pike RN and Whisstock JC (2002) Serpins in prokaryotes. *Molecular biology and evolution* 19(11): 1881–90.

Ivanov D, Emonet C, Foata F, Affolter M, Delley M, Fisseha M, Blum-Sperisen S, Kochhar S and Arigoni F (2006) A serpin from the gut bacterium Bifidobacterium longum inhibits eukaryotic elastase-like serine proteases. *Journal of Biological Chemistry*. ASBMB 281(25): 17246–17252.

Jain R and Wagner M (2010) Kolmogorov-Smirnov scores and intrinsic mass tolerances for peptide mass fingerprinting. *Journal of proteome research* 9(2): 737–42.

Jakobsson P-J, Mancini JA, Riendeau D and Ford-Hutchinson AW (1997) Identification and characterization of a novel microsomal enzyme with glutathione-dependent transferase and peroxidase activities. *Journal of Biological Chemistry*. ASBMB 272(36): 22934–22939.

Jakobsson P-J, Morgenstern R, Mancini J, Ford-Hutchinson A and Persson B (2000) Membrane-associated Proteins in Eicosanoid and Glutathione Metabolism (MAPEG) A Widespread Protein Superfamily. *American Journal of Respiratory and Critical Care Medicine*. Am Thoracic Soc 161(supplement_1): S20–S24.

Järnum S, Bockermann R, Runström A, Winstedt L and Kjellman C (2015) The Bacterial Enzyme IdeS Cleaves the IgG-Type of B Cell Receptor (BCR), Abolishes BCR-Mediated Cell Signaling, and Inhibits Memory B Cell Activation. *The Journal of Immunology*. Am Assoc Immnol 195(12): 5592–5601.

Jedrychowski MP, Huttlin EL, Haas W, Sowa ME, Rad R and Gygi SP (2011) Evaluation of HCD-and CID-type fragmentation within their respective detection platforms for murine phosphoproteomics. *Molecular & Cellular Proteomics*. ASBMB 10(12): M111–009910.

Jepson MA and Clark M (2001) The role of M cells in *Salmonella* infection. *Microbes and infection*. Elsevier 3(14): 1183–1190.

Jiang W and Hearn MT (1996) Protein interaction with immobilized metal ion affinity ligands under high ionic strength conditions. *Analytical biochemistry* 242(1): 45–54.

Johnson RJ, Savas CJ, Kartje Z and Hoops GC (2014) Rapid and Adaptable Measurement of Protein Thermal Stability by Differential Scanning Fluorimetry: Updating a Common Biochemical Laboratory Experiment. *Journal of Chemical Education*. ACS Publications 91(7): 1077–1080.

Jones AR, Siepen JA, Hubbard SJ and Paton NW (2009) Improving sensitivity in proteome studies by analysis of false discovery rates for multiple search engines. *Proteomics*. Wiley Online Library 9(5): 1220–1229.

Jouve M, Garcia M-I, Courcoux P, Labigne A, Gounon P and Le Bouguénec C (1997) Adhesion to and invasion of HeLa cells by pathogenic Escherichia coli carrying the afa-3 gene cluster are mediated by the AfaE and AfaD proteins, respectively. *Infection and immunity*. Am Soc Microbiol 65(10): 4082–4089.

Jubelin G, Chavez CV, Taieb F, Banfield MJ, Samba-Louaka A, Nobe R, Nougayrède J-P, Zumbihl R, Givaudan A, Escoubas J-M and others (2009) Cycle inhibiting factors (CIFs) are a growing family of functional cyclomodulins present in invertebrate and mammal bacterial pathogens. *PloS one*. Public Library of Science 4(3): e4855.

Jubelin G, Taieb F, Duda DM, Hsu Y, Samba-Louaka A, Nobe R, Penary M, Watrin C, Nougayrède J-P, Schulman BA and others (2010) Pathogenic bacteria target NEDD8-conjugated cullins to hijack host-cell signaling pathways. *PLoS Pathog*. Public Library of Science 6(9): e1001128.

Jung C, Hugot J-P and Barreau F (2010) Peyer's patches: the immune sensors of the intestine. *International journal of inflammation*. Hindawi Publishing Corporation 2010.

Kaboord B and Perr M (2008) Isolation of proteins and protein complexes by immunoprecipitation. *2D PAGE: Sample Preparation and Fractionation*. Springer 349–364.

Kadonaga JT (2004) Regulation of RNA polymerase II transcription by sequence-specific DNA binding factors. *Cell*. Elsevier 116(2): 247–257.

Kadonaga JT (2012) Perspectives on the RNA polymerase II core promoter. *Wiley Interdisciplinary Reviews: Developmental Biology*. Wiley Online Library 1(1): 40–51.

Kainulainen V and Korhonen TK (2014) Dancing to another tune—adhesive moonlighting proteins in bacteria. *Biology*. Multidisciplinary Digital Publishing Institute 3(1): 178–204.

Kannan N, Nguyen LV, Makarem M, Dong Y, Shih K, Eirew P, Raouf A, Emerman JT and Eaves CJ (2014) Glutathione-dependent and-independent oxidative stress-control mechanisms distinguish normal human mammary epithelial cell subsets. *Proceedings of the National Academy of Sciences*. National Acad Sciences 111(21): 7789–7794.

Karaszkiewicz JW (2005) Critical factors in immunoassay optimization. *Gaithersburg, MD: Kirkegaard \& Perry Laboratories, Inc*.

Karpinski K (1990) Optimality assessment in the enzyme-linked immunosorbent assay (ELISA). *Biometrics*. JSTOR 381–390.

Katahira T, Imamura Y and Kitamura D (2006) The BASH/BLNK/SLP-65-associated protein BNAS1 regulates antigen-receptor signal transmission in B cells. *International immunology* 18(4): 545–53.

Kaufman RJ (2002) Orchestrating the unfolded protein response in health and disease. *The Journal of clinical investigation*. Am Soc Clin Investig 110(10): 1389–1398.

Kaur J and Jain SK (2012) Role of antigens and virulence factors of *Salmonella enterica* serovar Typhi in its pathogenesis. *Microbiological research* 167(4): 199–210.

Keller A, Nesvizhskii AI, Kolker E and Aebersold R (2002) Empirical statistical model to estimate the accuracy of peptide identifications made by MS/MS and database search. *Analytical chemistry*. ACS Publications 74(20): 5383–5392.

Kelly SM, Jess TJ and Price NC (2005) How to study proteins by circular dichroism. *Biochimica et Biophysica Acta (BBA)-Proteins and Proteomics*. Elsevier 1751(2): 119–139.

Kelly SM and Price NC (2000) The use of circular dichroism in the investigation of protein structure and function. *Current protein and peptide science*. Bentham Science Publishers 1(4): 349–384.

Kenney JM, Knight DP, Dicko C and Vollrath F (2000) Linear and circular dichroism can help us to understand the molecular nature of spider silk. *European Arachnology 2000* 123–126.

Kessenbrock K, Dau T and Jenne DE (2011) Tailor-made inflammation: how neutrophil serine proteases modulate the inflammatory response. *Journal of molecular medicine (Berlin, Germany)* 89(1): 23–8.

Kessner D, Chambers M, Burke R, Agus D and Mallick P (2008) ProteoWizard: open source software for rapid proteomics tools development. *Bioinformatics*. Oxford Univ Press 24(21): 2534–2536.

Khan F, Ahmad A and Khan MI (2007) Chemical, thermal and pH-induced equilibrium unfolding studies of Fusarium solani lectin. *IUBMB life* 59(1): 34–43.

Khan SS and Lee FJ (2014) Delineation of domains within the cannabinoid CB1 and dopamine D2 receptors that mediate the formation of the heterodimer complex. *Journal of Molecular Neuroscience*. Springer 53(1): 10–21.

Kim D and Herr AE (2013) Protein immobilization techniques for microfluidic assays. *Biomicrofluidics*. AIP Publishing 7(4): 041501.

Kim JS, Eom JS, Jang JI, Kim HG, Seo DW, Bang I-S, Bang SH, Lee IS and Park YK (2011) Role of *Salmonella* Pathogenicity Island 1 protein IacP in *Salmonella enterica* serovar typhimurium pathogenesis. *Infection and immunity* 79(4): 1440–50.

Kimple ME, Brill AL and Pasker RL (2013) Overview of affinity tags for protein purification. *Current protocols in protein science / editorial board, John E. Coligan ... [et al.]* 73: Unit 9.9.

Kimple ME and Sondek J (2004) Overview of affinity tags for protein purification. *Current Protocols in Protein Science*. Wiley Online Library 9–9.

Kinnula VL (2005) Focus on antioxidant enzymes and antioxidant strategies in smoking related airway diseases. *Thorax* 60(8): 693–700.

Kirkegaard T and Jäättelä M (2009) Lysosomal involvement in cell death and cancer. *Biochimica et Biophysica Acta (BBA)-Molecular Cell Research*. Elsevier 1793(4): 746–754.

Kirschnek S, Ying S, Fischer SF, Häcker H, Villunger A, Hochrein H and Häcker G (2005) Phagocytosis-induced apoptosis in macrophages is mediated by up-regulation and activation of the Bcl-2 homology domain 3-only protein Bim. *The Journal of Immunology*. Am Assoc Immnol 174(2): 671–679.

Knochenmuss R, Stortelder A, Breuker K and Zenobi R (2000) Secondary ion-molecule reactions in matrix-assisted laser desorption/ionization. *Journal of mass spectrometry*. Wiley Online Library 35(11): 1237–1245.

Knochenmuss R and Zenobi R (2003) MALDI ionization: the role of in-plume processes. *Chemical reviews*. ACS Publications 103(2): 441–452.

Knodler LA, Nair V and Steele-Mortimer O (2014) Quantitative assessment of cytosolic *Salmonella* in epithelial cells. *PloS one* 9(1): e84681.

Knodler LA, Vallance BA, Celli J, Winfree S, Hansen B, Montero M and Steele-Mortimer O (2010) Dissemination of invasive *Salmonella* via bacterial-induced extrusion of mucosal epithelia. *Proceedings of the National Academy of Sciences of the United States of America* 107(41): 17733–8.

Kobayashi SD, Voyich JM, Burlak C and DeLeo FR (2005) Neutrophils in the innate immune response. *ARCHIVUM IMMUNOLOGIAE ET THERAPIAE EXPERIMENTALIS-ENGLISH EDITION-*. OSSOLINEUM PUBLISHING HOUSE 53(6): 505.

Kolaczkowska E and Kubes P (2013) Neutrophil recruitment and function in health and inflammation. *Nature Reviews Immunology*. Nature Publishing Group 13(3): 159–175.

Koller H, Hochegger K, Zlabinger GJ, Lhotta K, Mayer G and Rosenkranz AR (2004) Apoptosis of human polymorphonuclear neutrophils accelerated by dialysis membranes via the activation of the complement system. *Nephrology Dialysis Transplantation*. ERA-EDTA 19(12): 3104–3111.

Kong J and Yu S (2007) Fourier transform infrared spectroscopic analysis of protein secondary structures. *Acta biochimica et biophysica Sinica* 39(8): 549–59.

Korhonen T (2015) Fibrinolytic and procoagulant activities of Yersinia pestis and *Salmonella enterica*. *Journal of Thrombosis and Haemostasis*. Wiley Online Library 13(S1): S115–S120.

Korkmaz B, Horwitz MS, Jenne DE and Gauthier F (2010) Neutrophil elastase, proteinase 3, and cathepsin G as therapeutic targets in human diseases. *Pharmacological reviews*. ASPET 62(4): 726–759.

Kosobokova E, Skrypnik K and Kosorukov V (2016) Overview of fusion tags for recombinant proteins. *Biochemistry (Moscow)*. Springer 81(3): 187–200.

Krachler AM and Orth K (2013) Targeting the bacteria-host interface: strategies in anti-adhesion therapy. *Virulence*. Taylor & Francis 4(4): 284–294.

Ksiazek M, Mizgalska D, Enghild JJ, Scavenius C, Thogersen IB and Potempa J (2015) Miropin, a novel bacterial serpin from the periodontopathogen Tannerella forsythia, inhibits a broad range of proteases by using different peptide bonds within

the reactive center loop. *Journal of Biological Chemistry*. ASBMB 290(1): 658–670.

Kumar SD and Kumar DH (2012) Importance of RP-HPLC in analytical method development: a review. *International Journal of Pharmaceutical Sciences and Research*. International Journal of Pharmaceutical Sciences and Research 3(12): 4626.

La D, Kong M, Hoffman W, Choi YI and Kihara D (2013) Predicting permanent and transient protein-protein interfaces. *Proteins: Structure, Function, and Bioinformatics*. Wiley Online Library 81(5): 805–818.

Laemmli UK (1970) Cleavage of structural proteins during the assembly of the head of bacteriophage T4. *nature* 227: 680–685.

Laguna RK, Creasey EA, Li Z, Valtz N and Isberg RR (2006) A Legionella pneumophila-translocated substrate that is required for growth within macrophages and protection from host cell death. *Proceedings of the National Academy of Sciences*. National Acad Sciences 103(49): 18745–18750.

Lahiri A, Lahiri A, Iyer N, Das P and Chakravortty D (2010) Visiting the cell biology of *Salmonella* infection. *Microbes and infection / Institut Pasteur* 12(11): 809–18.

Lai X-H, Xu Y, Chen X-M and Ren Y (2015) Macrophage cell death upon intracellular bacterial infection. *Macrophage*. NIH Public Access 2: e779.

Lam GY, Fattouh R, Muise AM, Grinstein S, Higgins DE and Brumell JH (2011) Listeriolysin O suppresses phospholipase C-mediated activation of the microbicidal NADPH oxidase to promote Listeria monocytogenes infection. *Cell host & microbe*. Elsevier 10(6): 627–634.

Lamazares E, Clemente I, Bueno M, Velázquez-Campoy A and Sancho J (2015) Rational stabilization of complex proteins: a divide and combine approach. *Scientific reports*. Nature Publishing Group 5: 9129.

Lancellotti M, Brocchi M and da Silveira WD (2006) Bacteria-induced apoptosis: an approach to bacterial pathogenesis. *Braz J Morphol Sci* 23(1): 75–86.

Lanucara F, Holman SW, Gray CJ and Eyers CE (2014) The power of ion mobility-mass spectrometry for structural characterization and the study of conformational dynamics. *Nature chemistry* 6(4): 281–94.

Larsen AC, Gillig A, Shah P, Sau SP, Fenton KE and Chaput JC (2014) General approach for characterizing in vitro selected peptides with protein binding affinity. *Analytical chemistry*. ACS Publications 86(15): 7219–7223.

Larsson T, Bergström J, Nilsson C and Karlsson K-A (2000) Use of an affinity proteomics approach for the identification of low-abundant bacterial adhesins as applied on the Lewisb-binding adhesin of Helicobacter pylori. *FEBS letters*. Wiley Online Library 469(2-3): 155–158.

Lauri A, Castiglioni B and Mariani P (2011) Comprehensive analysis of *Salmonella* sequence polymorphisms and development of a LDR-UA assay for the detection and characterization of selected serotypes. *Applied microbiology and biotechnology*. Springer 91(1): 189–210.

Laursen BS, Sørensen HP, Mortensen KK and Sperling-Petersen HU (2005) Initiation of protein synthesis in bacteria. *Microbiology and Molecular Biology Reviews*. Am Soc Microbiol 69(1): 101–123.

Law RH, Zhang Q, Mcgowan S, Buckle AM, Silverman GA, Wong W, Rosado CJ and others (2006) Review An overview of the serpin superfamily. Citeseer.

Lea WA and Simeonov A (2012) Differential scanning fluorometry signatures as indicators of enzyme inhibitor mode of action: case study of glutathione S-transferase. *PloS one*. Public Library of Science 7(4): e36219.

Lebiedzinska M, Szabadkai G, Jones AW, Duszynski J and Wieckowski MR (2009) Interactions between the endoplasmic reticulum, mitochondria, plasma membrane and other subcellular organelles. *The international journal of biochemistry \& cell biology*. Elsevier 41(10): 1805–1816.

Ledeboer NA, Frye JG, McClelland M and Jones BD (2006) *Salmonella enterica* serovar Typhimurium requires the Lpf, Pef, and Tafi fimbriae for biofilm formation on HEp-2 tissue culture cells and chicken intestinal epithelium. *Infection and immunity*. Am Soc Microbiol 74(6): 3156–3169.

Lee DG, An SY, Um MS, Choi WJ, Noh SM, Jung HW and Oh JK (2016) Photo-induced thiol-ene crosslinked polymethacrylate networks reinforced with Al 2 O 3 nanoparticles. *Polymer*. Elsevier.

Lee JW, Kim WH, Yeo J and Jung MH (2010) ER stress is implicated in mitochondrial dysfunction-induced apoptosis of pancreatic beta cells. *Molecules and cells* 30(6): 545–9.

Leng J, Butcher BA and Denkers EY (2009) Dysregulation of macrophage signal transduction by Toxoplasma gondii: past progress and recent advances. *Parasite immunology* 31(12): 717–28.

Lequin RM (2005) Enzyme immunoassay (EIA)/enzyme-linked immunosorbent assay (ELISA). *Clinical chemistry*. Am Assoc Clin Chem 51(12): 2415–2418.

Li H, Xu H, Zhou Y, Zhang J, Long C, Li S, Chen S, Zhou J-M and Shao F (2007) The phosphothreonine lyase activity of a bacterial type III effector family. *Science*. American Association for the Advancement of Science 315(5814): 1000–1003.

Liang X, Fonnum G, Hajivandi M, Stene T, Kjus NH, Ragnhildstveit E, Amshey JW, Predki P and Pope RM (2007) Quantitative comparison of IMAC and TiO 2 surfaces used in the study of regulated, dynamic protein phosphorylation. *Journal of the American Society for Mass Spectrometry*. Elsevier 18(11): 1932–1944.

Liévin-Le Moal V and Servin AL (2006) The front line of enteric host defense against unwelcome intrusion of harmful microorganisms: mucins, antimicrobial peptides, and microbiota. *Clinical microbiology reviews*. Am Soc Microbiol 19(2): 315–337.

Lin L, Wu Y, Li C and Zhao S (2001) Cloning, tissue expression pattern, and chromosome location of a novel human gene BRI3BP. *Biochemical genetics*. Springer 39(11-12): 369–377.

Liu L and Chen Z (2009) Separation of small molecular peptides with the same amino acid composition but different sequences by high performance liquid chromatography-electrospray ionization-mass spectrometry. *Science in China Series B: Chemistry*. Springer 52(12): 2264–2268.

Liu H and May K (2012) Disulfide bond structures of IgG molecules: structural variations, chemical modifications and possible impacts to stability and biological function. *MAbs*, 17–23.

Liu JZ, Jellbauer S, Poe AJ, Ton V, Pesciaroli M, Kehl-Fie TE, Restrepo NA, Hosking MP, Edwards RA, Battistoni A, Pasquali P, Lane TE, Chazin WJ, Vogl T, Roth J, Skaar EP and Raffatellu M (2012) Zinc sequestration by the neutrophil protein calprotectin enhances *Salmonella* growth in the inflamed gut. *Cell host & microbe* 11(3): 227–39.

Liu L and Chen Z (2009) Separation of small molecular peptides with the same amino acid composition but different sequences by high performance liquid

chromatography-electrospray ionization-mass spectrometry. *Science in China Series B: Chemistry*. Springer 52(12): 2264–2268.

Liu W, Sohn HW, Tolar P and Pierce SK (2010) It's all about change: the antigen-driven initiation of B-cell receptor signaling. *Cold Spring Harbor perspectives in biology*. Cold Spring Harbor Lab 2(7): a002295.

Lord CC, Thomas G and Brown JM (2013) Mammalian alpha beta hydrolase domain (ABHD) proteins: Lipid metabolizing enzymes at the interface of cell signaling and energy metabolism. *Biochimica et Biophysica Acta (BBA)-Molecular and Cell Biology of Lipids*. Elsevier 1831(4): 792–802.

Louis-Jeune C, Andrade-Navarro MA and Perez-Iratxeta C (2012) Prediction of protein secondary structure from circular dichroism using theoretically derived spectra. *Proteins: Structure, Function, and Bioinformatics*. Wiley Online Library 80(2): 374–381.

Low S, Shaimi R, Thandaithabany Y, Lim J, Ahmad A and Ismail A (2013) Electrophoretic interactions between nitrocellulose membranes and proteins: Biointerface analysis and protein adhesion properties. *Colloids and Surfaces B: Biointerfaces*. Elsevier 110: 248–253.

Lu I-C, Lee C, Lee Y-T and Ni C-K (2015) Ionization Mechanism of Matrix-Assisted Laser Desorption/Ionization. *Annual Review of Analytical Chemistry*. Annual Reviews 8: 21–39.

Luke CJ, Pak SC, Askew YS, Naviglia TL, Askew DJ, Nobar SM, Vetica AC, Long OS, Watkins SC, Stolz DB and others (2007) An intracellular serpin regulates necrosis by inhibiting the induction and sequelae of lysosomal injury. *Cell*. Elsevier 130(6): 1108–1119.

Luo K and Cao SS (2015) Endoplasmic reticulum stress in intestinal epithelial cell function and inflammatory bowel disease. *Gastroenterology research and practice*. Hindawi Publishing Corporation 2015.

Luo L, King NP, Yeo JC, Jones A and Stow JL (2014) Single-step protease cleavage elution for identification of protein-protein interactions from GST pull-down and mass spectrometry. *Proteomics*. Wiley Online Library 14(1): 19–23.

Lushchak VI (2012) Glutathione homeostasis and functions: potential targets for medical interventions. *Journal of amino acids*. Hindawi Publishing Corporation 2012.

Lutay N, Ambite I, Grönberg Hernandez J, Rydström G, Ragnarsdóttir B, Puthia M, Nadeem A, Zhang J, Storm P, Dobrindt U, Wullt B and Svanborg C (2013) Bacterial control of host gene expression through RNA polymerase II. *The Journal of clinical investigation* 123(6): 2366–79.

Ma Z, Guan Y, Liu X and Liu H (2005) Covalent immobilization of albumin on micron-sized magnetic poly (methyl methacrylate-divinylbenzene-glycidyl methacrylate) microspheres prepared by modified suspension polymerization. *Polymers for advanced technologies*. Wiley Online Library 16(7): 554–558.

Mabbott NA, Donaldson DS, Ohno H, Williams IR and Mahajan A (2013) Microfold (M) cells: important immunosurveillance posts in the intestinal epithelium. *Mucosal immunology* 6(4): 666–77.

Machado FS, Dutra WO, Esper L, Gollob KJ, Teixeira MM, Factor SM, Weiss LM, Nagajyothi F, Tanowitz HB and Garg NJ (2012) Current understanding of immunity to Trypanosoma cruzi infection and pathogenesis of Chagas disease. *Seminars in immunopathology* 34(6): 753–70.

Macht M, Marquardt A, Deininger S-O, Damoc E, Kohlmann M and Przybylski M (2004) " Affinity-proteomics": direct protein identification from biological material using mass spectrometric epitope mapping. *Analytical and bioanalytical chemistry*. Springer 378(4): 1102–1111.

MacPhee DJ (2010) Methodological considerations for improving Western blot analysis. *Journal of pharmacological and toxicological methods*. Elsevier 61(2): 171–177.

Magdeldin S and Moser A (2012) Affinity chromatography: Principles and applications. *S. Magdeldin, InTech, Croatia* 1–28.

Main-Hester KL, Colpitts KM, Thomas GA, Fang FC and Libby SJ (2008) Coordinate regulation of *Salmonella* pathogenicity island 1 (SPI1) and SPI4 in *Salmonella enterica* serovar Typhimurium. *Infection and immunity* 76(3): 1024–35.

Majowicz SE, Musto J, Scallan E, Angulo FJ, Kirk M, O'Brien SJ, Jones TF, Fazil A, Hoekstra RM and others (2010) The global burden of nontyphoidal *Salmonella* gastroenteritis. *Clinical Infectious Diseases*. Oxford University Press 50(6): 882–889.

Malhotra JD and Kaufman RJ (2011) ER stress and its functional link to mitochondria: role in cell survival and death. *Cold Spring Harbor perspectives in biology*. Cold Spring Harbor Lab 3(9): a004424.

Malik-Kale P, Winfree S and Steele-Mortimer O (2012) The bimodal lifestyle of intracellular *Salmonella* in epithelial cells: replication in the cytosol obscures defects in vacuolar replication. *PloS one*. Public Library of Science 7(6): e38732.

Manfredini V, Roehrs R, Peralba M do CR, Henriques JAP, Saffi J, Ramos ALL de P and Benfato M da S (2004) Glutathione peroxidase induction protects Saccharomyces cerevisiae sod1deltasod2delta double mutants against oxidative damage. *Brazilian journal of medical and biological research*. SciELO Brasil 37(2): 159–165.

Mansan-Almeida R, Pereira AL and Giugliano LG (2013) Diffusely adherent Escherichia coli strains isolated from children and adults constitute two different populations. *BMC microbiology*. BioMed Central 13(1): 1.

Marí M and Cederbaum AI (2001) Induction of catalase, alpha, and microsomal glutathione S-transferase in CYP2E1 overexpressing HepG2 cells and protection against short-term oxidative stress. *Hepatology*. Wiley Online Library 33(3): 652–661.

Mar'\in-Buera L, Garc'\ia-Bartolomé A, Morán M, López-Bernardo E, Cadenas S, Hidalgo B, Sánchez R, Seneca S, Arenas J, Mart'\in MA and others (2015) Differential proteomic profiling unveils new molecular mechanisms associated with mitochondrial complex III deficiency. *Journal of proteomics*. Elsevier 113: 38–56.

Marchès O, Ledger TN, Boury M, Ohara M, Tu X, Goffaux F, Mainil J, Rosenshine I, Sugai M, De Rycke J and others (2003) Enteropathogenic and enterohaemorrhagic Escherichia coli deliver a novel effector called Cif, which blocks cell cycle G2/M transition. *Molecular microbiology*. Wiley Online Library 50(5): 1553–1567.

Markham K, Bai Y and Schmitt-Ulms G (2007) Co-immunoprecipitations revisited: an update on experimental concepts and their implementation for sensitive interactome investigations of endogenous proteins. *Analytical and bioanalytical chemistry*. Springer 389(2): 461–473.

Maródi L and Notarangelo LD (2007) Immunological and genetic bases of new primary immunodeficiencies. *Nature Reviews Immunology*. Nature Publishing Group 7(11): 851–861.

Martínez-Lorenzo MJ, Meresse S, De Chastellier C and Gorvel J-P (2001) Unusual intracellular trafficking of *Salmonella* typhimurium in human melanoma cells. *Cellular microbiology*. Wiley Online Library 3(6): 407–416.

Mårtensson I-L, Almqvist N, Grimsholm O and Bernardi AI (2010) The pre-B cell receptor checkpoint. *FEBS letters*. Wiley Online Library 584(12): 2572–2579.

Martin SR and Bayley PM (2002) Absorption and circular dichroism spectroscopy. *Methods in molecular biology (Clifton, N.J.)* 173: 43–55.

Martínez-Lorenzo MJ, Méresse S, de Chastellier C and Gorvel JP (2001) Unusual intracellular trafficking of *Salmonella* typhimurium in human melanoma cells. *Cellular microbiology* 3(6): 407–16.

Marvin LF, Roberts MA and Fay LB (2003) Matrix-assisted laser desorption/ionization time-of-flight mass spectrometry in clinical chemistry. *Clinica chimica acta; international journal of clinical chemistry* 337(1-2): 11–21.

Massari P, Ho Y and Wetzler LM (2000) Neisseria meningitidis porin PorB interacts with mitochondria and protects cells from apoptosis. *Proceedings of the National Academy of Sciences*. National Acad Sciences 97(16): 9070–9075.

De Matos LL, Trufelli DC, de Matos GL and da Silva Pinhal A (2010) Immunohistochemistry as an important tool in biomarkers detection and clinical practice. *Biomarker insights*. Libertas Academica Ltd 5: 9.

Matsudaira P (1987) Sequence from picomole quantities of proteins electroblotted onto polyvinylidene difluoride membranes. *Journal of Biological Chemistry*. ASBMB 262(21): 10035–10038.

Matsumoto H, Koyama Y and Tanioka A (2003) Interaction of proteins with weak amphoteric charged membrane surfaces: effect of pH. *Journal of colloid and interface science*. Elsevier 264(1): 82–88.

Le Maux S, Nongonierma AB and FitzGerald RJ (2015) Improved short peptide identification using HILIC-MS/MS: Retention time prediction model based on the impact of amino acid position in the peptide sequence. *Food chemistry*. Elsevier 173: 847–854.

McCaffrey RL and Allen L-AH (2006) Francisella tularensis LVS evades killing by human neutrophils via inhibition of the respiratory burst and phagosome escape. *Journal of leukocyte biology*. Soc Leukocyte Biology 80(6): 1224–1230.

McFedries A, Schwaid A and Saghatelian A (2013) Methods for the elucidation of protein-small molecule interactions. *Chemistry & biology* 20(5): 667–73.

McGhee JR and Fujihashi K (2012) Inside the mucosal immune system. *PLoS Biol*. Public Library of Science 10(9): e1001397.

McLafferty FW (2008) Mass spectrometry across the sciences. *Proceedings of the National Academy of Sciences of the United States of America* 105(47): 18088–9.

McMurray MA, Stefan CJ, Wemmer M, Odorizzi G, Emr SD and Thorner J (2011) Genetic interactions with mutations affecting septin assembly reveal ESCRT functions in budding yeast cytokinesis. *Biological chemistry* 392(8-9): 699–712.

Medina-Kauwe LK (2007) "Alternative" endocytic mechanisms exploited by pathogens: new avenues for therapeutic delivery? *Advanced drug delivery reviews*. Elsevier 59(8): 798–809.

Medzihradszky KF, Campbell JM, Baldwin MA, Falick AM, Juhasz P, Vestal ML and Burlingame AL (2000) The characteristics of peptide collision-induced dissociation using a high-performance MALDI-TOF/TOF tandem mass spectrometer. *Analytical chemistry*. ACS Publications 72(3): 552–558.

Medzihradszky KF and Chalkley RJ (2015) Lessons in de novo peptide sequencing by tandem mass spectrometry. *Mass spectrometry reviews*. Wiley Online Library 34(1): 43–63.

Melville S and Craig L (2013) Type IV pili in Gram-positive bacteria. *Microbiology and molecular biology reviews*. Am Soc Microbiol 77(3): 323–341.

Menzel C, Dreisewerd K, Berkenkamp S and Hillenkamp F (2001) Mechanisms of energy deposition in infrared matrix-assisted laser desorption/ionization mass spectrometry. *International Journal of Mass Spectrometry*. Elsevier 207(1): 73–96.

Menzel C, Dreisewerd K, Berkenkamp S and Hillenkamp F (2002) The role of the laser pulse duration in infrared matrix-assisted laser desorption/ionization mass spectrometry. *Journal of the American Society for Mass Spectrometry*. Elsevier 13(8): 975–984.

Von Mering C, Jensen LJ, Snel B, Hooper SD, Krupp M, Foglierini M, Jouffre N, Huynen MA and Bork P (2005) STRING: known and predicted protein-protein associations, integrated and transferred across organisms. *Nucleic acids research*. Oxford Univ Press 33(suppl 1): D433–D437.

Meyer T, Schirrmann T, Frenzel A, Miethe S, Stratmann-Selke J, Gerlach GF, Strutzberg-Minder K, Dübel S and Hust M (2012) Identification of immunogenic

proteins and generation of antibodies against *Salmonella* Typhimurium using phage display. *BMC biotechnology*. BioMed Central 12(1): 1.

For Microbiology SS of the NC of the IS and others (1934) The genus *Salmonella* lignieres, 1900. *The Journal of hygiene*. Cambridge University Press 34(3): 333.

Miedel MT, Zeng X, Yates NA, Silverman GA and Luke CJ (2014) Isolation of serpin-interacting proteins in C. elegans using protein affinity purification. *Methods*. Elsevier 68(3): 536–541.

Miles A and Wallace B (2016) Circular dichroism spectroscopy of membrane proteins. *Chemical Society Reviews*. Royal Society of Chemistry.

Miles AJ and Wallace BA (2006) Synchrotron radiation circular dichroism spectroscopy of proteins and applications in structural and functional genomics. *Chemical Society reviews* 35(1): 39–51.

Miller SI (1991) PhoP/PhoQ: macrophage-specific modulators of *Salmonella* virulence? *Molecular microbiology* 5(9): 2073–8.

Millioni R, Tolin S, Puricelli L, Sbrignadello S, Fadini GP, Tessari P and Arrigoni G (2011) High abundance proteins depletion vs low abundance proteins enrichment: comparison of methods to reduce the plasma proteome complexity. *PloS one*. Public Library of Science 6(5): e19603.

Mogensen TH (2009) Pathogen recognition and inflammatory signaling in innate immune defenses. *Clinical microbiology reviews*. Am Soc Microbiol 22(2): 240–273.

Mohammad A and Jabeen N (2003) Reversed-phase chromatography of amines, phenols, and metal cations on silica layers impregnated with tributyl phosphate, using surfactant-mediated mobile phases. *Acta Chromatographica*. UNIVERSITY OF SILESIA 13.

Molestina RE, El-Guendy N and Sinai AP (2008) Infection with Toxoplasma gondii results in dysregulation of the host cell cycle. *Cellular microbiology* 10(5): 1153–65.

Molíková M and Jandera P (2010) Characterization of stationary phases for reversed-phase chromatography. *Journal of separation science* 33(4-5): 453–63.

Molina DM, Eshaghi S and Nordlund P (2008) Catalysis within the lipid bilayer—structure and mechanism of the MAPEG family of integral membrane proteins.

Current opinion in structural biology. Elsevier 18(4): 442–449.

De Monerri NCS and Kim K (2014) Pathogens hijack the epigenome: a new twist on host-pathogen interactions. *The American journal of pathology*. Elsevier 184(4): 897–911.

Morpeth SC, Ramadhani HO and Crump JA (2009) Invasive non-Typhi *Salmonella* disease in Africa. *Clinical infectious diseases : an official publication of the Infectious Diseases Society of America* 49(4): 606–11.

Morris JH, Knudsen GM, Verschueren E, Johnson JR, Cimermancic P, Greninger AL and Pico AR (2014) Affinity purification-mass spectrometry and network analysis to understand protein-protein interactions. *Nature protocols*. Nature Publishing Group 9(11): 2539–2554.

Mostowy S and Shenoy AR (2015) The cytoskeleton in cell-autonomous immunity: structural determinants of host defence. *Nature Reviews Immunology*. Nature Publishing Group.

Moumene A and Meyer DF (2016) Ehrlichia's molecular tricks to manipulate their host cells. *Microbes and Infection*. Elsevier 18(3): 172–179.

Mueller SJ and Reski R (2015) Mitochondrial Dynamics and the ER: The Plant Perspective. *Frontiers in cell and developmental biology*. Frontiers Media SA 3.

Müller AJ, Kaiser P, Dittmar KE, Weber TC, Haueter S, Endt K, Songhet P, Zellweger C, Kremer M, Fehling H-J and others (2012) *Salmonella* gut invasion involves TTSS-2-dependent epithelial traversal, basolateral exit, and uptake by epithelium-sampling lamina propria phagocytes. *Cell host \& microbe*. Elsevier 11(1): 19–32.

Naganathan AN, Doshi U and Muñoz V (2007) Protein folding kinetics: Barrier effects in chemical and thermal denaturation experiments. *Journal of the American Chemical Society*. ACS Publications 129(17): 5673–5682.

Nagao H, Shimma S, Hayakawa S, Awazu K and Toyoda M (2010) Development of a tandem time-of-flight mass spectrometer with an electrospray ionization ion source. *Journal of mass spectrometry : JMS* 45(8): 937–43.

Nagarkar-Jaiswal S, Lee P-T, Campbell ME, Chen K, Anguiano-Zarate S, Gutierrez MC, Busby T, Lin W-W, He Y, Schulze KL and others (2015) A library of MiMICs allows tagging of genes and reversible, spatial and temporal knockdown of proteins

in Drosophila. *Elife*. eLife Sciences Publications Limited 4: e05338.

Nagatomo S, Nagai M, Ogura T and Kitagawa T (2013) Near-UV circular dichroism and UV resonance Raman spectra of tryptophan residues as a structural marker of proteins. *The Journal of Physical Chemistry B*. ACS Publications 117(32): 9343–9353.

Nesvizhskii AI, Keller A, Kolker E and Aebersold R (2003) A statistical model for identifying proteins by tandem mass spectrometry. *Analytical chemistry*. ACS Publications 75(17): 4646–4658.

Nguyen TN and Goodrich JA (2006) Protein-protein interaction assays: eliminating false positive interactions. *Nature methods* 3(2): 135–9.

Nielsen ML, Savitski MM and Zubarev RA (2005) Improving protein identification using complementary fragmentation techniques in Fourier transform mass spectrometry. *Molecular \& Cellular Proteomics*. ASBMB 4(6): 835–845.

Nikolov D and Burley S (1997) RNA polymerase II transcription initiation: a structural view. *Proceedings of the National Academy of Sciences*. National Acad Sciences 94(1): 15–22.

Nishida M, Harada S, Noguchi S, Satow Y, Inoue H and Takahashi K (1998) Three-dimensional structure of Escherichia coli glutathione S-transferase complexed with glutathione sulfonate: catalytic roles of Cys10 and His106. *Journal of molecular biology*. Elsevier 281(1): 135–147.

Normark S (2000) Anfinsen comes out of the cage during assembly of the bacterial pilus. *Proceedings of the National Academy of Sciences of the United States of America* 97(14): 7670–2.

Nougayrède J-P, Taieb F, De Rycke J and Oswald E (2005) Cyclomodulins: bacterial effectors that modulate the eukaryotic cell cycle. *Trends in microbiology*. Elsevier 13(3): 103–110.

Oakley A (2011) Glutathione transferases: a structural perspective. *Drug metabolism reviews* 43(2): 138–51.

Oberley-Deegan RE, Rebits BW, Weaver MR, Tollefson AK, Bai X, McGibney M, Ovrutsky AR, Chan ED and Crapo JD (2010) An oxidative environment promotes growth of Mycobacterium abscessus. *Free radical biology & medicine* 49(11): 1666–73.

Ochman H, Lawrence JG and Groisman EA (2000) Lateral gene transfer and the nature of bacterial innovation. *Nature*. Nature Publishing Group 405(6784): 299–304.

Ochoa IMF and Rodríguez AV (2005) Mecanismos moleculares de patogenicidad de *Salmonella* sp. *Revista Latinoamericana de Microbiología* 47(1-2): 25–42.

Ogu CC and Maxa JL (2000) Drug interactions due to cytochrome P450. *Baylor University Medical Center. Proceedings*, 421.

Olsen JV, Ong S-E and Mann M (2004) Trypsin cleaves exclusively C-terminal to arginine and lysine residues. *Molecular & cellular proteomics : MCP* 3(6): 608–14.

Omenn GS, States DJ, Adamski M, Blackwell TW, Menon R, Hermjakob H, Apweiler R, Haab BB, Simpson RJ, Eddes JS and others (2005) Overview of the HUPO Plasma Proteome Project: Results from the pilot phase with 35 collaborating laboratories and multiple analytical groups, generating a core dataset of 3020 proteins and a publicly-available database. *Proteomics*. Wiley Online Library 5(13): 3226–3245.

Oo HZ, Sentani K, Sakamoto N, Anami K, Naito Y, Oshima T, Yanagihara K, Oue N and Yasui W (2014) Identification of novel transmembrane proteins in scirrhous-type gastric cancer by the Escherichia coli ampicillin secretion trap (CAST) method: TM9SF3 participates in tumor invasion and serves as a prognostic factor. *Pathobiology*. Karger Publishers 81(3): 138–148.

Østergaard H, Rasmussen SK, Roberts TH and Hejgaard J (2000) Inhibitory Serpins from Wheat Grain with Reactive Centers Resembling Glutamine-rich Repeats of Prolamin Storage Proteins CLONING AND CHARACTERIZATION OF FIVE MAJOR MOLECULAR FORMS. *Journal of Biological Chemistry*. ASBMB 275(43): 33272–33279.

Ou Y, Geng P, Liao G-Y, Zhou Z and Wu W-T (2009) Intracellular GSH and ROS levels may be related to galactose-mediated human lens epithelial cell apoptosis: role of recombinant hirudin variant III. *Chemico-biological interactions*. Elsevier 179(2): 103–109.

Ozbabacan SEA, Engin HB, Gursoy A and Keskin O (2011) Transient protein-protein interactions. *Protein Engineering Design and Selection*. Oxford Univ Press 24(9): 635–648.

Padmanabhan B, Kuzuhara T, Adachi N and Horikoshi M (2004) The crystal structure of CCG1/TAFII250-interacting factor B (CIB). *Journal of Biological Chemistry*. ASBMB 279(10): 9615–9624.

Page R, Peti W, Wilson IA, Stevens RC and Wüthrich K (2005) NMR screening and crystal quality of bacterially expressed prokaryotic and eukaryotic proteins in a structural genomics pipeline. *Proceedings of the National Academy of Sciences of the United States of America*. National Acad Sciences 102(6): 1901–1905.

Paiva CN and Bozza MT (2014) Are reactive oxygen species always detrimental to pathogens? *Antioxidants & redox signaling*. Mary Ann Liebert, Inc. 140 Huguenot Street, 3rd Floor New Rochelle, NY 10801 USA 20(6): 1000–1037.

Paiva CN, Feijó DF, Dutra FF, Carneiro VC, Freitas GB, Alves LS, Mesquita J, Fortes GB, Figueiredo RT, Souza HSP, Fantappié MR, Lannes-Vieira J and Bozza MT (2012) Oxidative stress fuels Trypanosoma cruzi infection in mice. *The Journal of clinical investigation* 122(7): 2531–42.

Palace GP, Fitzpatrick R, Tran KV, Phoebe CH and Norton K (1999) Determination of amino acids in diverse polymeric matrices using HPLC, with emphasis on agars and agaroses. *Biochimica et Biophysica Acta (BBA)-General Subjects*. Elsevier 1472(3): 509–518.

Perera NC, Schilling O, Kittel H, Back W, Kremmer E and Jenne DE (2012) NSP4, an elastase-related protease in human neutrophils with arginine specificity. *Proceedings of the National Academy of Sciences*. National Acad Sciences 109(16): 6229–6234.

Perez-Lopez A, Behnsen J, Nuccio S-P and Raffatellu M (2016) Mucosal immunity to pathogenic intestinal bacteria. *Nature Reviews Immunology*. Nature Publishing Group 16(3): 135–148.

Perrin J, Le Coadic M, Vernay A, Dias M, Gopaldass N, Ouertatani-Sakouhi H and Cosson P (2015) TM9 family proteins control surface targeting of glycine-rich transmembrane domains. *J Cell Sci*. The Company of Biologists Ltd 128(13): 2269–2277.

Peterson LW and Artis D (2014) Intestinal epithelial cells: regulators of barrier function and immune homeostasis. *Nat Rev Immunol* 14(3): 141–53.

Peyser YM, Ajtai K, Burghardt TP and Muhlrad A (2001) Effect of Ionic Strength on the Conformation of Myosin Subfragment1-Nucleotide Complexes. *Biophysical journal*. Elsevier 81(2): 1101–1114.

Phalen DN, Drew ML, Simpson B, Roset K, Dubose K and Mora M (2010) *Salmonella enterica* subsp. enterica in Cattle Egret (Bubulcus ibis) chicks from central Texas: prevalence, serotypes, pathogenicity, and epizootic potential. *Journal of wildlife diseases*. BioOne 46(2): 379–389.

Phizicky EM and Fields S (1995) Protein-protein interactions: methods for detection and analysis. *Microbiological reviews*. Am Soc Microbiol 59(1): 94–123.

Picotti P, Marabotti A, Negro A, Musi V, Spolaore B, Zambonin M and Fontana A (2004) Modulation of the structural integrity of helix F in apomyoglobin by single amino acid replacements. *Protein science*. Wiley Online Library 13(6): 1572–1585.

Pillich H, Loose M, Zimmer K-P and Chakraborty T (2016) Diverse roles of endoplasmic reticulum stress sensors in bacterial infection. *Molecular and cellular pediatrics*. Springer Berlin Heidelberg 3(1): 1.

Polaskova V, Kapur A, Khan A, Molloy MP and Baker MS (2010) High-abundance protein depletion: Comparison of methods for human plasma biomarker discovery. *Electrophoresis*. Wiley Online Library 31(3): 471–482.

Pompach P, Man P, Novak P, Havl'\i\vcek V, Fi\vserová A and Bezou\vska K (2004) Mass spectrometry is a powerful tool for identification of proteins associated with lipid rafts of Jurkat T-cell line. *Biochemical Society Transactions*. Portland Press Limited 32(5): 777–779.

Porath J, Carlsson J, Olsson I and Belfrage G (1975) Metal chelate affinity chromatography, a new approach to protein fractionation. *Nature* 258: 598–599.

Prasanna RR and Vijayalakshmi MA (2010) Immobilized metal-ion affinity systems for recovery and structure-function studies of proteins at molecular, supramolecular, and cellular levels. *Pure and Applied Chemistry* 82(1): 39–55.

Priller JPR, Reid S, Konein P, Dietrich P and Sonnewald S (2016) The Xanthomonas campestris pv. vesicatoria Type-3 Effector XopB Inhibits Plant Defence Responses by Interfering with ROS Production. *PloS one*. Public Library of Science 11(7): e0159107.

Proft T and Baker E (2009) Pili in Gram-negative and Gram-positive bacteria—structure, assembly and their role in disease. *Cellular and molecular life sciences*. Springer 66(4): 613–635.

Pruvot B, Laurens V, Salvadori F, Solary E, Pichon L and Chluba J (2010) Comparative analysis of nonaspanin protein sequences and expression studies in zebrafish. *Immunogenetics* 62(10): 681–99.

Pugsley AP (1993) The complete general secretory pathway in gram-negative bacteria. *Microbiological reviews* 57(1): 50–108.

Pukáncsik M, Orbán Á, Nagy K, Matsuo K, Gekko K, Maurin D, Hart D, Kézsmárki I and Vertessy BG (2016) Secondary structure prediction of protein constructs using random incremental truncation and vacuum-ultraviolet CD spectroscopy. *PloS one*. Public Library of Science 11(6): e0156238.

Qi R and Liu XY (2006) New advance in caspase-independent programmed cell death and its potential in cancer therapy. *International journal of biomedical science : IJBS* 2(3): 211–6.

Rabsch W, Andrews HL, Kingsley RA, Prager R, Tschäpe H, Adams LG and Bäumler AJ (2002) *Salmonella enterica* serotype Typhimurium and its host-adapted variants. *Infection and Immunity*. Am Soc Microbiol 70(5): 2249–2255.

Rajalingam K, Al-Younes H, Müller A, Meyer TF, Szczepek AJ and Rudel T (2001) Epithelial cells infected with Chlamydophila pneumoniae (Chlamydia pneumoniae) are resistant to apoptosis. *Infection and immunity* 69(12): 7880–8.

Rajewsky K (1996) Clonal selection and learning in the antibody system. *Nature* 381(6585): 751–758.

Ramsden AE, Holden DW and Mota LJ (2007) Membrane dynamics and spatial distribution of *Salmonella*-containing vacuoles. *Trends in microbiology* 15(11): 516–24.

Rao VS, Srinivas K, Sujini G and Kumar G (2014) Protein-protein interaction detection: methods and analysis. *International journal of proteomics*. Hindawi Publishing Corporation 2014.

Raran-Kurussi S and Waugh DS (2012) The ability to enhance the solubility of its fusion partners is an intrinsic property of maltose-binding protein but their folding is either spontaneous or chaperone-mediated. *PloS one*. Public Library of Science 7(11): e49589.

Raussens V, Ruysschaert J-M and Goormaghtigh E (2003) Protein concentration is not an absolute prerequisite for the determination of secondary structure from circular dichroism spectra: a new scaling method. *Analytical biochemistry*. Elsevier 319(1): 114–121.

Ravishankar S, Zhu L and Jaroni D (2010) Assessing the cross contamination and transfer rates of *Salmonella enterica* from chicken to lettuce under different food-handling scenarios. *Food microbiology*. Elsevier 27(6): 791–794.

Reed CJ, Bushnell S and Evilia C (2014) Circular dichroism and fluorescence spectroscopy of cysteinyl-tRNA synthetase from Halobacterium salinarum ssp. NRC-1 demonstrates that group I cations are particularly effective in providing structure and stability to this halophilic protein. *PloS one*. Public Library of Science 9(3): e89452.

Reis EMF dos, Rodrigues D dos P, Freitas-Almeida AC de and Hofer E (2011) Prevalence of R-type ACSSuT in strains of *Salmonella* serovar Typhimurium DT193 isolated from human infections in Brazil. *Revista Panamericana de Salud Pública*. SciELO Public Health 29(6): 387–392.

Remaut H, Rose RJ, Hannan TJ, Hultgren SJ, Radford SE, Ashcroft AE and Waksman G (2006) Donor-strand exchange in chaperone-assisted pilus assembly proceeds through a concerted beta strand displacement mechanism. *Molecular cell* 22(6): 831–42.

Ren L, Chang E, Makky K, Haas AL, Kaboord B and Qoronfleh MW (2003) Glutathione S-transferase pull-down assays using dehydrated immobilized glutathione resin. *Analytical biochemistry*. Elsevier 322(2): 164–169.

Rheingold SR, Brown VI, Fang J, Kim JM and Grupp SA (2003) Role of the BCR complex in B cell development, activation, and leukemic transformation. *Immunologic research* 27(2-3): 309–30.

Ribet D and Cossart P (2015) How bacterial pathogens colonize their hosts and invade deeper tissues. *Microbes and Infection*. Elsevier 17(3): 173–183.

Rippa V, Cirulli C, Di Palo B, Doti N, Amoresano A and Duilio A (2010) The ribosomal protein L2 interacts with the RNA polymerase alpha subunit and acts as a transcription modulator in Escherichia coli. *Journal of bacteriology*. Am Soc Microbiol 192(7): 1882–1889.

Rizzuto R, Pinton P, Carrington W, Fay FS, Fogarty KE, Lifshitz LM, Tuft RA and Pozzan T (1998) Close contacts with the endoplasmic reticulum as determinants of

mitochondrial Ca2+ responses. *Science*. American Association for the Advancement of Science 280(5370): 1763–1766.

Roark EA and Haldar K (2008a) Effects of lysosomal membrane protein depletion on the *Salmonella*-containing vacuole. *PloS one* 3(10): e3538.

Roark EA and Haldar K (2008b) Effects of lysosomal membrane protein depletion on the *Salmonella*-containing vacuole. *PloS one*. Public Library of Science 3(10): e3538.

Roberts TH and Hejgaard J (2008) Serpins in plants and green algae. *Functional & integrative genomics* 8(1): 1–27.

Roberts TH, Hejgaard J, Saunders NFW, Cavicchioli R and Curmi PMG (2004) Serpins in unicellular Eukarya, Archaea, and Bacteria: sequence analysis and evolution. *Journal of molecular evolution* 59(4): 437–47.

Rolando M and Buchrieser C (2014) Legionella pneumophila type \IV\ effectors hijack the transcription and translation machinery of the host cell. *Trends in Cell Biology* (12):771-8.

Roman M (2009) Model cellulosic surfaces: History and recent advances. *ACS symposium series*, 3–53.

Rosales-Reyes R, Alpuche-Aranda C, de la Luz Ram'\irez-Aguilar M, Castro-Eguiluz AD and Ortiz-Navarrete V (2005) Survival of *Salmonella enterica* serovar Typhimurium within late endosomal-lysosomal compartments of B lymphocytes is associated with the inability to use the vacuolar alternative major histocompatibility complex class I antigen-processing pathway. *Infection and immunity*. Am Soc Microbiol 73(7): 3937–3944.

Rose RJ, Welsh TS, Waksman G, Ashcroft AE, Radford SE and Paci E (2008) Donor-strand exchange in chaperone-assisted pilus assembly revealed in atomic detail by molecular dynamics. *Journal of molecular biology* 375(4): 908–19.

Rosenberger CM, Scott MG, Gold MR, Hancock RE and Finlay BB (2000) *Salmonella* typhimurium infection and lipopolysaccharide stimulation induce similar changes in macrophage gene expression. *The Journal of immunology*. Am Assoc Immnol 164(11): 5894–5904.

Rosenfeld Y and Shai Y (2006) Lipopolysaccharide (Endotoxin)-host defense antibacterial peptides interactions: role in bacterial resistance and prevention of sepsis. *Biochimica et Biophysica Acta (BBA)-Biomembranes*. Elsevier 1758(9): 1513–1522.

Rossez Y, Wolfson EB, Holmes A, Gally DL and Holden NJ (2015) Bacterial flagella: twist and stick, or dodge across the kingdoms. *PLoS Pathog*. Public Library of Science 11(1): e1004483.

Round JL and Mazmanian SK (2009) The gut microbiota shapes intestinal immune responses during health and disease. *Nature Reviews Immunology*. Nature Publishing Group 9(5): 313–323.

Roy PH, Tetu SG, Larouche A, Elbourne L, Tremblay S, Ren Q, Dodson R, Harkins D, Shay R, Watkins K, Mahamoud Y and Paulsen IT (2010) Complete genome sequence of the multiresistant taxonomic outlier Pseudomonas aeruginosa PA7. *PloS one* 5(1): e8842.

Ruddock LW and Molinari M (2006) N-glycan processing in ER quality control. *Journal of cell science*. The Company of Biologists Ltd 119(21): 4373–4380.

Ruer S, Stender S, Filloux A and de Bentzmann S (2007) Assembly of fimbrial structures in Pseudomonas aeruginosa: functionality and specificity of chaperone-usher machineries. *Journal of bacteriology* 189(9): 3547–55.

Ruiz L, Hevia A, Bernardo D, Margolles A and Sánchez B (2014) Extracellular molecular effectors mediating probiotic attributes. *FEMS microbiology letters*. The Oxford University Press 359(1): 1–11.

Rutherfurd SM and Dunn BM (2011) Quantitative amino acid analysis. *Current Protocols in Protein Science*. Wiley Online Library 3–2.

Rychlik I, Karasova D, Sebkova A, Volf J, Sisak F, Havlickova H, Kummer V, Imre A, Szmolka A and Nagy B (2009) Virulence potential of five major pathogenicity islands (SPI-1 to SPI-5) of *Salmonella enterica* serovar Enteritidis for chickens. *BMC microbiology*. BioMed Central 9(1): 1.

Salih O, Remaut H, Waksman G and Orlova EV (2008) Structural analysis of the Saf pilus by electron microscopy and image processing. *Journal of molecular biology* 379(1): 174–87.

Salvemini F, Franzé A, Iervolino A, Filosa S, Salzano S and Ursini MV (1999) Enhanced glutathione levels and oxidoresistance mediated by increased glucose-6-phosphate dehydrogenase expression. *The Journal of biological chemistry* 274(5): 2750–7.

Salzano AM and Crescenzi M (2005) Mass spectrometry for protein identification and the study of post translational modifications. *Ann Ist Super Sanita* 41(4): 443–450.

Samatey FA, Matsunami H, Imada K, Nagashima S, Shaikh TR, Thomas DR, Chen JZ, DeRosier DJ, Kitao A and Namba K (2004) Structure of the bacterial flagellar hook and implication for the molecular universal joint mechanism. *Nature*. Nature Publishing Group 431(7012): 1062–1068.

Samson JE, Magadán AH, Sabri M and Moineau S (2013) Revenge of the phages: defeating bacterial defences. *Nature reviews. Microbiology* 11(10): 675–87.

Samuelsson B, Morgenstern R and Jakobsson P-J (2007) Membrane prostaglandin E synthase-1: a novel therapeutic target. *Pharmacological reviews* 59(3): 207–24.

Sánchez B, Schmitter J-M and Urdaci MC (2009) Identification of novel proteins secreted by Lactobacillus rhamnosus GG grown in de Mann-Rogosa-Sharpe broth. *Letters in applied microbiology* 48(5): 618–22.

Santos AJ, Durkin CH, Helaine S, Boucrot E and Holden DW (2016) Clustered intracellular *Salmonella* Typhimurium Blocks Host Cell Cytokinesis. *Infection and immunity*. Am Soc Microbiol IAI–00062.

Sapra R, Gaucher S, Lachmann J, Buffleben G, Chirica G, Comer J, Peterson J, Chopra A and Singh A (2006) Proteomic analyses of murine macrophages treated with Bacillus anthracis lethal toxin. *Microbial pathogenesis*. Elsevier 41(4): 157–167.

Sauer FG, Pinkner JS, Waksman G and Hultgren SJ (2002) Chaperone priming of pilus subunits facilitates a topological transition that drives fiber formation. *Cell* 111(4): 543–51.

Sauer FG, Remaut H, Hultgren SJ and Waksman G (2004) Fiber assembly by the chaperone-usher pathway. *Biochimica et biophysica acta* 1694(1-3): 259–67.

Schell MA, Karmirantzou M, Snel B, Vilanova D, Berger B, Pessi G, Zwahlen M-C, Desiere F, Bork P, Delley M, Pridmore RD and Arigoni F (2002) The genome sequence of Bifidobacterium longum reflects its adaptation to the human gastrointestinal tract. *Proceedings of the National Academy of Sciences of the United States of America* 99(22): 14422–7.

Scherl A, Shaffer SA, Taylor GK, Hernandez P, Appel RD, Binz P-A and Goodlett DR (2008) On the benefits of acquiring peptide fragment ions at high measured mass accuracy. *Journal of the American Society for Mass Spectrometry* 19(6): 891–901.

Schikora A, Garcia AV and Hirt H (2012) Plants as alternative hosts for *Salmonella*. *Trends in plant science*. Elsevier 17(5): 245–249.

Schimmöller F, Díaz E, Mühlbauer B and Pfeffer SR (1998) Characterization of a 76 kDa endosomal, multispanning membrane protein that is highly conserved throughout evolution. *Gene* 216(2): 311–8.

Schleker S, Sun J, Raghavan B, Srnec M, Müller N, Koepfinger M, Murthy L, Zhao Z and Klein-Seetharaman J (2012) The current *Salmonella*-host interactome. *PROTEOMICS-Clinical Applications*. Wiley Online Library 6(1-2): 117–133.

Schmid F-X (2001) Biological Macromolecules: UV-visible Spectrophotometry. *eLS*. Wiley Online Library.

Schmidt H and Hensel M (2004) Pathogenicity islands in bacterial pathogenesis. *Clinical microbiology reviews*. Am Soc Microbiol 17(1): 14–56.

Schneider AG, Abdallah DSA, Butcher BA and Denkers EY (2013) Toxoplasma gondii triggers phosphorylation and nuclear translocation of dendritic cell STAT1 while simultaneously blocking IFN gamma-induced STAT1 transcriptional activity. *PLoS One*. Public Library of Science 8(3): e60215.

Schroeder N, Mota LJ and Méresse S (2011) *Salmonella*-induced tubular networks. *Trends in microbiology* 19(6): 268–77.

Schwartz RH (1992) Costimulation of T Lymphocytes: Minireview The Role of 0D28, CTLA-4, and B7/BB1 in Interleukin-2 Production and Immunotherapy. *Cell*. Elsevier 71: 1065–1068.

Scorrano L, Oakes SA, Opferman JT, Cheng EH, Sorcinelli MD, Pozzan T and Korsmeyer SJ (2003) BAX and BAK regulation of endoplasmic reticulum Ca2+: a control point for apoptosis. *Science*. American Association for the Advancement of Science 300(5616): 135–139.

Seaborn T, Ravni A, Au R, Chow BK, Fournier A, Wurtz O, Vaudry H, Eiden LE and Vaudry D (2014) Induction of serpinb1a by PACAP or NGF is required for PC12 cells survival after serum withdrawal. *Journal of neurochemistry*. Wiley Online Library 131(1): 21–32.

Seabrook SA and Newman J (2013) High-throughput thermal scanning for protein stability: making a good technique more robust. *ACS combinatorial science*. ACS Publications 15(8): 387–392.

Searle BC (2010) Scaffold: a bioinformatic tool for validating MS/MS-based proteomic studies. *Proteomics* 10(6): 1265–9.

Sebastiani G, Blais V, Sancho V, Vogel SN, Stevenson MM, Gros P, Lapointe J-M, Rivest S and Malo D (2002) Host immune response to *Salmonella enterica* serovar Typhimurium infection in mice derived from wild strains. *Infection and immunity* 70(4): 1997–2009.

Seidler J, Zinn N, Boehm ME and Lehmann WD (2010) De novo sequencing of peptides by MS/MS. *Proteomics* 10(4): 634–49.

Sendoel A and Hengartner MO (2014) Apoptotic cell death under hypoxia. *Physiology*. Am Physiological Soc 29(3): 168–176.

Seymour S, Booy A, Gundry R, Van Eyk J and Hunter C (2010) Assessing the Complementarities of MALDI and ESI for Protein Identification in Complex Mixtures. *Technical Note, AB SCIEX* 1–5.

Shao C, Zhang Y and Sun W (2014) Statistical characterization of HCD fragmentation patterns of tryptic peptides on an LTQ Orbitrap Velos mass spectrometer. *Journal of proteomics*. Elsevier 109: 26–37.

Shen A, Lupardus PJ, Morell M, Ponder EL, Sadaghiani AM, Garcia KC and Bogyo M (2009) Simplified, enhanced protein purification using an inducible, autoprocessing enzyme tag. *PLoS One*. Public Library of Science 4(12): e8119.

Sherratt PJ and Hayes JD (2001) 9 Glutathione S-transferases. *Enzyme systems that metabolise drugs and other xenobiotics* 319.

Shields PA and Farrah SR (1983) Influence of salts on electrostatic interactions between poliovirus and membrane filters. *Applied and environmental microbiology*. Am Soc Microbiol 45(2): 526–531.

Sikdar S, Gill R and Datta S (2016) Improving protein identification from tandem mass spectrometry data by one-step methods and integrating data from other platforms. *Briefings in bioinformatics*. Oxford Univ Press 17(2): 262–269.

Siligardi G, Hussain R, Patching SG and Phillips-Jones MK (2014) Ligand-and drug-binding studies of membrane proteins revealed through circular dichroism spectroscopy. *Biochimica et Biophysica Acta (BBA)-Biomembranes*. Elsevier 1838(1): 34–42.

Silverman GA, Whisstock JC, Bottomley SP, Huntington JA, Kaiserman D, Luke CJ, Pak SC, Reichhart J-M and Bird PI (2010) Serpins flex their muscle I. Putting the clamps on proteolysis in diverse biological systems. *Journal of Biological Chemistry*. ASBMB 285(32): 24299–24305.

Singh V (2013) *Salmonella* serovars and their host specificity. *Journal of Veterinary Science & Animal Husbandry*. Annex Publishers 1(3): 1.

Singhal N, Kumar M, Kanaujia PK and Virdi JS (2015) MALDI-TOF mass spectrometry: an emerging technology for microbial identification and diagnosis. *Frontiers in microbiology*. Frontiers Media SA 6.

Sipos F and Muzes G (2011) Isolated lymphoid follicles in colon: switch points between inflammation and colorectal cancer. *World J Gastroenterol* 17(13): 1666–73.

Siuzdak G, Blackledge RD and Hollenbeck TP (1999) Electrospray and MALDI mass spectrometry in the identification of spermicides in criminal investigations. *Journal of Forensic Science*. ASTM International 44(4): 783–788.

Sjögren T, Nord J, Ek M, Johansson P, Liu G and Geschwindner S (2013) Crystal structure of microsomal prostaglandin E2 synthase provides insight into diversity in the MAPEG superfamily. *Proceedings of the National Academy of Sciences of the United States of America* 110(10): 3806–11.

Snapyan M, Lecocq M, Guével L, Arnaud M-C, Ghochikyan A and Sakanyan V (2003) Dissecting DNA-protein and protein-protein interactions involved in bacterial transcriptional regulation by a sensitive protein array method combining a near-infrared fluorescence detection. *Proteomics*. Wiley Online Library 3(5): 647–657.

Snyder LR, Kirkland JJ and Glajch JL (1997) Appendix III: Retention in Reversed-Phase and Normal-Phase HPLC as a Function of Sample Molecular Structure. *Practical HPLC Method Development, Second Edition*. Wiley Online Library 729–734.

Soeriyadi AH, R Whittaker M, Boyer C and Davis TP (2013) Soft ionization mass spectroscopy: insights into the polymerization mechanism. *Journal of Polymer Science Part A: Polymer Chemistry*. Wiley Online Library 51(7): 1475–1505.

Song Q, Gou W-L and Zhang R (2016) FAM3A attenuates ER stress-induced mitochondrial dysfunction and apoptosis via CHOP-Wnt pathway. *Neurochemistry international*. Elsevier 94: 82–89.

Soupene E, Rothschild J, Kuypers FA and Dean D (2012) Eukaryotic protein recruitment into the Chlamydia inclusion: implications for survival and growth. *PloS one* 7(5): e36843.

Sousa MM, Steen KW, Hagen L and Slupphaug G (2011) Antibody cross-linking and target elution protocols used for immunoprecipitation significantly modulate signal-to noise ratio in downstream 2D-PAGE analysis. *Proteome science*. BioMed Central 9(1): 1.

Souwer Y, Griekspoor A, Jorritsma T, de Wit J, Janssen H, Neefjes J and van Ham SM (2009) B cell receptor-mediated internalization of *salmonella*: a novel pathway for autonomous B cell activation and antibody production. *The journal of immunology*. Am Assoc Immnol 182(12): 7473–7481.

Souwer Y, Griekspoor A, de Wit J, Martinoli C, Zagato E, Janssen H, Jorritsma T, Bar-Ephraím YE, Rescigno M, Neefjes J and others (2012) Selective infection of antigen-specific B lymphocytes by *Salmonella* mediates bacterial survival and systemic spreading of infection. *PloS one*. Public Library of Science 7(11): e50667.

Sowell RA, Koeniger SL, Valentine SJ, Moon MH and Clemmer DE (2004) Nanoflow LC/IMS-MS and LC/IMS-CID/MS of protein mixtures. *Journal of the American Society for Mass Spectrometry* 15(9): 1341–53.

Spahn T and Kucharzik T (2004) Modulating the intestinal immune system: the role of lymphotoxin and GALT organs. *Gut*. BMJ Publishing Group Ltd and British Society of Gastroenterology 53(3): 456–465.

Srihari S, Yong CH, Patil A and Wong L (2015) Methods for protein complex prediction and their contributions towards understanding the organisation, function and dynamics of complexes. *FEBS letters*. Elsevier 589(19): 2590–2602.

Stapels DA, Ramyar KX, Bischoff M, von Köckritz-Blickwede M, Milder FJ, Ruyken M, Eisenbeis J, McWhorter WJ, Herrmann M, van Kessel KP and others (2014) Staphylococcus aureus secretes a unique class of neutrophil serine protease inhibitors. *Proceedings of the National Academy of Sciences*. National Acad Sciences 111(36):

13187–13192.

Stead DA, Preece A and Brown AJ (2006) Universal metrics for quality assessment of protein identifications by mass spectrometry. *Molecular \& Cellular Proteomics*. ASBMB 5(7): 1205–1211.

Stecher B, Robbiani R, Walker AW, Westendorf AM, Barthel M, Kremer M, Chaffron S, Macpherson AJ, Buer J, Parkhill J and others (2007) *Salmonella enterica* serovar typhimurium exploits inflammation to compete with the intestinal microbiota. *PLoS Biol*. Public Library of Science 5(10): e244.

Steele-Mortimer O (2008) The *Salmonella*-containing vacuole—moving with the times. *Current opinion in microbiology*. Elsevier 11(1): 38–45.

Steen H and Mann M (2004) The ABC's (and XYZ's) of peptide sequencing. *Nature reviews Molecular cell biology*. Nature Publishing Group 5(9): 699–711.

Stoilova-McPhie S, Ali S and Laezza F (2013) Protein-protein interactions as new targets for ion channel drug discovery. *Austin journal of pharmacology and therapeutics*. NIH Public Access 1(2).

Strausberg RL, Feingold EA, Grouse LH, Derge JG, Klausner RD, Collins FS, Wagner L, Shenmen CM, Schuler GD, Altschul SF, Zeeberg B, Buetow KH, Schaefer CF, Bhat NK, Hopkins RF, Jordan H, Moore T, Max SI, Wang J, Hsieh F, Diatchenko L, Marusina K, Farmer AA, Rubin GM, Hong L, Stapleton M, Soares MB, Bonaldo MF, Casavant TL, Scheetz TE, Brownstein MJ, Usdin TB, Toshiyuki S, Carninci P, Prange C, Raha SS, Loquellano NA, Peters GJ, Abramson RD, Mullahy SJ, Bosak SA, McEwan PJ, McKernan KJ, Malek JA, Gunaratne PH, Richards S, Worley KC, Hale S, Garcia AM, Gay LJ, Hulyk SW, Villalon DK, Muzny DM, Sodergren EJ, Lu X, Gibbs RA, Fahey J, Helton E, Ketteman M, Madan A, Rodrigues S, Sanchez A, Whiting M, Madan A, Young AC, Shevchenko Y, Bouffard GG, Blakesley RW, Touchman JW, Green ED, Dickson MC, Rodriguez AC, Grimwood J, Schmutz J, Myers RM, Butterfield YSN, Krzywinski MI, Skalska U, Smailus DE, Schnerch A, Schein JE, Jones SJM and Marra MA (2002) Generation and initial analysis of more than 15,000 full-length human and mouse cDNA sequences. *Proceedings of the National Academy of Sciences of the United States of America* 99(26): 16899–903.

Strindelius L, Folkesson A, Normark S and Sjöholm I (2004) Immunogenic properties of the *Salmonella* atypical fimbriae in BALB/c mice. *Vaccine* 22(11-12): 1448–56.

Stroschein-Stevenson SL, Foley E, O'Farrell PH and Johnson AD (2005) Identification of Drosophila gene products required for phagocytosis of Candida albicans. *PLoS Biol*. Public Library of Science 4(1): e4.

Suckau D, Resemann A, Schuerenberg M, Hufnagel P, Franzen J and Holle A (2003) A novel MALDI LIFT-TOF/TOF mass spectrometer for proteomics. *Analytical and bioanalytical chemistry*. Springer 376(7): 952–965.

Sugasawa T, Lenzen G, Simon S, Hidaka J, Cahen A, Guillaume JL, Camoin L, Strosberg AD and Nahmias C (2001) The iodocyanopindolol and SM-11044 binding protein belongs to the TM9SF multispanning membrane protein superfamily. *Gene* 273(2): 227–37.

Sukhan A, Kubori T and Galán JE (2003) Synthesis and localization of the *Salmonella* SPI-1 type III secretion needle complex proteins PrgI and PrgJ. *Journal of bacteriology* 185(11): 3480–3.

Sun L, Li Y, Yang P, Zhu G and Dovichi NJ (2012) High efficiency and quantitatively reproducible protein digestion by trypsin-immobilized magnetic microspheres. *Journal of Chromatography A*. Elsevier 1220: 68–74.

Swearingen MC, Porwollik S, Desai PT, McClelland M and Ahmer BM (2012) Virulence of 32 *Salmonella* strains in mice. *PLoS One*. Public Library of Science 7(4): e36043.

Switt AIM, Orsi RH, den Bakker HC, Vongkamjan K, Altier C and Wiedmann M (2013) Genomic characterization provides new insight into *Salmonella* phage diversity. *BMC genomics*. BioMed Central 14(1): 1.

Tagami S, Sekine S, Minakhin L, Esyunina D, Akasaka R, Shirouzu M, Kulbachinskiy A, Severinov K and Yokoyama S (2014) Structural basis for promoter specificity switching of RNA polymerase by a phage factor. *Genes & development* 28(5): 521–31.

Tahoun A, Mahajan S, Paxton E, Malterer G, Donaldson DS, Wang D, Tan A, Gillespie TL, O'Shea M, Roe AJ and others (2012) *Salmonella* transforms follicle-associated epithelial cells into M cells to promote intestinal invasion. *Cell host \& microbe*. Elsevier 12(5): 645–656.

Tang L, Wang C-X, Zhu S-L, Li Y, Deng X, Johnston RN, Liu G-R and Liu S-L (2013) Genetic boundaries to delineate the typhoid agent and other *Salmonella* serotypes into distinct natural lineages. *Genomics*. Elsevier 102(4): 331–337.

Terpe K (2003) Overview of tag protein fusions: from molecular and biochemical fundamentals to commercial systems. *Applied microbiology and biotechnology* 60(5):

523–33.

Tewari P and Singh A (1999) Amberlite XAD-2 functionalized with chromotropic acid: synthesis of a new polymer matrix and its applications in metal ion enrichment for their determination by flame atomic absorption spectrometry. *Analyst*. Royal Society of Chemistry 124(12): 1847–1851.

Thiede B, Höhenwarter W, Krah A, Mattow J, Schmid M, Schmidt F and Jungblut PR (2005) Peptide mass fingerprinting. *Methods*. Elsevier 35(3): 237–247.

Thorns C (1995) *Salmonella* fimbriae: novel antigens in the detection and control of *Salmonella* infections. *British Veterinary Journal*. Elsevier 151(6): 643–658.

Tieng V, Le Bouguénec C, Du Merle L, Bertheau P, Desreumaux P, Janin A, Charron D and Toubert A (2002) Binding of Escherichia coli adhesin AfaE to CD55 triggers cell-surface expression of the MHC class I-related molecule MICA. *Proceedings of the National Academy of Sciences*. National Acad Sciences 99(5): 2977–2982.

Tindall B, Grimont P, Garrity G and Euzeby J (2005) Nomenclature and taxonomy of the genus *Salmonella*. *International journal of systematic and evolutionary microbiology*. Microbiology Society 55(1): 521–524.

Tolstikov VV and Fiehn O (2002) Analysis of highly polar compounds of plant origin: combination of hydrophilic interaction chromatography and electrospray ion trap mass spectrometry. *Analytical biochemistry*. Elsevier 301(2): 298–307.

Towbin H, Staehelin T and Gordon J (1979) Electrophoretic transfer of proteins from polyacrylamide gels to nitrocellulose sheets: procedure and some applications. *Proceedings of the National Academy of Sciences*. National Acad Sciences 76(9): 4350–4354.

Tribalat L, Paisse O, Dessalces G and Grenier-Loustalot M-F (2006) Advantages of LC-MS-MS compared to LC-MS for the determination of nitrofuran residues in honey. *Analytical and bioanalytical chemistry*. Springer 386(7-8): 2161–2168.

Tu C, Rudnick PA, Martinez MY, Cheek KL, Stein SE, Slebos RJ and Liebler DC (2010) Depletion of abundant plasma proteins and limitations of plasma proteomics. *Journal of proteome research*. ACS Publications 9(10): 4982–4991.

Tziatzios C, Schubert D, Lotz M, Gundogan D, Betz H, Schägger H, Haase W, Duong F and Collinson I (2004) The bacterial protein-translocation complex: SecYEG dimers associate with one or two SecA molecules. *Journal of molecular biology*

340(3): 513–24.

Ueda E, Gout P and Morganti L (2003) Current and prospective applications of metal ion-protein binding. *Journal of Chromatography A*. Elsevier 988(1): 1–23.

Uhl O, Glaser C, Demmelmair H and Koletzko B (2011) Reversed phase LC/MS/MS method for targeted quantification of glycerophospholipid molecular species in plasma. *Journal of Chromatography B*. Elsevier 879(30): 3556–3564.

Ullah R, Shah MA, Tufail S, Ismat F, Imran M, Iqbal M, Mirza O and Rhaman M (2016) Activity of the Human Rhinovirus 3C Protease Studied in Various Buffers, Additives and Detergents Solutions for Recombinant Protein Production. *PloS one*. Public Library of Science 11(4): e0153436.

Umezawa K, Ohnishi N, Tanaka K, Kamiya S, Koga Y, Nakazawa H and Ozawa A (1995) Granulation in livers of mice infected with *Salmonella* typhimurium is caused by superoxide released from host phagocytes. *Infection and immunity* 63(11): 4402–8.

Uzzau S, Brown DJ, Wallis T, Rubino S, Leori G, Bernard S, Casadesús J, Platt DJ and Olsen JE (2000) Host adapted serotypes of *Salmonella enterica*. *Epidemiology and infection*. Cambridge Univ Press 125(02): 229–255.

Vatansever F, de Melo WC, Avci P, Vecchio D, Sadasivam M, Gupta A, Chandran R, Karimi M, Parizotto NA, Yin R and others (2013) Antimicrobial strategies centered around reactive oxygen species-bactericidal antibiotics, photodynamic therapy, and beyond. *FEMS microbiology reviews*. The Oxford University Press 37(6): 955–989.

Vazquez-Torres A, Jones-Carson J, Bäumler AJ, Falkow S, Valdivia R, Brown W, Le M, Berggren R, Parks WT and Fang FC (1999) Extraintestinal dissemination of *Salmonella* by CD18-expressing phagocytes. *Nature*. Nature Publishing Group 401(6755): 804–808.

Veiga E and Cossart P (2006) The role of clathrin-dependent endocytosis in bacterial internalization. *Trends in cell biology* 16(10): 499–504.

Veitch NC (2004) Horseradish peroxidase: a modern view of a classic enzyme. *Phytochemistry* 65(3): 249–59.

Van Veld P and Lee R (1988) Intestinal glutathione S-transferase activity in flounder Platichthys flesus collected from contaminated and reference sites. *Marine ecology progress series. Oldendorf* 46(1): 61–63.

Vernikos GS, Thomson NR and Parkhill J (2007) Genetic flux over time in the *Salmonella* lineage. *Genome biology*. BioMed Central 8(6): 1.

Vetsch M, Erilov D, Molière N, Nishiyama M, Ignatov O and Glockshuber R (2006) Mechanism of fibre assembly through the chaperone-usher pathway. *EMBO reports* 7(7): 734–8.

Vigueras-Santiago E, Hernández-López S and Rodr'\iguez-Romero A (2006) Photochemical cross-linking study of polymers containing diacetylene groups in their main chain and azobenzene compounds as pendant groups. *Superficies y vac'\io*. Sociedad Mexicana de Ciencia y Tecnolog'\ia de Superficies y Materiales AC 19(1): 1–7.

Vitale A and Boston RS (2008) Endoplasmic reticulum quality control and the unfolded protein response: insights from plants. *Traffic (Copenhagen, Denmark)* 9(10): 1581–8.

Vizcarra IA, Hosseini V, Kollmannsberger P, Meier S, Weber SS, Arnoldini M, Ackermann M and Vogel V (2016) How type 1 fimbriae help Escherichia coli to evade extracellular antibiotics. *Scientific reports*. Nature Publishing Group 6.

Vollrath F, Hawkins N, Porter D, Holland C and Boulet-Audet M (2014) Differential Scanning Fluorimetry provides high throughput data on silk protein transitions. *Scientific reports*. Nature Publishing Group 4.

Vreede FT, Chan AY, Sharps J and Fodor E (2010) Mechanisms and functional implications of the degradation of host RNA polymerase II in influenza virus infected cells. *Virology*. Elsevier 396(1): 125–134.

Wallace B and Janes RW (2001) Synchrotron radiation circular dichroism spectroscopy of proteins: secondary structure, fold recognition and structural genomics. *Current opinion in chemical biology*. Elsevier 5(5): 567–571.

Wallace B, Lees J, Orry A, Lobley A and Janes RW (2003) Analyses of circular dichroism spectra of membrane proteins. *Protein Science*. Wiley Online Library 12(4): 875–884.

Wallace BA, Janes RW and Wallace BA (2003) Circular dichroism and synchrotron radiation circular dichroism spectroscopy: tools for drug discovery. *Biochemical Society transactions* 31(Pt 3): 631–3.

Wang J, Li T, Bai Y, Zhu Y and Lu Z (2003) Fabrication of unimolecular double-stranded DNA microarrays on solid surfaces for probing DNA-protein/drug interactions. *Molecules*. Molecular Diversity Preservation International 8(1): 153–168.

Wang P and Wilson SR (2013) Mass spectrometry-based protein identification by integrating de novo sequencing with database searching. *BMC bioinformatics* 14 Suppl 2: S24.

Wasylnka JA, Bakowski MA, Szeto J, Ohlson MB, Trimble WS, Miller SI and Brumell JH (2008) Role for myosin II in regulating positioning of *Salmonella*-containing vacuoles and intracellular replication. *Infection and immunity*. Am Soc Microbiol 76(6): 2722–2735.

Weinrauch Y and Zychlinsky A (1999) The induction of apoptosis by bacterial pathogens. *Annual Reviews in Microbiology*. Annual Reviews 4139 El Camino Way, PO Box 10139, Palo Alto, CA 94303-0139, USA 53(1): 155–187.

Wells JM and McLuckey SA (2005) Collision-induced dissociation (CID) of peptides and proteins. *Methods in enzymology*. Elsevier 402: 148–185.

Whitmore L and Wallace B (2004) DICHROWEB, an online server for protein secondary structure analyses from circular dichroism spectroscopic data. *Nucleic acids research*. Oxford Univ Press 32(suppl 2): W668–W673.

Wiedow O and Meyer-Hoffert U (2005) Neutrophil serine proteases: potential key regulators of cell signalling during inflammation. *Journal of internal medicine* 257(4): 319–28.

Williams DL, Risse B, Kim S, Saunders D, Orlin S, Baker MS, Jensen PJ and Lavker RM (1999) Plasminogen activator inhibitor type 2 in human corneal epithelium. *Investigative ophthalmology & visual science* 40(8): 1669–75.

Williams JG and Tomer KB (2004) Disposable chromatography for a high-throughput nano-ESI/MS and nano-ESI/MS-MS platform. *Journal of the American Society for Mass Spectrometry* 15(9): 1333–40.

Winstanley C and Hart CA (2001) Type III secretion systems and pathogenicity islands. *Journal of medical microbiology* 50(2): 116–26.

Winter SE, Thiennimitr P, Winter MG, Butler BP, Huseby DL, Crawford RW, Russell JM, Bevins CL, Adams LG, Tsolis RM and others (2010) Gut inflammation provides a respiratory electron acceptor for *Salmonella*. *Nature*. Nature Publishing Group 467(7314): 426–429.

Winther-Larsen HC, Hegge FT, Wolfgang M, Hayes SF, Van Putten JP and Koomey M (2001) Neisseria gonorrhoeae PilV, a type IV pilus-associated protein essential to human epithelial cell adherence. *Proceedings of the National Academy of Sciences*. National Acad Sciences 98(26): 15276–15281.

De Wit J, Souwer Y, Jorritsma T, Bos HK, Ten Brinke A, Neefjes J and Van Ham SM (2010) Antigen-specific B cells reactivate an effective cytotoxic T cell response against phagocytosed *Salmonella* through cross-presentation. *PloS one*. Public Library of Science 5(9): e13016.

Woo M-K, Heo C-K, Hwang H-M, Ko J-H, Yoo H-S and Cho E-W (2011) Optimization of phage-immobilized ELISA for autoantibody profiling in human sera. *Biotechnology letters*. Springer 33(4): 655–661.

Wood DW (2014) New trends and affinity tag designs for recombinant protein purification. *Current opinion in structural biology*. Elsevier 26: 54–61.

Worley MJ, Nieman GS, Geddes K and Heffron F (2006) *Salmonella* typhimurium disseminates within its host by manipulating the motility of infected cells. *Proceedings of the National Academy of Sciences of the United States of America* 103(47): 17915–20.

Worrall LJ, Lameignere E and Strynadka NCJ (2011) Structural overview of the bacterial injectisome. *Current opinion in microbiology* 14(1): 3–8.

Wright HL, Moots RJ, Bucknall RC and Edwards SW (2010) Neutrophil function in inflammation and inflammatory diseases. *Rheumatology*. Br Soc Rheumatology 49(9): 1618–1631.

Wu H, Liu G, Li C and Zhao S (2003) bri3, a novel gene, participates in tumor necrosis factor-alpha-induced cell death. *Biochemical and biophysical research communications*. Elsevier 311(2): 518–524.

Wu J and FUutowiczK M (1999) Hexahistidme (Hise> tag dependent protein dimerization: A cautionary tale.

Wu X and Oppermann U (2003) High-level expression and rapid purification of rare-codon genes from hyperthermophilic archaea by the GST gene fusion system. *Journal of Chromatography B*. Elsevier 786(1): 177–185.

Wu Y, Xie J, Wang F and Chen Z (2009) Separation of small molecular peptides with same amino acid composition but different sequences by capillary electrophoresis. *Journal of separation science* 32(3): 437–40.

Xiao Y and Isaacs SN (2012) Enzyme-linked immunosorbent assay (ELISA) and blocking with bovine serum albumin (BSA)-not all BSAs are alike. *Journal of immunological methods* 384(1-2): 148–51.

Xu Y, Xu L, Zhao M, Xu C, Fan Y, Pierce SK and Liu W (2014) No receptor stands alone: IgG B-cell receptor intrinsic and extrinsic mechanisms contribute to antibody memory. *Cell research*. Nature Publishing Group 24(6): 651–664.

Yamane M (2002) High-performance liquid chromatography-thermospray ionization-mass spectrometry of the oxidation products of polyunsaturated-fatty acids. *Analytica Chimica Acta*. Elsevier 465(1): 227–236.

Yamazaki T, Sasaki N, Nishi M, Yamazaki D, Ikeda A, Okuno Y, Komazaki S and Takeshima H (2007) Augmentation of drug-induced cell death by ER protein BRI3BP. *Biochemical and biophysical research communications*. Elsevier 362(4): 971–975.

Yan F and Polk DB (2002) Probiotic bacterium prevents cytokine-induced apoptosis in intestinal epithelial cells. *Journal of Biological Chemistry*. ASBMB 277(52): 50959–50965.

Yang S-F, Yeh C-B, Chou Y-E, Lee H-L and Liu Y-F (2016) Serpin peptidase inhibitor (SERPINB5) haplotypes are associated with susceptibility to hepatocellular carcinoma. *Scientific reports*. Nature Publishing Group 6.

Yang W, Steen H and Freeman MR (2008) Proteomic approaches to the analysis of multiprotein signaling complexes. *Proteomics*. Wiley Online Library 8(4): 832–851.

Yao Q, Cui J, Zhu Y, Wang G, Hu L, Long C, Cao R, Liu X, Huang N, Chen S, Liu L and Shao F (2009) A bacterial type III effector family uses the papain-like hydrolytic activity to arrest the host cell cycle. *Proceedings of the National Academy of Sciences of the United States of America* 106(10): 3716–21.

Ye S and Goldsmith EJ (2001) Serpins and other covalent protease inhibitors. *Current opinion in structural biology*. Elsevier 11(6): 740–745.

Yeretssian G, Lecocq M, Lebon G, Hurst HC and Sakanyan V (2005) Competition on Nitrocellulose-immobilized Antibody Arrays From Bacterial Protein Binding Assay to Protein Profiling in Breast Cancer Cells. *Molecular \& Cellular Proteomics*. ASBMB 4(5): 605–617.

Ying S, Seiffert BM, Häcker G and Fischer SF (2005) Broad degradation of proapoptotic proteins with the conserved Bcl-2 homology domain 3 during infection with Chlamydia trachomatis. *Infection and immunity*. Am Soc Microbiol 73(3): 1399–1403.

Young CL, Britton ZT and Robinson AS (2012) Recombinant protein expression and purification: a comprehensive review of affinity tags and microbial applications. *Biotechnology journal*. Wiley Online Library 7(5): 620–634.

Yu S (1989) Purification and characterization of glutathione transferases from five phytophagous Lepidoptera. *Pesticide Biochemistry and Physiology*. Elsevier 35(1): 97–105.

Zalazar L, Alonso C, De Castro R and Cesari A (2014) An alternative easy method for antibody purification and analysis of protein-protein interaction using GST fusion proteins immobilized onto glutathione-agarose. *Analytical and bioanalytical chemistry*. Springer 406(3): 911–914.

Zangi R, Hagen M and Berne B (2007) Effect of ions on the hydrophobic interaction between two plates. *Journal of the American Chemical Society*. ACS Publications 129(15): 4678–4686.

Zav'yalov V, Zavialov A, Zav'yalova G and Korpela T (2010) Adhesive organelles of Gram-negative pathogens assembled with the classical chaperone/usher machinery: structure and function from a clinical standpoint. *FEMS microbiology reviews*. The Oxford University Press 34(3): 317–378.

Zavialov A, Kersley J, Korpela T, Zav'yalov V, MacIntyre S and Knight S (2002) Donor strand complementation mechanism in the biogenesis of non-pilus systems. *Molecular microbiology*. Wiley Online Library 45(4): 983–995.

Zavialov A, Zav'yalova G, Korpela T and Zav'yalov V (2007) FGL chaperone-assembled fimbrial polyadhesins: anti-immune armament of Gram-negative bacterial pathogens. *FEMS microbiology reviews* 31(4): 478–514.

Zavialov AV, Berglund J, Pudney AF, Fooks LJ, Ibrahim TM, MacIntyre S and Knight SD (2003) Structure and biogenesis of the capsular F1 antigen from Yersinia pestis: preserved folding energy drives fiber formation. *Cell*. Elsevier 113(5): 587–596.

Zavialov AV, Tischenko VM, Fooks LJ, Brandsdal BO, Aqvist J, Zav'yalov VP, Macintyre S and Knight SD (2005) Resolving the energy paradox of chaperone/usher-mediated fibre assembly. *The Biochemical journal* 389(Pt 3): 685–94.

Zeng W-Z, Liu D-S, Duan B, Song X-L, Wang X, Wei D, Jiang W, Zhu MX, Li Y and Xu T-L (2013) Molecular mechanism of constitutive endocytosis of Acid-sensing ion channel 1a and its protective function in acidosis-induced neuronal death. *The Journal of Neuroscience*. Soc Neuroscience 33(16): 7066–7078.

Zenobi R and Knochenmuss R (1998) Ion formation in MALDI mass spectrometry. *Mass Spectrometry Reviews* 17(5): 337–366.

Zhang J (2012) *Protein-protein interactions in salt solutions*. INTECH Open Access Publisher.

Zhao P, Hou L, Farley K, Sundrud MS and Remold-O'Donnell E (2014) SerpinB1 regulates homeostatic expansion of IL-17+ gamma delta and CD4+ Th17 cells. *Journal of leukocyte biology*. Soc Leukocyte Biology 95(3): 521–530.

Zhao X, Li G and Liang S (2013) Several affinity tags commonly used in chromatographic purification. *Journal of analytical methods in chemistry*. Hindawi Publishing Corporation 2013.